Durham University

Durham E-Theses

Mars: the Durham magnetic automated

C.A. Ayre

How to cite:

Ayre, C.A. (1971) Mars: the Durham magnetic automated. Doctoral thesis, Durham University.

Use policy

The full-text may be used and/or reproduced, and given to third parties in any format or medium, without prior permission or charge, for personal research or study, educational, or not-for-profit purposes provided that:

- a full bibliographic reference is made to the original source
- a https://etheses.durham.ac.uk/id/eprint/9091/ is made to the metadata record in Durham E-Theses
- the full-text is not changed in any way

The full-text must not be sold in any format or medium without the formal permission of the copyright holders.

Please consult the full Durham E-Theses policy for further details.

Academic Support Office, The Palatine Centre, Durham University, Stockton Road, Durham, DH1 3LE
e-mail: e-theses.admin@durham.ac.uk Tel: +44 0191 334 6107
https://etheses.durham.ac.uk

M.A.R.S. - The Durham Magnetic Automated

Research Spectrograph

by

C.A. Ayre, B.Sc.

A Thesis submitted to the

University of Durham for the

Degree of Doctor of Philosophy

September, 1971.

27 JAN 1972
LIBRARY

ABSTRACT

A large solid iron spectrograph is described which will be used initially to measure the vertical spectrum and charge ratio of cosmic ray muons to momenta in excess of 5000 GeV/c. Scintillation counters and trays of digitised neon flash tubes are used as particle detectors and the spectrograph is connected to an I.B.M. 1130 computer for on-line data recording and analysis of the events. The spectrograph has an acceptance of 818 cm^2 ster. and an estimated maximum detectable momentum of approximately 6000 GeV/c.

A momentum selector is incorporated in the spectrograph equipment which selects, for further analysis by the computer, particles with momenta above a few hundred GeV/c from the information contained in trays of digitised flash tubes situated at three levels in the spectrograph. The computer calculates the momenta of particles selected in this way using the data contained in a further five trays of digitised flash tubes.

A flash tube digitisation technique has been developed for use in the spectrograph and is described in detail. The technique utilises a simple probe on the front of the flash tube to detect an electrical pulse when the tube discharges. The pulse is fed into an electronic memory for the flash tube made from integrated circuit logic elements.

The electronic circuits used for the flash tube data recording, the momentum selector, and the logic controlling the readout of data from the flash tube trays to the computer are described. The method of analysis of events by the computer is discussed.

PREFACE

The work described in this thesis was carried out in the period 1967-1970 while the author was a research student under the supervision of Dr. M.G. Thompson in the Cosmic Ray Group of the Physics Department of the University of Durham.

The design and construction of the spectrograph, its associated equipment and electronics, was shared with the author's colleagues. The author was solely responsible for the development of the digitisation technique, and the design and construction of the flash tube trays used in the spectrograph, the electronic circuits used in the Momentum Selector system, Measuring and Azimuth Trays, and the electronics for the tray steerage logic.

The digitisation technique has been reported by Ayre and Thompson (1969,1970) and preliminary details of the spectrograph by Ayre et al.(1970). The first results of the spectrograph have been reported by Ayre et al. (1971) and have also been presented at the XII International Conference on Cosmic Rays in Tasmania, August, 1971.

PLATE 1

M.A.R.S. - The Durham Magnetic Automated Research Spectrograph

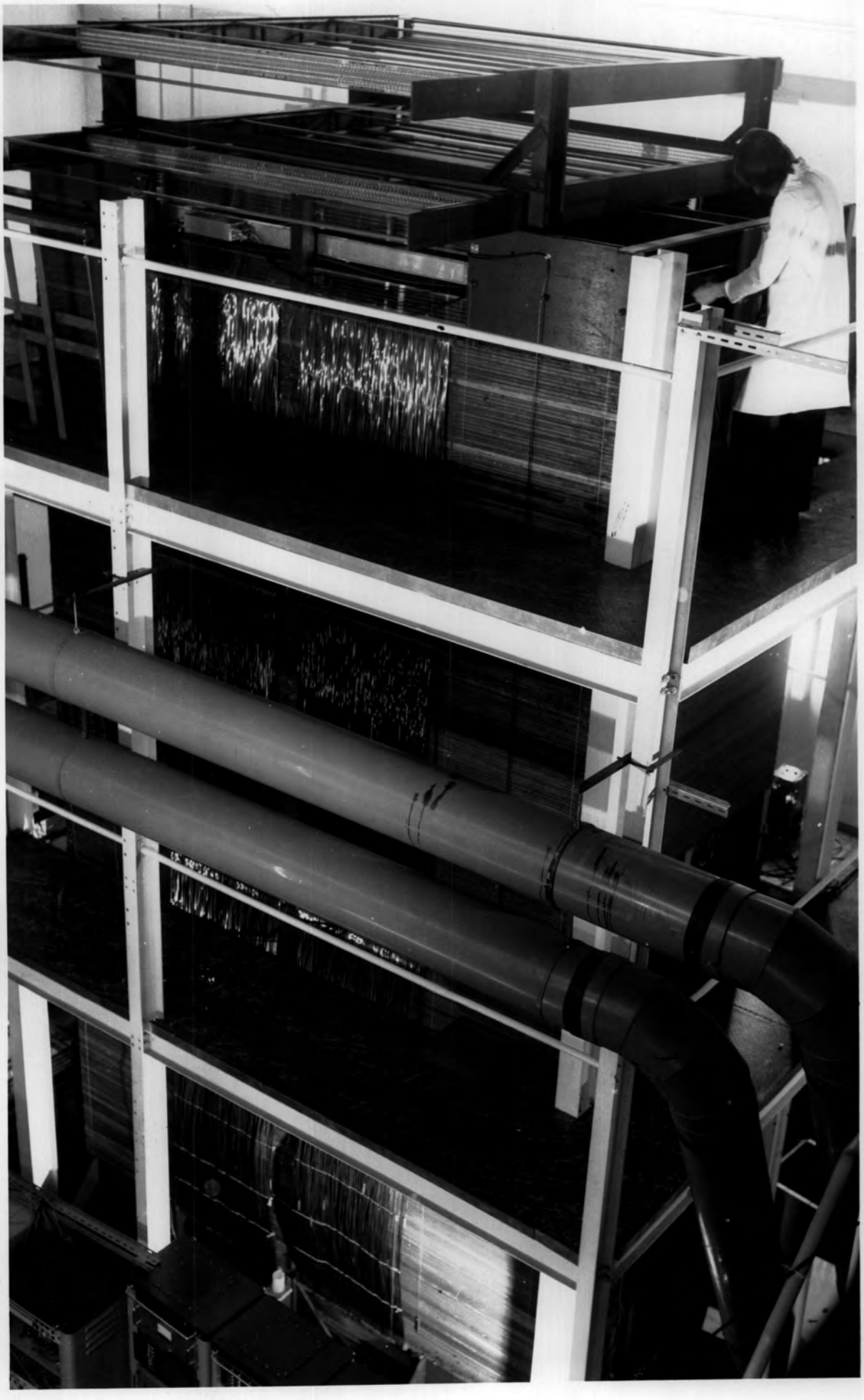

PLATE 2

M.A.R.S.: The Electronics of the

Spectrograph.

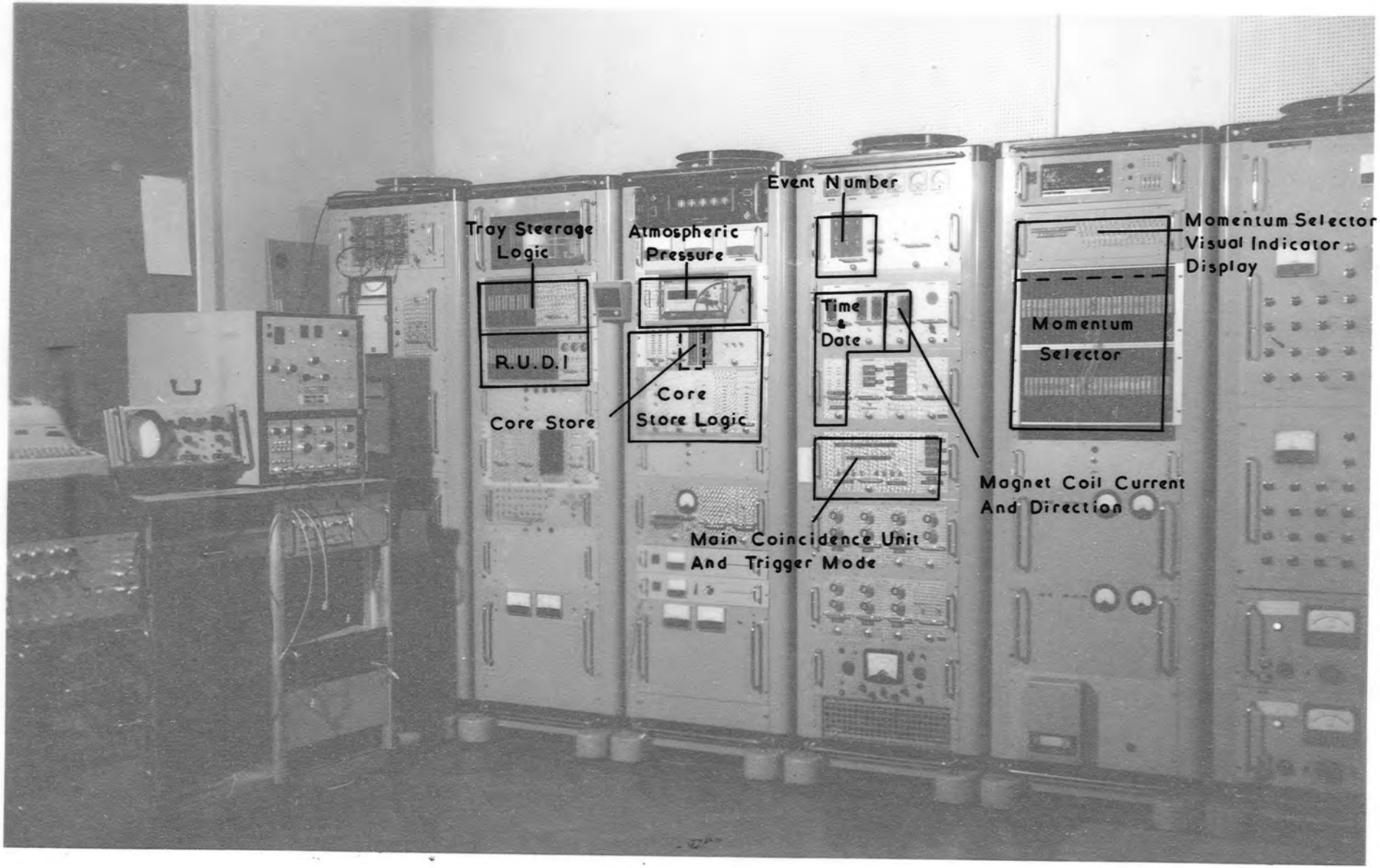
Event Number
Tray Steerage Logic
Atmospheric Pressure
Momentum Selector Visual Indicator Display
Time & Date
R.U.D.I
Momentum Selector
Core Store
Core Store Logic
Magnet Coil Current And Direction
Main Coincidence Unit And Trigger Mode

CONTENTS

CHAPTER 1

Introduction.

1.1 General Introduction

Cosmic Rays, since their discovery by Hess in 1912, have been the subject of intense study. Basically they are studied from two aspects, astrophysics and nuclear physics. The astrophysical work is concerned with the origin of the cosmic rays and the processes required in possible sources and the medium between the source and the earth to explain the energy spectrum, mass composition, and time variation of the primary cosmic rays incident on the earth. The primary cosmic rays are a source of high energy particles far in excess of the energies obtained with present day particle accelerators. Hence a study of their interactions in the atmosphere will enable the results obtained from machine data to be extended to higher energies. Similarly, the secondary muons arriving at sea level, which are produced as a consequence of the interactions of the primary particles in the atmosphere, can be used in experiments to study their properties at energies above machine values.

1.2 The Primary Cosmic Radiation

It is now known that the primary cosmic radiation consists of about 86% protons, 13% helium nuclei, and 1% of other elements, and at energies above 10 GeV it arrives isotropically at the earth. The energy spectrum of the primary particles is very dependent on the particle energy. Greisen (1966) quotes an integral spectrum varying with the particle energy E, measured in eV, as

$$
\begin{aligned}
I(>E) &= 2.5 \times 10^{18}\, E^{-1.6} && && 10^{10}\text{eV} < E < 10^{15}\ \text{eV} \\
&= 5 \times 10^{27}\, E^{-2.2} && \text{m.}^{-2}\text{sec.}^{-1}\text{ster.}^{-1} && 10^{15}\text{eV} < E < 10^{18}\ \text{eV} \\
&= 4 \times 10^{16}\, E^{-1.6} && && 10^{18}\text{eV} < E
\end{aligned}
$$

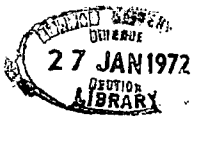

The low energy cut off depends on the geomagnetic latitude for the point of observation as the primary particles of low energy (a few GeV) are greatly effected by the earth's magnetic field. Consequently, there is a minimum energy for each point of observation below which particles cannot reach the earth. No high energy cut off has yet been determined though experimental difficulties arise due to the extremely low rate of particles having energies in excess of 10^{19}eV.

Direct measurements on the primary spectrum have been carried out using balloons and satellites up to energies of about 10^{12}eV. Above this value the primary intensity is small, being about 1.6×10^{-1} m.$^{-2}$sec.$^{-1}$ster.$^{-1}$ for $E > 10^{12}$ eV, with the integral spectrum having an exponent of - 1.6. The spectrum has been determined at these high energies by a study of the interactions of the primary particles and subsequent secondary particles in the atmosphere, which produce a large number of particles at sea level. This series of interactions results in the phenomenon known as an Extensive Air Shower (E.A.S.).

From a study of the arrival direction of the primary particles, their composition, time variation, and energy spectrum, some understanding of their origin and subsequent trajectory in space under the influence of the galactic magnetic field can be obtained.

1.3 Interactions in the Atmosphere by the Primary Particles

On passing through the earth's atmosphere, the primary cosmic rays interact with the nuclei of the air molecules to produce secondary particles. The primary protons interact, on average, every 80 gm cm.$^{-2}$ of the atmosphere and lose about 50% of their energy at each interaction. The secondary particles are mainly composed of pions with a smaller number of kaons, hyperons, and nucleons. The number of secondary particles, n, depends on the energy of the primary particle, E, and obeys to a good approximation the relation $n \propto E^{\frac{1}{4}}$ (Cocconi (1966), de Beer et al.(1966)).

The pions produced in the interaction exist almost equally in their three modes, π^+, π^-, and π^o. The neutral pions have a decay time at rest of about 10^{-16} sec. and each decays into two photons. The two photons then produce an electron photon cascade in the atmosphere. The number of electrons and positrons is increased by the photons from the decay of the other neutral pions produced in the interaction and by the electron photon cascades produced by π^o decay from the further interactions of the primary particle in the atmosphere.

For a primary energy of 10^{12} eV, the electron photon cascade is sufficiently large to reach sea level to produce an Extensive Air Shower. The shower is detected by the simultaneous arrival of a large number of particles over a large area and detectors placed at suitable points will record the shower as a coincident signal between several of the detectors. As the energy of the primary particle increases, the number of particles in the shower and the lateral extent of the shower increase and by measuring the number of particles in a shower an estimate of the primary energy can be made.

The charged pions and kaons produced by the interactions of the primary particle can either interact with an air nucleus to produce further pions or they can decay to produce muons. The decay probabilities of the pions and kaons are a function of their energy and zenith angle. For a given zenith angle, these particles have a greater probability of interacting than of decaying as their energy increases. As the zenith angle increases, the density of the region in which the pions and kaons of a given energy are produced at the same slant depth in the atmosphere decreases. Thus the interaction probabilities of the pions and kaons decrease as the zenith angle increases and hence a greater number of particles decay into muons. This results in the so called Sec θ enhancement in the intensity variation with zenith angle (θ).

The muons produced from pion and kaon decay are weakly interacting particles and have a high chance of reaching sea level without decay or

interaction. Hence a study of the spectrum and charge ratio of sea level muons will enable information to be obtained on the interactions in the atmosphere of the primary particles.

1.4 The Momentum Spectrum and Charge Ratio of Cosmic Ray Muons

1.4.1 Introduction

The muon momentum spectrum is an important datum of cosmic ray physics and experiments of increasing precision have been performed over a wide variety of zenith angles. The basic method of measurement has been that of direct measurement using magnetic spectrographs. The muons are deflected on traversing a magnetic field and a measurement of the deflection enables the momentum of the muon to be estimated. The direction of the deflection enables the charge of the muon to be found if the magnetic field direction is known. A survey of the recent major spectrographs used to measure the spectrum over a wide range of zenith angles is given in Chapter 2.

From the measured values of momenta, the spectrum and charge ratio, defined as the ratio of the intensities of positive to that of negative muons of a given momentum, can be determined. By comparing the behaviour of the spectrum and charge ratio as a function of the zenith angle it is possible to predict the ratio of kaons to pions produced in the interactions in the atmosphere. However, the analysis assumes a vertical spectrum which has only been measured to the required accuracy to a few hundred GeV/c in momentum. Consequently, the errors in the kaon to pion ratio increase rapidly above this momentum.

To reduce the statistical uncertainty in the ratio, the measurement of the vertical muon spectrum needs to be extended to momenta in excess of a few thousand GeV/c. The practical difficulties involved in an extension of the spectrum measurements to these values of momenta are discussed in Chapter 2.

1.4.2 Measurements of the Vertical Muon Spectrum and Charge Ratio

The results of several experiments to measure the vertical muon differential momentum spectrum using magnetic spectrographs are shown in figure 1.1.

The spectrum measured by Hayman and Wolfendale (1962) was obtained using an air gap magnet to deflect the muons and the trajectories were determined by four trays of neon flash tubes, two trays being placed above the magnet and two below the magnet. The more recent experiments of Baber et al. (1968a) and Allkofer et al. (1970) used solid iron magnets to deflect the muon. Baber et al. used four trays of neon flash tubes and Allkofer et al. six optical spark chambers to locate the trajectories of particles traversing the respective spectrographs. Further details of the spectrographs are given in Chapter 2.

An examination of the spectrum measurements in figure 1.1 show that there is an appreciable uncertainty in the spectrum above about 200 GeV/c due to the large experimental errors. The large errors are mainly due to the steepness of the spectrum at momentum values above 200 GeV/c producing a low rate of particles through the spectrographs with momenta greater than 200 GeV/c and the fact that the maximum detectable momentum, which is defined in §2.1, of each spectrograph has a value in this momentum region. These factors are discussed further in Chapter 2.

The variation in the charge ratio of vertical muons with momentum is shown in figure 1.2. The results were obtained by Baber et al. (1968b) and Allkofer et al. (1970) from a further analysis of the results for the spectrum measurements described above. The results of Aurela et al. (1966) were obtained using a modified form of the spectrograph used by Hayman and Wolfendale (1962) for their spectrum measurements. The large uncertainties in the measurements above 100 GeV/c produced by the low rate of particles in this momentum region is again seen in figure 1.2.

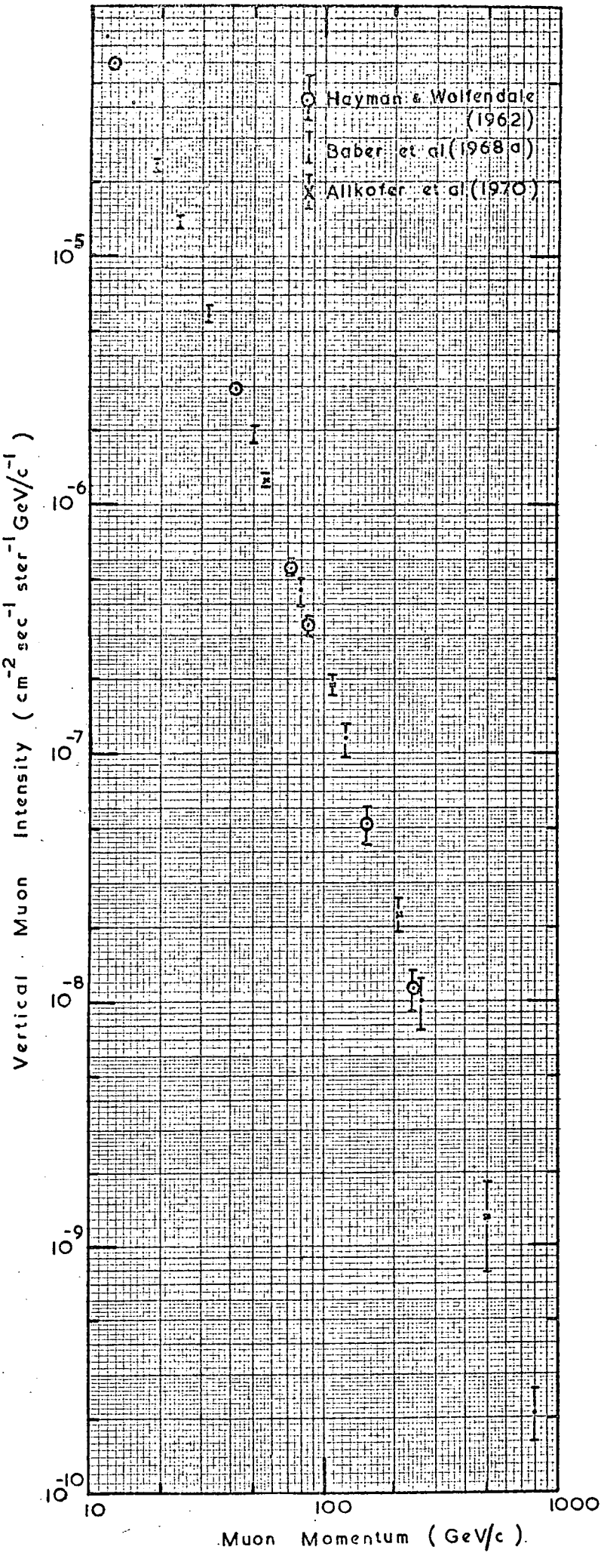

Figure 1.1 The Vertical Muon Differential Momentum Spectrum.

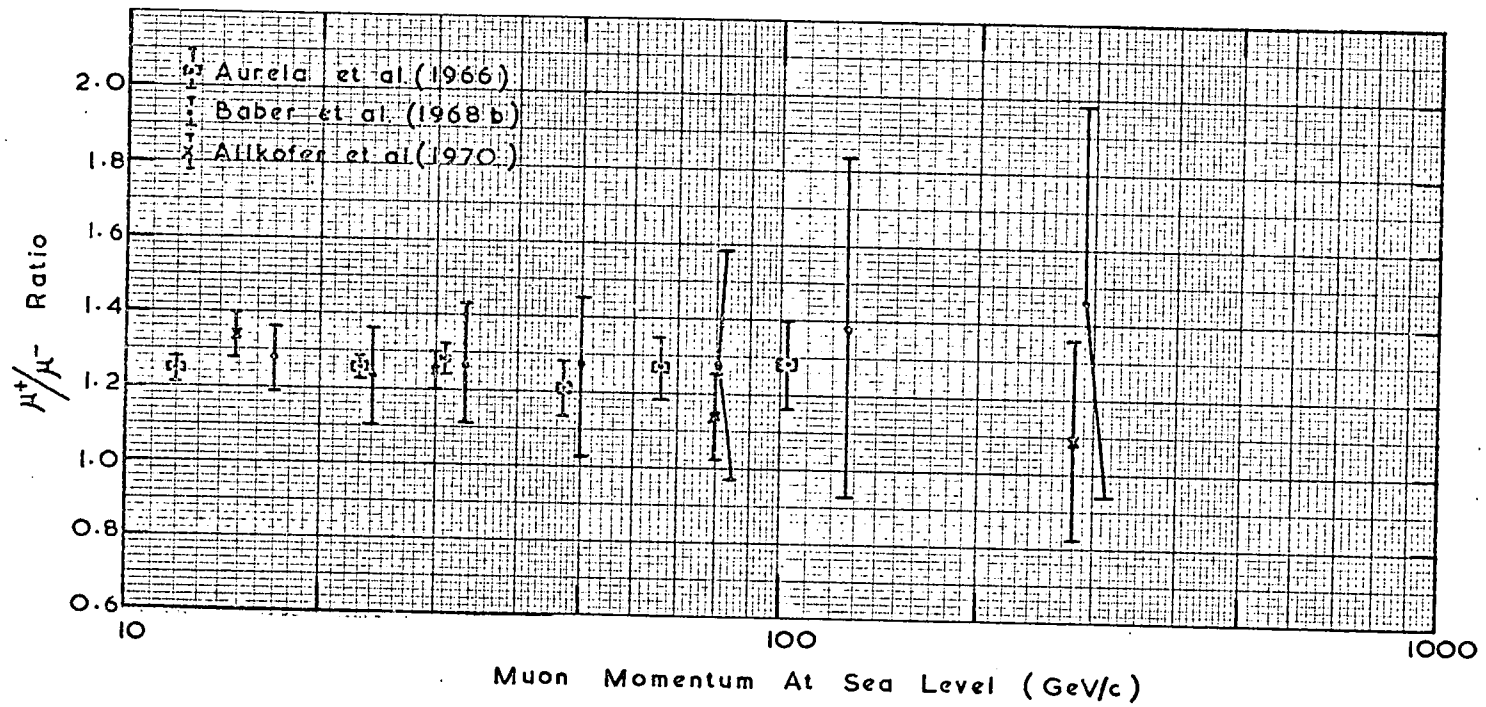

Figure 1.2 The Variation of the Charge Ratio of Vertical Muons with Momentum.

To extend the measurements of the spectrum and charge ratio up to momenta of a few thousand GeV/c using a magnetic spectrograph, the acceptance of the instrument will have to be sufficient to produce a reasonable rate of particles with momenta greater than a few thousand GeV/c. Also the maximum detectable momentum of the spectrograph is required to be at least in this momentum region. With such an instrument, the statistical uncertainties in the spectrum and charge ratio measurements in the hundred GeV/c region will be considerably reduced.

It should be pointed out that there are several indirect measurements of the spectrum in excess of momenta obtained with magnetic spectrographs. These include the measurement of the variation in the intensity of muons as a function of the depth underground (Miyake et al. (1964)) and the investigation of the electromagnetic interactions of high energy muons (Chin et al.(1970)).

With the first method, an analysis of the data gives an integral muon spectrum if the rate of energy loss with depth and energy is known. This however, brings some uncertainty into the results due to the fluctuation in the energy loss of the muon, and uncertainties in the behaviour of the energy loss expression and in the amount of matter traversed by the muon underground. Similarly, the second method also produces some uncertainty in that the interaction cross-section of high energy muons has to be assumed.

1.5 The Utah Experiment

A further indication of the necessity for a determination of the vertical spectrum to momenta of a few thousand GeV/c has come from the results of the University of Utah Underground Neutrino Detector as initially reported by Bergesson et al. (1967). The detector is built underground and utilises Cerenkov detectors and sonic spark chambers as particle detectors. In a study of the muon background with the detector, the muon intensity has been measured as a function of the slant depth and zenith angle.

Their results show that above an energy of about 1000 GeV there is no

increase in the intensity at a given slant depth and zenith angle when compared with the vertical intensity at the depth corresponding to the slant depth. This is in complete contradition to the expected results if the muons come from pion or kaon decay. Then an increase approximately proportional to Sec θ, where θ is the zenith angle, would have been expected.

A consequence of these results is that the majority of the muons, whose energies are above 1000 GeV, are not produced by pion or kaon decay. They are either produced directly in the primary particle-air nucleus collision or are the decay products of a particle which has a lifetime much less than the kaon lifetime. The process producing this isotropy has been given the name X-process.

The more recent results of the Utah group (Keuffel et al. (1970), Bergesson et al. (1971)) have suggested that the fraction of X-process muons is not as high as previously thought. The authors suggest that the fraction of X-process muons is about 2% compared to pions produced at the same energy. Also the isotropic component varies with muon energy such that it has a maximum contribution of about 50% to the vertical muon intensity in the energy range 1000 to 3000 GeV and subsequently decreases with increasing muon energy. These results will be reflected in the vertical muon momentum spectrum as an increase over that expected if the muons are produced by pion or kaon decay.

The Utah effect has not been found by Krishnaswamy et al. (1970) who have measured the angular distribution of underground muons in the Kolar Gold Mines in India. They find that their observations are consistent with the fact that the muons are produced from pion or kaon decay. However, possibly the most direct way of checking the Utah effect is to measure the vertical muon spectrum to energies in excess of a few thousand GeV using a magnetic spectrograph. Then, the results will not be effected by the errors associated with underground measurements.

1.6 The Present Work

A new spectrograph (M.A.R.S.) has recently been constructed in Durham which will be used to measure the momentum spectrum and charge ratio of muons

in the vertical direction. The spectrograph is connected on-line to a computer for analysis of the events.

The measurements will enable the spectrum to be analysed to momenta in excess of 5000 GeV/c. Particles with momenta between about fifty GeV/c and a few hundred GeV/c will be analysed automatically by the spectrograph equipment. The large rate of low energy particles (see Table 3.1) will enable the low energy spectrum to be determined with an accuracy of a few per cent over this region after a reasonable running time.

When the initial vertical measurements are completed, the spectrograph will be rebuilt in the near horizontal direction. After the spectrum and charge ratio measurements, the spectrograph will be a copious source of high energy muons which can be used in a variety of experiments.

The various components of the spectrograph are described in subsequent chapters but initially Chapter 2 gives a survey of the recent spectrographs and a brief outline of the theory of spectrograph measurements. Chapter 3 gives a general description of the instrument and basic details of the individual elements of the spectrograph, and in Chapter 4 a new technique for the digitisation of the flash tubes used in the spectrograph is described. Because of the high rate of low energy particles, a momentum selector is incorporated to detect so called high momentum events and is described in detail in Chapter 5. Chapter 6 describes the flash tube trays used to analyse a high momentum event and also discusses the electronic circuitry used for feeding digitised information pertaining to an event from the spectrograph to the computer for storage on a magnetic disc. In Chapter 7, the method of analysis of events together with the geometrical characteristics of the instrument are discussed. Finally, in Chapter 8 the present status of the work is discussed together with future plans.

CHAPTER 2

A Survey of Recent Cosmic Ray Spectrographs.

2.1 Introduction

Magnet spectrographs have been used extensively to measure the momentum spectra of cosmic ray muons. Measurements were originally carried out on the vertical spectrum using air gap electromagnets to deflect the muons. Spectrographs have since been constructed to measure the spectrum over a wide range of zenith angles.

Each spectrograph has a characteristic momentum above which errors in track location do not allow a good estimate of the true momentum of the particle to be made. The value of this momentum is known as the maximum detectable momentum (m.d.m.) of the instrument. The m.d.m. is defined as the momentum of that particle, the deflection of which is equal to the standard deviation of the error in the deflection. As an alternative, the most probable value of the error is sometimes used by workers to represent the error in the deflection. In this case, the m.d.m. is higher by the factor 1.483 than the m.d.m. using the standard deviation of the error if the error distribution is Gaussian. The formulae for determining the momentum of a particle from its deflection in a magnetic field are discussed in §2.2.

The acceptance of a spectrograph should also be sufficient to ensure that a reasonable rate of muons is obtained with momenta greater than the m.d.m. of the instrument. This enables the spectrum to be measured up to the m.d.m. with a comparatively short running time.

The acceptance is defined as the integral $\int_A \int_\Omega dA d\Omega$, where $d\Omega$ is the solid angle subtended by the area dA in the spectrograph, dA being taken at a convenient level in the spectrograph. The acceptance is then equal to the magnetic acceptance at the highest momenta, there being a reduction in acceptance as the momentum decreases due to the spectrograph's magnetic field. The acceptance is normally measured in units of cm^2 ster.

Air gap magnets have the disadvantage that the air gap must be quite small to ensure that a value of magnetic field is obtained which can produce a measurable deflection of muons with momenta of several hundred GeV/c. This generally results in an instrument having a small acceptance. It should be mentioned that air gap magnets can be larger if the electromagnet is especially designed for the purpose. In general, this results in an electromagnet with a high power consumption and the extra cost could outweigh the advantages. Several recent air gap spectrographs, for example Kasha et al. (1968) and Asbury et al. (1970), have used magnets which were originally designed to be used with particle accelerators or with bubble chambers. These magnets have then been used in further experiments on the cosmic ray muon flux and are discussed in §2.3.

The disadvantages of air gap magnets discussed above, have led to the development of solid iron magnets which can produce magnetic fields over a larger volume than conventional air gap magnets. This increases the line integral, $\int B\,dl$, where B is the flux density and l is measured along the track of a particle traversing the spectrograph when the track is projected on to a plane at right angles to the magnetic field direction. It will be shown in §2.2 that the angular deflection of the particle caused by the magnetic field is proportional to this integral. Thus the greater the line integral, the greater the angular deflection for a given momentum and hence the larger the m.d.m.

Solid iron spectrographs, however, do suffer from problems that arise due to multiple scattering in the iron. This will result in a flattening of the spectrum at high momentum due to the low momentum particles being scattered such that they seem to be of high momentum. The r.m.s. value of the angle of scatter, $\langle\theta\rangle$, when measured in the deflection plane, is given by the relation (Rossi and Greisen (1941))

$$\langle\theta\rangle = \frac{14.99}{\beta p} (\Sigma t)^{\frac{1}{2}} \text{ radians} \qquad 2.1$$

where p is the momentum of the particle in MeV/c and Σt is the total thickness

of matter traversed measured in radiation lengths. For a uniform magnetic field the magnetic deflection, ϕ, is given by the relation

$$\phi = \frac{k_1}{p} l \qquad 2.2$$

where k_1 is a constant and l is the length of the magnet. This formula is derived in §2.2.

Now, for an iron magnet, most of the matter traversed will be in the iron. So we have $\Sigma t = k_2 l$, where k_2 is a constant.

$$\text{Hence } \frac{\phi}{\langle\theta\rangle} \propto \sqrt{l} \quad \text{as } \beta \to 1 \qquad 2.3$$

Thus the signal to noise ratio increases as $\sqrt{l}$, implying the greater the thickness of iron traversed by the particles, the better is the spectrograph. For momentum spectrum measurements a correction has to be applied to the results to take into account the above scattering effects.

2.2 Derivation of the Deflection Equations used in Magnetic Spectrographs

Figure 2.1 shows the deflection of a charged particle of momentum p eV/c in the deflection plane, when the particle passes through a magnetic field of flux density B gauss. The deflection plane is at right angles to the magnetic field direction.

For a singly charged particle, the momentum (p) and radius of curvature (ρ) of the trajectory at any point are related to the magnetic flux density (B) by the equation:

$$p = 300\, B\rho \qquad 2.4$$

when p is measured in eV/c, B in gauss, and ρ in cm.

If there is no loss in momentum during the traversal of the magnetic field, then ρ is a constant and the trajectory is the arc of a circle. In practice the particle loses some momentum and a correction has to be applied, the magnitude of the correction depending upon the incoming energy and the amount of matter traversed by the particle.

From figure 2.1 $dl = \rho d\theta$ 2.5

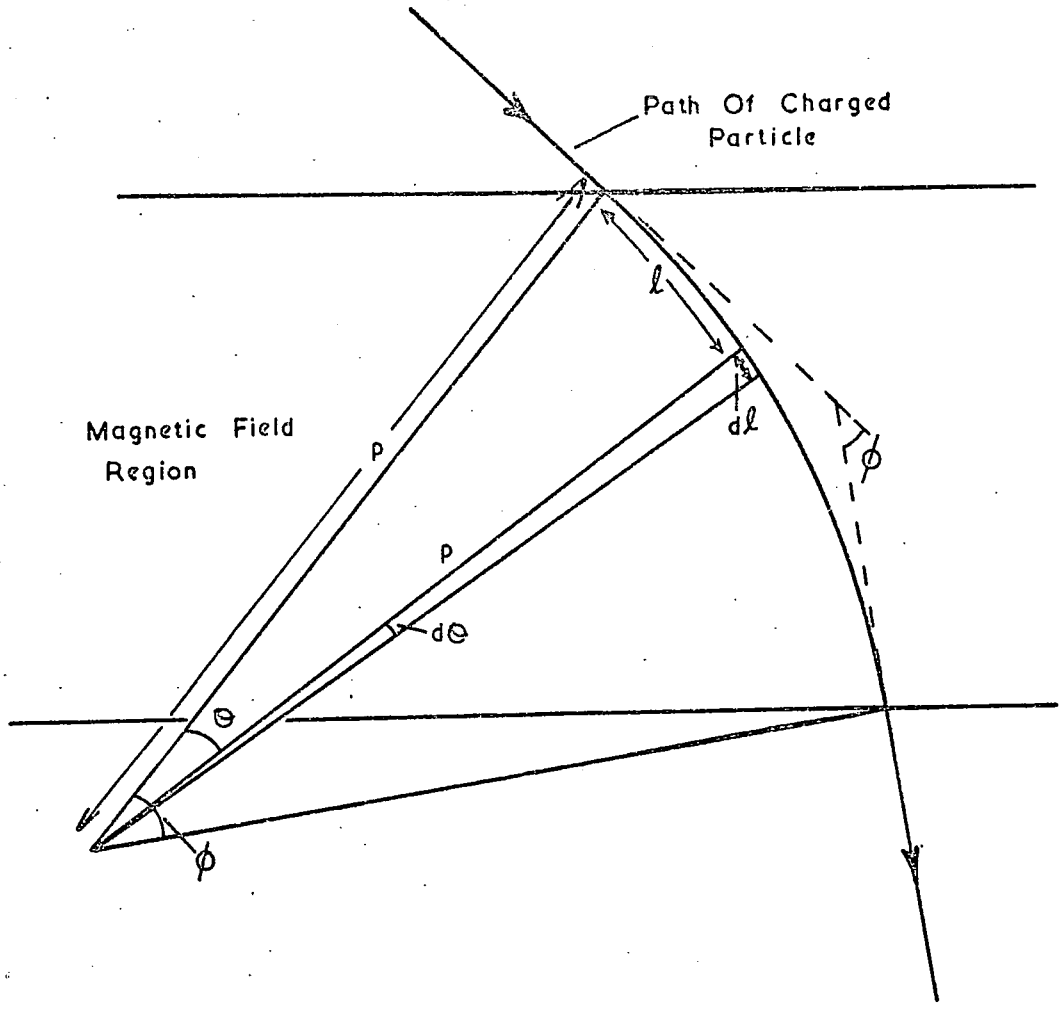

Figure 2.1 The Path of a Charged Particle in a Uniform Magnetic Field.

where θ is measured from the magnetic field entry point and l is the length of the trajectory in the magnetic field for the angle θ.

Substituting for ρ from equation 2.5 into equation 2.4 gives

$$p = 300B \frac{dl}{d\theta}$$

$$\text{or} \quad pd\theta = 300Bdl \qquad 2.6$$

The particle is deflected by an angle ϕ in the magnetic field as shown in figure 2.1.

Hence, from equation 2.6

$$\int_0^{\phi} p\, d\theta = 300 \int Bdl \qquad 2.7$$

If the momentum loss is small compared to the incident momentum, then p can be taken as constant and equation 2.7 becomes

$$p\phi = 300 \int Bdl \qquad 2.8$$

Equation 2.8 is used to determine the momentum of a particle in so called conventional spectrographs. In this type of spectrograph the angular deflection ϕ is measured by determining the trajectory of the particle before and after its passage through the magnetic field. The angular deflection is converted into a linear deflection when the deflections are measured at a suitable measuring level. Figure 2.2 shows the general arrangement of a conventional spectrograph. Several detecting levels are placed on either side of the magnetic field volume to determine the track of a particle. The types of detectors used in spectrographs are mentioned in §2.3 and §2.4.

Using the notation of figure 2.2, equation 2.8 becomes if ϕ is small

$$p \frac{\Delta}{d} = 300 \int Bdl$$

$$\text{or} \quad p\Delta = 300d \int Bdl \qquad 2.9$$

where d is the distance between the measuring levels.

Hence by measuring Δ, the momentum p can be determined from a knowledge of the spectrograph dimensions and magnetic flux density. If the magnetic field is uniform then the angular deflection is proportional to the length of the magnet.

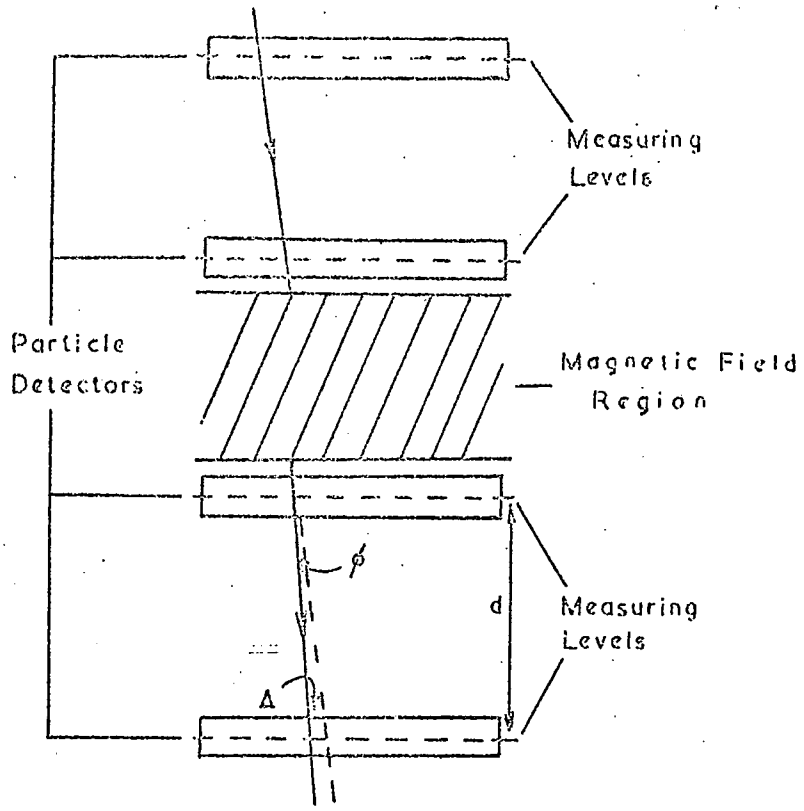

Figure 2.2 Schematic Form of a Conventional Spectrograph.

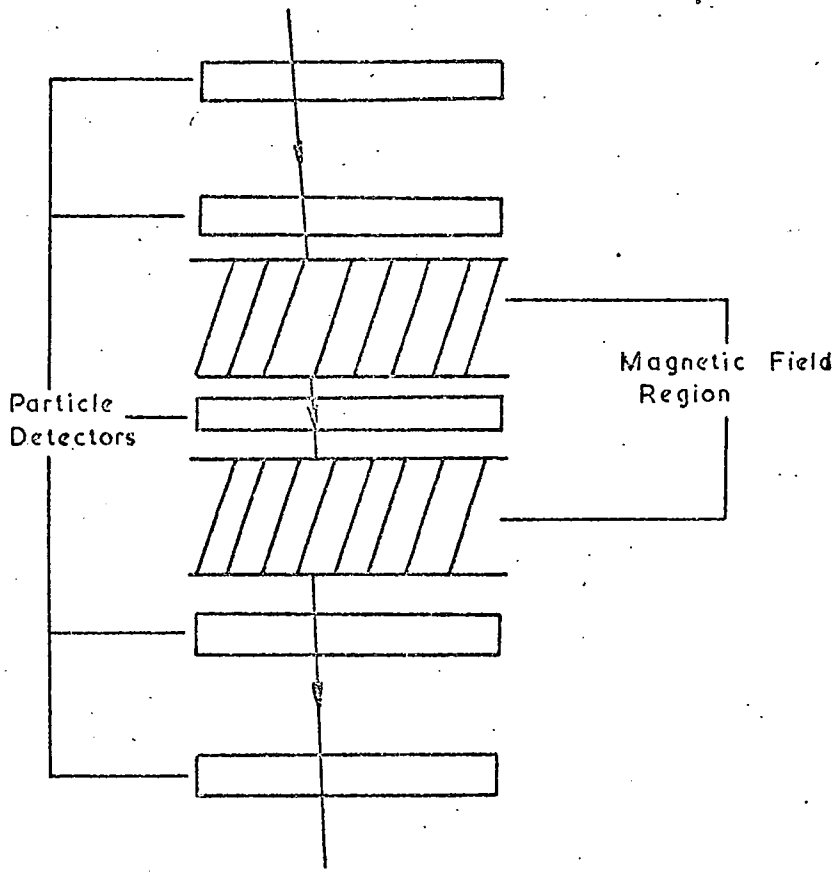

Figure 2.3 Schematic Form of a Multilayer Spectrograph.

In so called multilayer spectrographs, particle detectors are also placed in gaps in the magnetic field volume. Figure 2.3 shows the general arrangement of a multilayer spectrograph. The effect of the air gaps between the magnets has to be taken into account in the derivation of the momentum of a particle.

In order to compare the deflecting power of spectrographs, the value of $\int B dl$ is often quoted for the particular case of a trajectory passing normally through the magnet and having a small deflection. In this case the integral is taken as the product of the magnetic flux density and the magnet length and is normally measured in units of gauss cm. The values of this integral for several cosmic ray spectrographs are listed in Tables 2.1, 2.2, and 2.3.

For a uniform magnetic field equation 2.8 reduces to

$$p\phi = 300\, B \int dl \qquad 2.10$$

If the deflection is small then for a conventional spectrograph equation 2.10 becomes

$$p\phi = 300\, Bl \qquad 2.11$$

where l is the total length of the magnet which is equivalent to equation 2.2 if $k_1 = 300\, B$.

2.3 Air Gap Spectrographs

Table 2.1 lists the main air gap spectrographs built since 1950. Also shown are the main characteristics of each spectrograph. Several of the spectrographs are described in greater detail below.

Several spectrographs (Hyams et al. (1950), Caro et al. (1951), Brooke et al. (1962)) used Geiger counters as detecting elements. By analysing the triggered counters in the measuring levels, the deflection in terms of the Geiger counter widths could be found. The spectrum could then be found from a knowledge of the rates in the various counter width categories and the variation of the acceptance of the instrument with deflection.

TABLE 2.1

The Major Air Gap Spectrographs (Post 1950)

Authors	Location	m.d.m. (GeV/c)	Acceptance (cm^2 ster.)	Zenith Angle	$\int B.dl$ (gauss cm)	Detectors
Hyams et al. (1950)	Manchester U.K.	21	0.93	0°	6.5×10^5	G.M.
Holmes et al. (1961)		240	0.93	0°	5.97×10^6	G.M. and C.C.
Caro et al. (1951)	Melbourne, Australia	50	0.69	0°	$\sim 6.6 \times 10^5$ *	G.M.
Moroney and Parry (1954)		50	0.69	0°,30°,60°	$\sim 6.6 \times 10^5$ *	G.M.
Pine et al. (1959)	Cornell, U.S.A.	176	6.9	0°	$\sim 1.5 \times 10^6$ *	G.M. and C.C.
Pak et al. (1961)		120		0°,68°	$\sim 1.5 \times 10^6$ *	G.M. and F.T.
Brooke et al. (1962)	Durham, U.K.	18	8.0	0°	6.41×10^5	G.M.
Hayman and Wolfendale (1962)		443	8.0	0°	6.03×10^5	G.M. and F.T.
Coates and Nash (1962)	Nottingham, U.K.	29	0.73	0°,30°, 45°	1.07×10^5	G.M. and F.T.
Judge and Nash (1965a+b)		28	0.73	30°,45°, 60°,83°-90°	1.05×10^5	G.M. and F.T.
Kasha et al. (1968)	Brookhaven, U.S.A.	950	100	75°	1.64×10^6	S. and O.S.C.
Asbury et al. (1970)	Argonne, U.S.A.	830	500	75°,80°,85°	3.4×10^6	S. and O.S.C.
Flatté et al. (1971)	Stanford, U.S.A.	2000	570	60°-87°	3×10^6	S. and O.S.C.

* Estimated

Key: C.C. = Cloud Chambers
F.T. = Flash Tubes
G.M. = Geiger Counters
O.S.C. = Optical Spark Chambers
S. = Scintillation Counters

Figure 2.4 shows a diagram of the Manchester vertical spectrograph described by Hyams et al.(1950). The spectrograph consisted of two air gap magnets with Geiger counters placed as shown in figure 2.4. The deflection of a particle traversing the spectrograph was obtained by recording the Geiger counters which had discharged in the three measuring levels. The spectrograph was triggered by a five fold coincidence between a counter in each of the measuring levels and two counters at right angles to the counters in the measuring levels, which were situated in the air gaps of the two magnets. The discharged counters were indicated on a neon bulb hodoscope array which was photographed. By examining the discharged counters a deflection in terms of the counter numbers could be obtained.

Several of the spectrographs were modified to include further detectors which could define the track of a particle with greater accuracy. These secondary detectors were triggered only when the Geiger counters recorded a deflection in the lowest category and so the Geiger counters were being used as a form of momentum selector.

The m.d.m.'s of the spectrographs modified in this way consequentially increased. For example, Holmes et al. (1961) added three cloud chambers near to the three measuring levels of the Manchester spectrograph described above which were then used as the track locating detectors. This increased the m.d.m. of the spectrograph from 21 GeV/c to 240 GeV/c.

The form of the Durham vertical spectrograph described by Hayman and Wolfendale (1962) is shown in figure 2.5. The spectrograph was a modification of that described by Brooke et al. (1962). Four trays of neon flash tubes of internal diameter 5.9 mm and pressure 2.3 atmospheres were placed near to the four layers of Geiger counters shown in figure 2.5. A momentum selector was incorporated in the Geiger counter system and the flash tubes were triggered only when the deflection of the particle traversing the spectrograph was less than a certain value set by the momentum selector electronics. The events were photographed and the film scanned to determine the trajectories of the particles.

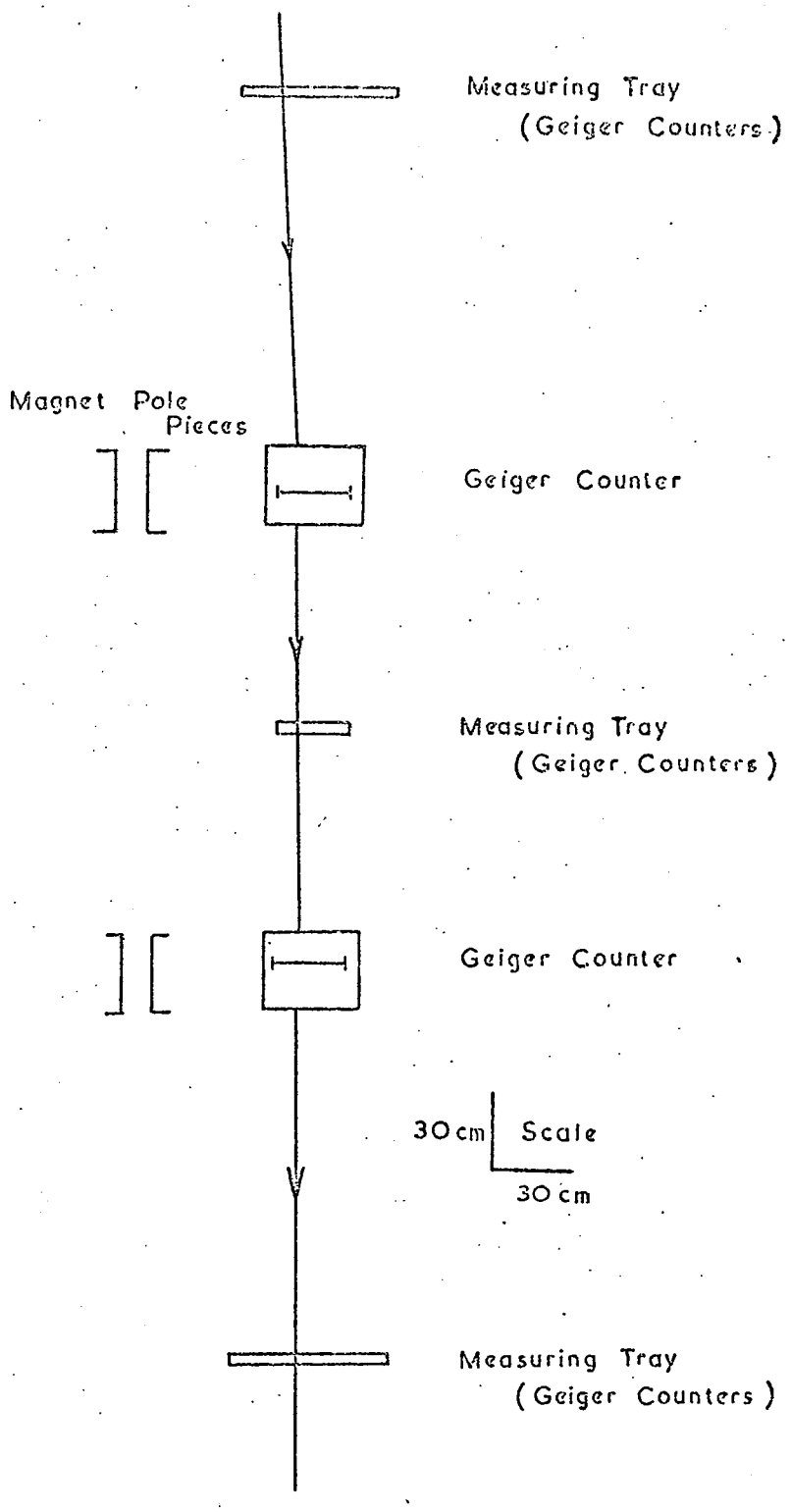

Figure 2.4 The Manchester Vertical Airgap Spectrograph Described by Hyams et al. (1950).

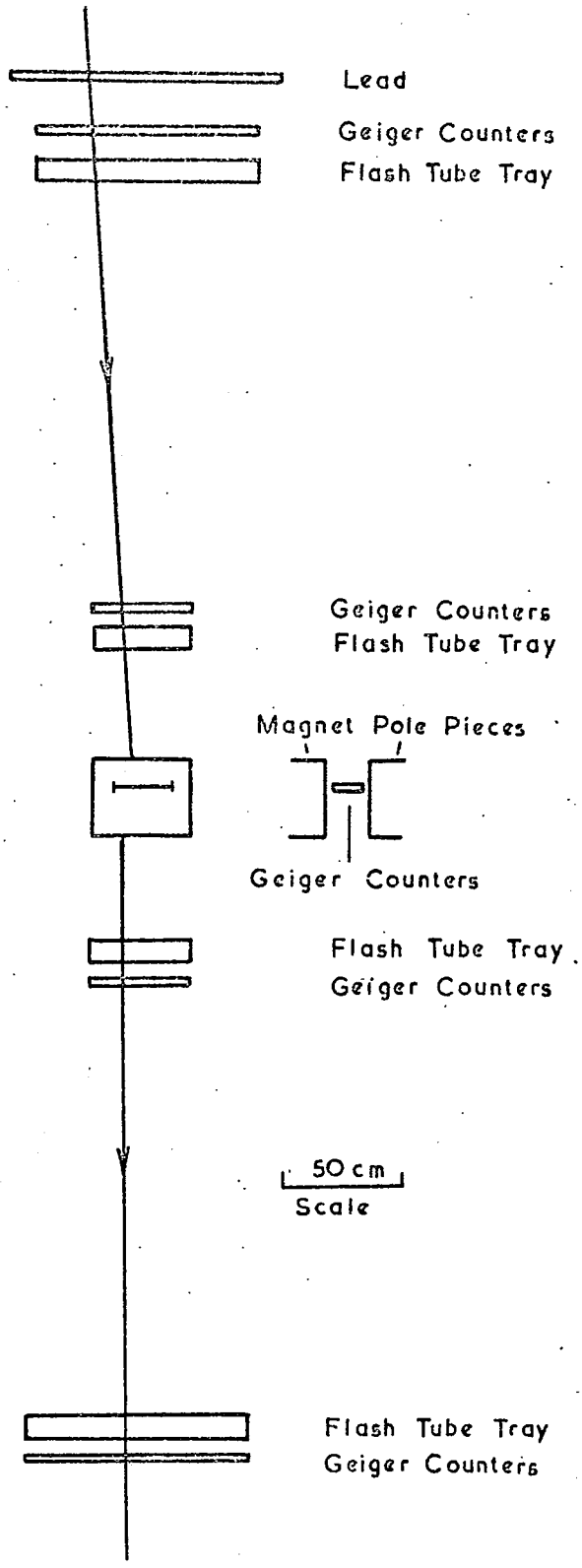

Figure 2.5 The Durham Vertical Airgap Spectrograph Described by Hayman and Wolfendale (1962).

The recent spectrographs of Kasha et al. (1968) and Asbury et al. (1970) used air gap magnets which had been used originally for accelerator experiments at the Brookhaven National Laboratory, U.S.A. and the Argonne National Laboratory,U.S.A. respectively. The sizesof these magnets are thus bigger than conventional cosmic ray magnets. The spectrographs used scintillation counters to detect the muon and optical spark chambers to locate the trajectory of the particle traversing the spectrograph. Scintillation counters have an advantage over trays of Geiger counters in that there is no dead space across the detecting level so the acceptance of the spectrograph is easier to calculate.

2.4 Solid Iron Spectrographs

Table 2.2 lists the main solid iron spectrographs built since 1960 together with their main characteristics. Further details of some of the spectrographs are described below.

Several of the spectrographs have been modified by using improved detecting systems. For example, the Durham spectrograph of Ashton and Wolfendale (1963) was subsequently modified (see Ashton et al. (1966)) by the addition of trays of neon flash tubes which were used to define the muon trajectory with greater accuracy. This resulted in the increase of the m.d.m. of the instrument from 40 GeV/c to 198 GeV/c.

Figure 2.6 shows a diagram of the modified spectrograph. The flash tubes used in the spectrograph had an internal diameter of 1.5 cm and contained commercial neon gas at a pressure of 60 cm of mercury. The spectrograph was triggered by a four fold coincidence in the Geiger counter trays ABCD used with two anticoincidence Geiger counter trays E and F placed above the spectrograph. These anticoincidence counters reduced the frequency of extensive air showers triggering the arrangement. A high voltage pulse was applied to the flash tubes when a trigger pulse was obtained from the Geiger counter coincidence system. The flash tubes were then photographed and the

TABLE 2.2

The Major Solid Iron Spectrographs

Authors	Location	m.d.m. (GeV/c)	Acceptance (cm^2 ster.)	Zenith Angle	$\int B.dl$ (gauss cm)	Detectors
Kamiya et al. (1962)	Nagoya, Japan	~100		75°-90°	~4 x 10^6*	S. and F.T.
Ashton and Wolfendale (1963)	Durham, U.K.	~ 40		80°	9.8 x 10^5	G.M.
Ashton et al. (1966)		198	30	77.5°-90°	9.82x 10^5	G.M. and F.T.
Bull et al. (1965)	Nottingham, U.K.					
Baber et al. (1968a+b)		360	18.6	0°	2.63x 10^6	G.M. and F.T.
Mackeown et al. (1966)	Durham, U.K.	1045		82.5°- 90°	1.95 x 10^6	G.M. and F.T.
Aurela and Wolfendale (1967)		270	13	0°	8.2 x 10^5	G.M. and F.T.
Alchudjian et al. (1968)	Mount Aragatz, U.S.S.R.	~3000	105	83°-90°	3.65 x 10^6	G.M. and W.S.C.
Palmer and Nash (1969)	Nottingham, U.K.	420		80°	1.90 x 10^6	G.M. and F.T.
Flint and Nash(1970)		428		80°	1.87 x 10^6	S. and F.T.
Nandi and Sinha (1970)	Durgapur, India	560	11.7	0°	3.24 x 10^6	G.M. and F.T.
Fugii et al. (1969)	Nagoya, Japan	1280	85	79°- 90°	3.5 x 10^6	S. and F.T.
Allkofer et al. (1970)	Kiel, W. Germany	~1000	16	Variable	3.2 x 10^6	S. and O.S.C.

* Estimated

Key: F.T. = Flash Tubes
G.M. = Geiger Counters
O.S.C. = Optical Spark Chambers
S. = Scintillation Counters
W.S.C. = Wire Spark Chamber

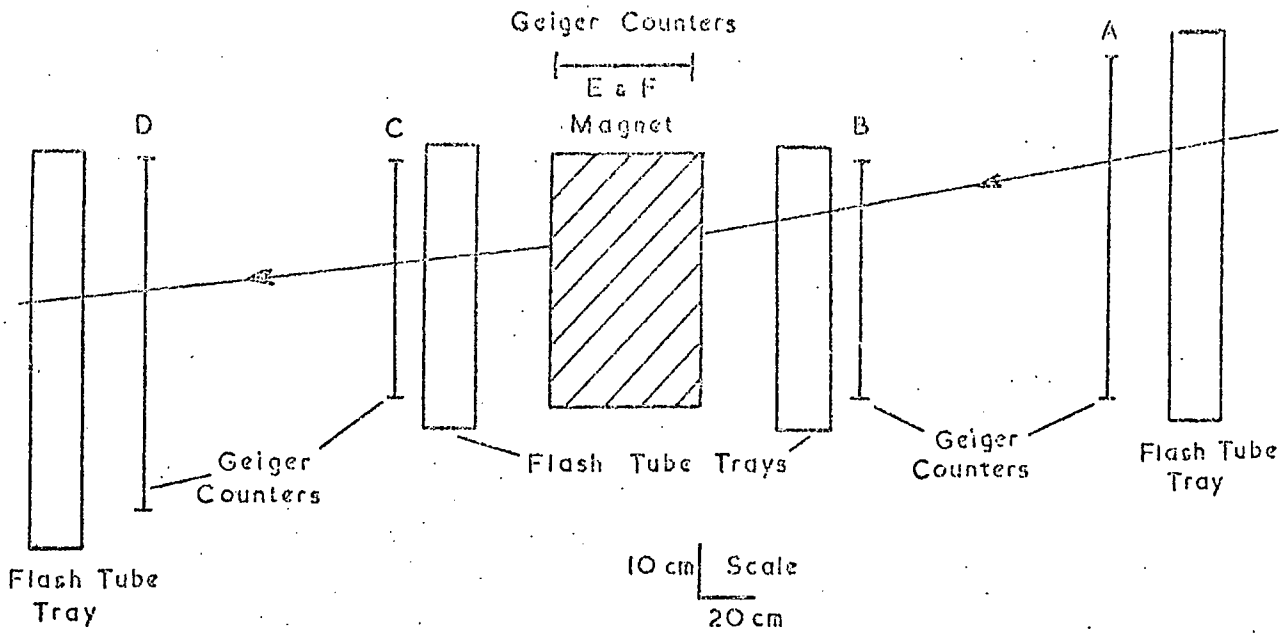

Figure 2.6 The Modified Durham Horizontal Solid Iron Spectrograph Described by Ashton et al. (1966).

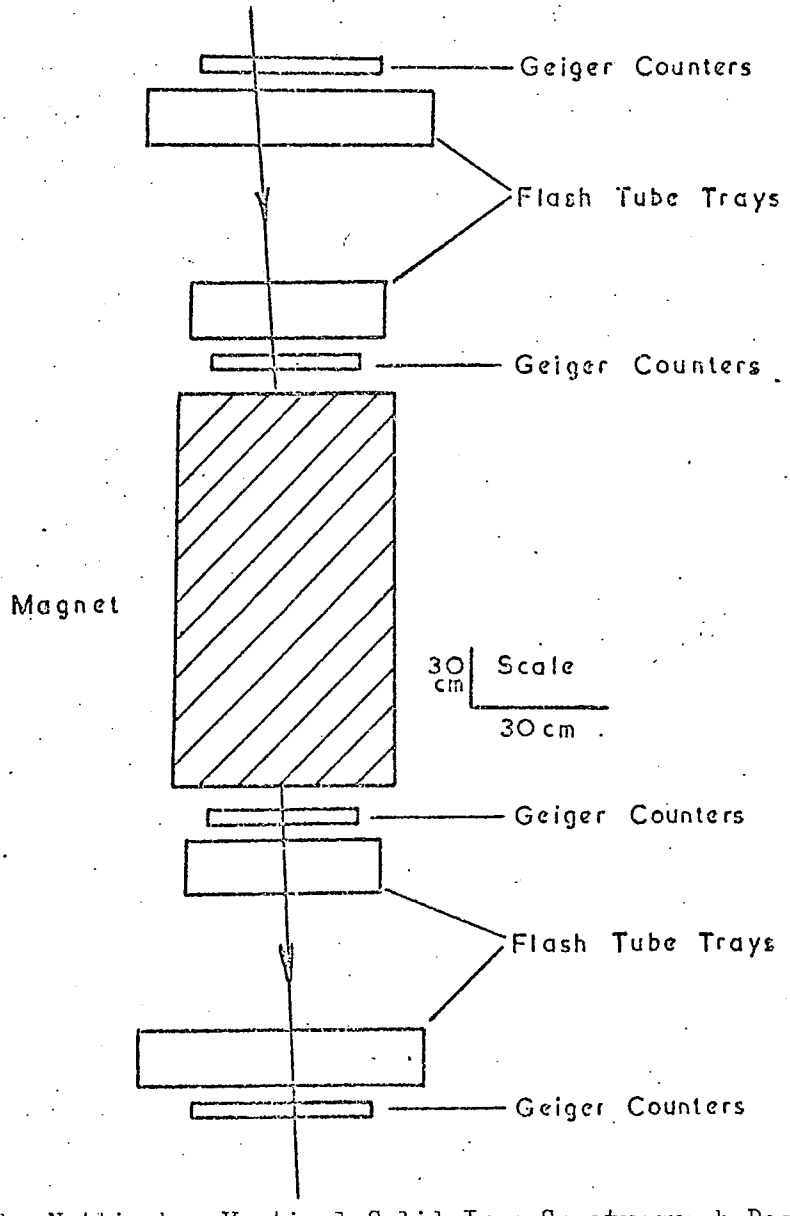

Figure 2.7 The Nottingham Vertical Solid Iron Spectrograph Described by Bull et al. (1962).

film scanned to determine the trajectories of the particles. The spectrograph was built in the near horizontal direction and accepted particles in the zenith angle range 77.5° - 90°.

The Nottingham vertical spectrograph described by Bull et al. (1965) is shown in figure 2.7. Trays of Geiger counters were used to detect the particle traversing the spectrograph and the trajectory was located by trays of neon flash tubes. The spectrograph was used by Baber et al. (1968a + b) to measure the momentum spectrum and charge ratio of vertical muons; their results are shown in figures 1.1 and 1.2 for the vertical spectrum and charge ratio respectively.

The spectrographs listed in Table 2.2 have enabled measurements of the muon spectrum to be undertaken over a wide range of zenith angles. However, although solid iron spectrographs have normally larger values for the m.d.m. than air gap spectrographs, the acceptances in most cases are still relatively small. This results in a low particle rate above the m.d.m. of the instrument and hence uncertainty of the spectrum near to the m.d.m.

2.5 Large Spectrographs under Construction or Design

The results of Bergeson et al. (1967), which were described in §1.5 have stimulated the design of spectrographs having m.d.m's of greater than several thousand GeV/c and also large acceptances. The spectrographs now under construction or design are shown in Table 2.3. The Durham spectrograph, M.A.R.S., is included in the table for comparison, though a more detailed list is given in Table 3.1. These spectrographs are described briefly below.

Adair, Kasha and colleagues (Kasha, 1971, private communication) are building a joint Yale University-Brookhaven National Laboratory spectrograph at Brookhaven, U.S.A. The spectrograph consists of a solid iron magnet, supporting two arms, each of which holds two scintillation counter hodoscope arrays and three optical spark chambers. The spectrograph is contained in a steel framework which enables it to be rotated to any required zenith angle.

TABLE 2.3

Large Spectrographs Under Construction or Design

Authors	Location	m.d.m. (GeV/c)	Acceptance (cm^2 ster.)	Zenith Angle	$\int B\,dl$ (gauss cm)	Detectors
Adair et al.	Brookhaven, U.S.A.	>2000	150	Variable	4.48×10^6	S. and O.S.C.
Masek et al.	San Diego, U.S.A.	~4500	3000	Variable	3×10^6	S. and W.S.C.
Cousins et al. (1970)	Nottingham, U.K.	~3000	120	0^o	2.7×10^6	G.M. and F.T. (Vidicon Camera)
Reines et al.	Irvine, U.S.A.	~15000	2500	90^o	1.8×10^6	S. and W.S.C.
Allkofer et al.	Tel Aviv, Israel	~7000	1466	85^o	4.8×10^6	S. and W.S.C.
(M.A.R.S.)	Durham, U.K.	~6000	818	0^o	8.09×10^6	S. and F.T. (Digitised)

Key: F.T. = Flash Tubes
G.M. = Geiger Counters
O.S.C. = Optical Spark Chambers
S. = Scintillation Counters
W.S.C. = Wire Spark Chambers

A momentum selector is incorporated in the spectrograph by using three of the four scintillation counter arrays. The hodoscope arrays consist of a plane of scintillation counters and a coincidence pulse between counters at the three levels for which the deflection is apparently a straight line causes the six spark chambers to be pulsed. The spectrograph has been built and is currently under test.

Masek and co-workers at the University of California in San Diego, U.S.A., are testing a solid iron spectrograph which has been designed to operate over a wide variety of zenith angles. The spectrograph will use four wire spark chambers with magnetostrictive readout, two of which are placed on either side of the magnet.

The new Nottingham spectrograph (Cousins et al. (1970)) is a modification of the spectrograph described by Bull et al. (1965). The Geiger counters and flash tube trays of the original spectrograph (figure 2.7) have been modified and the distances from the magnet increased. This has resulted in an increased m.d.m. and acceptance of the instrument. The flash tubes will not be photographed on film in the conventional way but instead will be photographed by a vidicon camera, whose photocathode is scanned to find the tubes which flashed. This method of obtaining information from an array of flash tubes is described by Harrison and Rastin (1970) and discussed further in §4.8.5.

At the University of California in Irvine, U.S.A., Reines and colleagues are building a prototype spectrograph which is approximately one third the size of the spectrograph in Table 2.3. This prototype spectrograph will be used in the near horizontal direction and will have a m.d.m. of 6000 GeV/c and an acceptance of 480 cm^2ster. After tests on this smaller spectrograph, work will begin on building the large spectrograph.

Design studies are being carried out on a multilayer spectrograph to be built by the Universities of Tel Aviv, Israel and Kiel, W. Germany (Allkofer, 1971, private communication). The spectrograph will be built in Tel Aviv and will consist of six magnet blocks of size 3.7m. x 1.8m. x 0.5m. The traversing particles will be detected by scintillation counters, and wire

spark chambers with magnetostrictive readout, which will be placed at the two ends of the spectrograph and in the gaps between the magnet blocks, will be used for the trajectory determination of a particle. The spectrograph will initially be used for the study of near horizontal particles.

CHAPTER 3

M.A.R.S. : The General Features of the Instrument

3.1 Introduction

The form of the Durham Magnetic Automated Research Spectrograph (M.A.R.S.) is shown in the scale diagrams of figures 3.1 and 3.2, which show the front and side views of the instrument respectively, and Plates 1 and 2, which show the spectrograph and the spectrograph electronics respectively. As can be seen from figures 3.1 and 3.2, it basically consists of four magnet blocks, blocks A, B, C, and D, each block containing 78 iron plates of thickness $^5/_8$" and having an overall size of approximately 3.66m x 2.13m x 1.24m. A magnetic field of approximately 16 kilogauss is produced in each block when an electric current of about 50A. is passed through the energising coils of the blocks. This magnetic field is discussed in §3.2.3.

Between the blocks are placed scintillation counters and trays containing neon flash tubes as shown in figure 3.1. The scintillation counters are used to detect particles traversing the spectrograph and the flash tubes to determine the trajectories of the particles. The spectrograph is symmetric about a vertical plane through its centre, parallel to the two larger sides, so as to utilise a large part of the uniform field region of the magnet. This vertical plane is the plane AA' in figure 3.1 and it makes an angle of 27° East of Geomagnetic North. For the purpose of discussion the two sides of the spectrograph are known as the Red and Blue sides and these are the Western and Eastern sides of the spectrograph respectively. The main characteristics of the instrument are listed in Table 3.1. Also included in Table 3.1 are the particle rates originally expected in the spectrograph, estimated from the vertical muon integral spectrum of Hayman and Wolfendale (1962).

Because of the extremely large rate of low momentum particles passing through the spectrograph (see Table 3.1), a momentum selector has been designed and incorporated in the spectrograph, based upon trays of neon flash tubes.

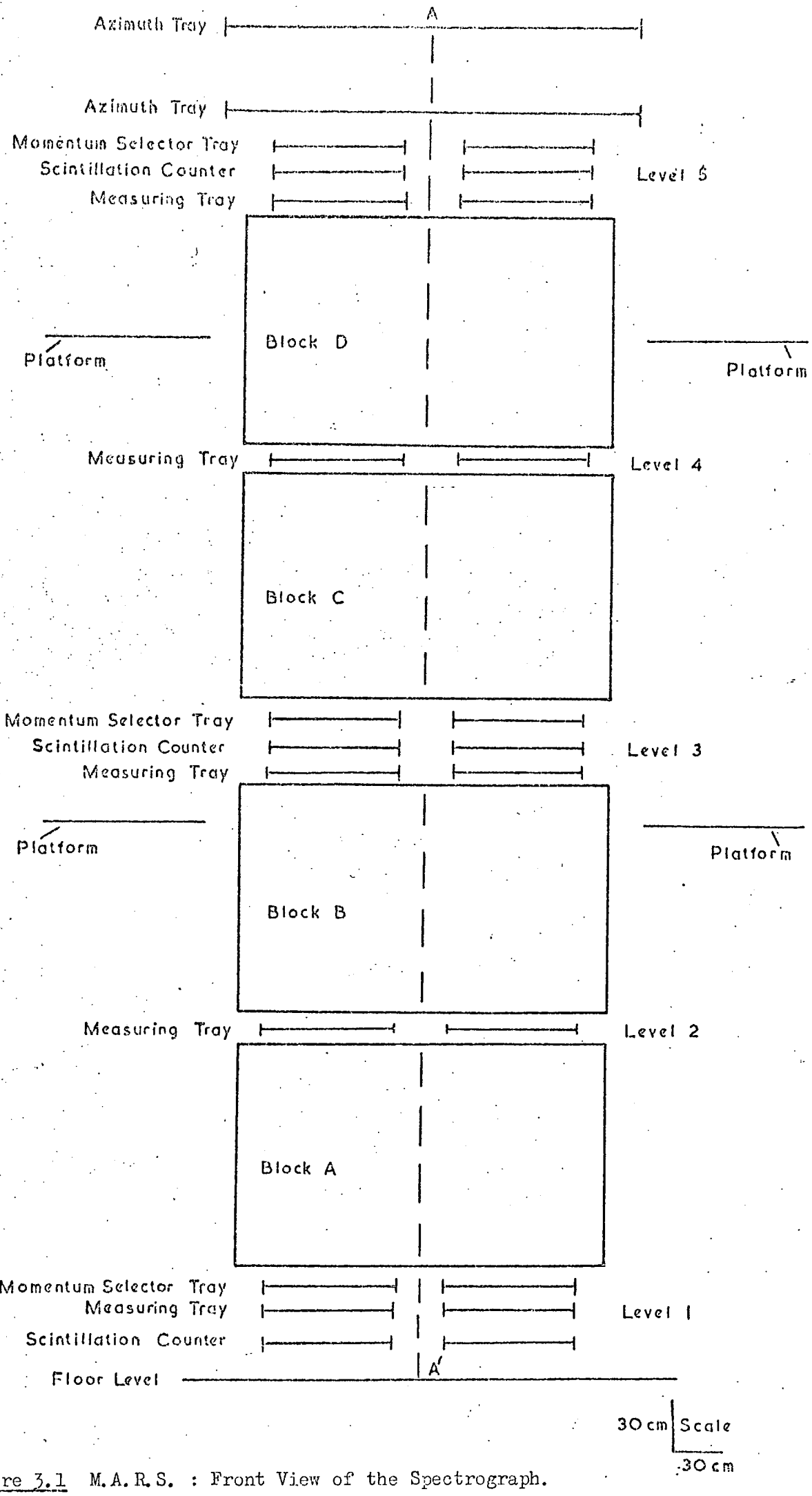

Figure 3.1 M.A.R.S. : Front View of the Spectrograph.

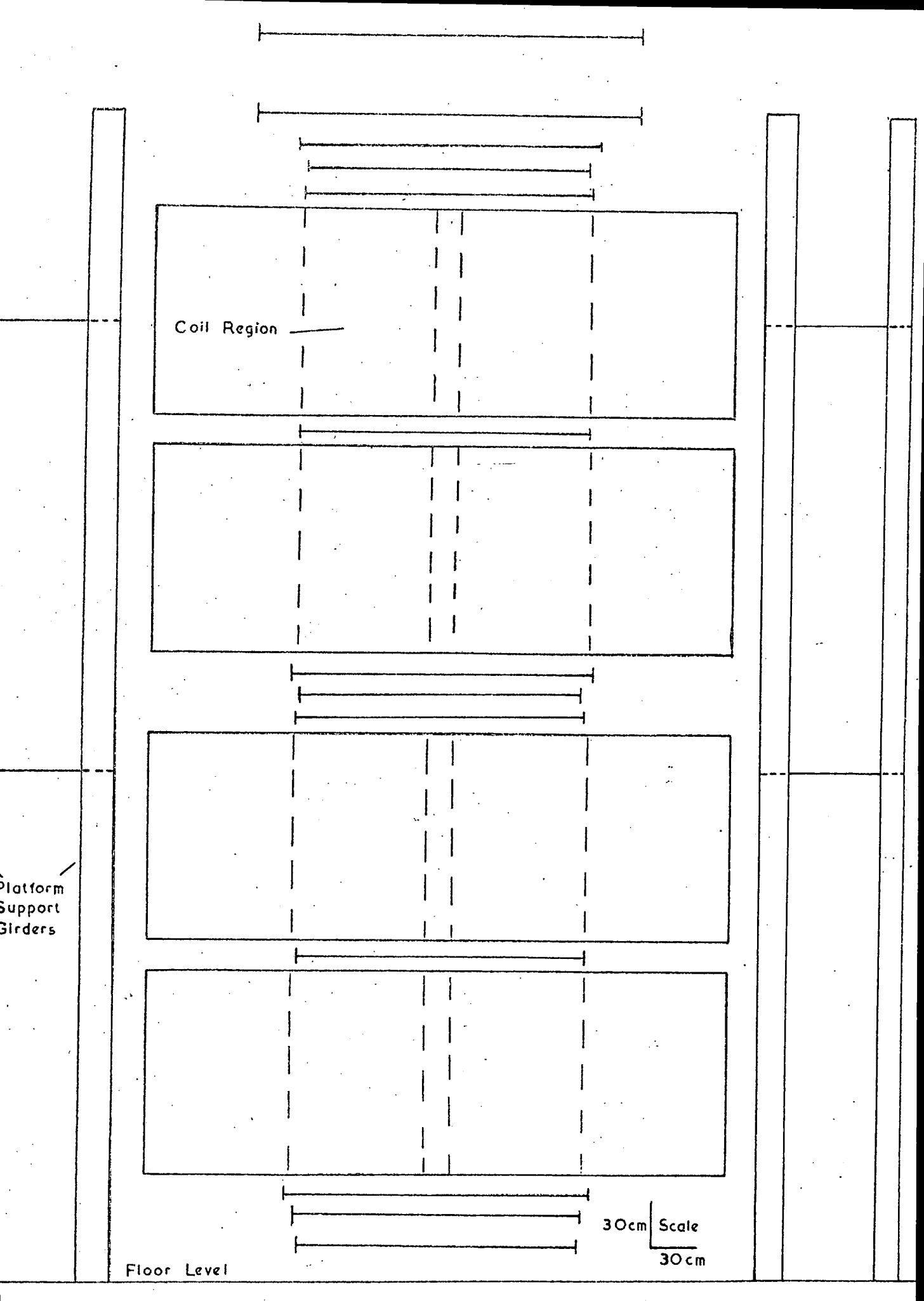

Figure 3.2 M.A.R.S. : Side View of the Spectrograph.

TABLE 3.1

M.A.R.S. : The Main Characteristics of the Instrument

Dimensions of a Magnet Block	3.66m x 2.13m x 1.24m
Weight of a Magnet Block	71 tons
Overall Height	7.62m
Acceptance	818 cm^2 ster.
Angular Range (neglecting magnetic deflection and multiple scattering)	
(i) Deflection Plane	$\pm 7^\circ$
(ii) Rear Plane	$\pm 15.5^\circ$
Magnetic Flux	16.3 $\pm$ 0.1 kilogauss
$\int$ Bdl	8.09×10^6 gauss cm
$\frac{<\theta> \text{ scatt}}{\phi \text{ mag}}$	~0.12
Minimum Detectable Momentum	6.9 GeV/c
Maximum Detectable Momentum	~ 6000 GeV/c

Momentum Selector Efficiencies (for Vertical Incident Particles)

Momentum = 220 GeV/c Efficiency = 0%

Momentum = 560 GeV/c Efficiency = 100%

Expected Rates through each side of the Spectrograph using Integral Spectrum of Hayman and Wolfendale (1962), (Magnetic Flux Density = 16.3 k gauss, no paralysis)

Momentum (GeV/c)	Rate
> 50	63.6 $hr.^{-1}$
> 100	14.8 $hr.^{-1}$
> 200	3.1 $hr.^{-1}$
> 500	7.8 day^{-1}
>1000	1.3 day^{-1}

The flash tube trays used in the momentum selector are called Momentum Selector Trays and are situated in the spectrograph as shown in figure 3.1. The trays each contain four layers of flash tubes of length 2m. The tubes have a mean internal diameter of 1.53 cm and contain commercial neon gas at a pressure of 60 cm of mercury.

Further trays of eight layers of small diameter flash tubes are located in the spectrograph at the positions shown in figure 3.1. These trays are called Measuring Trays and are used to determine the trajectory of certain particles, which, as will be explained below, are known as high momentum particles. The flash tubes used in the Measuring Trays are 2m. long, have a mean internal diameter of 5.55mm, and contain commercial neon gas at a pressure of 2.4 atmospheres.

Both the flash tubes in the Momentum Selector Trays and Measuring Trays are digitised using the technique discussed in Chapter 4. More detailed descriptions of the Momentum Selector Trays and Measuring Trays are given in Chapter 5 and Chapter 6 respectively.

The Momentum Selector Trays are used in conjunction with an electronic device, which is described in Chapter 5, to determine whether a particular particle traversing the spectrograph is of relatively high momentum. This device together with the Momentum Selector Trays constitute the Momentum Selector. A so called high momentum event could be detected by the Momentum Selector if the momentum is greater than about 200 GeV/c, the efficiency of the Momentum Selector varies from zero at about 220 GeV/c to 100% at about 560 GeV/c for particles incident in the vertical direction as explained in §7.2.

If a high momentum event is flagged from the Momentum Selector, the digitised information from the Measuring Trays on the triggered side is fed into a Mullard core store, which can hold 1024 8 bit words. Also held in the core store is digitised information of the event number, time of the event, date, magnet current and field direction, trigger mode of the event, and

atmospheric pressure. The contents of the core store are then transferred via an I.B.M. 1130 computer to a magnetic disc store. The event is processed by the 1130 computer when required. The computer is also used by the High Energy Nuclear Physics group to control the on-line scanning of bubble chamber film.

The majority of the triggering particles, being of low momentum, are analysed by the Momentum Selector in conjunction with a specially built digital device known as the Restricted Use Digital Instrument (R.U.D.I). This device calculates the deflection of the particle recorded by the Momentum Selector and stores the deflection in digital form on a 400 channel pulse height analyser (P.H.A.). This device is discussed further in §5.10.

Two transverse trays of digitised flash tubes are placed at the top of the spectrograph as shown in figure 3.2. These trays enable an estimate to be made of the entry angle of each particle in the back plane of the spectrograph to $\pm 0.5^{\circ}$. The trays are called the Azimuth Trays and use 2.5m. long flash tubes of the same diameter and pressure as the flash tubes used in the Momentum Selector Trays. The information in these trays is stored on the computer disc whenever a high momentum event is flagged, irrespective of the side through which the particle passed. A more detailed account of the Azimuth Trays is given in §6.7.

Access to each level of the spectrograph is obtained by a two storey platform supported by ten steel girders of length 23' as shown in figures 3.1 and 3.2, which is constructed around the four sides of the spectrograph.

The flash tube trays and scintillation counters in both sides of the spectrograph rest on $\frac{1}{2}$" steel rollers, which fit into bearings fixed in the magnet block supports. This facilitates ease of movement of the various components into their correct position in the spectrograph. The Azimuth Trays are placed in a framework made of 6" x 3" x $\frac{1}{4}$" steel channel, which rests on the top of the supports for the components of level 5. The trays rest in the channel and can be moved into their correct positions as they are easily accessible compared to the rest of the flash tube trays and scintillators in the spectrograph.

3.2 The Magnet

3.2.1 Construction of the Magnet

Because of the large weight of the magnet, supports, and detectors (over 300 tons), the magnet was constructed on a specially designed base. The floor of the laboratory is made from wooden blocks 1" thick mated together over 2" of cement and packing. Below this packing is a layer of reinforced concrete 5" thick. The wooden blocks and packing were removed and a webbing of 8" x 8" steel girders were mated into the concrete. The supports for the magnet were placed in position on top of the girders and welded to the girders.

Each magnet block consists of 78 iron plates. Each plate weights 18 cwt. and figure 3.3 shows the plan view of a plate. The plates were made and cut to the required size with a tolerance of $^{1}/_{16}$" (1.6mm) on the length and width by the British Steel Corporation works at Consett. The plates are made of low carbon content steel and Table 3.2 shows the chemical constitution of the plates. The corners of the slit cut out of each plate are rounded following the results of Bennett and Nash (1960) who found that rounded corners increased the field uniformity.

TABLE 3.2

Chemical Constitution of the Iron used in the Magnet

Element	C	S	P	Mn	Si	Cr	Ni	Cu	Sn	Fe
% by weight	.082	.028	.073	.370	.018	.011	.024	.030	.003	99.361

The magnet was constructed one block at a time. The plates comprising the first block, block A, were stacked on top of one another. Two plumb-lines were used to facilitate ease of stacking the plates vertically. Two of the edges of the slit cut in each plate were used as the reference lines for the plumb-lines.

When the required number of plates for the first block had been stacked, the coils were wound on the block. The coils are made from 4 S.W.G. copper wire

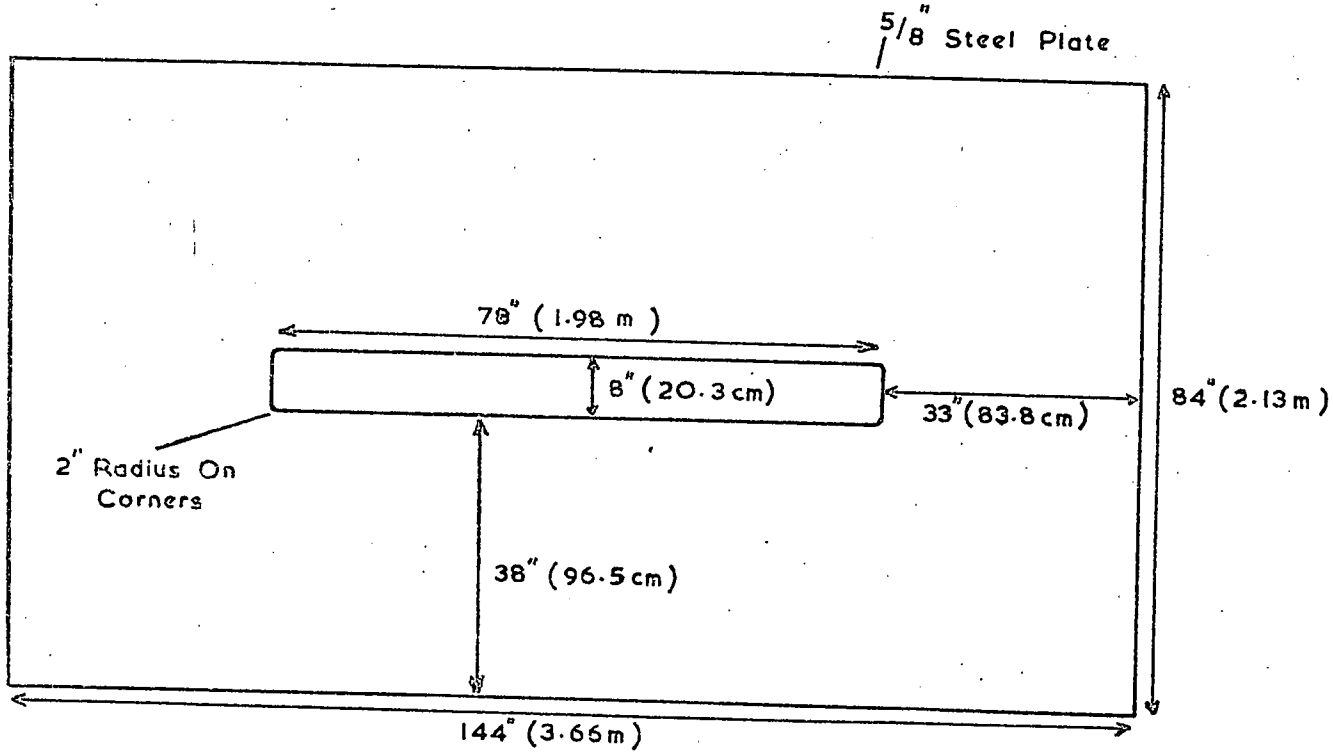

Figure 3.3 Plan View of a Magnet Plate.

(ϕ = 5.9mm), there being 184 turns on each side of the block. The coils are held in position by wooden formers placed at each of the four corners. Slits were machined in the formers, of width and depth equal to the wire diameter, into which the wire fitted. The wire was wound on to the block using the procedure described below.

About 20 turns of wire were wound loosely around the block off the wire drum. The wire was then wound tightly round the block one turn at a time starting at the end of the wire furthest from the wire drum. The slack was taken up on the drum as the number of turns was increased.

When the 20 turns had been wound on the block, the wire was cut and a further 20 turns wound loosely on to the block. The ends of the wire were joined by a brass ferrule into which the two wires were soft soldered. The process was repeated until one side had been completed. The opposite side of the magnet was wound in the same way and the two sides connected in series.

To keep the wires taut and parallel, string was looped between the coils at three points on each of the four sides of the turns. Plate 3 shows part of the first magnet block, block A, during the winding of the coils, the wooden formers and the loose turns of wire can easily be seen. To prevent the coils touching the block, sheets of elephant hide were placed between the coils and the block.

When the first magnet block was completed, the supports for the next block, block B, were placed on top of the first block and welded into position. The gap between the first and second blocks is only 7" . To make the coil winding easier, the second block was built on a packing of steel plates at the four corners of the block such that the gap was about 20" . After the block had been built and the coils wound, the packing was slowly removed with the help of two twenty-ton jacks and the block placed on to its supports. This packing procedure was also used on block D as the gap between it and the lower block is also 7" . The gap between blocks B and C is 19" so block C was built on to its supports without any packing.

PLATE 3

View of the Magnet Block A during the Winding of the Coils.

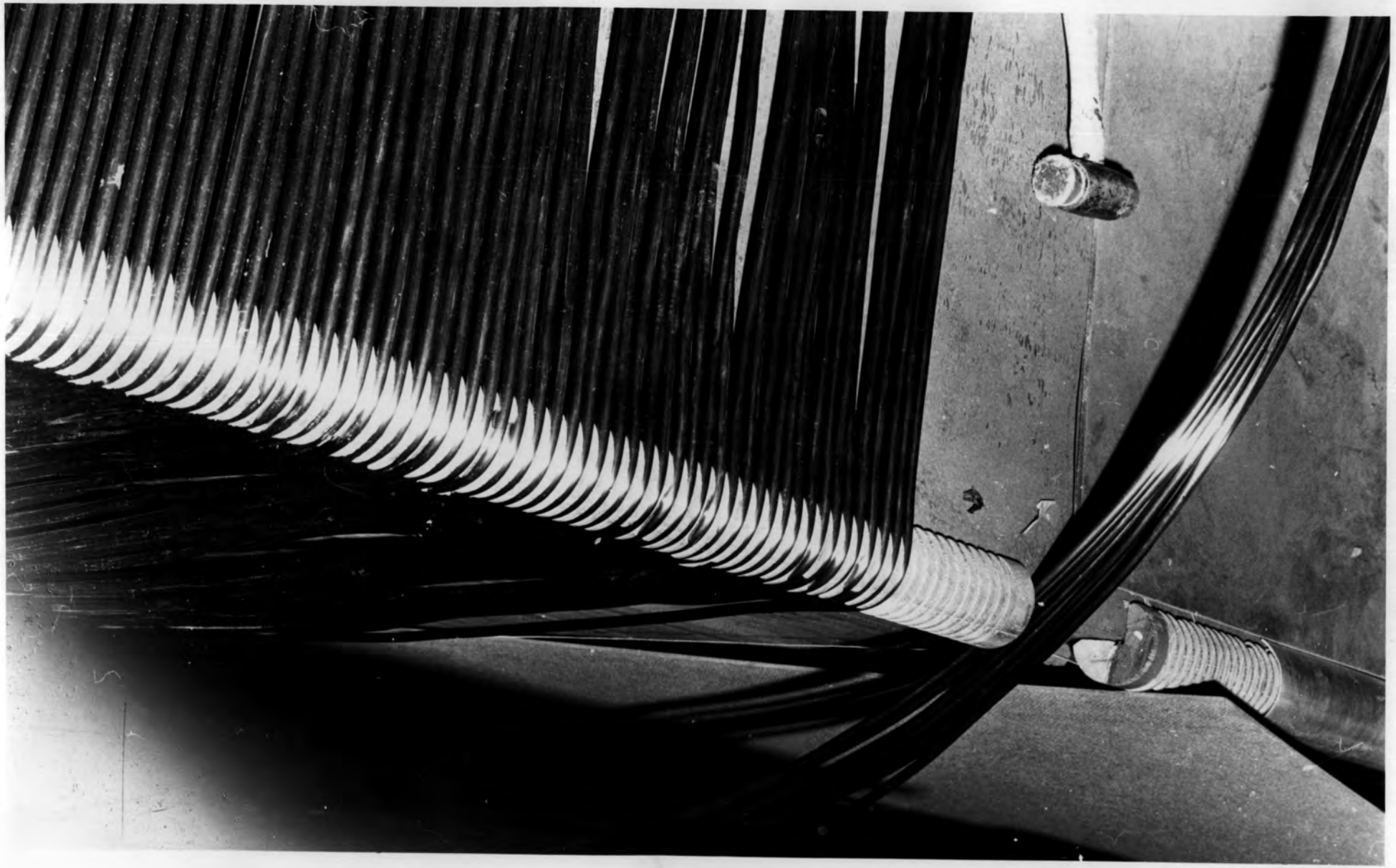

3.2.2 The Rectifier System

The coils on blocks A and C are joined in series. The coils on blocks B and D are joined in a similar manner. The two sets of coils are connected in parallel via reversing switches across a rectifier unit. The rectifier produces a D.C. voltage of 120 volts from a three phase input. When all the coils are connected to the rectifier a current of 50 A. flows through each coil, thus giving an output current of 100 A. from the rectifier. A power output of 12 KW is thus dissipated in the coils.

3.2.3 The Magnetic Field

The magnetic field was measured at various positions in the magnet blocks A,C, and D to determine the uniformity of the field. Search coils were placed in several plates during the construction of the blocks. Figure 3.4 shows the arrangement of these plates in the blocks. Figure 3.5 shows the positions of the search coils in a plate and figure 3.6 the form of an individual search coil. The search coils were made from plastic coated stranded tinned copper wire type 7/00048.

The flux through each search coil was determined by reversing the direction of the magnetic field and observing the deflection on a fluxmeter connected to the search coil. As the magnet coils have an inductance of about 12H., it was impossible to reverse the field instantaneously. Hence the following procedure was carried out.

The magnet energising current was switched on and the fluxmeter connected to a search coil. The current was switched off and after a certain waiting period the field was reversed using the reversing switches and the current again switched on. The resulting change of the fluxmeter reading was noted. The procedure was repeated for several values of waiting time and a graph plotted of waiting time against flux reading. The waiting time was never less than 30 sec. because of the possibility that the back e.m.f. due to the large inductance of the coils would cause sparking at the reversing switches if the

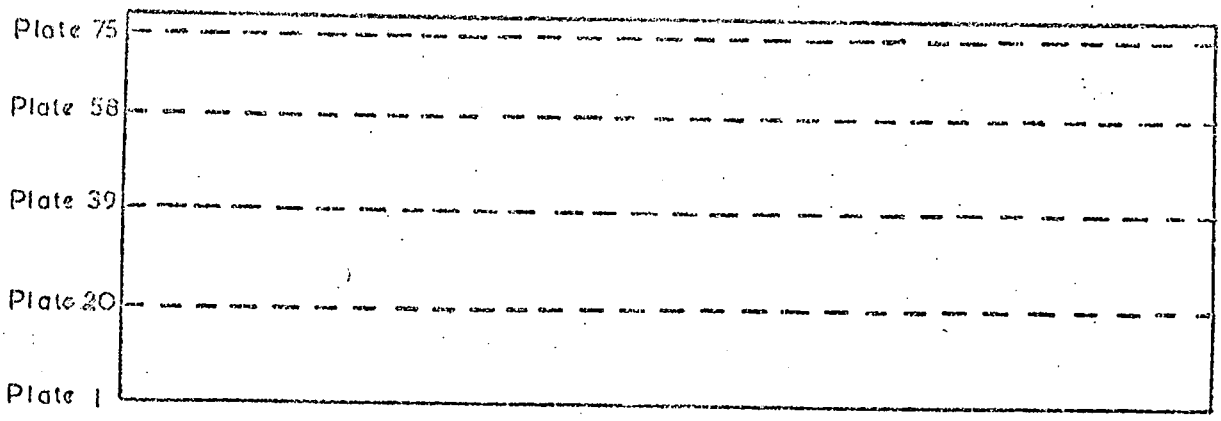

Figure 3.4 The Positions of the Magnet Plates with Search Coils.

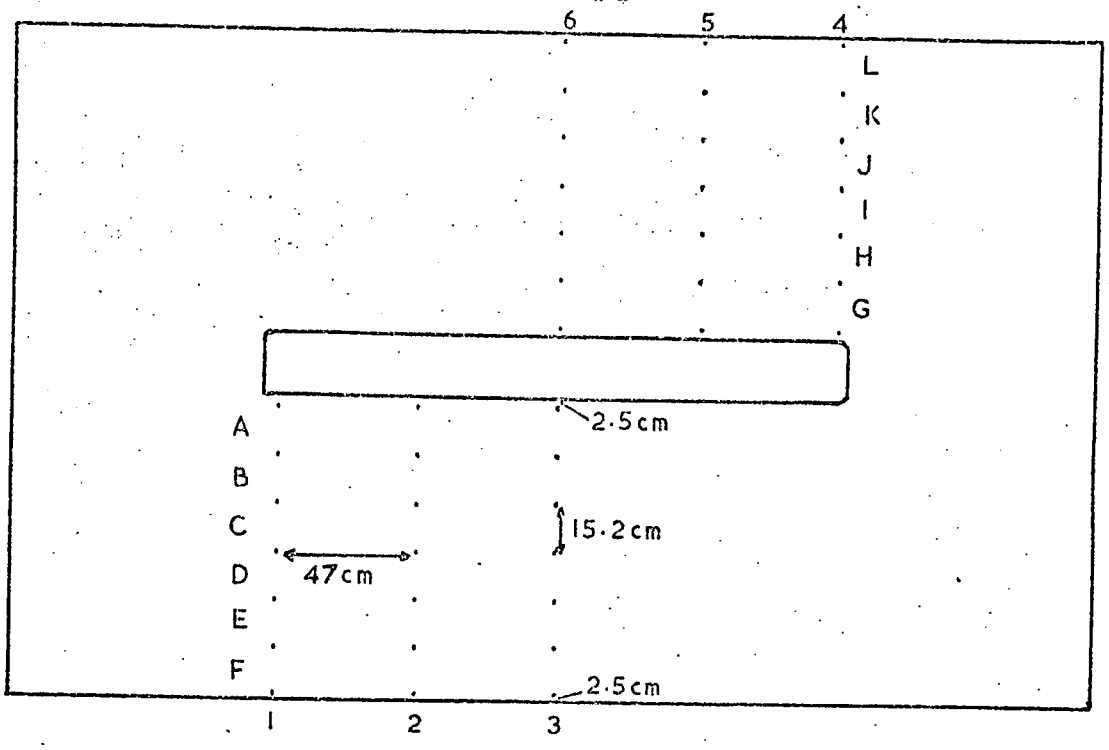

Figure 3.5 The Positions of the Search Coils in the Plates.

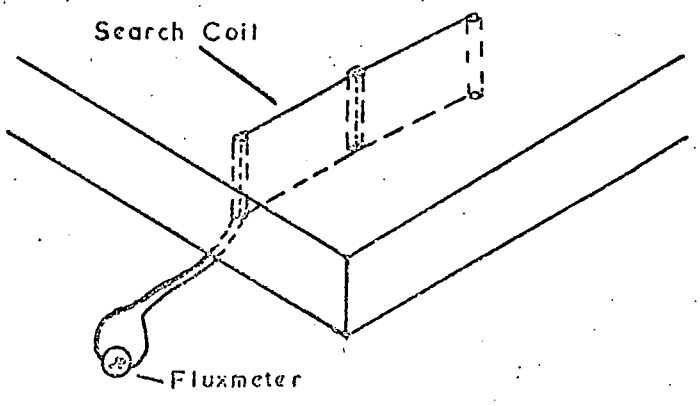

Figure 3.6 The Form of a Search Coil

waiting time was less than this. The fluxmeter reading at zero time was then extrapolated from the graph. Figure 3.7 shows a typical graph corresponding to one of the search coils obtained using this method.

The variation in the field in the planes perpendicular to the magnetic field when averaged over all the search coils in the planes is shown in figure 3.8 for block C. Also for this block, figure 3.9 shows the variation of the field along the planes parallel to the plane A A' in figure 3.1 when again averaged over all the search coils in the planes. In figures 3.8 and 3.9 the corresponding planes on both sides of the magnet have been taken together and plotted as a single point. The field variation for blocks A,B, and D is also similar to that of block C.

The above graphs show that a uniform field, the maximum non uniformity being about $\pm 2\%$ can be obtained in the volume of the magnet used for the deflection of a traversing particle.

The average magnetic field within a block was measured by the use of a single coil of wire around the centre of the block which was connected to the Y terminals of an X - Y plotter. The X axis terminals were connected to a voltage which increased linearly with time.

The voltage (V) produced across the ends of the coil is given by the usual relation: $V = -\frac{dN}{dt}$, where N is the flux linking the coil. Hence the flux change, N, is given by $N = -\int V\,dt$. The area under a curve of V against time gives N from which the magnetic field can be determined.

The same procedure was used with the X - Y plotter as with the search coils connected to a fluxmeter. The X-Y plotter was started when the magnet energising current was on. The current was switched off and after 30 seconds the field was reversed using the reversing switches and the current switched on again. Corrections were made to the resulting pen recording for the response time of the plotter, which was longer than the rise time of the input voltage pulse from the coil, and for the dead time of the plotter between successive sweeps.

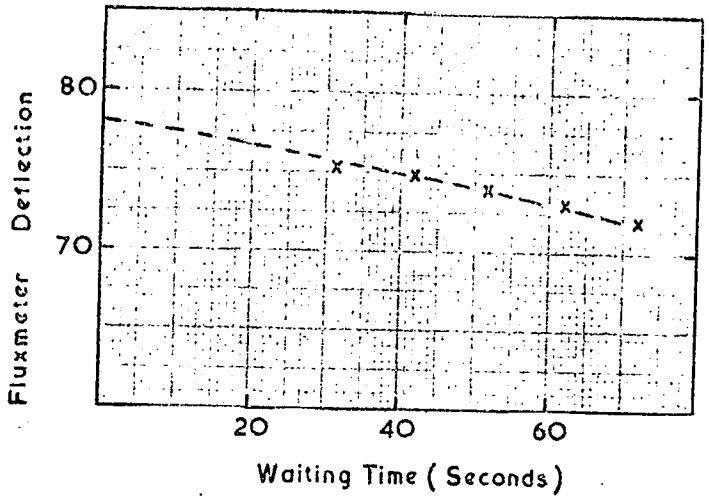

Figure 3.7 Graph of Fluxmeter Deflection against Waiting Time for a Search Coil.

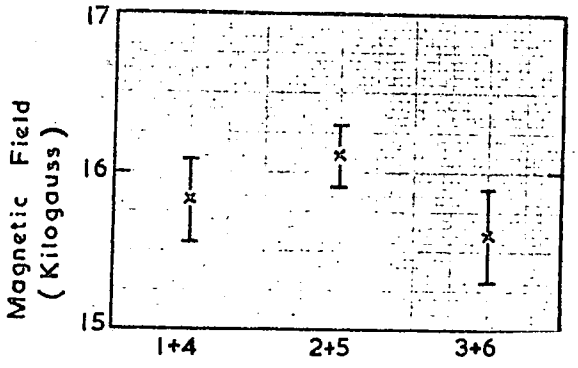

Figure 3.8 The Variation in the Magnetic Field in the Planes at Right Angles to the Magnetic Field Direction.

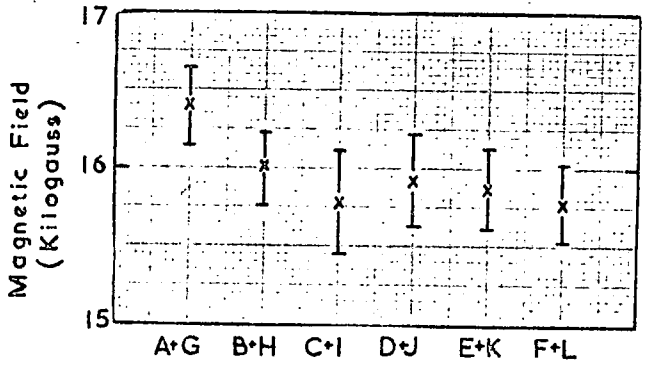

Figure 3.9 The Variation in the Magnetic Field in the Planes Parallel to the Magnetic Field Direction.

The area under the curve, after applying the corrections mentioned above, was measured by three independent methods: counting the squares, Simpson's Rule, and cutting out an outline of the curve and weighing. The results for the three methods are given in Table 3.3 for the four magnet blocks. The resultant mean magnetic field over the sensitive region of the magnet was found to be 16.3 ± 0.1 kilogauss.

TABLE 3.3

Results of the Magnetic Field Measurements for the Magnet Blocks using a X-Y Plotter

	Method of Measurement					
Block	Counting Squares			Simpson's Rule	Weighing	Average
A	16.24	16.23	16.27	16.36	16.56	16.33
B	16.47	16.01	15.79	16.57	16.22	16.21
C	16.18	16.14	16.20	16.87	16.52	16.38
D	16.45	16.44	16.01	16.29	16.03	16.24
Average	16.34	16.21	16.07	16.52	16.33	-

Measurements in Kilogauss.

Average Value of Magnetic field = 16.3 ± 0.1 Kilogauss

3.3 The Scintillation Counters

The scintillation counters are made from plastic scintillator material type number NE 102a and have an overall size of approximately 177 cm x 75 cm x 5 cm. The light output from the scintillators is collected using the technique discussed by Barnaby and Barton (1960) and Ashton et al. (1965). Four photomultipliers (Mullard type 53 AVP) are fixed on to Perspex light guides on the ends of the scintillators by means of optical cement. The light guides are similarly joined to the scintillators by optical cement. Figure 3.10(a) shows the form of the light guides and the positions of the photomultipliers.

The response of a photomultiplier is effected by stray magnetic fields so each photomultiplier is shielded by a μ metal shield and a soft iron shield

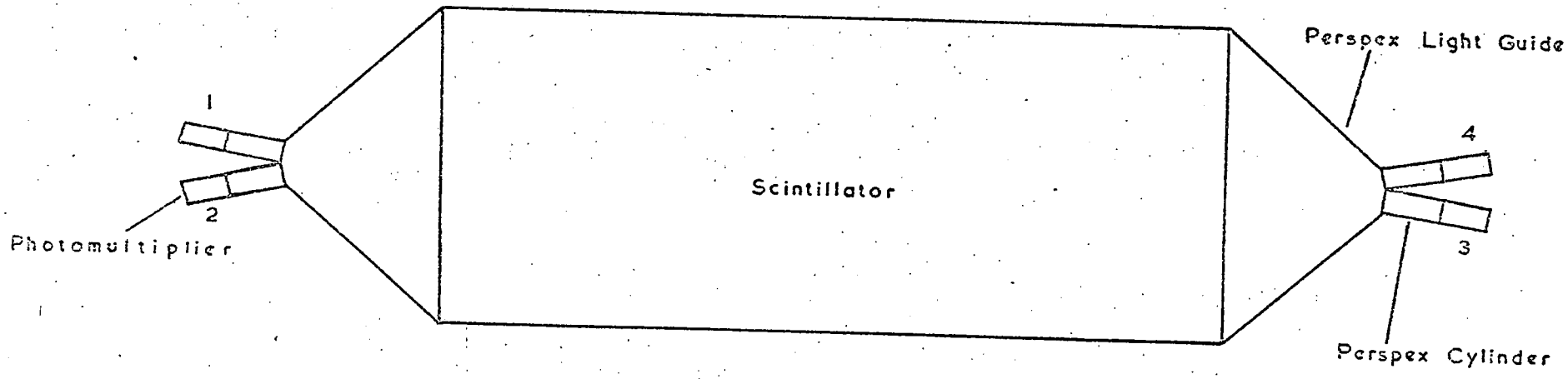

Figure 3.10(a) The Scintillation Counter.

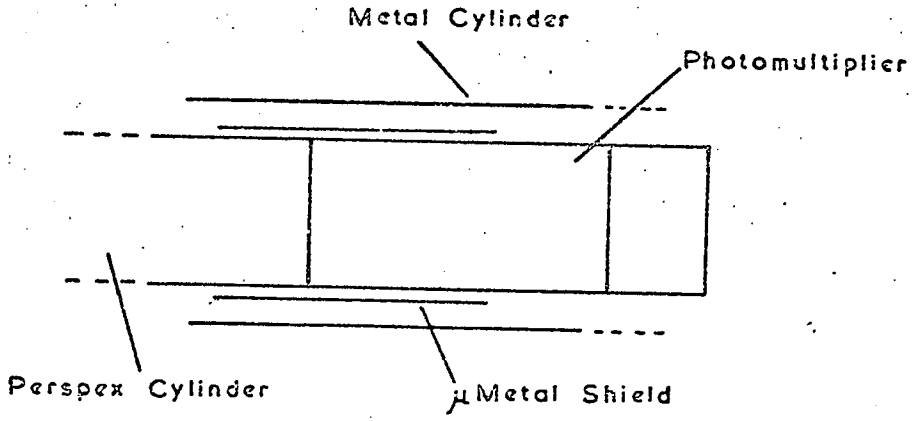

Figure 3.10(b) The Shielding Arrangement on a Photomultiplier.

as shown in figure 3.10(b). The Perspex cylindrical light guides, to which the photomultipliers are joined in figure 3.10(a), enable the shields to fit over each photomultiplier.

The scintillator and photomultipliers are contained inside a light tight box. The sides of the box are made of aluminium alloy channel of size 3" x 2" x $\frac{1}{4}$", the overall size of the box being 330cm x 76cm x 7.6cm. The top and bottom of the box are made from hardboard sheet fixed to the channel by aluminium strips placed around the sides of the hardboard. The strips are held in position by 0 B.A. countersunk screws passing through the strips and hardboard into the channel. Aluminium sheet is placed over the hardboard and is located between the hardboard and aluminium strips.

Before being placed in the light tight box, the scintillator and light guides were polished and then covered with aluminium foil. This reduces the light lost from the outer surfaces. A sheet of black plastic is used to cover the scintillator and light guides to prevent any external light from entering the system.

The dynode resistance chain for the photomultiplier bases is shown in figure 3.11. The dynode chain is contained in the photomultiplier base and is shielded by a metal cylinder. The E.H.T. to each photomultiplier can be varied by means of a switch arrangement of resistors which is also shown in figure 3.11 connected to a stabilised high voltage power supply.

The E.H.T. of each photomultiplier was adjusted, so that they each had the same gain, with the aid of a small scintillator telescope so positioned as to selected only particles passing through the centre of the counter. The two small scintillation counters of the telescope were placed above and below the large scintillation counter and an output pulse from the telescope coincidence unit was used to gate a 400 channel pulse height analyser (P.H.A.). The output pulses from each photomultiplier were fed into the P.H.A. and the E.H.T. for the photomultiplier adjusted until the peak of the distribution, which

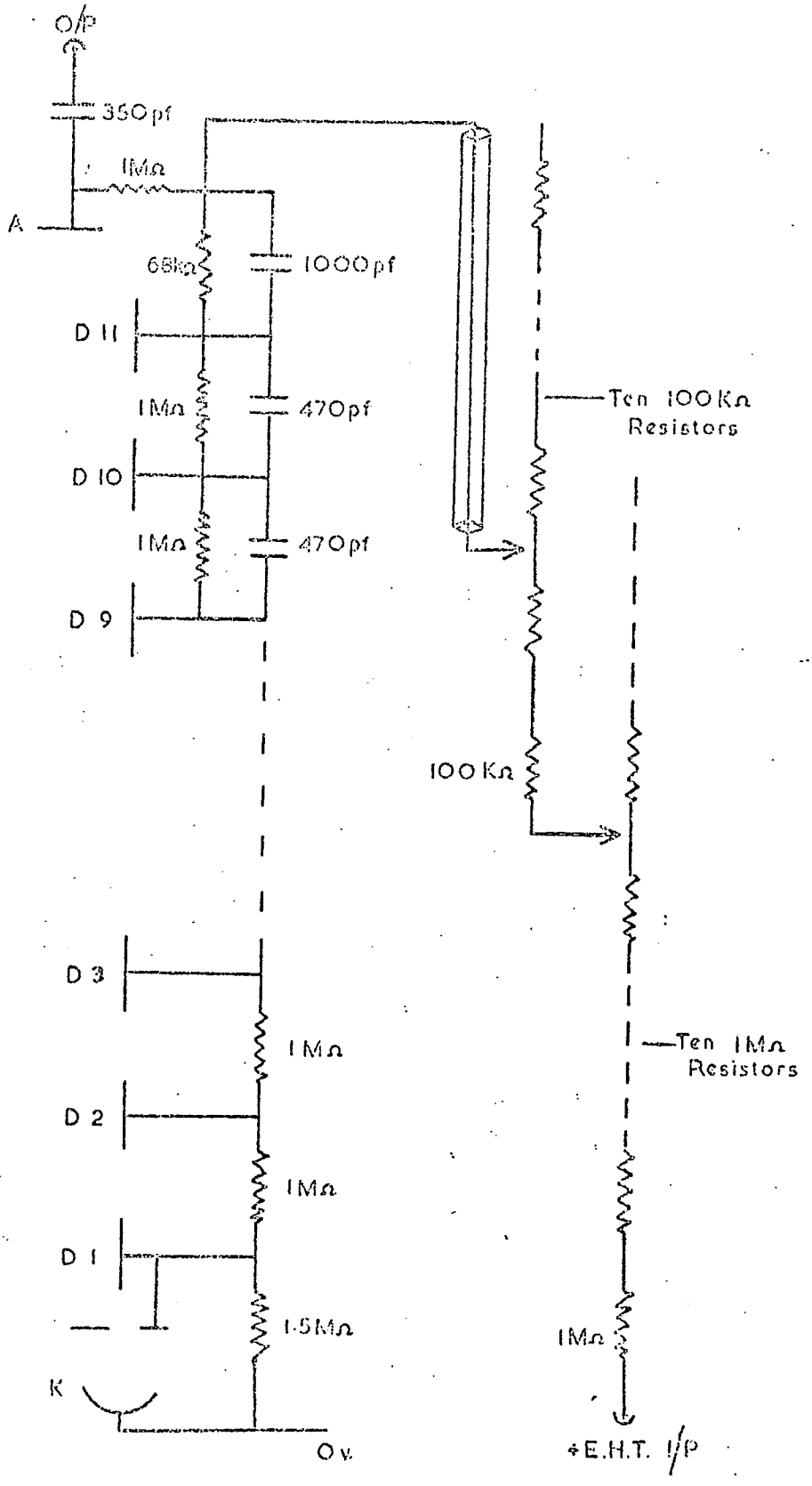

Figure 3.11 The Dynode Resistance Chain for the Photomultiplier Bases.

is the most probable pulse height, due to the traversal of the central region of the counter by a particle, occurred at a certain channel number on the P.H.A., this channel number being the same for each of the four photomultipliers.

To obtain a uniform response over the scintillator, the four photomultipliers on each scintillator are taken in pairs as shown in figure 3.12, which shows the block diagram for the scintillation counter electronics. The numbers shown on each photomultiplier are the same as those in figure 3.10(a).

The output pulses from the two paired photomultipliers after passing through head amplifiers are fed into a pulse adding circuit. The pulse from the adding circuit is amplified and fed via co-axial cable to a discriminator and pulse shaper. The head amplifiers and adding circuits are in shielding boxes on the outside of the box holding the scintillator, this enables easy access to be obtained in case of a fault.

The optimum discriminator level for each of the paired photomultipliers was selected by gating the P.H.A. on the discriminator output whilst feeding the pulses from the scintillation counter into the P.H.A. The discrimination level could then be seen from the P.H.A. record and could be adjusted until most of the noise from the counter was eliminated.

The added pulses from the second pair of photomultipliers in the scintillation counter are also fed to a discriminator and pulse shaper. The shaped outputs from the two discriminators are fed into a two fold coincidence circuit as shown in figure 3.12. An output pulse from the coincidence circuit is usually only obtained when at least one particle went through the counter. The resolving time of the system is 0.7 μs.

A constant check is made on the counting rate of each scintillation counter by means of six ratemeters, which drive a six channel pen recorder. Each channel of the recorder is sampled once a minute. A potentiometer is incorporated in each ratemeter to enable a steady D.C. voltage to be applied to the pen recorder, upon which a voltage proportional to the scintillator counting rate is applied.

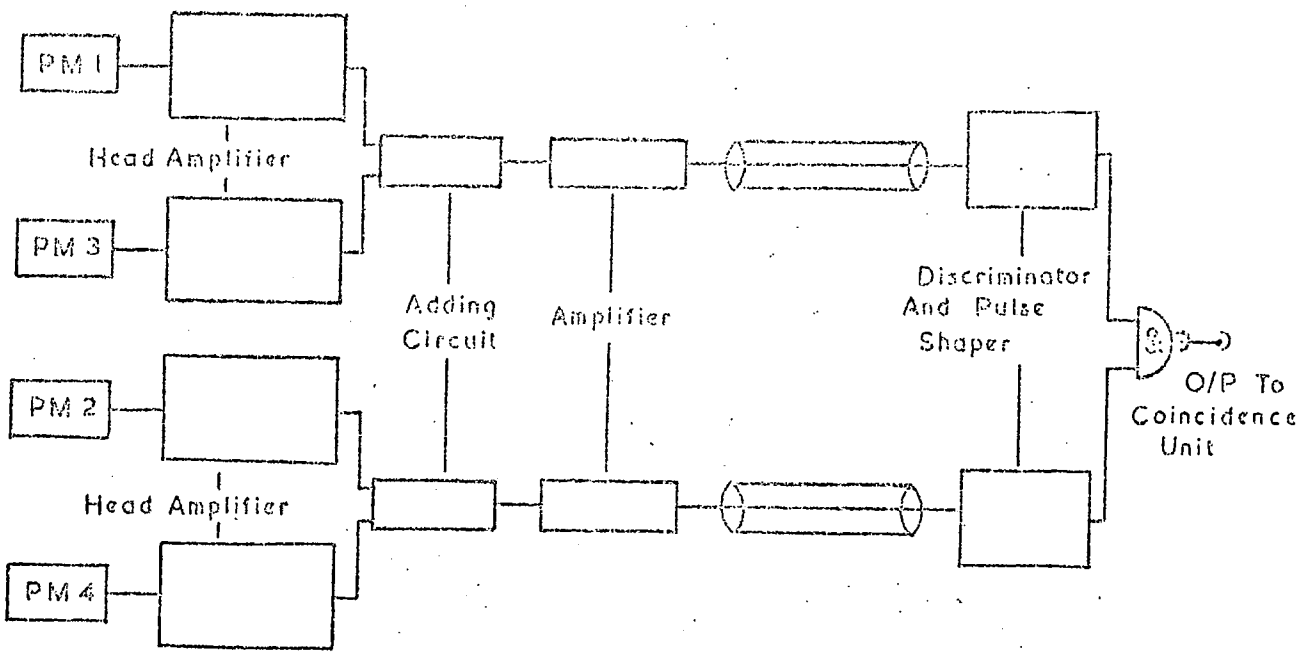

Figure 3.12 Block Diagram of the Scintillation Counter Electronics.

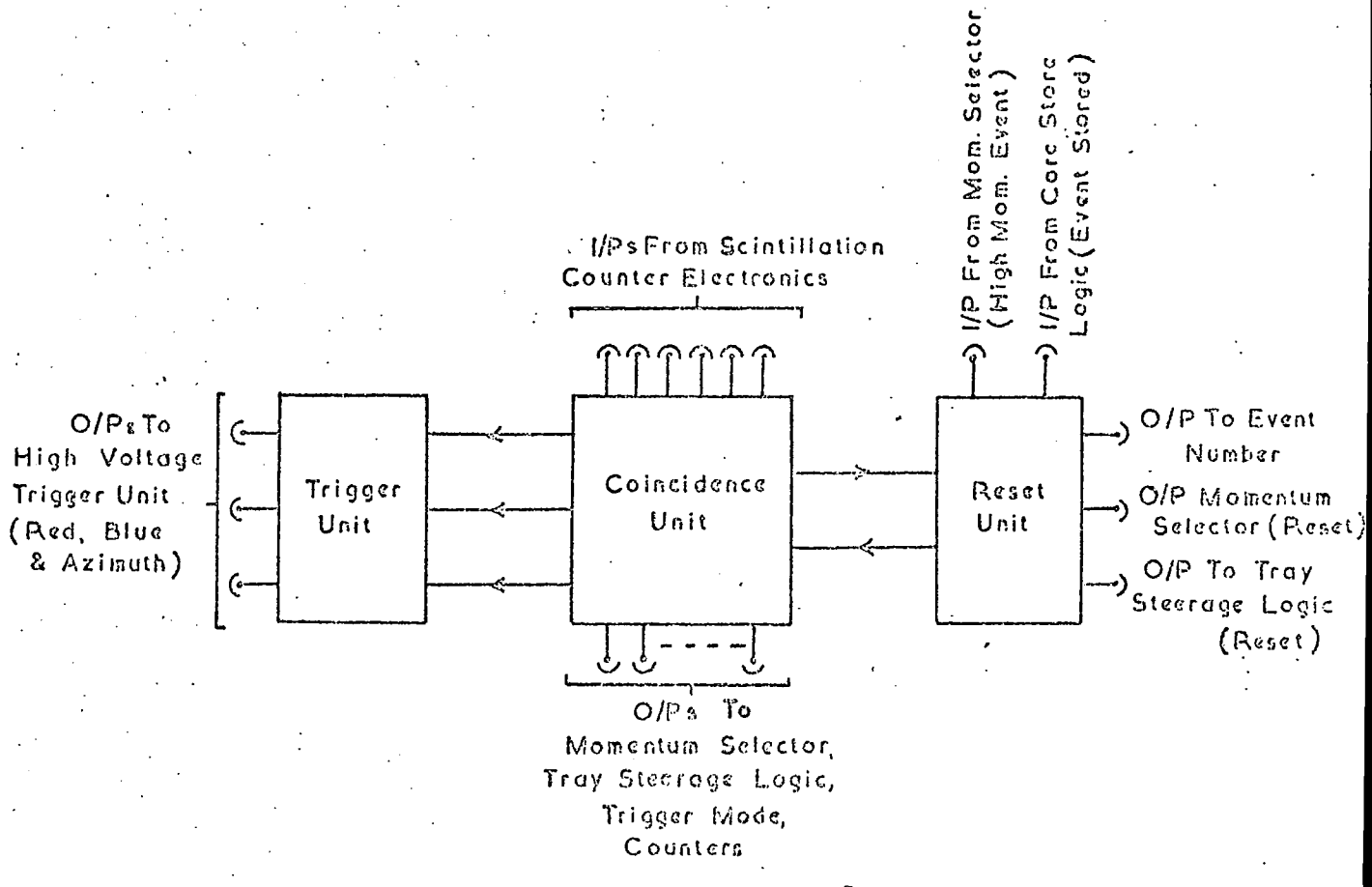

Figure 3.13 Block Diagram of the Main Coincidence System.

This enables the record for each scintillation counter to be recorded at different positions on the pen recorder chart.

3.4 The Main Coincidence System

3.4.1 Introduction

This system is responsible for controlling the triggering of the flash tube trays and for producing output pulses to the controlling electronics of the Momentum Selector and Measuring Tray systems. The system can be subdivided into several smaller systems which are each responsible for producing output pulses to other controlling electronic systems. Figure 3.13 shows a block diagram of the system showing the various sub-units and the outputs and inputs to the rest of the electronics. The main coincidence system is contained in a rack near to the spectrograph and is marked in Plate 2. The form and function of the various sub-units are described below.

3.4.2 The Coincidence Unit

The output pulses from the discriminator unit corresponding to each scintillation counter are fed into the coincidence system as shown in figure 3.14. Also shown in the figure are the logic levels in the steady state. The circuits used for the monostables (M/S in figure 3.14) and delay units are described in Appendix A. A monostable, or pulse shaping circuit, produces an output pulse of constant length irrespective of the length of the input pulse and a delay unit delays the passage of a pulse by a certain value.

Several switches have been included in the unit as shown in figure 3.14 to control the form of coincidence from the unit. These switches are placed on the front panel of the unit. A further switch is situated near to the 1130 computer so that the computer operator can stop the system if the need arises.

When a three fold coincidence is obtained from the scintillation counters on one side of the spectrograph, two output pulses are fed to the trigger unit, a pulse is fed to the reset unit, and an automatic paralysis of 1.5 ms. is applied to the complete apparatus. The trigger unit, which is described in §3.4.4, controls the pulsing of the flash tube trays. The reset unit is described in §3.4.3 and is the controlling logic for the length of paralysis set by a

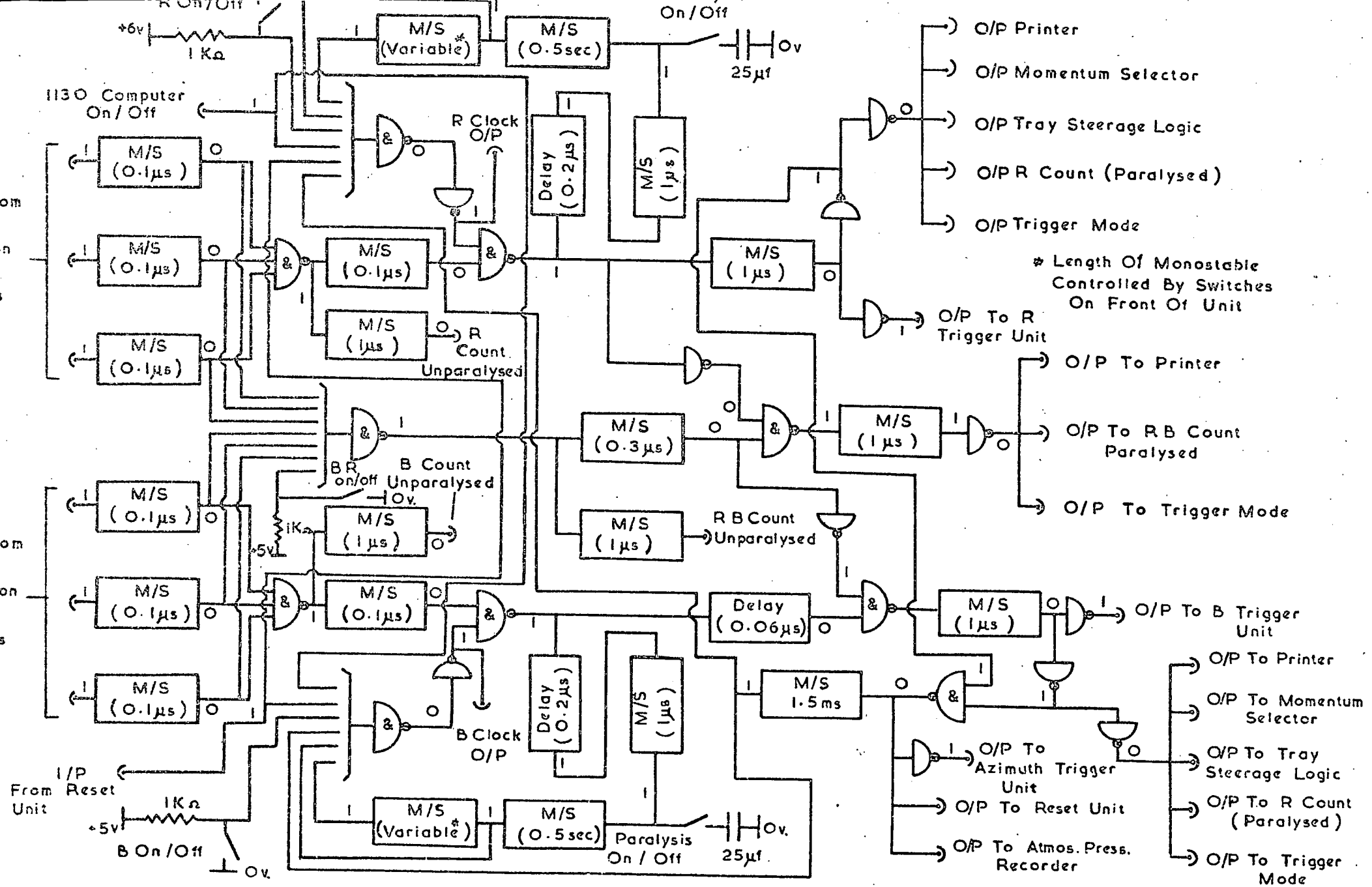

Figure 3.14 The Coincidence Unit.

high momentum event. The procedure after the paralysis of 1.5 ms on the apparatus depends on whether the event is a high or low momentum event. If the event is a low momentum event then the paralysis on the side not triggered is removed. The length of the paralysis on the triggered side can be varied from 0.5 sec. to 7 sec. by two series of switches, one for each side, on the front of the unit and can, if required, be removed.

If the event is a high momentum event then a further paralysis is applied to the apparatus by the reset unit which is not removed until the information for the event has been stored in the computer. This high momentum paralysis will have been applied to the apparatus during the automatic paralysis stage as the Momentum Selector will have determined whether or not the event is a high momentum event after about 110 μs from the initial three fold coincidence. After the removal of the high momentum paralysis the side not triggered will have its paralysis removed. The triggered side may still be paralysed depending on the length of the paralysis set in the electronics.

If a six fold coincidence pulse is obtained from all the scintillation counters, then the trigger output for the Blue side is vetoed and high voltage pulses are only applied to the flash tube trays on the Red side and the Azimuth Trays. This is because the core store is only of sufficient size to store information from one side and the Azimuth Trays. This will be discussed further in §6.8.

Output pulses are provided from the unit to the Momentum Selector, trigger mode, and tray steerage logic to indicate which side has been triggered. The trigger mode records the triggered side for the core store and is described in §6.9.7. Further output pulses are provided to count the coincidence rates of the scintillation counters in both paralysed and unparalysed modes and to trigger a digital voltmeter recording the atmospheric pressure as explained in §6.9.8. The rate of particles passing through each side and the six fold counts in the paralysis mode are recorded by a printer unit. In particular the number of muon traversals are printed out every 20 minutes on to a paper reel together with the time and date. After printing, the counters start from zero

and again print out after a further 20 minutes. Mechanical counters, which can be reset at will, also record the total number of events and the high momentum events obtained in the three trigger modes. The unparalysed counting rates are not intended to be recorded permanently but will be used to check the counting rates if required.

The coincidence unit also provides outputs to a circuit which records the running time of each side of the spectrograph. The running times are recorded by two mechanical counters graduated in hours, minutes, and seconds.

3.4.3 The Reset Unit.

The circuit diagram for the reset unit is shown in figure 3.15. As well as providing the paralysis on the apparatus when a high momentum event is recorded, it also provides pulses to the Momentum Selector Control unit and the tray steerage logic to reset the electronic memories on the flash tubes.

The series of output pulses from the reset unit depends on whether the event is a low or high momentum event. If the event is a low momentum event then the input pulse from the coincidence unit, after being delayed by 1 ms, produces output pulses to the Momentum Selector and tray steerage logic to reset the memories on the flash tube trays. The automatic paralysis on the apparatus is removed 0.5 ms after the reset pulses to the electronic memories.

If the event is a high momentum event, then an input pulse is received from the Momentum Selector. This produces an output pulse to trigger the event number counter, which is described in §6.9.2. A flip-flop is also triggered by this output pulse which applies a paralysis to the apparatus. This trigger pulse is of length 60 μs to prevent the flip-flop being reset by any noise produced during the application of the high voltage pulse.

The output pulses from the unit to reset the memories are vetoed by the application of this paralysis. When the event has been stored in the computer, a pulse is received from the core store logic. This produces the output pulses for the memory resets. After a further 25 μs the paralysis is removed from the

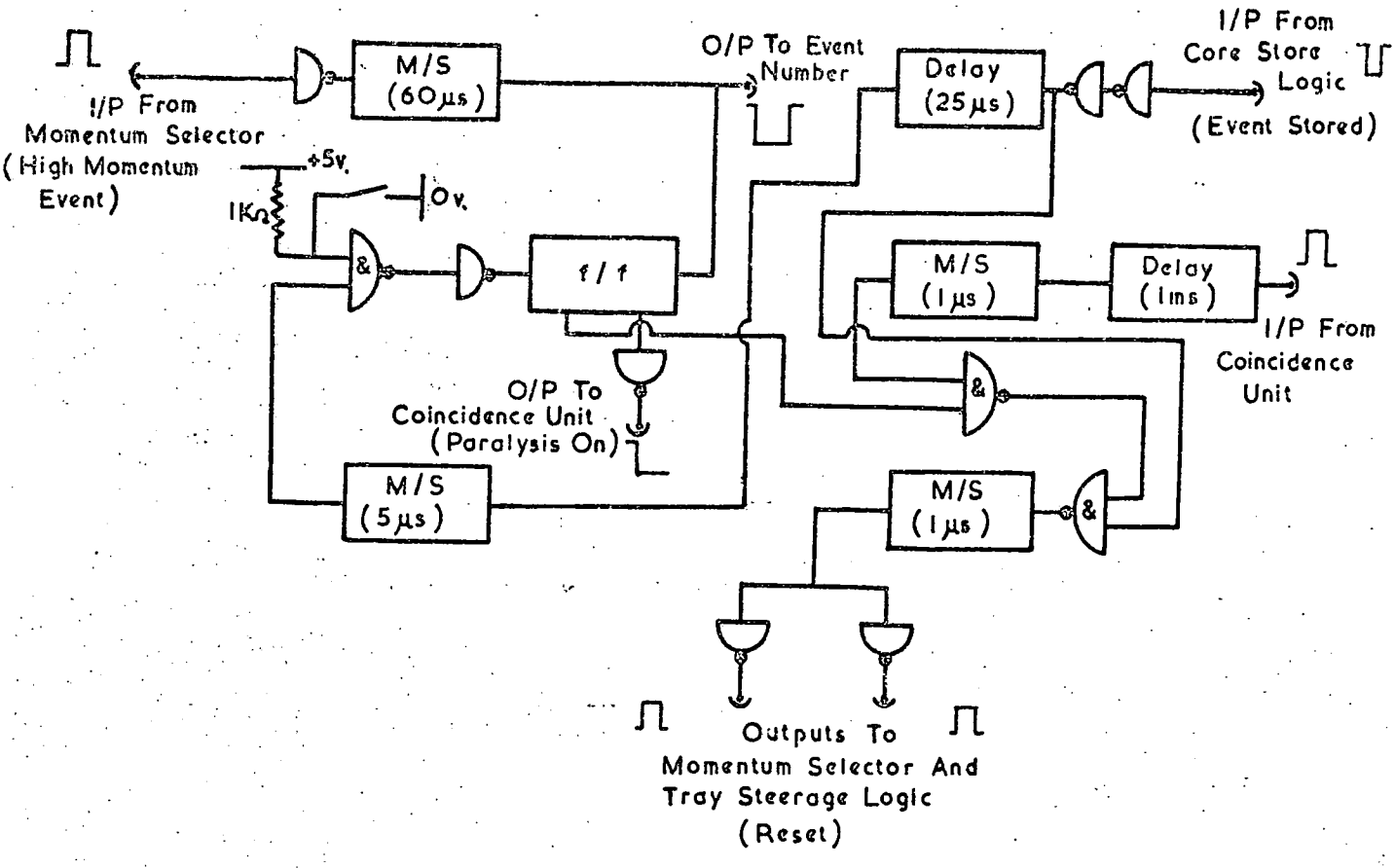

Figure 3.15 The Reset Unit.

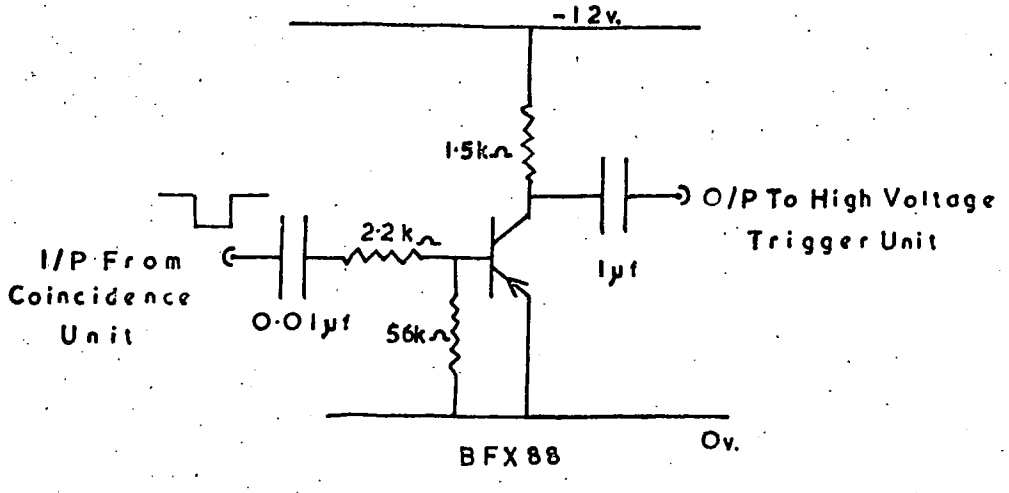

Figure 3.16 The Trigger Unit.

whole apparatus. The paralysis of the triggered side may still be applied after the removal of the paralysis controlled by the reset unit as this depends on the paralysis time set inside the coincidence unit.

A push button switch is incorporated in the front of the unit, which enables the paralysis flip-flop to be set to the off mode when the power is switched on. The state of the flip-flop is shown by an indicator bulb on the front of the unit.

3.4.4. The Trigger Unit

This unit provides output pulses for the three high voltage trigger units which are described in § 3.5. Figure 3.16 shows a diagram of the arrangement for one of the circuits, the remaining two circuits are similar in form. When a coincidence pulse is obtained in the coincidence unit, two output pulses are sent to the trigger unit. One of these pulses corresponds to the side to be triggered and the other pulse is the trigger pulse for the Azimuth Trays. This latter pulse is produced every event. If a six fold coincidence is obtained from the scintillation counters, then only the trigger units for the Red side and Azimuth Trays are pulsed for the reason mentioned in § 3.4.2.

Transistors are used to produce the output trigger pulse to the high voltage trigger unit for two reasons; to prevent feedback from the high voltage trigger unit effecting the rest of the electronics and also to prevent the high voltage trigger unit being triggered by noise pickup from adjacent apparatus.

3.5 The High Voltage Trigger Units

Three high voltage trigger units are incorporated in the spectrograph electronics. They are used to apply high voltage pulses to the flash tube trays on each side of the spectrograph and to the Azimuth Trays.

The high voltage pulse applied to a flash tube tray is obtained by discharging a lumped parameter delay line through a resistor by means of a spark gap. A square negative pulse is obtained across the resistor, which is

applied to the flash tube trays. Two types of delay line are used in the spectrograph, each having a different characteristic impedance and pulse length. For the Measuring and Azimuth Trays a delay line of characteristic impedance 22 ohms is used which gives a pulse length on open circuit of 1.5 μs. The Momentum Selector Trays use a delay line of characteristic impedance 47 ohms and pulse length of 3 μs on open circuit. The inductances used in the delay line are wound on dowel rod. Recesses have been machined in the rod to allow the inductances to be a tight fit and not to move. The inductances are made from 18 S.W.G. copper wire (ϕ = 1.22mm) which is shellaced to prevent breakdown between adjacent turns.

The delay lines for the Measuring and Azimuth Trays comprise 15 elements and the inductances consist of 8 turns of wire wound on a dowel rod of diameter 2.5 cm with the recesses machined so that the internal diameter of the inductance winding is 2 cm. The delay lines for the Momentum Selector Trays are made from 12 elements and the inductances consist of 22 turns of wire of internal diameter 3 cm wound on a dowel rod of diameter 3.2 cm. The capacitors used on both types of delay line are of value 2500 pf. and are joined to the mid point of the inductances and to a common line, which is a $\frac{3}{4}$" x $\frac{1}{4}$" brass rod of length equal to the delay lines.

The resistor used with the delay line is a Morganite disc shaped ceramic resistor. Contact is made to the resistor by means of brass discs fixed to the ends of the resistor with conducting cement.

The value of this resistor governs the pulse height obtained for a fixed delay line voltage and when the delay line is connected to a tray it effects the rise time of the pulse. However, for the trays used in the spectrograph, it is the capacitance of the trays which is the dominant factor. The Momentum Selector Trays, Measuring Trays, and Azimuth Trays have capacitances of 0.005 μf, 0.028 μf, and 0.019 μf respectively. The rise time of the high voltage pulse applied to a flash tube tray is important because during a

slowly rising pulse, the electrons produced in a particular flash tube by the traversing particle will be swept to the walls before the applied electric field is sufficient to produce a discharge in the tube, and such a pulse will thus result in a loss of efficiency for the flash tube.

The value of the resistor was determined by measuring the variation in layer efficiency of the flash tube trays as a function of the applied pulse height for various values of the resistor. The layer efficiency was measured by photographing the flash tube trays in the spectrograph. The value of the resistor and the form of the high voltage pulse applied to the trays are described in §5.8.3 for the Momentum Selector Trays and §6.4.2 for the Measuring Trays.

Each flash tube tray has its own delay line. These delay lines are grouped together in three groups, two groups for the Red and Blue sides of the spectrograph and the third group for the Azimuth Trays. The delay lines for the Red and Blue sides are arranged to stand vertically on a sheet of Tufnol on the first level of the spectrograph gantry. The Azimuth Tray delay lines stand on the second level of the gantry. The delay lines in the three groups are enclosed by an aluminium box. The resistances for the delay lines and the high voltage trigger unit fit above the delay lines and are also shielded by the aluminium box. Plate 4 shows a photograph of a delay line unit when removed from its box, in which the various components of the unit are indicated.

The Measuring and Momentum Selector Trays on one side are triggered by different spark gaps because the voltage on the delay lines is different for the two cases. The Azimuth Trays are triggered by one spark gap.

The spark gaps are triggered by discharging a condenser of capacity 0.05 μf through the primary of a transformer using a thyristor type BTX 64. Figure 3.17 shows a diagram of the circuit. For the Red and Blue sides the circuit is repeated as shown in figure 3.17, the two circuits being for the Measuring Trays and Momentum Selector Trays. The circuit is triggered by a pulse from

PLATE 4

A Delay Line Unit

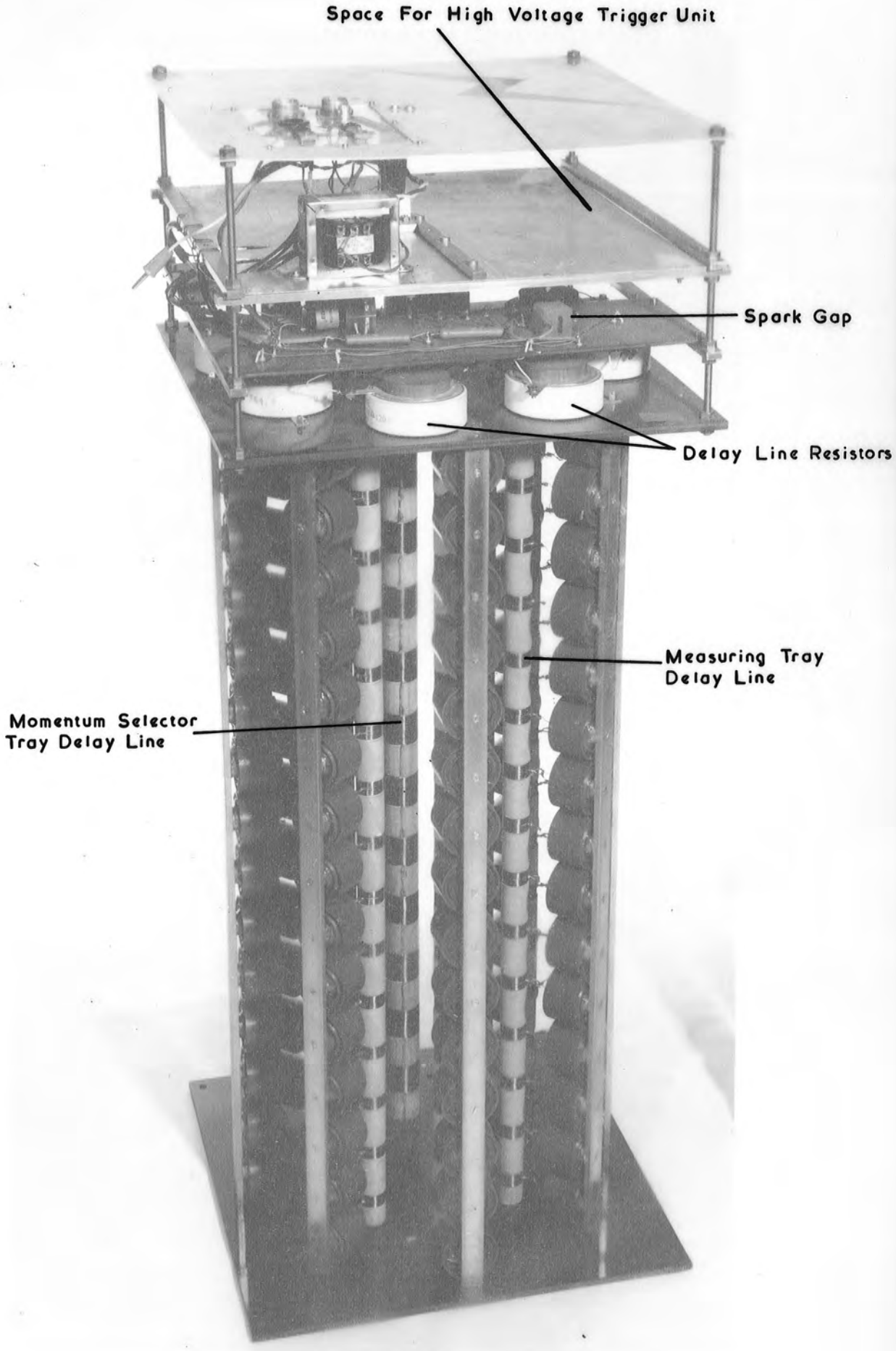
Space For High Voltage Trigger Unit
Spark Gap
Delay Line Resistors
Measuring Tray
Delay Line
Momentum Selector
Tray Delay Line

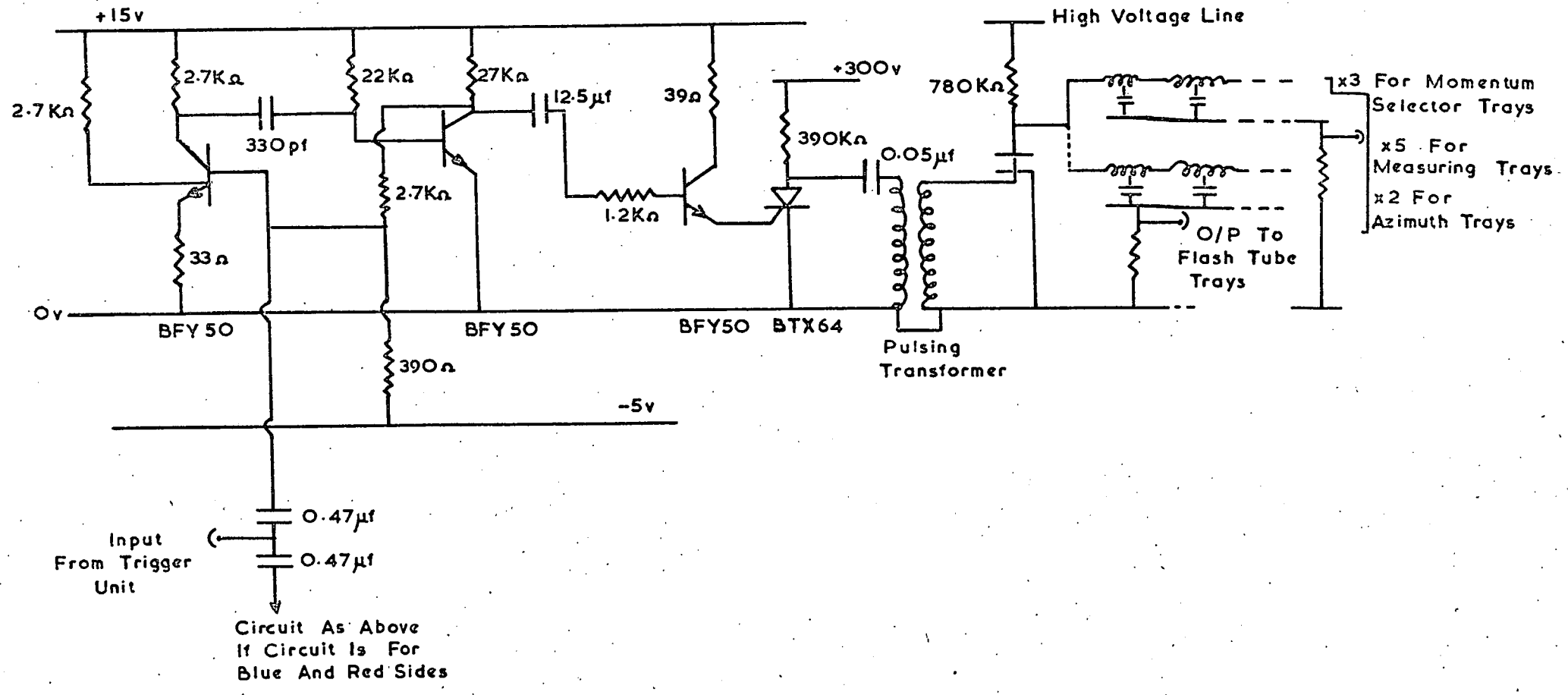

Figure 3.17 The Circuit for the High Voltage Trigger Unit.

the corresponding trigger unit as described in §3.4.4. After the delay lines have been discharged, they are charged again through the 780kΩ resistor from the high voltage supply as shown in figure 3.17. With this circuit the high voltage pulse can be applied to the flash tube trays after a time of 1.5 μs from the passage of a triggering particle through the spectrograph.

The electronics is mounted in an aluminium box above the delay lines shown in Plate 4. The pulse transformers, spark gaps, and charging resistors for the delay lines are contained in the section above the delay line resistors. The rest of the electronics fit into the space above. Co-axial cable is used from the delay lines to the flash tube trays, the cable being connected to the trays by two brass connectors as explained in §5.4.

3.6 Summary of the Triggering Procedure in M.A.R.S.

A résumé of the sequence of events which takes place when an event is detected in one of the sides of the spectrograph is given below. A block diagram of the electronics system is shown in figure 3.18.

(i) A three fold coincidence pulse is obtained from the scintillation counters on one side of the spectrograph, for instance the Red side. This results in pulses being fed to the following units:

(a) the high voltage trigger units for the Red Side and the Azimuth Trays to apply high voltage pulses to the required trays;

(b) the tray steerage logic to indicate that the digitised information in the Measuring Trays on the Red Side and the Azimuth Trays is to be fed into the core store if the event is a high momentum event;

(c) the Momentum Selector control unit to start the procedure for the readout of pulses from the Momentum Selector Trays;

(d) the digital device R.U.D.I. to indicate which side has been triggered and to prepare the device for accepting information from the Momentum Selector.

The spectrograph is paralysed for at least 1.5 ms.

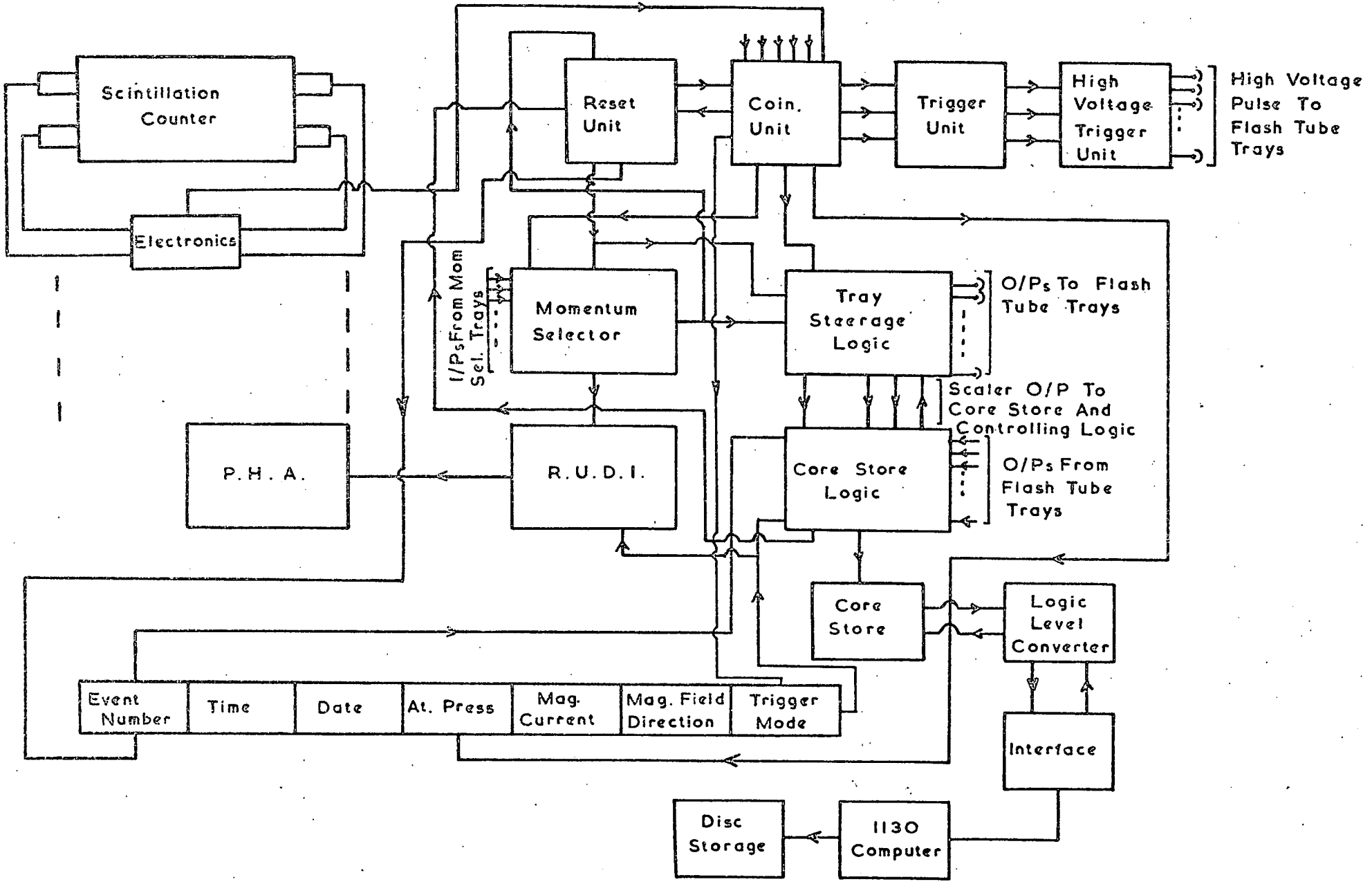

Figure 3.18 Block Diagram of the Spectrograph Electronics.

(ii) The Momentum Selector and the tray steerage logic then apply a reset pulse to the electronic memories of the flash tubes. This pulse is also a veto as it prevents the memories from being set during the time the pulse is applied. The pulse is applied during the rising edge of the high voltage pulse to prevent the memories being triggered by noise.

(iii) After a delay of 1.5 μs from the initial coincidence pulse, the high voltage pulses are applied to the flash tube trays in the Red Side and to the Azimuth Trays; the tubes which have flashed are recorded by the electronic memories. After a further delay of 8.5 μs, the Momentum Selector control unit allows pulses to be fed from the logic on the Momentum Selector Trays to the Momentum Selector, indicating the position of the particle in the trays. The Momentum Selector then analyses the event and decides whether it is possibly a high or low momentum event. R.U.D.I. also analyses the event in conjunction with the Momentum Selector and stores any result in a 400 channel pulse height analyser. The next sequence of events depends on whether the event is classed as a low or high momentum event.

(iv) If the event is found by the Momentum Selector to be a low momentum event then, after a time of 1 ms from the initial coincidence pulse, pulses are fed from the reset unit to the Momentum Selector control unit and tray steerage logic to reset the electronic memories on the flash tubes and to reset the controlling logic back to their normal off mode. After a further interval of 0.5 ms, the automatic paralysis is removed although there will still be a paralysis on the triggered side.

(v) If a high momentum event is found by the Momentum Selector, then a pulse is fed from the Momentum Selector to the reset unit to set a flip-flop which applies a further paralysis to the apparatus. The Momentum Selector will indicate whether the particle is a high momentum event about 110 μs after the initial three fold coincidence. The Momentum Selector also feeds a pulse via the tray steerage logic to the core store logic indicating that information

is required to be stored from the flash tube trays. The core store logic then feeds into the core store the digital information which accompanies every high momentum event - the event number, time and date of the event, the atmospheric pressure, the magnetic field direction, the magnet coil current, and the trigger mode. When this has been stored, the digitised information of the flash tubes which have discharged in the Measuring Trays of the Red Side and the Azimuth Trays is fed into the core store.

(vi) When all the digitised information associated with an event has been stored, the computer is interrupted. As the computer is used by the High Energy Nuclear Physics group for on-line control of scanning machines, it may not be ready immediately to accept the readout of the core store into the computer. The computer has been programmed, however, to accept an interrupt from the core store as soon as possible. The output states from the core store are fed into an intermediary interface into which are also fed the outputs from the scanning machines. Before passing into the interface, the output lines from the core store are fed into a logic level converter to produce output logic level voltages of +18 volts and 0 volts for logic levels of 1 and 0 respectively. These two voltages are the logic voltages for the interface. The event is then stored in an allocated part of the computer core and transferred to a magnetic disc when the allocated part is full as explained in § 6.8.

(vii) When the computer has stored the event, a pulse is sent from the core store logic to the reset unit, which removes the paralysis from the apparatus. The spectrograph is then ready for the next event.

The total rate of triggered events is recorded by the 20 minute printer. Mechanical counters record the total number of events and the number of high momentum events in the three trigger modes.

CHAPTER 4

The Flash Tube Digitisation Technique

4.1 Introduction

The neon flash tube was first introduced by Conversi and Gozzini (1955) and has subsequently been developed by various workers, for example, Gardener et al. (1957) and Coxell and Wolfendale (1960). Basically the flash tube is a soda glass tube filled with commercial neon gas and sealed with a plain front at one end, which enables the tube to be easily photographed. The flash tube is placed with other tubes between parallel plate electrodes. An array of flash tubes is made by building several layers of tubes with electrodes between each layer or, in some cases, alternate layers.

The flash tubes can be made to flash with the characteristic neon colour if, a few microseconds after the traversal of an ionising particle, a strong electric pulse is applied to the electrodes. The flashed tubes can then be recorded on film. The pulse characteristics depend on the flash tube diameter and pressure of the gas but typical values are a square pulse producing a peak field of 2.5 kV cm^{-1} and length 3μs.

Ashton et al. (1958) and Bull et al. (1962) have shown that the flash tube can be used for locating the trajectory of a particle to an accuracy of less than one millimetre if the flash tubes are used in specially designed arrays. Consequently, flash tubes have been used in cosmic ray magnetic spectrographs to determine the particle trajectory by several workers. Several of these spectrographs have been mentioned in Chapter 2 and are listed in Tables 2.1, 2.2, and 2.3.

Flash tubes have also been used in a wide variety of other cosmic ray experiments. These have included experiments on the structure of muons in Extensive Air Showers (Earnshaw et al. (1967)), the measurement of the muon burst spectrum (Ashton and Coates (1966)), and the investigation of neutrino interactions deep underground (Achar et al. (1965) and Reines (1967)).

It can be seen from the types of experiments mentioned above that the flash tube has shown over the years to beaversatile and reliable device. In most of these experiments the discharged flash tubes have been recorded photographically and the film scanned with the use of a suitable projection system to reconstruct the event. However, as experiments have become larger, the problems of photography and scanning have increased, due to the increase in rate through larger apparatus, or, in fact, due to difficulties in photography because of the large size of the instrument. With the ready access to computers, an obvious solution to these problems is to digitise the flash tubes and read the experimental data directly into a computer, which could be programmed to analyse the event.

Because of the high rate of particles through M.A.R.S., a digitised flash tube system is an ideal solution since the dead time of the apparatus, which is required when a photographic method is used to enable the camera to be wound on to the next frame, can be considerably reduced.

4.2 Preliminary Investigation

The main requirement in this investigation was to produce a digitising technique which was simple, reliable, and cheap since it would be required for about 9000 flash tubes when used in M.A.R.S. The use of a neon bulb on the front of a flash tube could possibly satisfy these requirements as explained below.

It can be shown that adjacent flash tubes can be set off by a flashed tube if the outer wall of the tube is not made opaque by black paint or plastic material. It was thus thought that the neon bulb would respond in a likewise manner. A small neon bulb was thus arranged in front of a flash tube as shown in figure 4.1. The earthed copper cylinder was used to shield the bulb from pickup when the high voltage pulse was applied. Figure 4.2 shows the circuit used with the neon bulb. The voltage across the neon bulb was adjusted so that it was two volts below its striking voltage of 87 volts. The flash tube

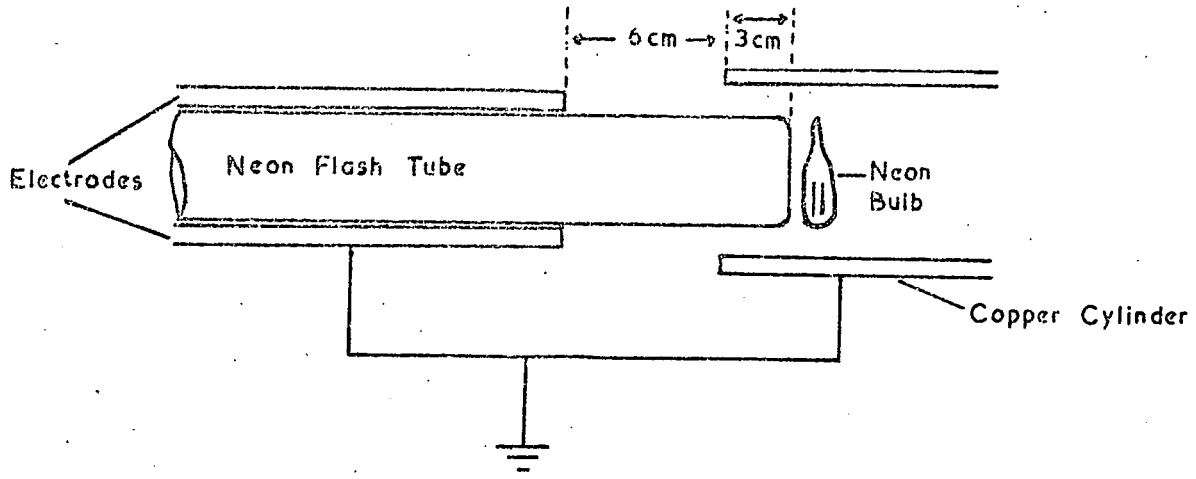

Figure 4.1 The Experimental Arrangement for the Preliminary Investigation.

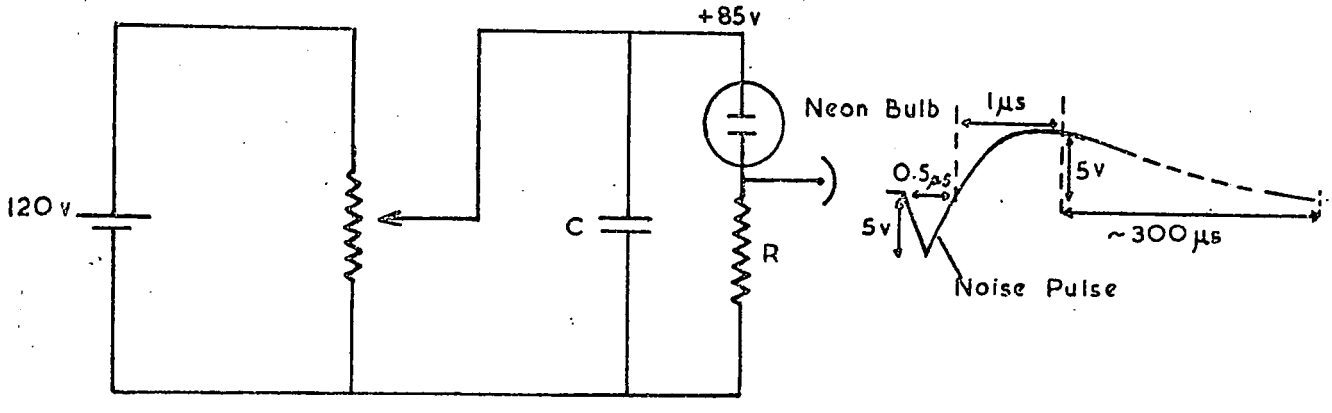

Figure 4.2 The Circuit Used with the Neon Bulb and the Output Pulse obtained with R = 3.3kΩ and C = 0.01μf.

was of length 1 metre, filled with commercial neon gas to a pressure of 60 cm of mercury, and had a mean internal diameter of 1.5 cm and mean external diameter of 1.75 cm. The high voltage pulse applied to the flash tube was obtained by discharging a 0.1μf. capacitor charged to a potential of 10 kV through a 100 ohm resistor. The pulse was negative in shape and had a peak height of 10 kV, giving an applied peak field of 5.6 kV cm^{-1}, and had a total length of 40μs.

The high voltage pulse was applied to the flash tube every three seconds. The flash tube was a special tube in the sense that it flashed every time a pulse was applied. This is probably due to radioactive contamination in the glass or gas or due to impurities on the glass surface producing a point discharge in the gas and hence a flash. It was found that a pulse was obtained when the tube flashed which was significantly different from the noise pulse obtained when the tube did not fire. A typical pulse obtained when the tube fired is shown in figure 4.2. The negative noise pulse was always present but the positive pulse was only obtained when the tube flashed. This pulse was for values of the resistor (R) of 3.3 kΩ and capacitor (C) of 0.01μf shown in figure 4.2 with the neon bulb arranged so that it was in contact with the front of the tube.

It was whilst carrying out tests on the efficiency of the system that it was noticed that if the front of the tube was blacked out the neon bulb still flashed whenever the tube fired. It was also found that when an earthed aluminium disc was placed between the flash tube and the neon bulb, no pulse was detected when the tube fired.

This suggested that there was an electric field effect producing the discharge of the neon bulb and not, as was first thought, a photon effect. It was this output effect from the flash tube which was subsequently investigated.

4.3. Further Investigation

For the investigation the flash tube was placed between parallel plate electrodes as shown in figure 4.3. The high voltage pulse was similar to that

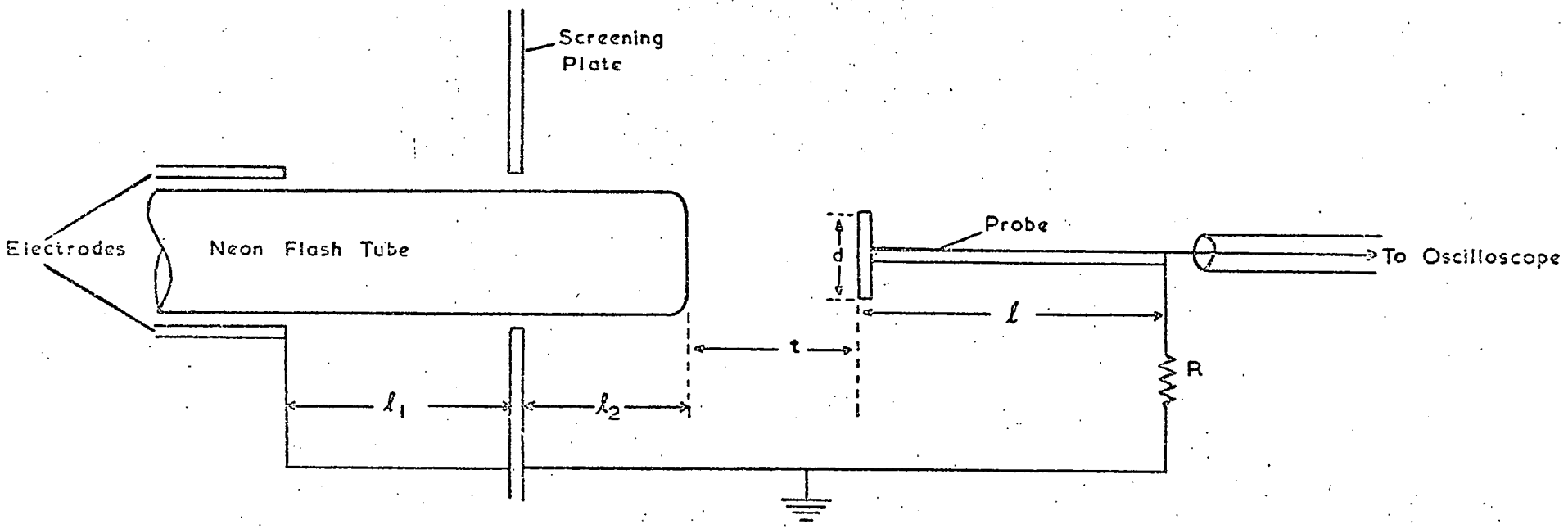

Figure 4.3 The Experimental Arrangement and Parameters Varied in the Examination of the Output Pulse from the Flash Tube.

used in the preliminary investigation.

A square screening plate of side 15cm was placed as shown in figure 4.3, its purpose being to reduce the noise pulse detected by the probe. This noise pulse comprised a short burst of high frequency oscillation lasting for about one microsecond, the magnitude of which was independent of whether or not the tube fired. When the flash tube discharged, an additional pulse was detected on the probe having a character different from that of the noise. It was found that there was a time delay of about one microsecond between the application of the high voltage pulse and the output pulse being detected if the tube flashed.

The useful pulse detected by the probe was similar in shape to the applied high voltage pulse. The form of the output pulse depends on the value of the probe resistance R in figure 4.3. The parameters shown in figure 4.3. had the values indicated in Table 4.1 throughout the investigation unless otherwise stated. The resistance R in Table 4.1 was the input impedance of the oscilloscope probe.

TABLE 4.1

The Values of the Parameters shown in Figure 4.3

l_1	l_2	l	t	d	R
2.5cm	1.0cm	1.25cm	0.1cm	0.71cm	$10^7\Omega$

The measured dependence of the pulse height on the length (l) and the diameter (d) of the probe are shown in figure 4.4 for the distances l_1 and l_2 in figure 4.3 equal to 3.5cm and 1.5cm respectively. Figures 4.4(a) and 4.4(b) show the variation of the output voltage on the probe diameter and length respectively.

Figure 4.5 shows the variation of pulse height and length as a function of the probe resistance R in figure 4.3 for the distance t in figure 4.3 equal to zero. As may be seen from figure 4.5 an output pulse of a desired length or height can be obtained by choosing a suitable value for the probe resistance. For a given pulse length the required pulse height can be obtained by tapping the required voltage across the probe resistance.

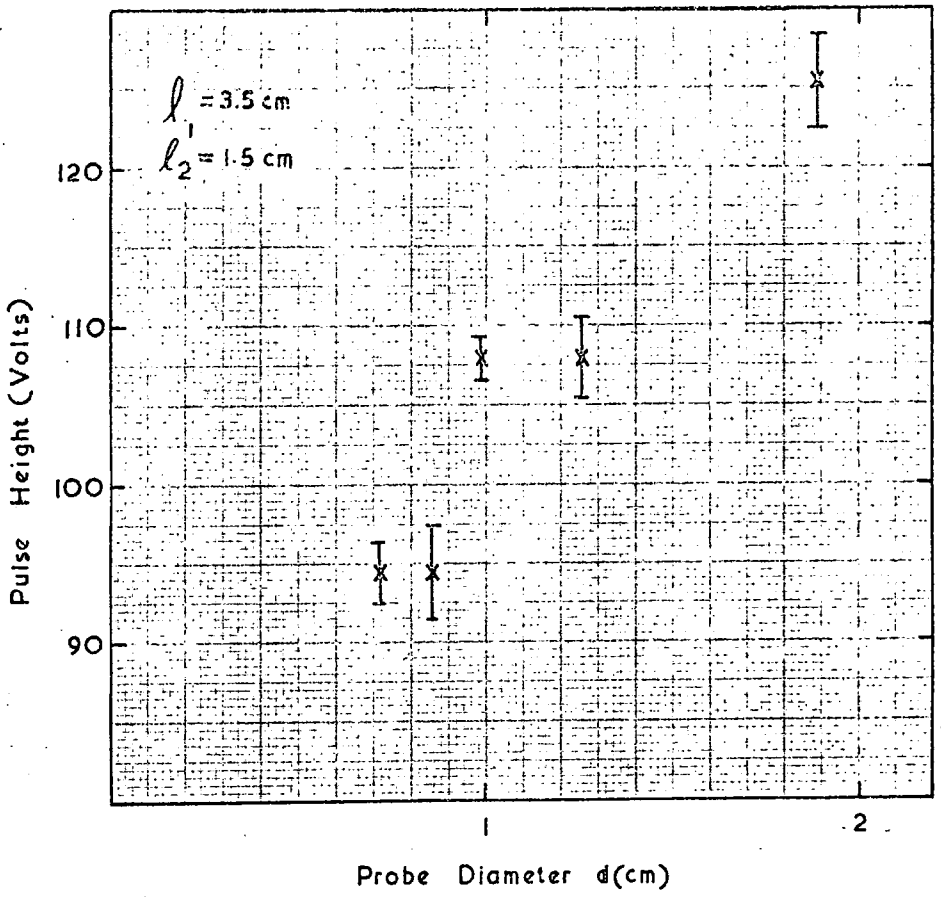

Figure 4.4(a) The Variation of Pulse Height with Probe Diameter.

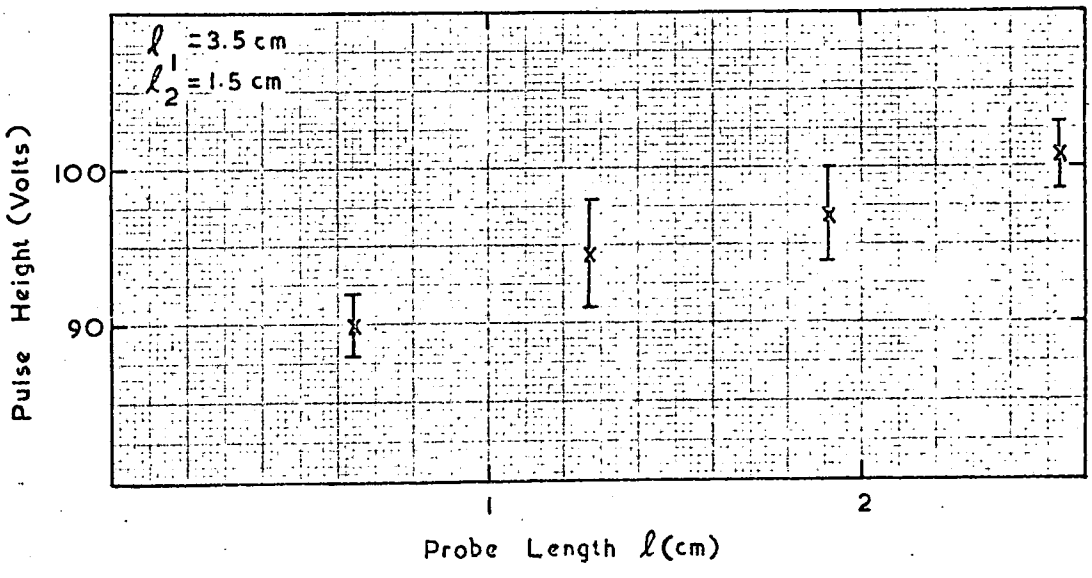

Figure 4.4(b) The Variation of Pulse Height with Probe Length.

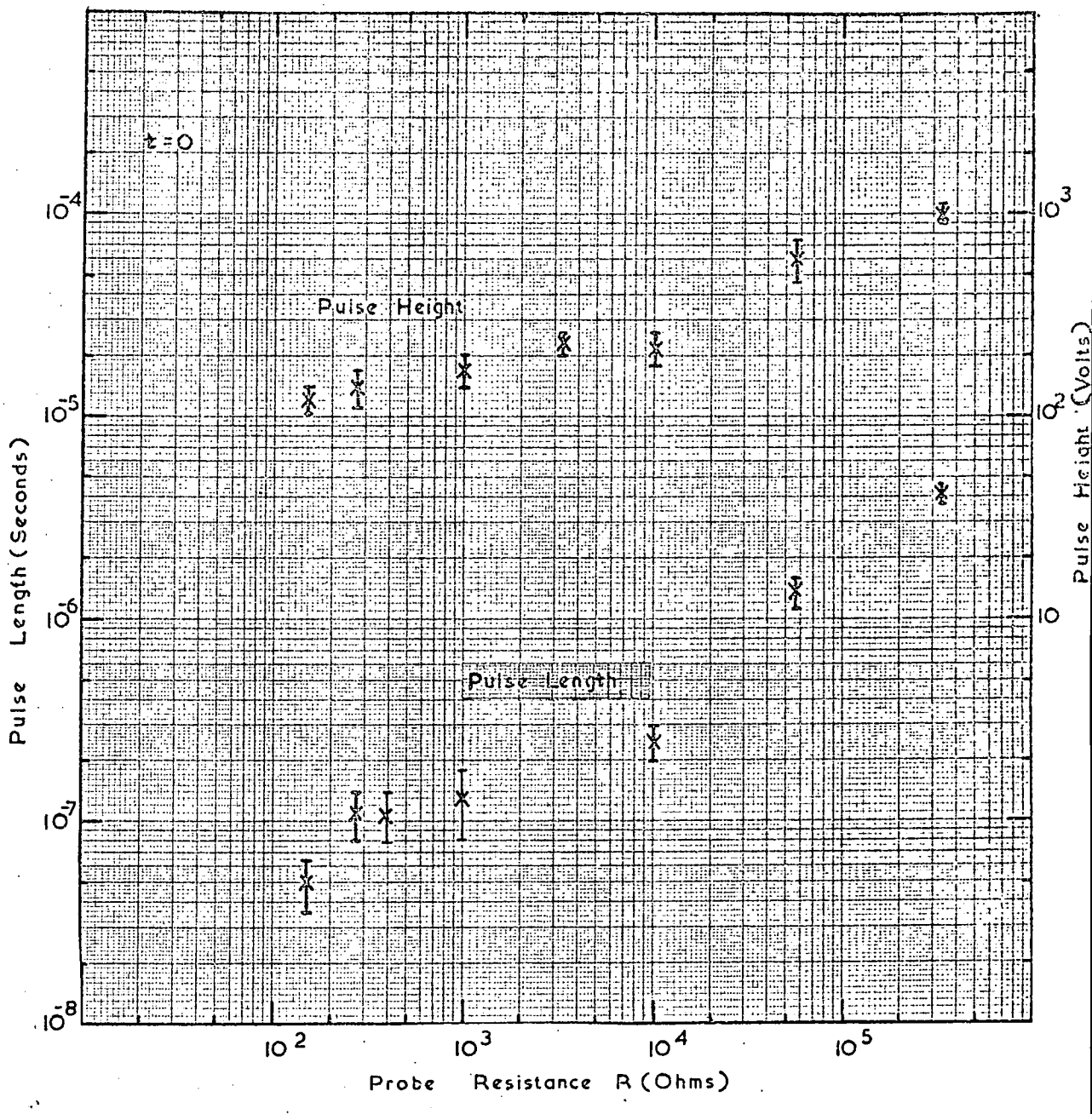

Figure 4.5 The Variation of Pulse Height and Pulse Length with the Probe Resistance.

The fluctuation in output voltage is shown in figure 4.6 for 200 pulses. A possible cause of the histogram having a cut off at high voltage values is discussed in §4.4. The variation of output pulse with distance of the probe from the tube (t) is shown in figure 4.7 for l_1 equal to 2.5cm and for values of l_2 of 0.5cm and 1.5cm, where l_1 and l_2 are the distances shown in figure 4.3.

A simple explanation of the detected pulse would be that it was due to free electrons, which have been produced in the discharge in the flash tube, diffusing into the end of the tube beyond the electrodes. The probe would then detect a voltage pulse due to the electronic charge density. A consequence of this argument is that the sign of the pulse detected by the probe will be independent of the sign of the high voltage pulse since electrons will diffuse irrespective of the sign of the high voltage pulse.

However, it was found that a positive pulse was detected when a positive high voltage pulse was applied across the tube. A delay line pulse was also applied to the flash tube. This was a square pulse of length 4μs. It was found that the output pulse was the same shape as the delay line applied pulse when the output from the probe was fed directly into the oscilloscope. These effects suggest that the pulse detected by the probe is caused by the effect of the main discharge in the tube, which is produced between the electrodes across the tube. The probe then picks up the main discharge through the glass surface by capacitive feed-through.

To investigate this effect further, the voltage inside the flash tube at its end was measured. A flash tube was constructed with a piece of platinum wire of diameter 20 S.W.G. (0.91mm) fixed in the plane end of the tube so that one cm of the wire was inside the tube. The flash tube had a mean external diameter of 1.75cm and contained commercial neon gas at a pressure of 60cm of mercury. It was placed between parallel plate electrodes as shown in figure 4.8(a) and pulsed randomly every three seconds. The same high voltage pulse was used as in the previous investigations. To ensure that the tube

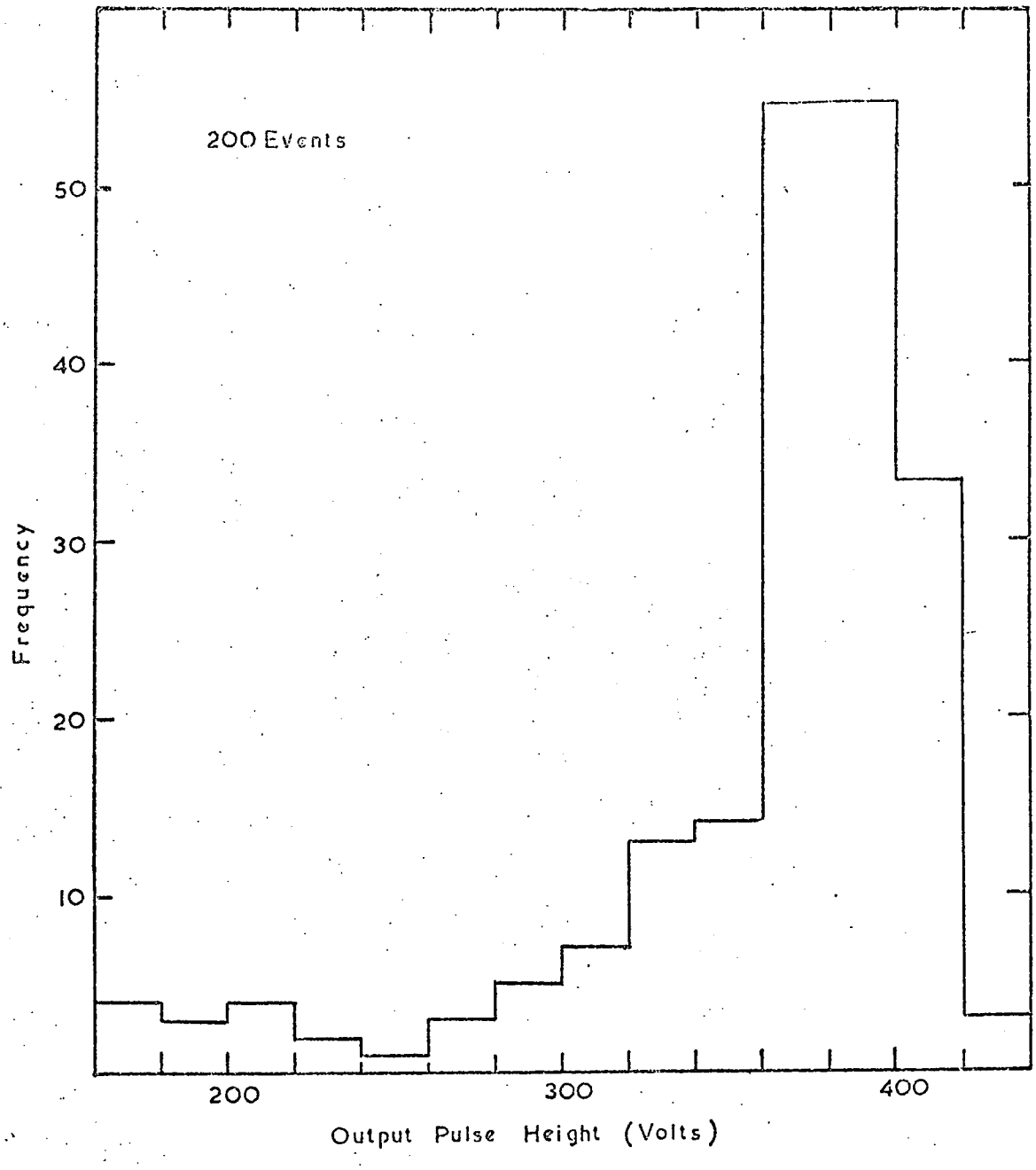

Figure 4.6 Histogram of the Pulse Height of 200 Events.

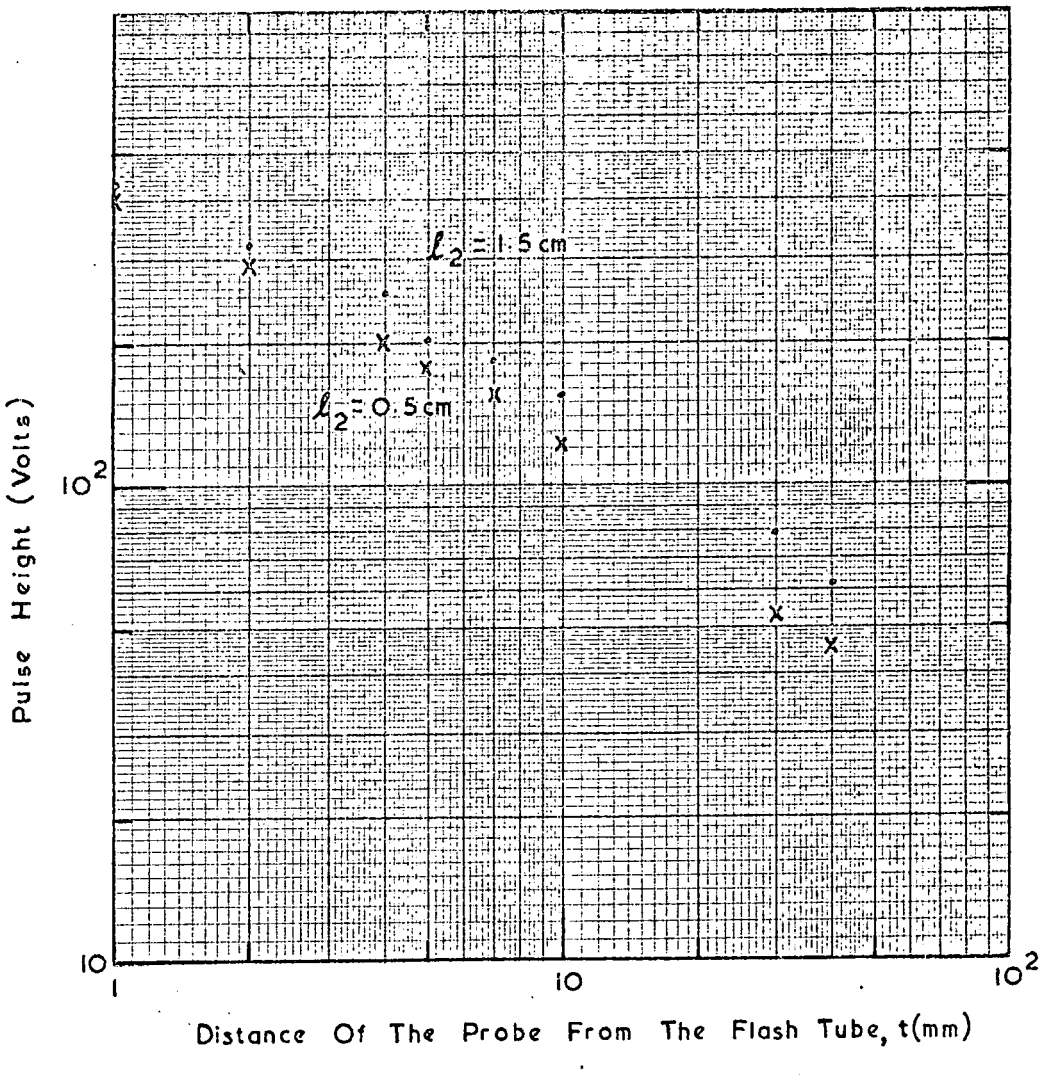

Figure 4.7 The Variation of Pulse Height with Distance of the Probe from the Flash Tube for Two Values of l_2.

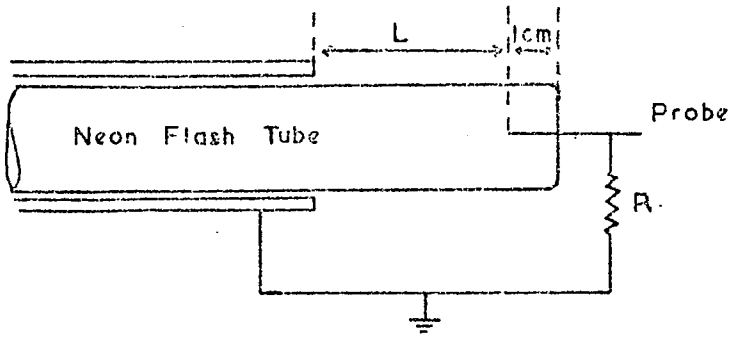

Figure 4.8(a) The Experimental Arrangement for Investigating the Voltage Pulse inside the Flash Tube.

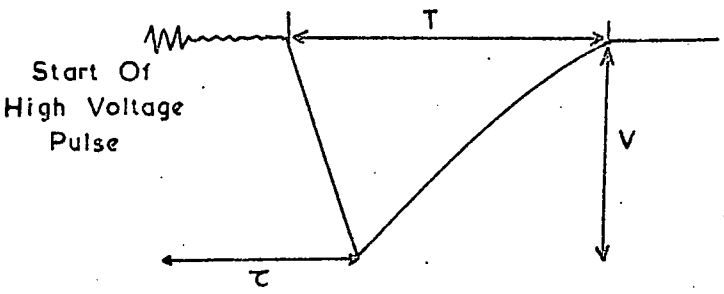

Figure 4.8(b) Form of Pulse obtained for an Applied Negative High Voltage Pulse and the Measured Parameters of the Pulse.

flashed nearly every time a small radioactive source was placed near to the flash tube.

It was found that there was a delay in the arrival of a pulse at the probe which depended on the distance (L) of the probe from the electrodes. The pulse height (V) and time (τ) required for the pulse to reach peak height from the start of the high voltage pulse were measured with an oscilloscope for various values of the distance (L) of the end of the probe from the electrodes, where V, τ, and L are shown in figure 4.8. Figure 4.8(b) shows the form of a typical output pulse for an applied negative high voltage pulse. The probe resistance R in figure 4.8(a) was equal to the oscilloscope probe impedance of 10^8 ohms.

The procedure was repeated using a high voltage positive pulse of the same peak height and length as the negative high voltage pulse. Figure 4.9 shows the variation of V and τ with L for an applied negative high voltage pulse and figure 4.10 shows the same variation but now for a positive applied pulse. A comparison of figures 4.9 and 4.10 show that the same peak output pulse and delay is obtained, within the experimental errors, for both positive and negative applied high voltage pulses. The results of this experiment are discussed in §4.4.

The pulse length of the output pulse, which is equal to T in figure 4.8(b), was found to be constant over all values of L for both positive and negative high voltage pulses and was of value 21μs. Similarly the total rise time of the pulse from zero to peak height was found to have a constant value of 0.3μs. over all values of L for both positive and negative applied high voltage pulses.

To investigate how the pulse obtained with the probe varied as a function of probe resistance R, the pulse height and length were measured for various probe resistances for a fixed value of L of 1cm and using a negative applied high voltage pulse. Figure 4.11 shows the variation in pulse height and pulse length as a function of the probe resistance R.

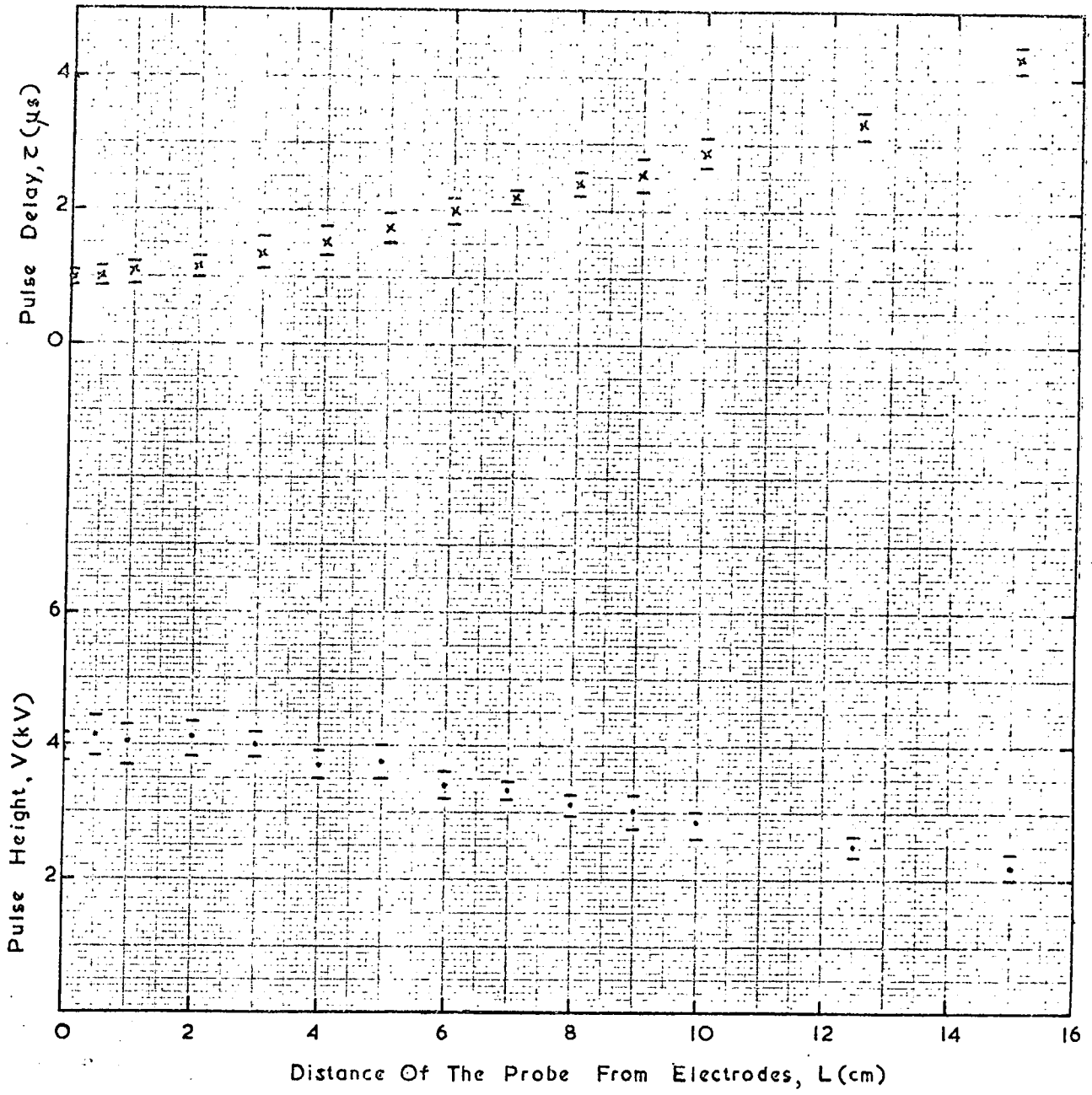

Figure 4.9. The Variation of Pulse Height and Pulse Delay with Probe Distance for an Applied Negative High Voltage Pulse.

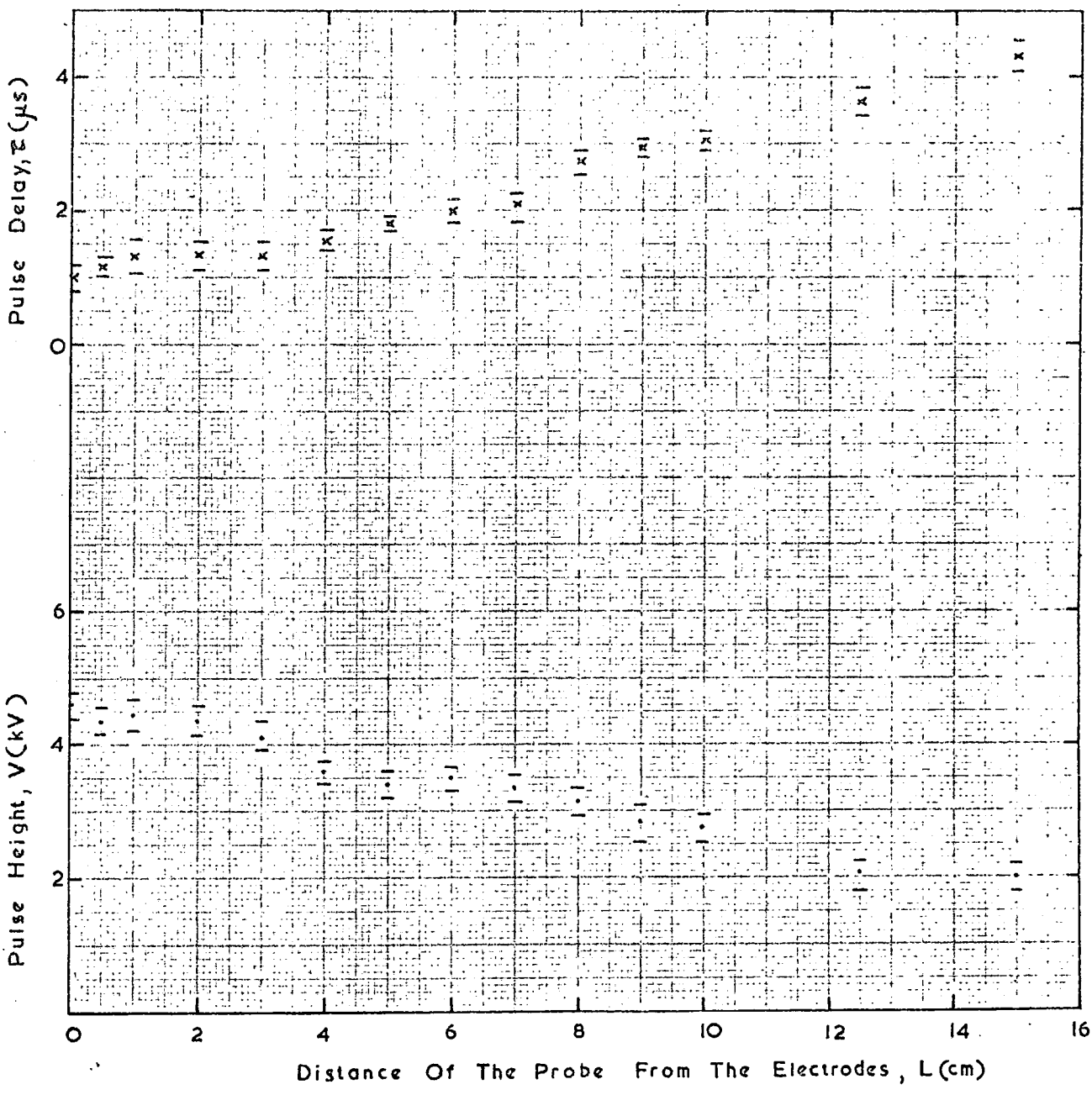

Figure 4.10 The Variation of Pulse Height and Pulse Delay with Probe Distance for an Applied Positive High Voltage Pulse.

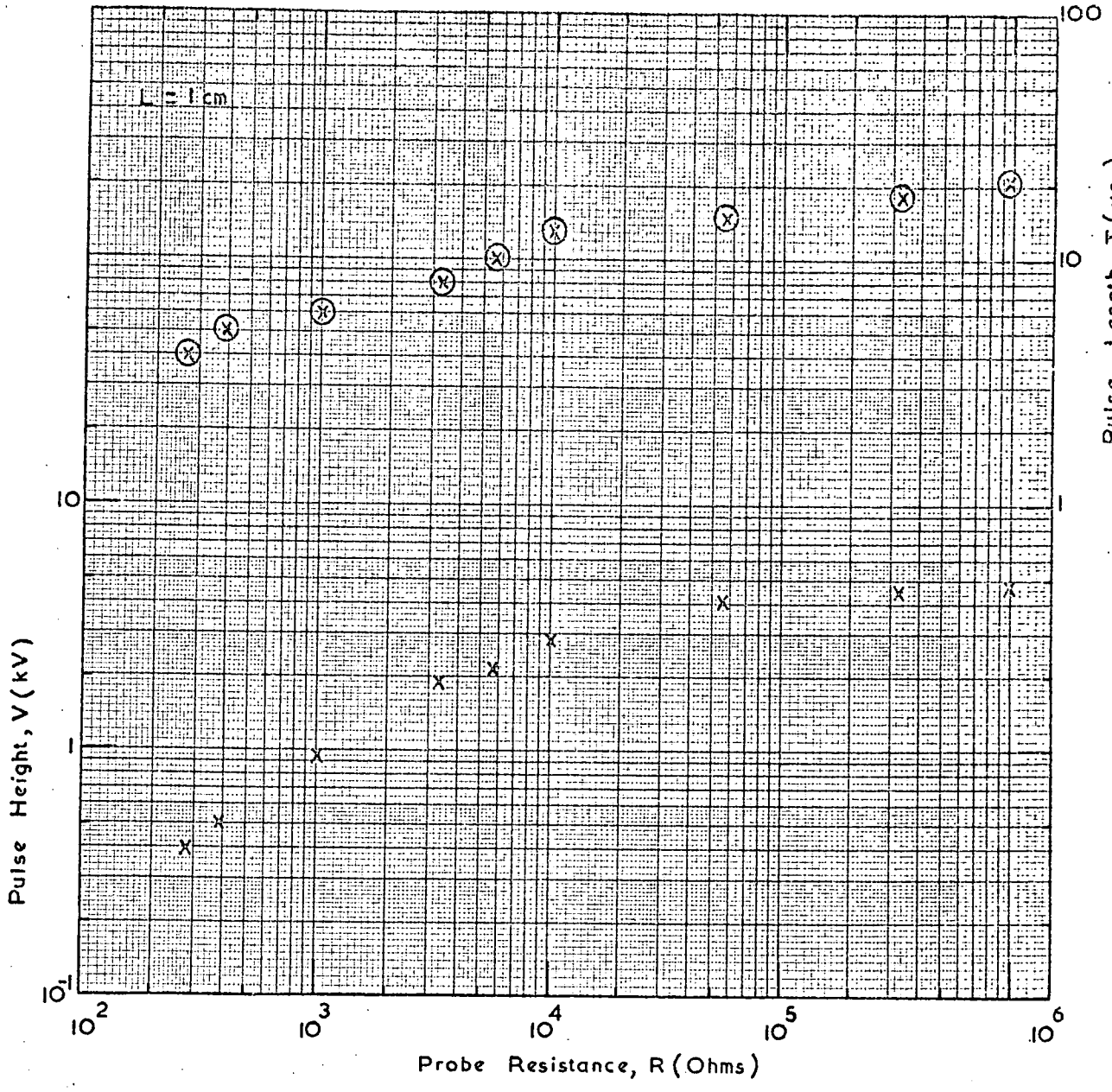

Figure 4.11 The Variation of Pulse Height and Length with Probe Resistance for an Applied Negative High Voltage Pulse.

4.4 Discussion

The results obtained with a wire probe fixed in the end of a tube show that an appreciable electric field is produced at the end of the flash tube which is not covered by the electrodes. This effect could be seen in the flash tube as a visible discharge to the probe end. The discharge to the probe became stronger as the distance of the extruded part of the flash tube was reduced. This is in accordance with the results of figures 4.9 and 4.10 which show that the probe voltage increases as the probe is moved closer to the electrodes. The discharge to the probe was independent of whether or not the probe was connected to the earth electrode. This is because the probe, as seen by the voltage in the tube, is effectively at earth potential.

So far the discharge in the end of the tube not covered by the electrodes has only been studied with the flash tube having a built in probe. To see whether the effect was present in a normal flash tube, an unpainted flash tube of the same size as the probe flash tube was placed between electrodes in a similar arrangement, shown in figure 4.8(a), to the probe flash tube with L equal to 15cm. The same negative high voltage pulse was applied as before and the tube was pulsed randomly every three seconds with a radioactive source close to the tube.

When the tube flashed, the discharge in the tube between the electrodes was of the normal streamer type, as reported by Coxell et al. (1961). However, in the region of the tube where no electrodes were present a diffused type of discharge was seen. It was easily shown that the effect was due to a discharge in the gas and not to light from the main discharge passing along the tube by touching the side of the glass wall. A discharge was seen to form in the gas to the point being touched. It was also noted that the discharge could be enhanced if a metal cylinder, which may or may not be earthed, was placed over the protruding end of the flash tube. The discharge in the tube covered by the cylinder was found to be greatly increased in intensity. This is due to the cylinder effecting the electric field direction and thus producing in the

gas a strong discharge. The effect is also present when the earth electrode was extended to cover the whole tube in the normal manner, with the high voltage electrode not covering the 15cm at the end of the tube. Then a strong discharge was produced along the inside flash tube surface nearest to the electrode.

The above results, which were obtained in a flash tube with no probe in its end, show that a discharge is still present in the gas outside the main discharge region covered by the electrodes. One possible, though qualitative, explanation of the effect is that the gas outside the electrodes is ionised by ultra violet photons produced in the main discharge. The electrons thus produced by the photoionisation will be effected by the electric potential produced in the main discharge, which will result in a potential being produced at the end of the tube by movement of the electrons. The positive ions produced in the photoionisation will not move during the effect of the main discharge because of their heavy mass compared to the electron.

The field effecting the electrons in the end of the tube not covered by the electrodes must be produced by the potential in the main discharge because the field due to the edge effects of the electrodes, when a high voltage pulse is applied, is negligible. Recent calculations by Ashton et al. (in the press) have shown that the applied high voltage pulse on the electrodes produces an electric field of strength less than $0.005\ E_o$ at distances along the axis of a flash tube greater than 4cm from the electrodes, where E_o is the value of the electric field in the unifrom region between the electrodes. As the discharge is seen for distances of the extruded tube greater than 10cm, the effect of the electrode field at those distances can be neglected.

The effect of the main discharge potential, takes a finite time to pass down the extruded tube. This is seen from the graphs shown in figures 4.9 and 4.10 which shows the delay time for a pulse to be detected by the probe for positive and negative high voltage pulses respectively. The graphs are approximately linear and an analysis of their gradients gives an approximate value of this velocity wave of $\sim 5 \times 10^6$ cm $sec.^{-1}$

The electrons produced by photoionisation at the end of the tube will move under the effect of the potential of the main discharge, the direction of movement depending on the sign of the applied high voltage pulse and during their motion produce the diffused discharge observed in the volume by collision with neon atoms.

Any external probe will pick up the discharge through the glass surface by capacitive feed-through. An interesting point to note is that with an external probe a pulse length is obtained for a high value of the probe impedance which is longer than the applied high voltage pulse as can be seen from the graph of figure 4.5. This is due to the charge distribution remaining at the tube end after the passage of the high voltage pulse. This effect is not present with an internal probe because the probe will distort the field inside the tube by producing a secondary discharge, as described above.

The graphs of the variation of the peak output voltage with the distance of the internal probe from the electrodes for positive and negative high voltage pulses, which are plotted in figures 4.10 and 4.9 respectively, show that the peak output voltage was never greater than half the appliedvoltage. This is an effect of the main discharge, which will be such that there is a very small potential difference across the tube during the discharge. The effect on an external probe will result in a maximum output voltage being detected by a probe.

This explains the cut off observed in the pulse height distribution found when a probe was used on the outside of the tube to detect the pulse as shown in figure 4.6. Smaller pulses than the maximum will be caused by the jitter in the tube flashing.

4.5 Design Considerations for Arrays using the Probe Digitisation Method

If an array of flash tubes is designed to use this digitisation method, then the individual probes must be shielded to prevent pickup when a neighbouring tube fires. A suitable form of shielding is an earthed metal cylinder which

fits over the probe and part of the flash tube to completely shield the probe. The probe could be held centrally inside the tube cylinder using a cylinder of suitable insulating material such as Perspex. It is also desirable to use the probe against the front of a tube so that it detects the highest possible output voltage. Any attenuation required can be obtained with a suitable resistor, or resistors, connected to the probe.

As the shield passes over part of the flash tube, the flash tube will have to protrude slightly from the electrodes to prevent breakdown from the high voltage electrodes to the shield. This distance also governs the peak height and delay of the pulse so the smallest distance of the end of the flash tube to the high voltage electrodes, which is within the safety range, should be used.

The use of cylinders as shields raises an obvious practical difficulty in the method of support of the shields in front of the tray so that the support holds the probes rigid against the front of the flash tubes. A solution to this is to use a thick metal block into which are drilled holes of sufficient diameter to accomodate a flash tube. The probe is held in a Perspex cylinder which is fixed symmetrically inside the block. The front of the flash tube then fits in the block against the probe.

The flash tube could be positioned correctly in an array by using similar, though less thick, plates at the front and back of the flash tube tray. These plates could be drilled at the same time as the probe shield using a special drilling machine. This would thus save man power in making further flash tube supports for any tray using this digitisation method.

This method of probe shield and flash tube supports was used on two prototype arrays for low and high pressure flash tubes as described in the following two sections.

4.6 The Prototype Array

So far investigations on only a single flash tube have been carried out. It was thus necessary to try an array of tubes to see whether the technique

would work satisfactorily on a large scale.

Consequently, a tray of flash tubes was constructed as shown in figure 4.12, which shows a cross-sectional view of the tray. The distances indicated in figure 4.12 are listed in Table 4.2, for the low pressure tubes. The tray consisted of four layers of one metre long tubes of mean external diameter 1.75cm containing commercial neon gas at a pressure of 60cm of mercury. There were fifteen tubes per layer with a tube spacing of 2cm in each layer. The earth screening plate was replaced by a dural shield of thickness $1\frac{1}{2}$" (3.81cm) into which were drilled holes to accomodate the probes. The probes were 1" long 6 B.A. brass countersunk screws with washers on their heads, so that the diameter of the probe head was 0.71 cm. The probes were held in Perspex cylinders of length 1.9cm inside the holes, the cylinders being fixed inside the holes by adhesive. The dural block, as well as shielding the probes from noise from the high voltage pulse and pickup when a neighbouring tube flashes, also ensures that the probes fit rigidly against the front of each flash tube.

TABLE 4.2

The Dimensions of the Prototype Flash Tube Arrays

l_1	l_2	d	Flash Tube
5.0cm	1.0cm	1.8cm	Low pressure
1.5cm	1.5cm	0.8cm	High pressure

Using the method discussed in §4.5, the flash tubes were held rigid and parallel in the tray by two $\frac{1}{8}$" thick plates of brass, having the same stagger as the holes for the probes, which were fixed at the front and back of each tray. The front plate then enabled the probe shield to be removed if required without moving the flash tubes.

The flash tubes used in the tray were covered by a tube of black plastic material to prevent the flashing of adjacent tubes. This plastic covering was

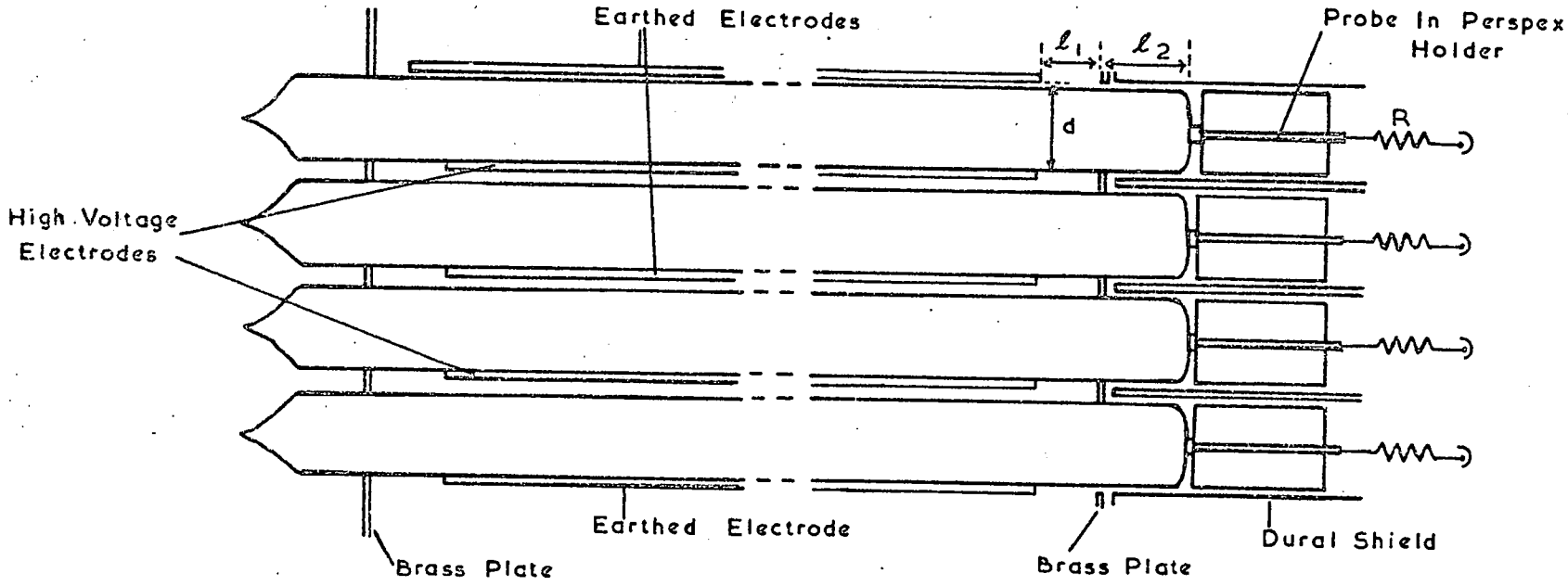

Figure 4.12 Cross-sectional View of the Prototype Arrays (Parameters shown in the figure are listed in Table 4.2).

clearly seen to be a disadvantage as it could easily be torn when the tubes were fed through the holes in the brass plates during the filling of the tray if extreme care was not taken. It was thus concluded that flash tubes using this method of support and digitisation should be painted black instead of using the plastic covering.

The tray being digitised was placed between two further trays of flash tubes as shown in figure 4.13. These trays contained the same type of flash tube as the special tray except that the tubes were closed packed in the trays and had no digitisation electronics. Two scintillation counters were placed above and below the stack. A coincidence pulse between the two scintillation counters was used to trigger a pulsing unit which applied a high voltage pulse to the flash tube trays. The pulse was of similar form as that used in the investigations with a single flash tube and produced efficient tracks in the array. The event was photographed by a camera and figure 4.14 shows a block diagram used in the experimental arrangement.

The flash tube tray to be digitised was first tested to examine the output pulse obtained from a flash tube when it fired. The variation in pulse height and length as a function of the probe resistance R in figure 4.12 is shown in figure 4.15, when the resistance is connected to earth. The resistance R which was finally used comprised two resistors in series so chosen that the output pulse when a tube flashed was of total length about four microseconds and peak height four to five volts. The pulse could then be used to trigger a suitable memory comprised of integrated circuit blocks. The values of the resistors chosen were 39kΩ and 1.8kΩ, the voltage produced across the 1.8kΩ resistor was then taken as the output. The 1.8kΩ resistors were fixed on a printed circuit board in front of the tray and the 39kΩ resistors were placed between the probe and the board. An aluminium box was fitted over the probe shield and printed circuit board to reduce electrical pickup. A typical output pulse is shown in Plate 5, the oscilloscope setting being 2 volts cm^{-1} and 1 μs cm^{-1}. Figure 4.16 shows a histogram of the output pulse for 240

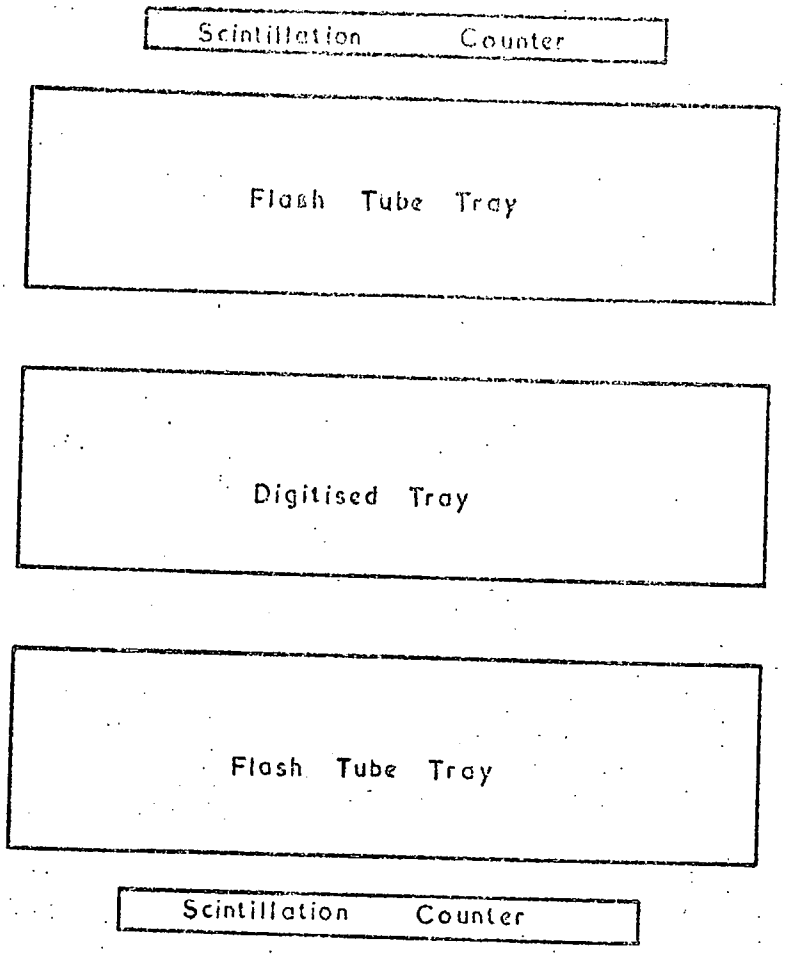

Figure 4.13 The Experimental Arrangement using the Prototype Array.

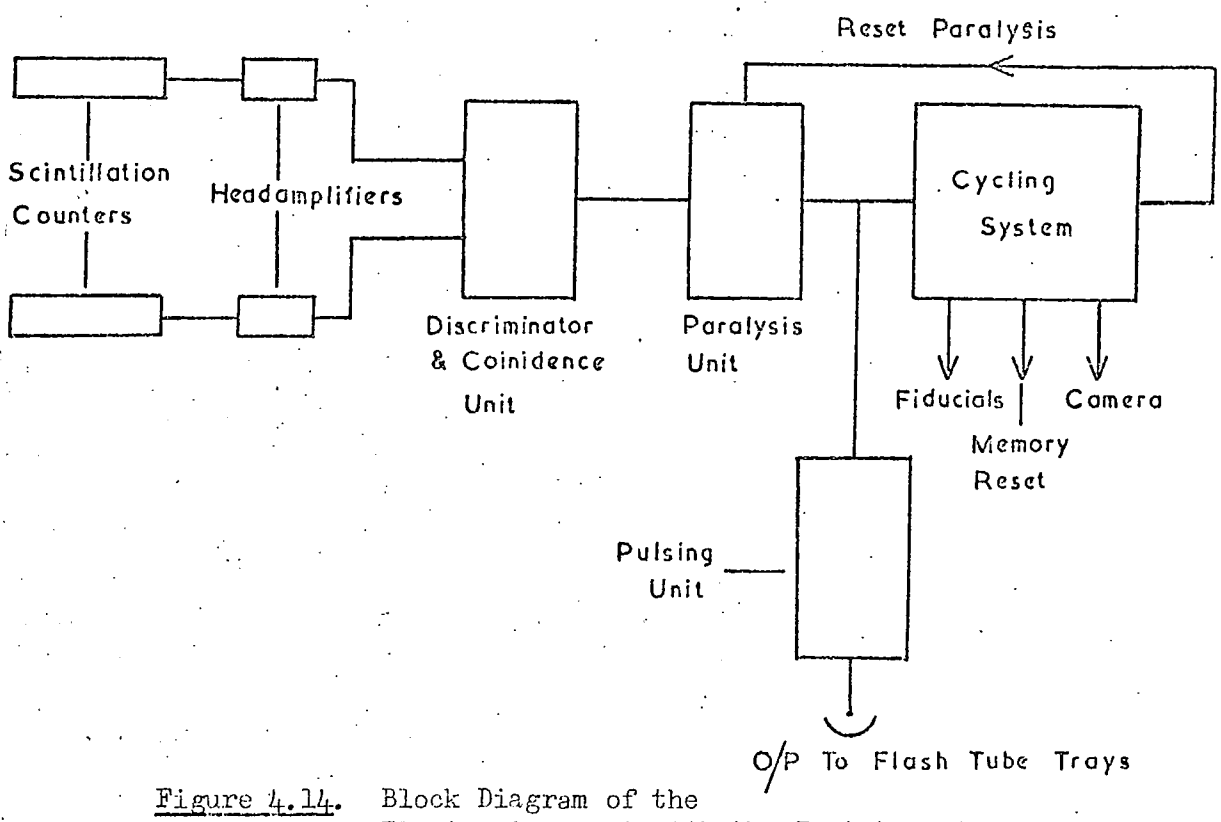

Figure 4.14. Block Diagram of the Electronics used with the Prototype Array.

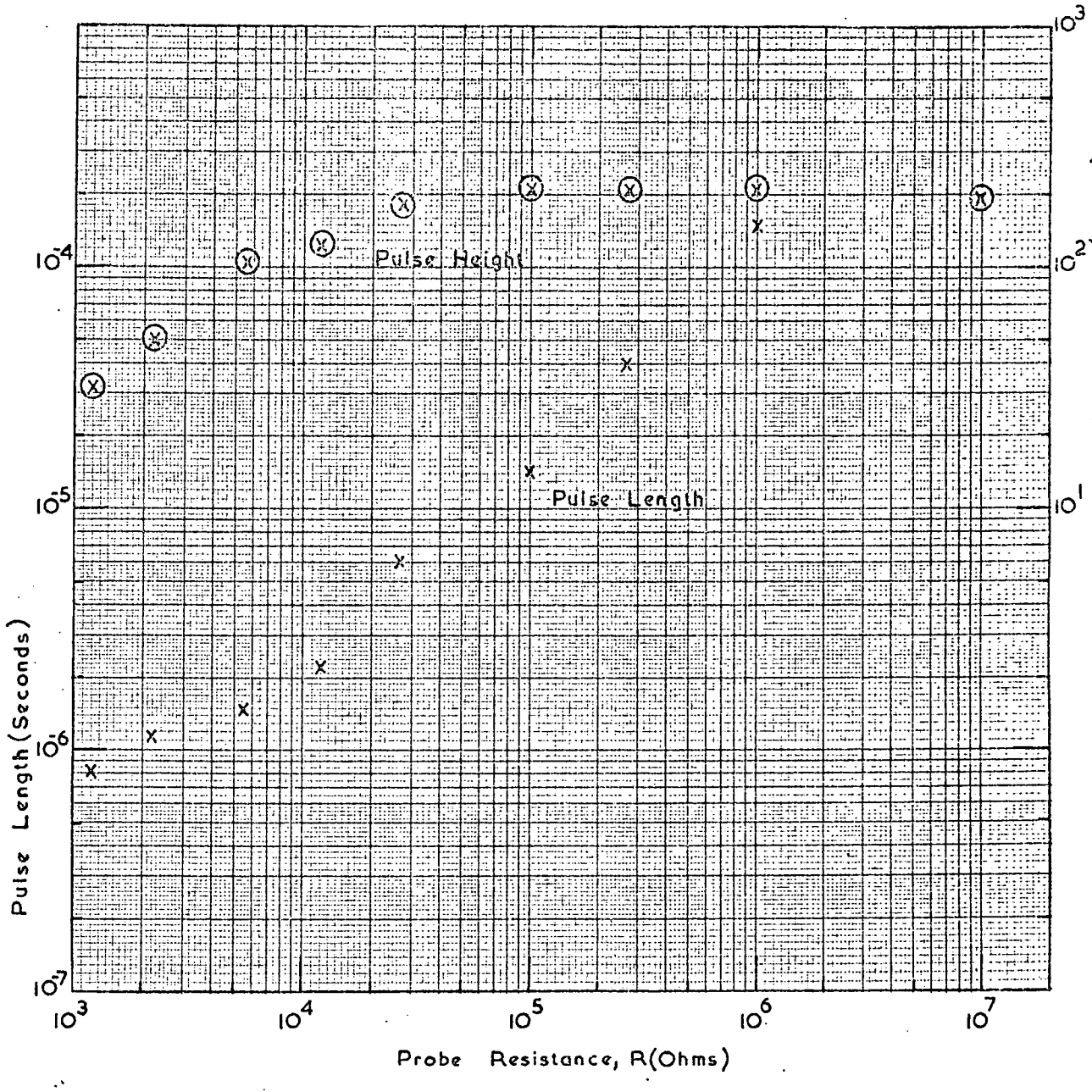

Figure 4.15 The Variation of Pulse Height and Length with Probe Resistance.

PLATE 5

A Typical Output Pulse from a

Flash Tube in the Prototype Array

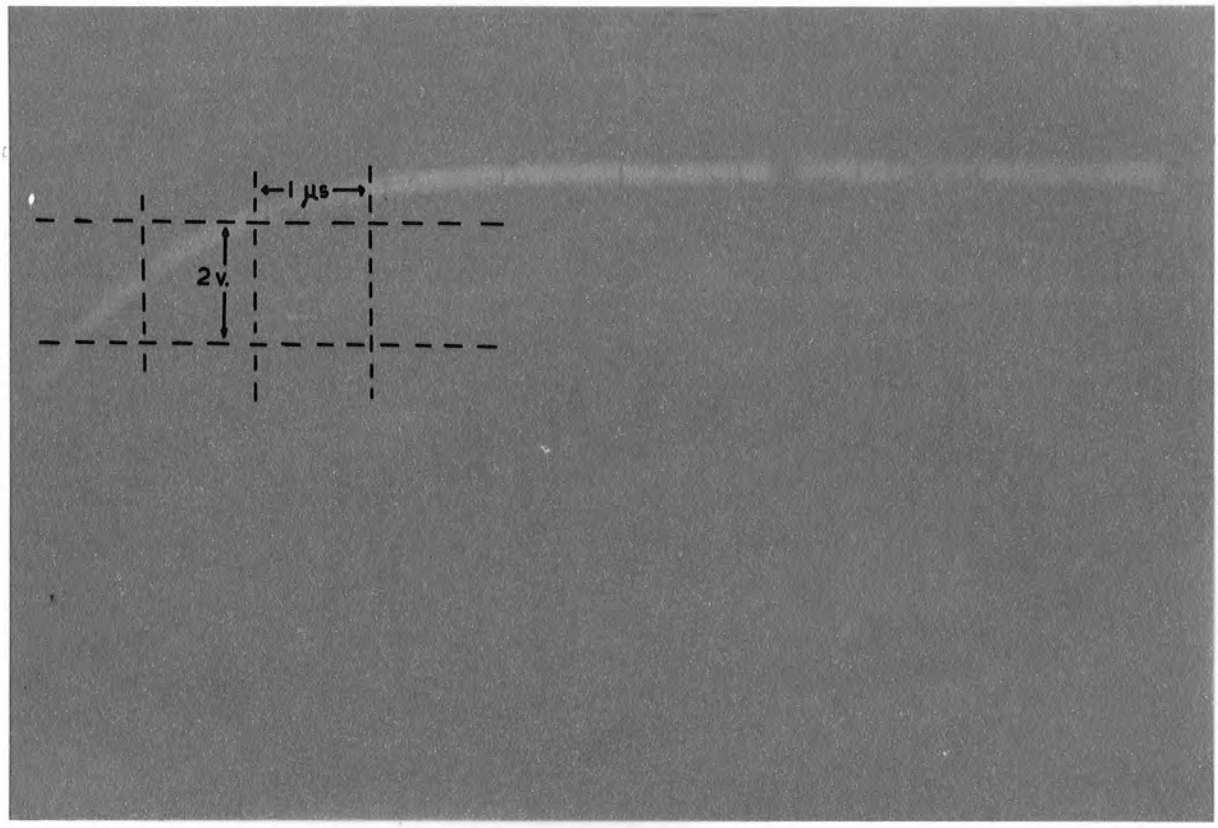
1 μs
2 v.

events when the output from the probe is fed directly into an oscilloscope of input impedance 10^7 ohm with no output resistor.

The results described above were obtained from flash tubes picked at random from the array. However, all the flash tubes were tested when the two output resistors were connected to the probes. The output pulses were found to be in the required voltage range for all the flash tubes in the array.

It should be mentioned that no direct comparison is possible between the results obtained in the earlier investigations and the prototype array results. This is because the shielding of the probes is different in the two cases although the same form of high voltage pulse is applied to the flash tube.

A block diagram of the digitisation electronics of each flash tube is shown in figure 4.17. The output from the probe resistors is connected to the input of an electronic memory composed of integrated circuit DTL nand gates. The output pulse from the probe is negative in shape so the input to the memory is held in the logical 1 state by connecting the 1.8kΩ resistor to a voltage level of +4 volts as shown in figure 4.17. The pulse from the flash tube probe causes the input level to the memory to switch from a logical 1 to a logical 0 state, thus causing the memory to be set. The memory is reset by the cycling system momentarily changing the reset line from a logical 1 state to a logical 0 state. A more detailed description of the electronics used for the flash tube memories is given in Chapters 5 and 6.

For the test tray, each flash tube memory had an indicator bulb as shown in figure 4.17. The bulb was in the on state if the memory had been changed from the normal off mode. The indicator bulbs are arranged so that they could be photographed by the same camera recording the particle track in the trays. The form of the indicator bulb used is described in Appendix A.

The flash tube fronts of the digitised tray could not be photographed because of the probes, printed circuit board, and shield over the front of the tray. Hence the backs of the flash tubes were photographed using a system of

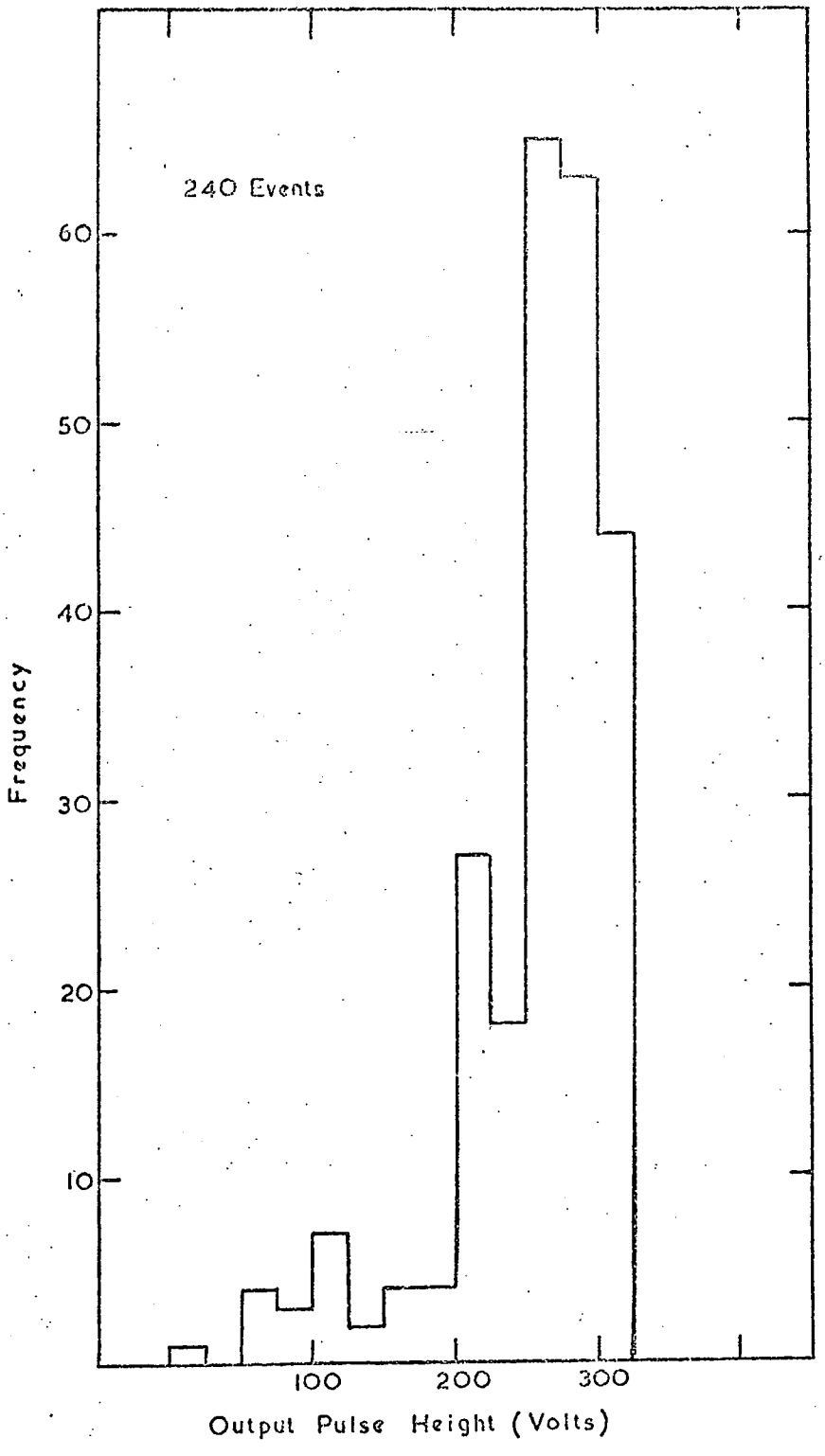

Figure 4.16 Histogram of the Pulse Height of 240 Events.

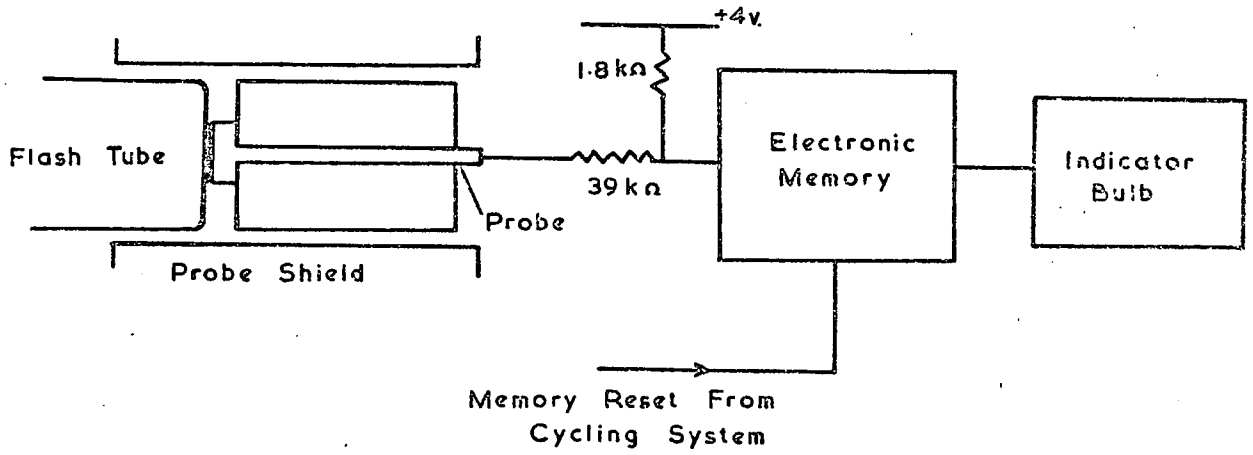

Figure 4.17 Block Diagram of the Digitisation Electronics.

mirrors at the back of the tray. The photograph of an event thus contained the flashed tubes from the three trays together with the output from the digitisation memories. A typical event is shown in Plate 6 . The trays and indicator bulbs are marked on the plate. The image of the backs of the digitised tray are weak and show the irregular shape because the light is viewed through the sealing nipple at the end of the tray. Each tray had two or more fiducial bulbs which were used to determine the flash tubes which had fired and the memories set when the events were scanned.

An analysis of the events showed that electronic recording of flash tube information is possible using a simple probe to detect a pulse when the flash tube fired.

4.7 The High Pressure Neon Flash Tube

The results so far described have been for tubes of mean external diameter 1.75 cm and pressure 60 cm of mercury. An investigation was also carried out on the small flash tubes which have an external diameter of about 8 mm and pressure 2.4 atmospheres. The properties of these tubes have been described by Coxell and Wolfendale (1960).

Flash tubes of a similar type are used in M.A.R.S. in the Measuring Trays, the only difference being that the tubes in M.A.R.S. are two metres long compared with the one metre length in a prototype array constructed with these tubes. The array contained four layers of tubes and was of similar form as the prototype array for the low pressure flash tubes shown in figure 4.12. The dimensions shown in figure 4.12 have the values listed in Table 4.2 for the high pressure tubes.

The probes used were 1" long 6 B.A. brass countersunk with washers on their heads so that the diameter of the probe head was 0.71 cm. The probes were fixed inside the dural shield in a similar manner to the probes for the large diameter flash tubes. The pulse applied to the flash tubes was also similar in form to the pulse used for the large diameter tubes. Scintillation counters

PLATE 6

A Typical Event Using the Proto-

type Array.

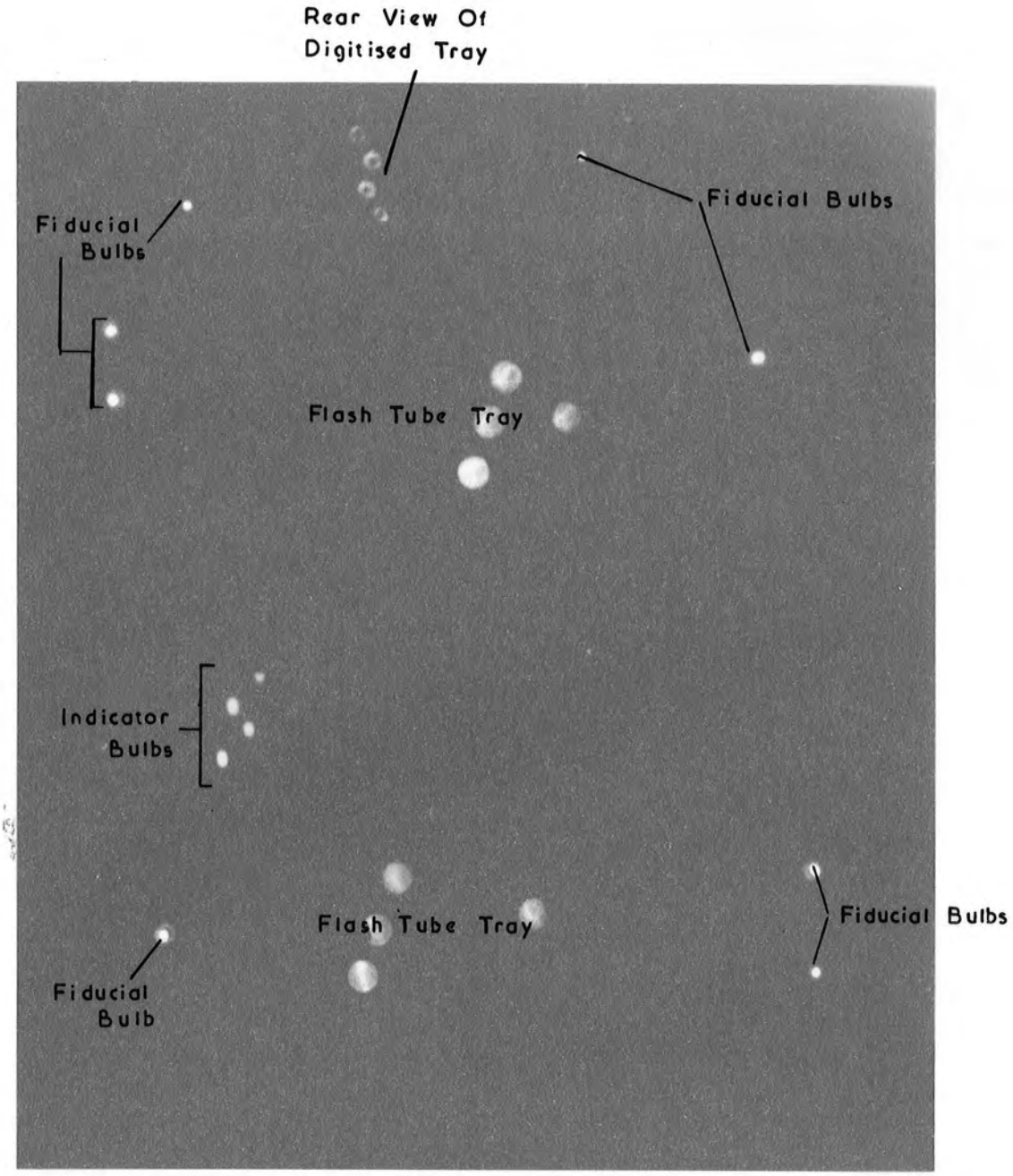
Rear View Of
Digitised Tray
Fiducial Bulbs
Fiducial Bulbs
Flash Tube Tray
Indicator Bulbs
Flash Tube Tray
Fiducial Bulbs
Fiducial Bulb

were placed above and below the flash tube tray and the high voltage pulse was applied to the tray when a two fold coincidence pulse was obtained from the scintillation counters.

The variation in pulse height and length as a function of the probe resistance R in figure 4.12 is shown in figure 4.18 when the resistance is connected to earth. These results are for one flash tube in the array picked at random, though several tubes were tested for the output pulse when the pulse was fed directly into an oscilloscope probe of impedance 10^7 ohms. The pulses examined in this way from several flash tubes were found to agree within the experimental error. A histogram of the pulse height from a flash tube is shown in figure 4.19 for events when the probe is connected directly into an oscilloscope of impedance 10^7 ohm.

A direct comparison between the pulse shapes obtained for the low and high pressure tubes for the same value of the resistance R is not possible. This arises from the fact that the distance of the probe for the high pressure tube is only 1.5 cm from the flash tube electrodes compared with a distance of 5 cm for the probes in the low pressure tubes. There will also be some effect in the pulse caused by the digitisation shield being nearer to the probe for the high pressure tubes, as these have smaller diameters, than for the low pressure tubes.

The results described above for the high pressure tubes show that a pulse suitable for the digitisation of the flash tube can be obtained from the high pressure tubes in a similar manner to the low pressure tubes. This method is used in M.A.R.S. as will be explained in Chapters 5 and 6 for both the low and high pressure flash tubes.

4.8 Previous Methods of Digitisation

4.8.1 Introduction

Several methods of obtaining the information from neon flash tubes other than the normal film photography have previously been developed. A brief outline of the methods used is given below.

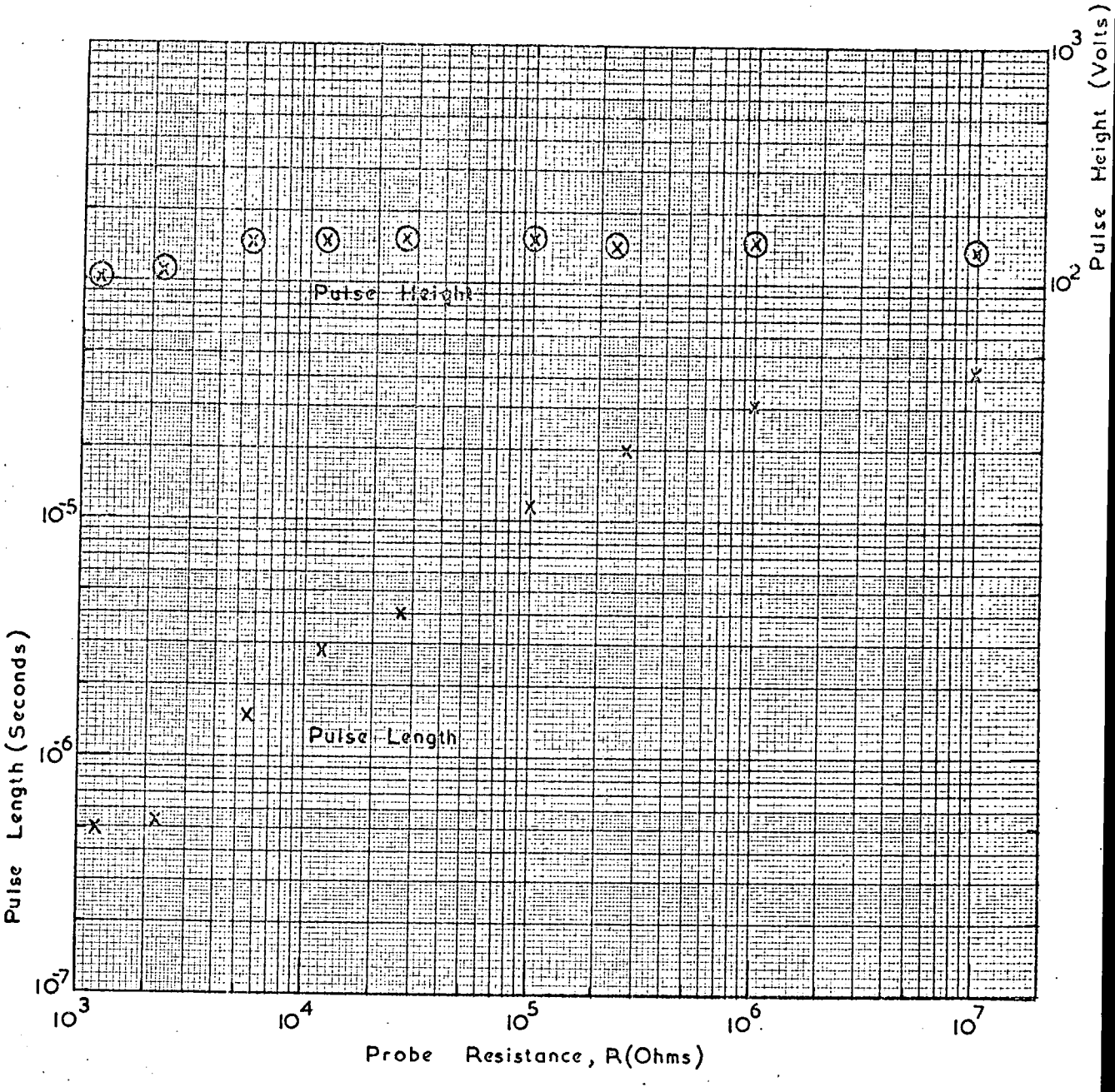

Figure 4.18 The Variation of the Pulse Height and Length of the High Pressure Flash Tubes with Probe Resistance.

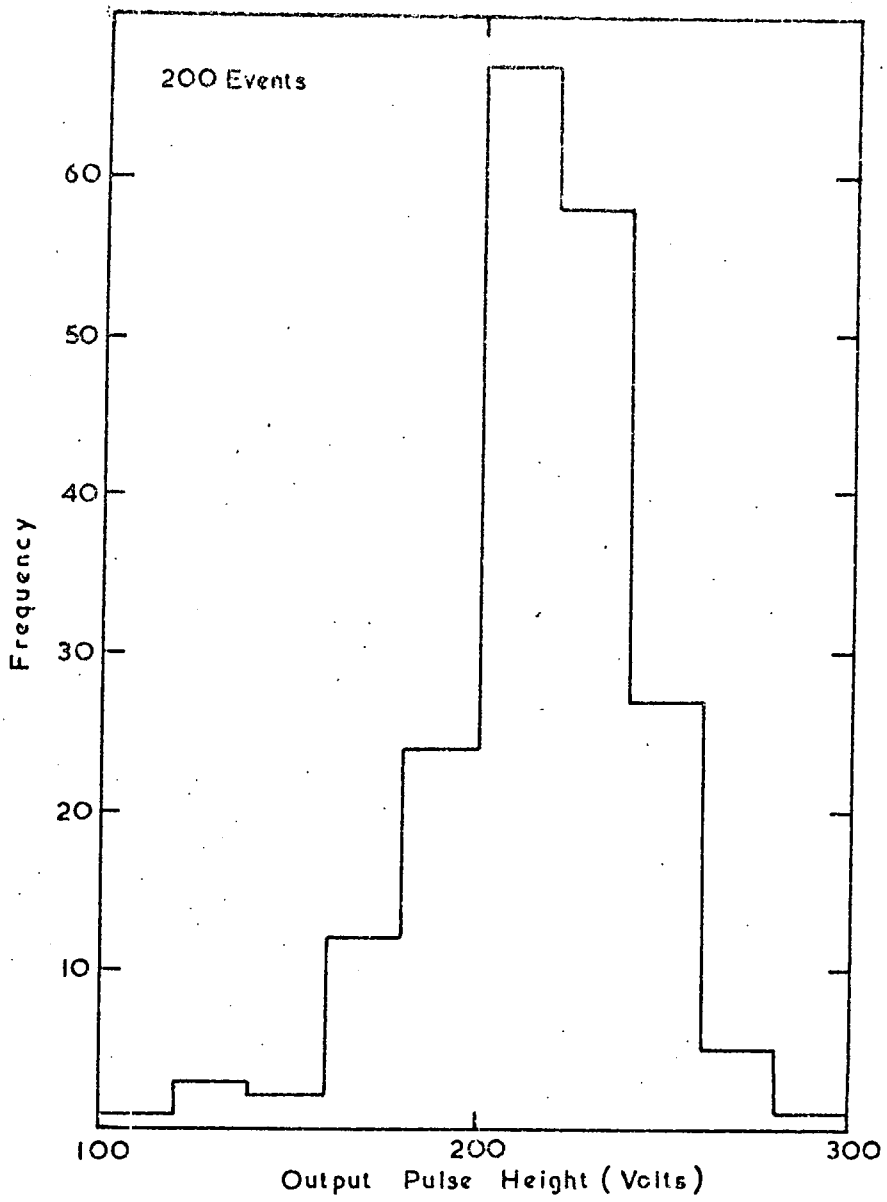

Figure 4.19 Histogram of the Pulse Height of the High Pressure Flash Tube for 200 Events.

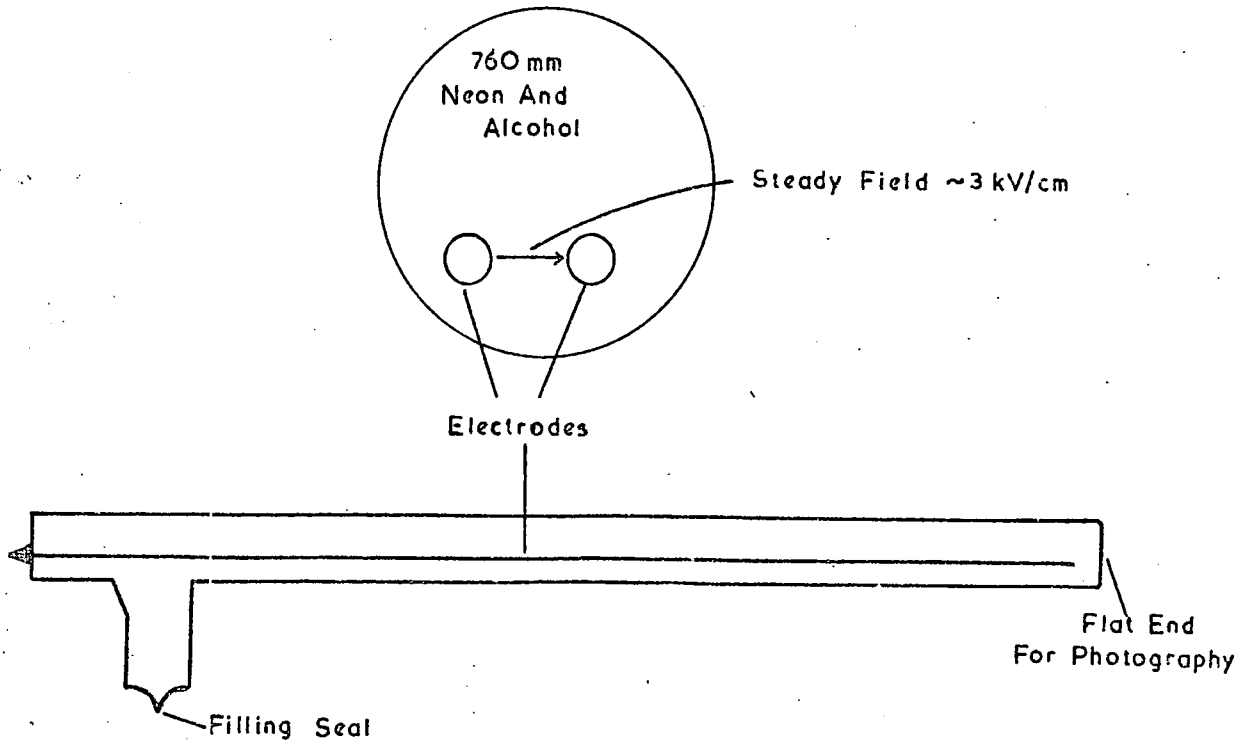

Figure 4.20 The Spark Tube Used by Bacon and Nash (1965)

4.8.2 The Photomultiplier Method

This method is described by Coxell et al. (1961). They discuss the possibility of using a photomultiplier to record the light output from an array of flash tubes and hence to correlate this output to the number of tubes which had flashed in the array. This would save the need to photograph the flash tubes, the only record required would be the output pulse from a photomultiplier. The authors suggest that this method has applications in density spectrum work on extensive air showers. The light output from the photomultiplier can be calibrated in terms of the number of flashed tubes in an array. This output pulse can then be recorded photographically using an oscilloscope or recorded directly by a pulse height analyser.

The authors also suggest that the photomultiplier can be used as a pre-selector of events. The array is triggered in the normal way after the passage of an extensive air shower and if the pulse height is greater than a pre-determined value, indicating on average that a certain number of tubes have flashed, a camera shutter is opened and the array triggered again.

If the time between pulses is of the order of milliseconds, the tubes which flashed on the first pulse have a high probability of flashing on the second pulse. They found for tubes of about 1.8 cm external diameter and pressure 60 cm of mercury a 0.5 probability of after-flashing if the interval between pulses is 90 ms. For tubes of about 8 mm external diameter and 2.3 atmospheres pressure the corresponding time was 30 ms.

4.8.3 The Spark Tube

Bacon and Nash (1965) reported the development of a system in which the flash tube contained sealed electrodes as shown in figure 4.20. The tube in their investigation was 20 cm long and internal diameter 1 cm. The electrodes were 1 mm wide copper strips on a thin paxolin card separated by 1 mm. A potential difference of about 300 volts was applied to the copper strips. When the tube flashed, a voltage pulse was obtained from the strips due to breakdown

across the inside of the tube.

They found that occasionally spurious discharges occurred between the strips but these were eliminated by the addition of a quencing agent, in this case ethyl alcohol at a pressure of 3 cm of mercury was used. They obtained detectable pulses with 85% efficiency. They attribute this efficiency of less than 100% to the internal electrodes not being parallel.

One advantage of the system is that it is still possible to photograph the tubes through the plain front in the conventional way but the increase in the cost of manufacturing the tube with a built in electrode system could be a disadvantage.

4.8.4 The Light Sensing Technique

Reines (1967) and Crouch (1968 - private communication) have reported a technique which has been developed for use in the South African Underground Neutrino Experiment. This large experiment is situated in a gold mine near Johannesburg at a depth of 8800 m.w.e. below the earth's surface. It is operated by groups from the Case Institute of Technology, Cleveland, U.S.A.; University of California in Irvine, U.S.A.; and the University of Witwatersrand, South Africa.

The experiment uses about 60,000 neon flash tubes of length 2 metres, mean external diameter 1.75 cm, and pressure of 60 cm of mercury. Because of the large area covered by the tubes, photography is made extremely difficult. A technique has been developed which records the tubes which have flashed electronically. The information is then displayed on a hodoscope system which can easily be photographed.

The method of digitising the flash tube is shown in figure 4.21. A cadmium selenide cell is placed in front of each flash tube and is shielded from external light by the shrink tubing. The cell is then connected via a silicon controlled rectifier and associated electronics to a light bulb on the hodoscope system.

When the flash tube fires, the light output from the tube is detected by

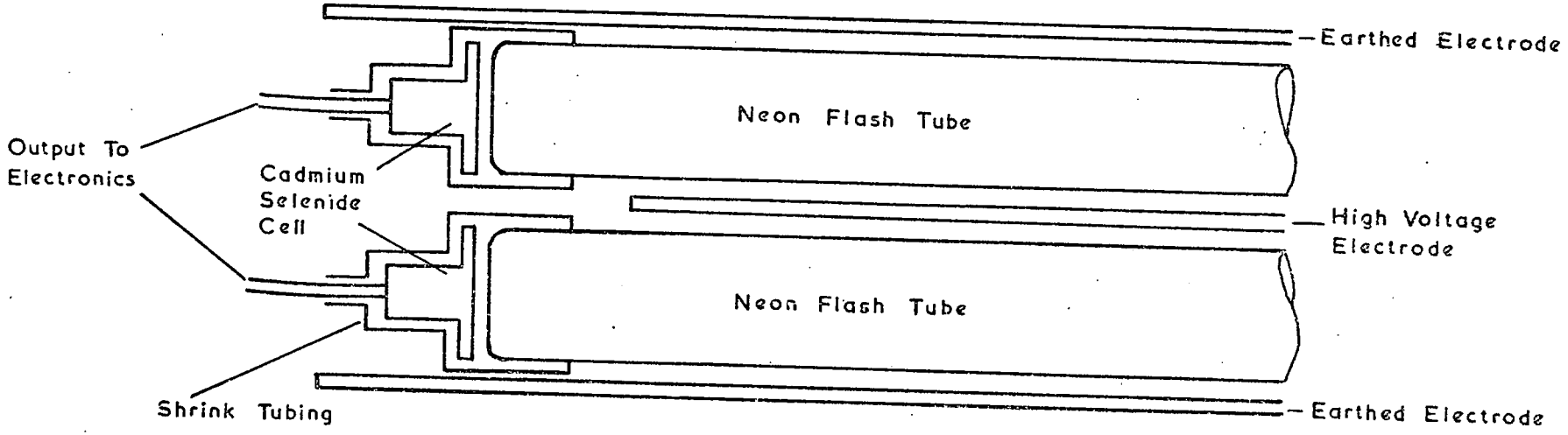

Figure 4.21 The Digitisation Method Used by Reines (1967).

the cadmium selenide cell as a change is resistance of the cell. This change is detected by the silicon controlled rectifier, which consequently switches on a bulb which is photographed. By scanning the events the tubes which have flashed can be determined.

4.8.5 The Vidicon System

Harrison and Rastin (1970) have developed a system in which a flash tube array is photographed by a vidicon camera. An intricate scanning procedure is used to scan each row of flash tube images on the vidicon photocathode and the co-ordinates of the flashed tube are recorded in terms of a standard scanning frequency. This information is then punched on to paper tape which can then be fed into a computer.

A disadvantage of the system as constructed is the built in rejection procedure which rejects the information for an event if three or more tubes flashed in a layer of the array. The authors state, however, that a more complex selection system could allow all the tubes to be recorded.

The technique is being used on the new Nottingham Spectrograph which was briefly outlined in §2.5.

4.9 Summary

The investigations which have been described above have shown that a pulse, suitable for the digitisation of a flash tube, can be obtained for both high and low pressure tubes. The method used is simple, reliable, and, above all, relatively cheap. This last point is not to be taken lightly, as the cost of any digitisation technique is an important factor in the design consideration when a large number of flash tubes are used in an experiment.

The important design considerations for an array of flash tubes using the digitisation technique are summarised below.

(i) The probes for each flash tube must be shielded to prevent pickup from adjacent tubes.

(ii) The probe touches the front of the flash tube as and is as close as possible to the flash tube electrodes.

This last point ensures that the best possible output pulse is obtained when the tube fires. There is, however, a lower limit to the distance of the probe from the electrodes due to the possible electrical breakdown between the high voltage electrode and the probe shield if the distance is small.

(iii) An output pulse suitable for the triggering of an electronic memory can be obtained by a suitable combination of probe resistance when the tubes are used at a voltage which gives efficient tracks in the flash tube array.

In this case, the value of the resistance governs the length of the pulse and the pulse height required, if it is less than the height obtained for the full resistance, is obtained by suitable tapping of the resistance.

(iv) The flash tubes using this technique should be painted black as the plastic covering used to cover each tube could easily be torn when the tubes are inserted into the array.

CHAPTER 5

The Momentum Selector

5.1 Introduction

A Momentum Selector has been incorporated in the spectrograph design because of the high rate of low energy particles traversing the apparatus. With the magnetic field at the running value of 16.3 kilogauss, the rate of particles through each side of the spectrograph is approximately 1110 $hr.^{-1}$. Of these particles about 15 $hr.^{-1}$ have momenta in excess of 100 GeV/c. The rate about 100 GeV/c has been calculated from the spectrograph dimensions and the measured integral spectrum of Hayman and Wolfendale (1962). The Momentum Selector has thus been designed to eliminate this low energy background and detect particles which have momenta above about 200 GeV/c. These so called high momentum events are signified by an output pulse from the Momentum Selector which initiates the readout of the information from each Measuring Tray on the triggered side into the core store.

The basic principles of the Momentum Selector design are described in this chapter together with the associated logic circuits for the selection of high momentum events. Also described briefly is the special device (R.U.D.I.) which calculates the deflection of the traversing particle from the information contained in the Momentum Selector and stores the deflection in a 400 channel pulse height analyser.

5.2 Principle of the Momentum Selector

The principle of the Momentum Selector is to determine the position of the trajectory of a particle traversing the spectrograph to a cell of width 5mm at three levels. This is achieved by the use of the Momentum Selector trays which are placed in the spectrograph as shown in figure 3.1.

A scale diagram of the flash tube pattern used in the trays is shown in figure 5.1. The number of tubes per layer and the 5 mm cell divisions along the measuring level are also shown in figure 5.1. The stagger of the tubes has

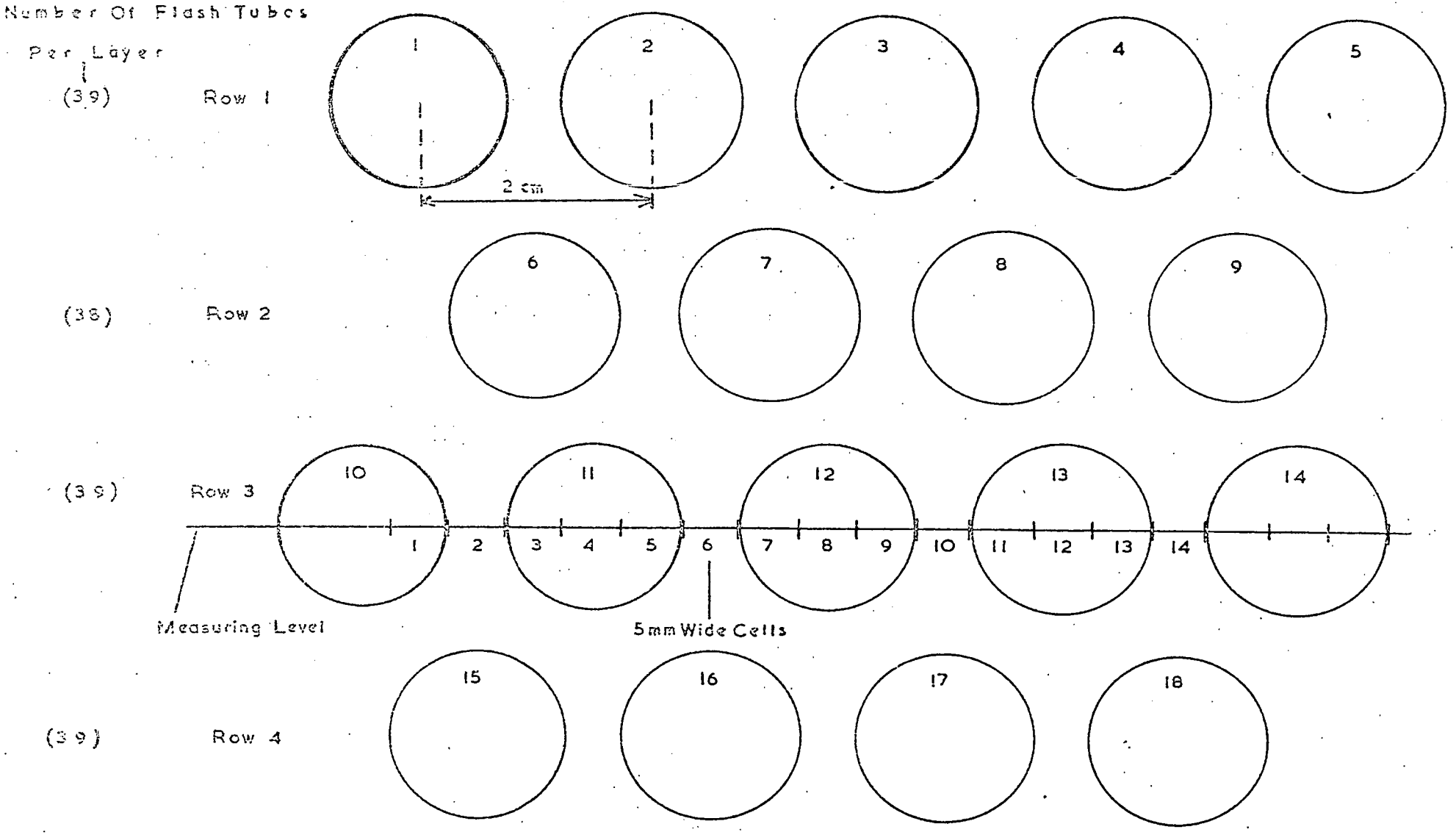

Figure 5.1 The Flash Tube Pattern of the Momentum Selector Trays.

been chosen so that at least two tubes flash on the traversal of a high momentum particle. The measuring level is along the central line of row 3 for the reasons mentioned in §5.8.2.

The trays are digitised using the method described in Chapter 4. It is possible, by examining the combination of tubes which flash after the traversal of a particle, to locate the position of the particle in one of the 5 mm wide cells, there being 152 cells across the tray width. The cell through which the particle passed in a tray is determined in practice by feeding the output pulse from the flash tube probe into an electronic memory made from integrated circuit blocks. The outputs from the memories are then gated into a further logic circuit which determines the particle cell. These circuits are discussed in §5.8.

The trajectory of any particle traversing the spectrograph is thus known to be in three cells, one at each measuring level. These cells are recorded in three shift registers made from integrated circuits as shown in figure 5.2. Each bit of the shift registers is basically an electronic memory and the information contained in a bit is shifted to its neighbour on the application of a clock pulse. The shift registers will be discussed in §5.9.

A high momentum event is defined as being when a straight line can be constructed through the cells in the three trays through which the particle passed. That is, if the particle passed through cell number a at level 5 and cell number c at level 1, then it is a high momentum event if it passed through cell number $\frac{a + c}{2}$ at level 3 as shown in figure 5.2. A correction is made for the fact that a true particle trajectory may be in an adjacent cell to the one allocated by the Momentum Selector logic as explained in §5.9. In practice a high momentum event is determined by shifting the information in each shift register in the direction shown in figure 5.2 and looking at all the possible three fold coincidences which give a straight line at the 76 th. and 152 nd. bits of shift register B. The shifting to the 76 th. or 152 nd. bits of shift

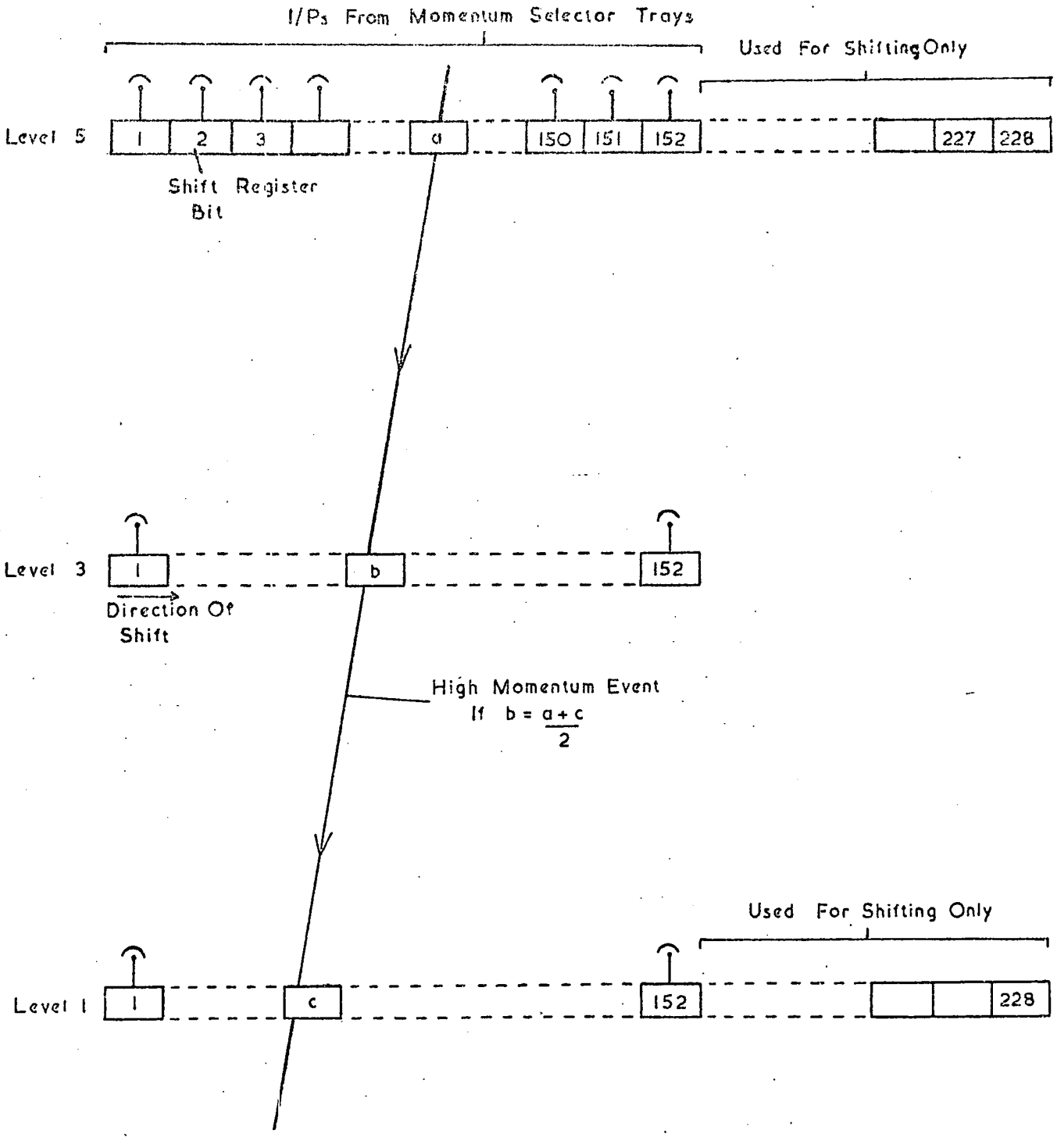

Figure 5.2 The Principle of Operation of the Momentum Selector.

register B is the reason for the extra 76 shift register bits in shift registers A and C. The shifting process is described fully in §5.9.

The advantage of this method is that there is no rejection of high momentum events due to accompanying particles in a tray produced, for example, by an interaction in one of the magnet blocks A or C. In fact a low momentum particle may be accepted as a high momentum event because of the presence of accompanying particles.

5.3 Other Forms of Momentum Selector

The use of a momentum selector in magnetic spectrographs is not new. Several workers have incorporated momentum selectors in their spectrographs to eliminate the low energy background. Holmes et al. (1961) used three levels of Geiger counters to detect the particle traversing the spectrograph. The deflection was calculated electronically by examining the Geiger counters which the particle traversed at the three levels. If the deflection was less than a certain value then three cloud chambers were triggered and the trajectory could be determined to a greater accuracy than with the Geiger counters. A similar Geiger counter momentum selector has been used by Pak et al. (1961) and Hayman and Wolfendale (1962) but flash tube arrays were used as the secondary detectors.

The new Yale-Brookhaven National Laboratory spectrograph (Kasha, 1971, private communication) uses scintillation counter hodoscopes at three levels in the spectrograph. The electronics used with the hodoscope arrays only initiates the application of a high voltage pulse to six optical spark chambers, which are equally spaced on either side of a solid iron magnet, if the deflection of a particle is less than a certain value. This arrangement produces a cut off in momentum at about 28 GeV/c, the efficiency in acceptance increasing with momentum so that it is unity at 200 GeV/c.

The momentum selector in M.A.R.S. is the first to use flash tubes in a momentum selector system. The advantage of the system over the types described above is that there is no dead space at the measuring levels of the

momentum selector and hence no correction has to be made for the dead space. There is also no rejection of events due to accompaniment which could result in a bias in the acceptance of high momentum particles. If scintillation counters had been used, although it would have replaced the present system of scintillation counters and Momentum Selector Trays by a single scintillation counter hodoscope system, there would have been the additional cost of photomultipliers and associated electronics for the scintillation counters. Also, the cut off in acceptance of high momentum events would have been at a considerably smaller value of momentum because the width of the scintillation counters would be larger than the cell width used with the flash tube trays.

5.4. The Momentum Selector Trays

The Momentum Selector flash tubes are supported in an outer framework made from 1" x $\frac{1}{2}$" bright steel bar of overall size 283 cm x 84 cm x 12.7 cm. Steps of 1" x 1" x $\frac{1}{2}$" were machined at each end of the bars. The framework locates together in the steps and is secured by four 2 B.A. countersunk screws at each of the eight corners of the tray. There are four layers of flash tubes in a tray with aluminium electrodes of thickness 18 S.W.G. (1.2 mm) placed between each layer. The electrodes are held in position by five $\frac{1}{2}$" wide Tufnol supports on each side of the tray, the supports are secured to the outer framework by 4 B.A. countersunk screws.

Figure 5.3 shows a diagram of the plan and side view of the tray and figure 5.4 a cross-section of an electrode support. As may be seen from figure 5.4 there is an overlap of $\frac{1}{4}$" (6.4 mm) between adjacent electrodes. This ensures that the tubes at the edge of each row are in a uniform field region.

The tubes are held in position by two $^{1}/_{8}$" thick brass plates fixed at the front and back of each tray into which are drilled holes to accommodate the flash tubes. These brass plates are used because a digitisation shield is required over the probes of each flash tube as discussed in Chapter 4. The

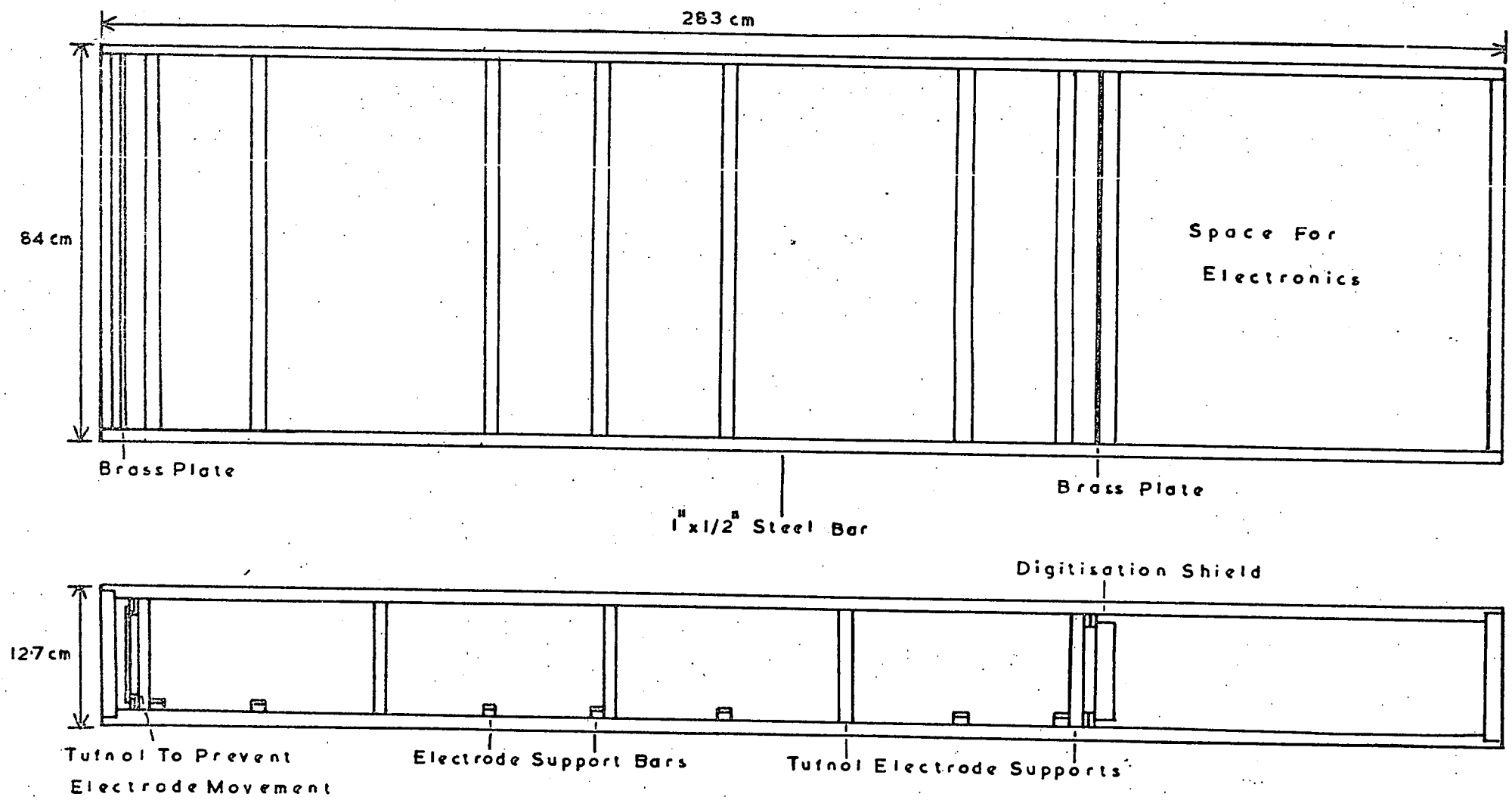

Figure 5.3 The Plan and Side View of a Momentum Selector Tray.

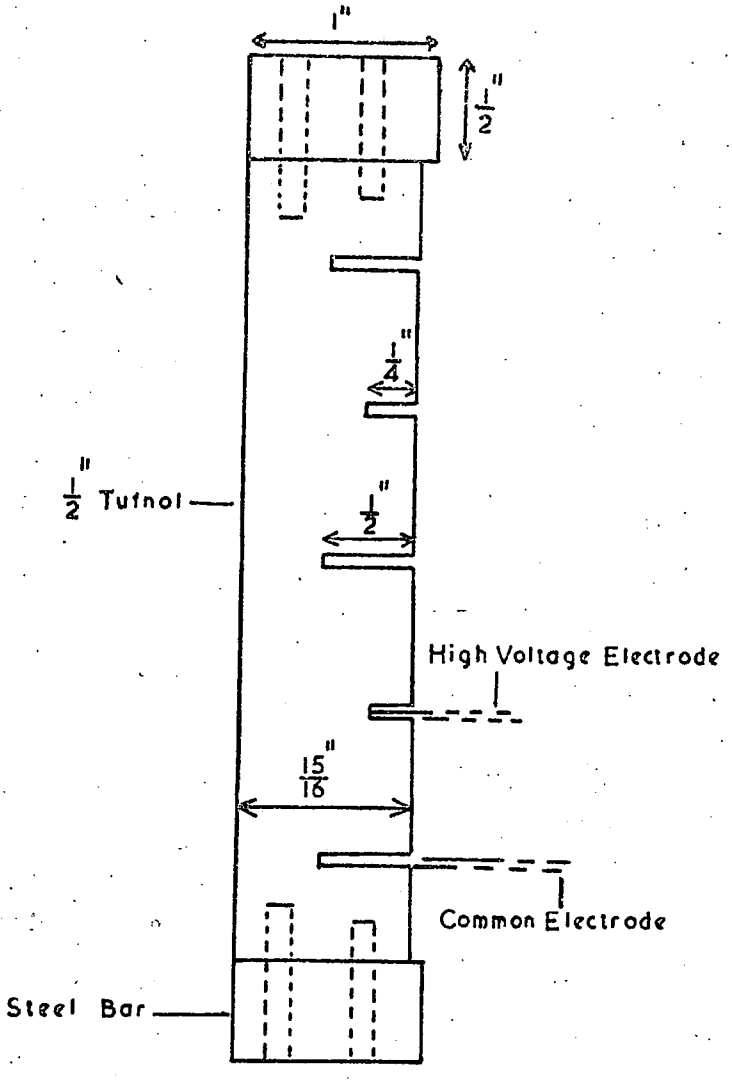

Figure 5.4 Cross-sectional View of a Tufnol Electrode Support.

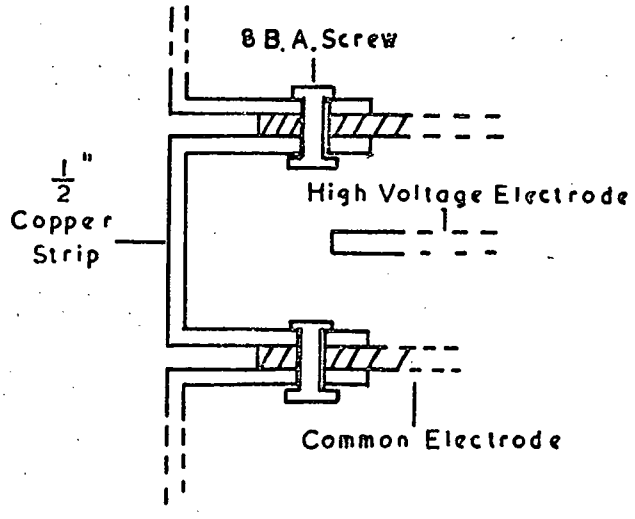

Figure 5.5 The Method of Interconnecting the Electrodes of a Flash Tube Tray.

digitisation shield is made from a $1\frac{1}{2}$" thick dural block. A description of the manufacture of the brass supports and dural shield is given in §5.5.

The brass support plates for the flash tubes are secured to lengths of $\frac{1}{2}$" x $\frac{1}{2}$" Tufnol bar along the two longer edges of the plate by six 4 B.A. countersunk screws along each edge. The Tufnol is itself fixed to the outer framework of the tray by two 4 B.A. countersunk screws at each corner. The flash tube digitisation shield fits over the top of the front plate and is held in position by six 2" long 4B.A. countersunk screws which screw into the Tufnol bars, there being clearance holes in the block and brass plate. Slits were cut out of the corners of the brass plates and the dural block so that there was a gap of at least $^1/8$" between the supports and shield and the outer framework. This is to prevent electrical contact between the common line of the power supplies and the earth of the mains in the laboratory. The outer framework of the tray will rest on metal rollers when the tray is in position in the magnet. The rollers and the magnet are at earth potential. The common line and earth are kept apart because of the earthing requirements of the 1130 computer.

The trays were filled using the method described below. This method was used in the filling of both the Momentum Selector Trays and the Measuring Trays.

The outer framework of the tray and the brass supports for the tubes were assembled near to the spectrograph with the Tufnol supports for the electrodes fixed in position on only one side of the tray. The bottom electrode was then placed in its correct position in the Tufnol supports.

The bottom electrode is supported at equal distances along its length by seven supports of $\frac{3}{4}$" x $\frac{3}{4}$" bright steel bar which fit between the outer lengths of the framework. Strips of $^1/8$" Perspex were fixed by adhesive to the top of the bars to prevent electrical contact between the framework and the bottom electrode. These supports are required to prevent the bowing of the electrodes along their length caused by the weight of tubes in the tray.

The bottom layer was then filled with flash tubes. The flash tubes had been tested previously for spurious flashing. The tubes were pulsed randomly at a rate of 1 pulse a second for 500 pulses. The pulse height was of similar amplitude as that to be used on the tray when in the spectrograph. Any tubes which flashed continuously were rejected. This spurious rate was found to be less than 1%. The tubes were also tested with a Tesla coil to ensure that they had the characteristic neon discharge and cleaned with a duster before inserting into the tray. The tubes were placed in the tray by inserting the tube in the correct hole in the back plate and pushing it along the tray to the front. If a tube was found to be difficult to insert, due to the variation in tube diameter, it was removed.

When the bottom layer of tubes had been filled, they were aligned parallel. The tubes were not parallel initially because of their natural bowing effect. This bowing effect on the parallelism of the tubes was reduced to a minimum by rotating the tubes such that they all bow in the same direction, in this case the vertical. After alignment the tubes were marked with a white paint spot at the back of the tube to indicate the correct position in the tray.

The second electrode was placed on top of the tubes in the bottom layer, care being taken that it did not disturb the layer of tubes. The second row was filled in a similar manner to the first layer and so on for the rest of the layers.

Interconnection of alternate electrodes across which the high voltage pulse is applied is made using strips of copper $\frac{1}{2}$" wide. The strips are of the form shown in figure 5.5. They were fixed to the electrodes by 8 B.A. countersunk screws cut to the required length. They are positioned centrally on the side of the tray nearest to the sides of the spectrograph so that they can be easily accessible when the tray is in position in the spectrograph.

When the tray had been filled, the remaining Tufnol electrode supports were fixed in position. Small pieces of $\frac{1}{2}$" wide Tufnol were then placed at the

four corners of the tray as shown in figure 5.3. Slits were machined in the Tufnol to enable them to fit between the Tufnol supports at the ends of the electrodes and the brass plates. They were used to prevent the electrodes from moving in a direction parallel to the flash tube axis when the tray was placed in position in the spectrograph. The sides of the tray were then covered by $\frac{1}{8}$" thick sheets of Perspex held in position by $\frac{1}{4}$" 8 B.A. countersunk screws into the sides of the outer framework. The Perspex sheets prevent dust from entering the tray and also act as a safety shield for the high voltage electrodes.

The high voltage pulse to the tray is produced by the high voltage trigger unit for the given side, which is described in §3.5. The pulse is fed to the tray along co-axial cable, which is connected to two brass connectors screwed to the inside of the Perspex sheet on the side nearest to the outside of the spectrograph when the tray is in position. A further co-axial cable passes along the inside of the Perspex side and is soldered to the copper strips joining the electrodes.

Because of the variation in flash tube diameters, the holes used in the brass plates and probe shields of the Momentum Selector Trays varied from tray to tray. Two hole diameters were used and these are listed in Table 5.1 for the six Momentum Selector Trays.

TABLE 5.1

The Hole Diameters Used in the Momentum Selector Tray Supports and Shield

Level	Blue Side	Red Side
1	17.75	17.75
3	17.86	17.75
5	17.86	17.75

Measurements in mm.

The electronics for the Momentum Selector, which allocates the cell the particle traversed, fits in the space at the front of the tray between the probe shield and the outer framework. A detailed description of the

electronics is given in § 5.8.4.

5.5 The Method of Construction of the Flash Tube Supports and Digitisation Shield

The same basic method for the construction of the supports and shield is used for all the trays in the spectrograph. A description is given for the construction of the supports and shield for the Momentum Selector Trays but those for the Measuring and Azimuth Trays were made in a similar manner.

Two plates of $^{1}/8$" thick brass were cut to the approximate correct size and were placed on top of a $1\frac{1}{2}$" thick dural block, which has also been cut to the approximate size required, on the machine bed of a milling machine. The materials lie on the bed of the machine in the order that they are fitted on the tray, that is, the top brass plate is the support at the back of the tray and the second brass plate is used on the front of the tray. This ensures that if there is any drilling irregularity for any hole, the probe shield will still fit over the flash tube fronts when it is placed in position. The brass and dural were then milled to the correct size which for the Momentum Selector Trays is 83.8 cm x 10.2 cm. After milling to the correct size, the machine operator aligned a small centre drill over the centre of the first hole in the top row. This hole centre is given as a co-ordinate from the top left hand corner of the block and plate arrangement when viewed from the front of the machine. The hole thus corresponds to the first tube in row 4 of figure 5.1.

The movement of the milling machine bed is controlled by an optical arrangement, which uses two accurately made metric rules placed along the two directions of motion of the machine bed and viewed through two lens systems. The origin of the co-ordinates, the top left hand corner of the block and plate arrangement, is known in terms of the readings of the metric rules. Thus, by adding the co-ordinates of the first hole centre to the readings of the metric rules, the centre drill can be located over the centre of the first hole. Using the optics on the machine the hole centre can be located to an accuracy of 0.01 mm.

After centre drilling the first hole, the next hole centre was located by moving the machine bed the required distance between centres of the holes, which is 2 cm for the Momentum Selector Trays. The second hole was centre drilled and the process repeated for all the holes in the row. The machine operator noted the co-ordinate of each hole in terms of the reading of the metric rules after the drilling of each hole.

When all the holes had been centre drilled in the row, the operator centred again on the first hole with the aid of the known co-ordinates for the hole. A pilot drill was used for all the holes in the row and then the final drill size was used. The pilot drill size was chosen such that a cut of about 1 mm is taken off on both sides of the hole by the final drill.

The centre drill was then used on the second row in a similar manner to the method used on the first row. The process was repeated for the third and fourth rows.

As the hole size is not the same for all the trays, because of the variation in flash tube diameters, the distance between the centre line of the holes in adjacent rows also varies. This distance is equal to the hole diameter plus the electrode thickness of 1.2 mm.

5.6 The Method of Allocation of a Particle Cell from the Flash Tube Pattern

It has been explained in § 5.2 that by observing the combination of flash tubes which flash when a particle traverses a Momentum Selector Tray, it is possible to place the path of the particle in a cell of width 5 mm.

For a high momentum event the spectrograph will accept particles whose incoming angles are within 7° of the vertical when the angle is measured in the deflection plane of the spectrograph. Larger angles than 7° are possible but these are low momentum particles, which are deflected into the magnet volume and trigger the scintillation counters by the magnetic field. As the Momentum Selector is required to be 100% efficient for these high momentum particles, the flash tube combinations set off by particles whose trajectories

are within 7° of the vertical were found for a tube spacing in a Momentum Selector Tray. Scale diagrams of the flash tube stagger were drawn and the combinations of flash tubes for a given cell produced by particles traversing the tray within 7.5° of the vertical were found. The flash tubes were assumed to be 100% efficient which is found in practice to be true within the experimental error.

The combinations of flash tubes possible for a given cell are shown in Table 5.2, the numbers of the flash tubes and cells in Table 5.2 correspond to the flash tube and cell numbers in figure 5.1. As may be seen from Table 5.2 the flash tube patterns for a cell are repeated every four cells which is equal to a tube spacing.

TABLE 5.2

The Flash Tube Combinations for the 5 mm Cells

Cell Number	Flash Tube Combinations for Cell
8	3,7,12,16*;3,12*;3,7,12;7,12;3,7,12,17*;7,12,17;
9	3,12*;3,8,12,17;3,12,17;3,7,12,17*;
10	8,17;3,8,17;3,17;
11	4,8,13,17*;8,13,17;3,8,13,17;3,8,13;
12	4,8,13,17*;4,13*;4,8,13;8,13;4,8,13,18*;8,13,18;
13	4,13*;4,9,13,18;4,13,18;4,8,13,18*;

*These combinations have two possible cells.

On examining the various combinations of flash tubes in Table 5.2, three combinations in a tube spacing can be produced by particles passing through adjacent cells. These combinations are marked with an asterisk in Table 5.2. The Momentum Selector requires, if possible, only one cell to be indicated after the passage of a single particle through a Momentum Selector Tray. This enables the digital device R.U.D.I. to accept the event for analysis, as explained in §5.10, and also prevents a smaller cut off in momentum for particles

selected as high momentum events by the Momentum Selector. The combinations of flash tubes giving two cells were allocated to one cell by examining the probability of the combination being produced by particles passing through the two cells within the angular range allowed by the spectrograph. The combination was then allocated to the cell having the greater probability.

On examining the probabilities, two combinations were found which had an equal chance of being in either cell. The two cells in question were the same for each combination so one combination was placed in one cell and the other combination in the remaining cell. The flash tube combinations giving two cells are listed in Table 5.3 together with the probabilities for each cell and the allocated cell. Table 5.4 lists the combination of flash tubes for a given cell after the reallocation.

TABLE 5.3

The Flash Tube Combinations Having Two Possible Cells

Flash Tube Combination	Cell Number	Probability	Cell Number	Probability	Allocated Cell
3,12	8	0.5	9	0.5	9
3,7,12,17	8	0.5	9	0.5	8
4,8,13,17	11	~0.6	12	~0.4	11

TABLE 5.4

The Flash Tube Combinations for the 5 mm Cells after Reallocation

Cell Number	Flash Tube Combinations for Cell
8	3,7,12;7,12;3,7,12,17;7,12,17;
9	3,12;3,8,12,17;3,12,17;
10	8,17;3,8,17;3,17;
11	4,8,13,17;8,13,17;3,8,13,17;3,8,13;
12	4,8,13;8,13;4,8,13,18;8,13,18;
13	4,13;4,9,13,18;4,13,18;

A check on the efficiency of correct cell determination can be obtained for various incoming angles to the tray. Parallel lines were drawn at a given angle to the vertical on scale diagrams of the flash tube pattern such that the intercepts on the measuring level of the tray were spaced 1 mm apart in real space. From the tubes which a particle traversed the allocated cell could be determined.

Angles from 0° to 8° on either side of the vertical were taken in 2° steps. For a given angle a graph could be plotted of error in location against the position of the particle in the measuring level. The error in location is defined as being equal to the true position of the particle in the measuring level minus the position of the cell mid point which is allocated to the particle, when the positions are measured in the direction of increasing cell number. Thus a particle whose error is within $\pm$ 2.5 mm is allocated to the correct cell.

Figure 5.6 shows graphs of the error in location of the particle against true position for angles of 0° and 4° on both sides of the vertical. The errors for a given angle repeat every tube spacing due to the symmetry of the flash tube pattern. The sign of the angle for the graphs in figure 5.6 indicates the direction of the incoming particle using the convention shown in figure 5.7.

For a given angle, the efficiency of correct cell allocation can be defined as the ratio of the width of a tube spacing over which the particle is in the correct cell to the total width of a tube spacing. The efficiency as a function of the angle of the incoming particle to the vertical is shown in figure 5.8. The assymmetry in efficiency for the same angle but for directions on opposite sides of the vertical is caused by the flash tube pattern. The overall efficiency for correct cell determination over the angular range 0° to 8° on both sides of the vertical is found from the graph to be 0.87.

From the graphs of the errors in location across a tube spacing a histogram can be plotted of the errors for the angles between 0° and 8° on both sides

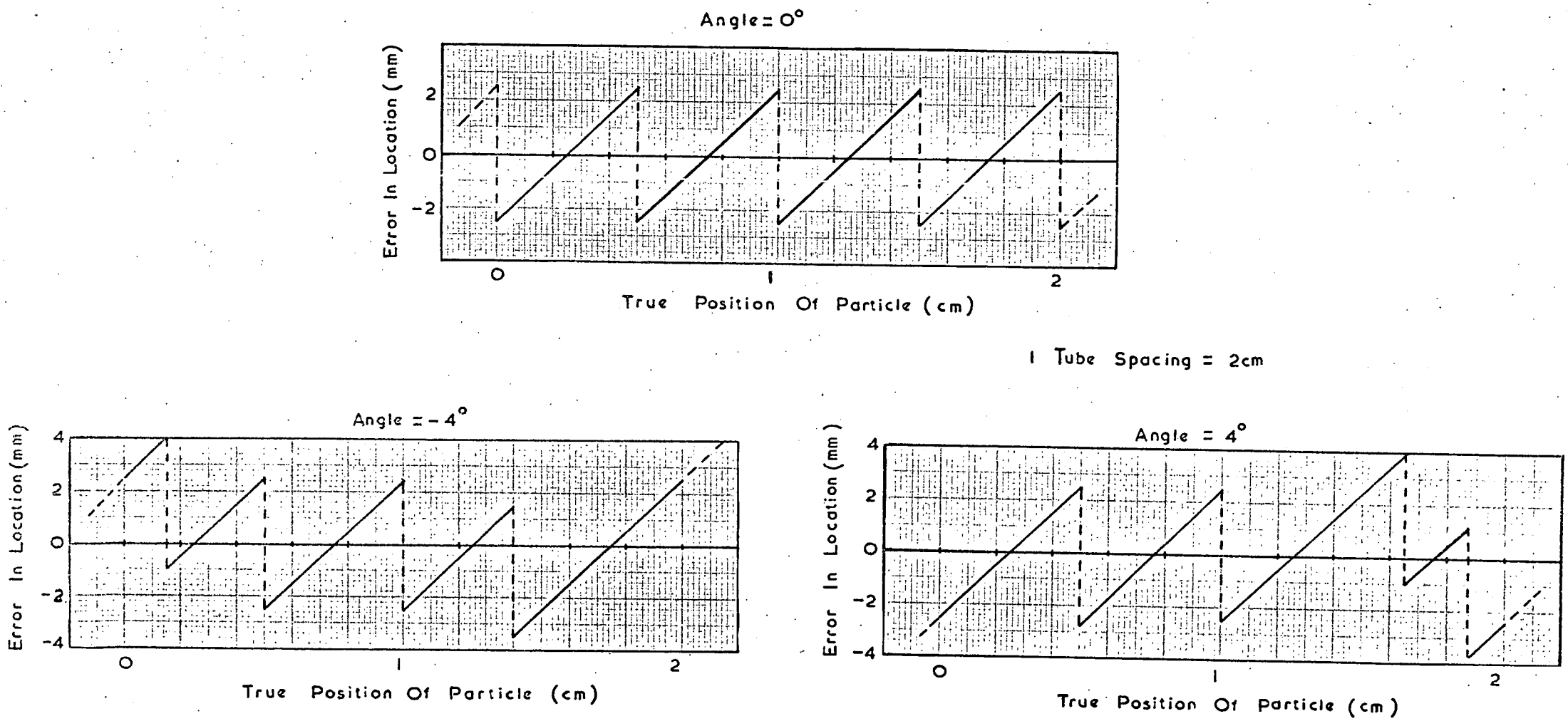

Figure 5.6 Graphs of Error in Location against True Position for Various Incoming Angles to a Momentum Selector Tray.

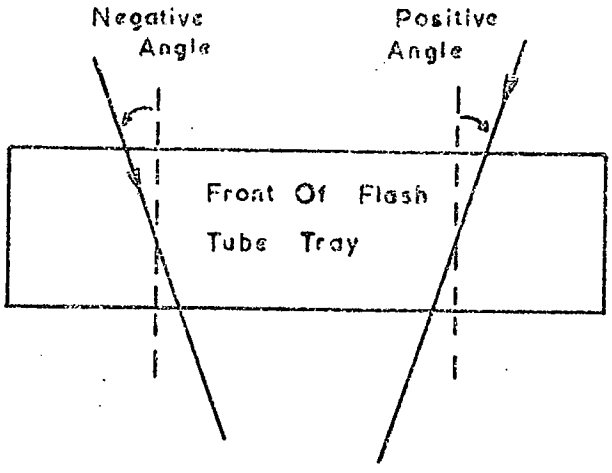

Figure 5.7 The Sign Convention Used for the Incoming Angles of Figure 5.6.

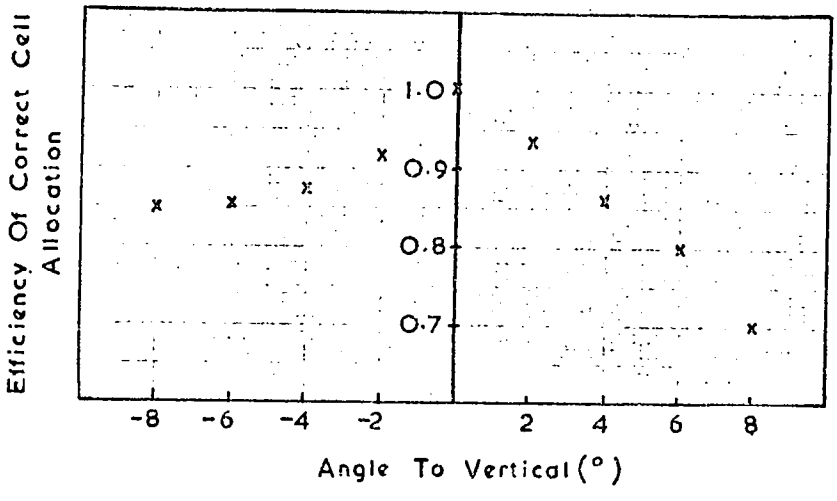

Figure 5.8 The Variation of the Efficiency of Correct Cell Allocation with Incoming Angle.

of the vertical. This histogram is shown in figure 5.9. The mean error from the histogram is 0.28 mm if the sign of the error is taken into account, and 1.49 mm if the sign is neglected. The standard deviation of the distribution is 1.78 mm. It can be seen from the histogram that the maximum error is $\pm$ 1 cell when the particle position is measured in terms of cell widths.

Other errors which could alter the cell allocation, such as inefficient flash tubes, the bowing of the flash tubes along their lengths and the variation of the internal diameter of a flash tube along its length are discussed in § 5.7.

5.7 Factors Governing the Correct Cell Determination

The efficiencies for the correct cell determination were measured above by assuming that the wrong cell is due only to the built in bias in the electronics. However, there are several other factors which will effect incorrect cell allocation. These are:

(i) Inefficient flash tubes.

(ii) The bowing of the flash tubes along their length and the variation in flash tube internal diameter.

(iii) Interactions in the iron of the magnet or more than one particle entering the spectrograph to give further particles traversing one or more Momentum Selector Tray.

The effect of (i) on the wrong cell allocation is small as the tests on the flash tubes have shown that their efficiency is 100% to within 3%. The efficiency measurements for the flash tubes are described in § 5.8.3. Similarly the effect of bowing tubes has been reduced to a minimum by arranging the bowing to be in the vertical direction when a tray was filled. The variation in the flash tube internal diameter can also be included in the effect of bowing of tubes and any effect will occur when the particle passes near to the edge of a flash tube.

By examining the flash tube pattern on a scale diagram it is possible to see where any possible edge effects could occur. An edge effect is the

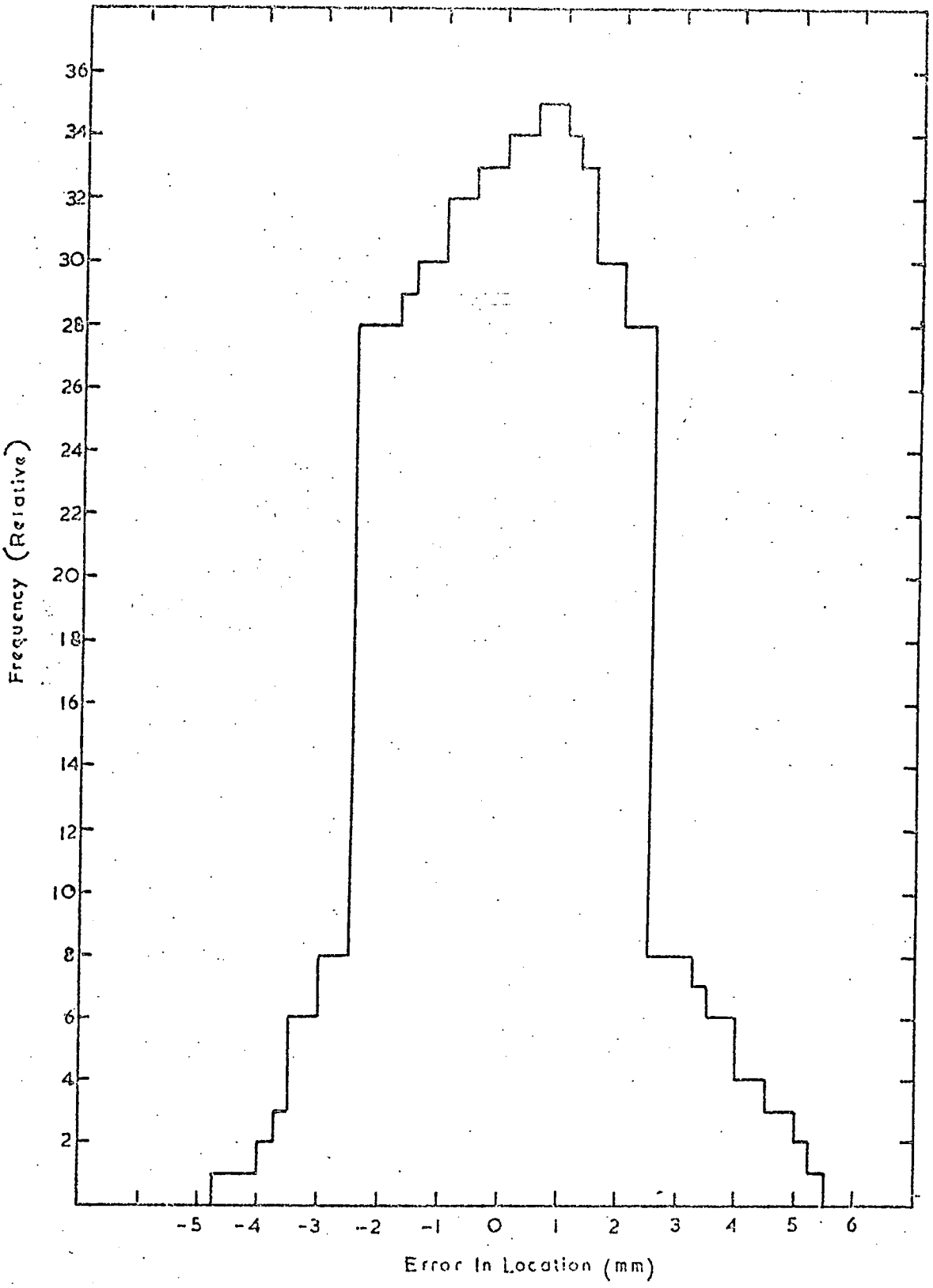

Figure 5.9 Histogram of the Error in Location for a Momentum Selector Tube Spacing.

case when the track of a particle passed close to the inside wall of a flash tube, either inside the gas or glass of the wall. The tube could then flash or not depending on the effect of (i) or (ii) above. An analysis of the possible edge effects in a tube spacing show that the particle will be allocated to its correct cell or to a neighbouring cell. Allowance is made for this effect by the Momentum Selector as explained in § 5.9.

The effect of more than one particle close together in a tray is difficult to estimate. It will certainly increase the chance of the particle being accepted as a high momentum event because the Momentum Selector will accept all events with a straight line combination between the cells at the three levels. Several cells will be indicated by the logic for the cell determination, the number depending on the tubes which flashed.

5.8 The Momentum Selector Electronics for the Cell Allocation

5.8.1 Introduction

The electronics for the cell allocation is contained in front of each Momentum Selector Tray. The flash tube probes are connected to electronic memories which are set by pulses from the probes. The memories are then gated into the logic to determine the correct cell by a pulse from the Momentum Selector control logic. A pulse is then produced at the output from the logic corresponding to the cell which the particle traversed. This output pulse is fed into the Momentum Selector which then determines, from the information obtained from the three Momentum Selector Trays on a side, whether the particle is a high momentum event. The logic for the Momentum Selector circuits are made from TTL circuit blocks. The electronic circuits for the cell determination are described below.

5.8.2 The Veto Requirements

The cell through which a particle passed in a Momentum Selector Tray is determined by the use of integrated circuit logic gates. However, if the outputs of each flash tube memory are fed into only coincidence gates, several

of the combinations will indicate that more than one cell in a measuring level is traversed. For example, from Table 5.4, flash tubes 8, 13, and 17 flashing would set off cell numbers 10 and 12, due to the coincidence of flash tubes 8 and 17, and 8 and 13 respectively, as well as the correct cell number 11. It is necessary to eliminate this effect for the reasons mentioned in §5.6. Hence veto logic is required to stop the additional cells being indicated.

To reduce the number of logic gates and veto circuits required in the electronics, the flash tubes in row 1 in figure 5.1 are only used if necessary. This will occur, for example, when only two flash tubes flash for a particular track and one of these is in row 1. Table 5.5 lists the flash tube combinations for each cell in a tube space when row 1 is used only when required. The flash tube number in parentheses indicates the flash tube in row 1 which is not used for this particular combination. By comparing Table 5.5 with Table 5.4 it can be seen that several flash tube combinations which include a flash tube from row 1 will also indicate the same cell if the tube in row 1 did not flash. Thus a saving in the logic gates required is obtained if the flash tubes in row 1 are not used in these cases.

TABLE 5.5

The Flash Tube Combinations for the Cells when Row 1 used only when necessary

Cell Number	Flash Tube Combination for Cell
8	(3),7,12;(3),7,12,17;
9	3,12;(3),8,12,17;3,12,17;
10	(3),8,17;3,17;
11	4,8,13,17;(3),8,13,17;3,8,13;
12	(4),8,13;(4),8,13,18;
13	4,13;(4),9,13,18;4,13,18;

( ) This flash tube is not used in coincidence with the other flash tubes in the combination.

The veto requirements are shown in Table 5.6 for a tube spacing. The number in parentheses indicates a flash tube which is not included in the logic

for that combination but may still flash (see Table 5.5). The number in brackets is the cell number for the veto combination. The electronic circuits for these veto requirements are discussed in §5.8.4.

TABLE 5.6

The Veto Requirements for a Tube Spacing

Flash Tube Combination Requiring Veto	Cell of Combination	Flash Tube Combination Producing Veto
3,12	9	3,7,12,16;[7] (3),7,12;[8] ;(3),7,12,17;[8]
3,17	10	(3),8,12,17;[9] 3,12,17;[9](3),8,13,17;[11]
8,17	10	(3),8,12,17;[9] 4,8,13,17;[11] (3),8,13,17;[11]
8,13	12	3,8,13;[11](3),8,13,17;[11]4,8,13,17;[11]
3,12,17	9	(3),7,12,17;[8]

( ) This flash tube is not used in coincidence with the other flash tubes in the combination.

[ ] The cell number of the Veto Combination.

The use of row 1 only when necessary explains why the measuring level for a Momentum Selector Tray is along row 3 as this is the central line for the three rows of tubes when row 1 is excluded.

5.8.3 The Digitisation System

The digitising system used on the Momentum Selector Trays is of the same form as that used on the prototype array described in §4.6. Figure 5.10 shows a cross-sectional view of the probe shield with the probes and other associated equipment in position. The probes used are 1" long 6 B.A. brass countersunk screws with washers on their heads so that the diameter of the probe head is 0.71 cm. The probes are held symmetrically in the shield by Perspex cylinders of length 1.9 cm which are fixed in the shield by filling the remainder of the hole above the probe with Araldite adhesive.

Connection is made to the probe by a wire which is soldered in a small hole drilled in the screw. The other end of the wire is connected to a printed circuit board which is fixed 4 cm from the shield by 12 small Perspex cylinders

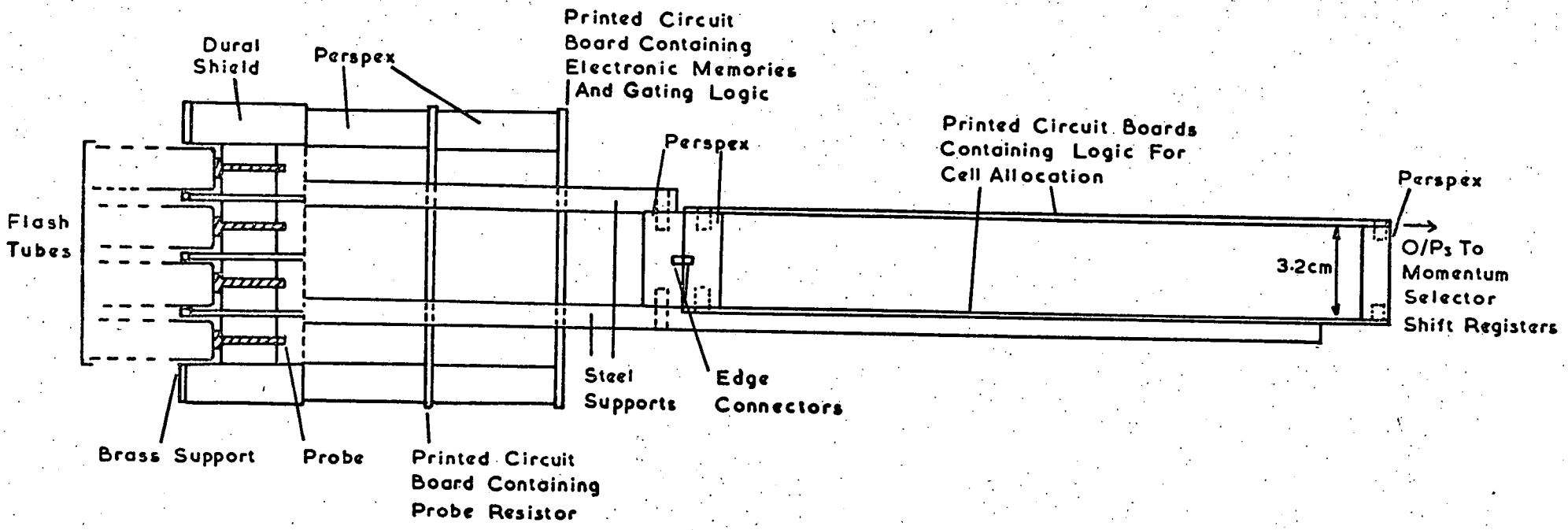

Figure 5.10 Cross-sectional View of a Probe Shield with Associated Equipment in position.

equally spaced around the board. This board contains the probe resistance of value 2.7 kΩ which is used to attenuate the pulse sufficiently to feed it into the logic gates comprising the electronic memory. A further printed circuit board is also fixed 4 cm in front of this board by Perspex cylinders. This second board contains the electronic memory and the gating logic for each flash tube. The form of the memory circuit and gating logic is described in §5.8.4. The logic for the cell allocation plugs into edge connectors on the front of the tray as described in §5.8.4.

The high voltage pulse applied to the Momentum Selector flash tubes is obtained by discharging a lumped parameter delay line through a resistor as explained in §3.5. The value of pulse height of the high voltage pulse used on the flash tubes was determined by measuring the layer efficiency of the flash tubes as a function of the pulse height for the minimum delay between the passage of the particle and the application of the high voltage pulse. Figure 5.11 shows a graph of the variation in layer efficiency as a function of the applied electric field for a delay of 1.5 μs, using a value of delay line resistance equal to its characteristic impedance of 47 ohm. The applied field is defined as the peak pulse height divided by the distance between electrodes. Assuming a 100% internal efficiency the layer efficiency for the stagger of tubes used in the Momentum Selector should be about 75%. As can be seen from the graph in figure 5.11 the layer efficiency is 75% within the experimental error so the tubes can be taken to be 100% efficient.

A voltage pulse was chosen which was on the plateau of the layer efficiency against voltage curve. This pulse produced a peak field of 2.6 kV cm^{-1} and total length 3 μs. This was for a pulse of peak height 4.5 kV corresponding to a voltage on the delay line of 10 kV. This voltage pulse will always be used on the trays as any change in the pulse will result in a corresponding change in the pulse used for the digitisation. If there is a reduction in output voltage due to a reduction in the applied pulse, the output pulse from

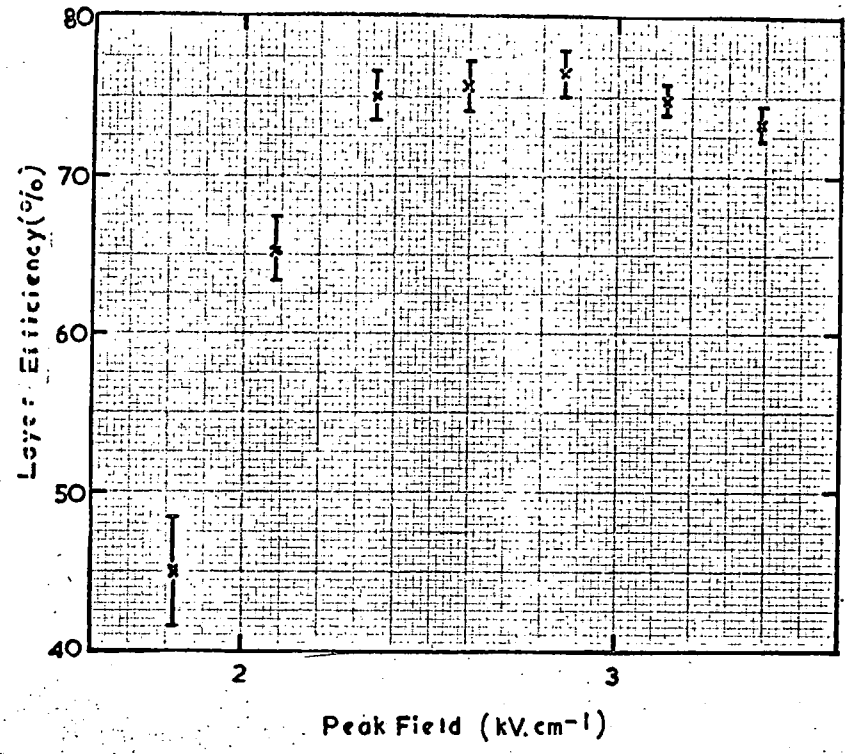

Figure 5.11 The Variation in the Layer Efficiency of the Momentum Selector Flash Tubes with Applied Field.

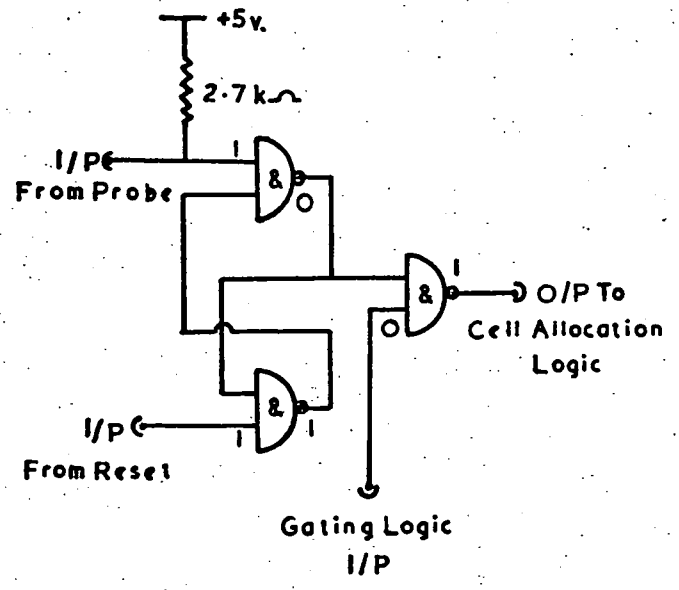

Figure 5.12 The Electronic Memory and Gating System used with each Flash Tube Probe.

the flash tube probes may not be sufficient to trigger the electronic memory.

The pulse obtained from the flash tube probe with a probe resistance of 2.7 kΩ is of peak height 5 volts and total length 0.5 μs when the pulse is fed into the electronic memory. The 2.7 kΩ resistor is connected to the positive supply line for the memories for the reason mentioned in §5.8.4. The pulse obtained for the memory input is then sufficient to set the memory.

It has already been mentioned in §4.3 that for an exponential shaped pulse there is a delay between the application of the high voltage pulse and the output pulse on the probe. For the Momentum Selector, this delay for the high voltage pulse characteristics described above was about 2.5 μs after the start of the high voltage pulse.

This time delay enables a veto to be applied to the electronic memory so that it is not set by any pickup during the application of the high voltage pulse.

5.8.4. The Electronic Circuits

The circuits on the tray fronts can be subdivided into two sections, the electronic memory circuits and the circuit to determine the cell which the particle traversed.

Figure 5.12 shows the form of the electronic memory and gating system used on the memory output. The memory has two output states which are complementary states of each other. The memories are reset by a pulse from the Momentum Selector which is fed via co-axial cable and buffer gates to the reset inputs to produce a negative pulse on the inputs. The output states of the memory are then as shown in figure 5.12. Each flash tube tray has 6 buffer gates which are connected to the 155 reset inputs on each tray, there being 155 flash tubes in a tray. Buffer gates are used as they are capable of being connected to a maximum of 30 gate inputs compared to the normal value of 10 for a nand gate.

The probe resistance of 2.7 kΩ is connected to the positive supply line to the gates so that the input to the gate is held in the logical 1 state. A

negative pulse from the probe sets the memory so that the output levels shown in figure 5.12 flip over. The output pulse to the cell determination logic is obtained by a positive pulse of length 1 μs on the blocking gate which is produced by the Momentum Selector via buffer gates on each tray. A negative pulse of length 1 μs is then fed to the logic only on those memories which have changed. The circuit controlling the memory reset and gating pulse is discussed in §5.9.

The blocks containing the logic gates for the memories and gating system are mounted on a printed circuit board in front of the tray as shown in figure 5.10. The blocks are so arranged on the board that they can easily be removed if they are faulty. This is achieved by placing the blocks on the side of the board nearest to the outer tray framework and soldering the pins of the block on to the copper strips of the board on that side. Interconnection between blocks is made by using minature stranded wire.

The inputs to the memories are from the first printed circuit board in front of the probe shield shown in figure 5.10. The outputs to the board are fed to the logic for cell determination via edge connector inputs as described below.

The circuit for the logic to determine the cell through which a particle passed is shown in figure 5.13. For comparison purposes, the numbers of the flash tubes and cells in figure 5.13 are the same as those in figure 5.1. The circuit is repeated every tube space, which is equal to four cells, across the tray. The logic levels when the gates are in the off mode are also shown in figure 5.13.

The pulse obtained from the flash tube gating logic is negative in shape and is of length 1 μs. After input to a board, the pulse is inverted and fed into the coincidence nand gates which determine the cell the particle traversed. The output from these gates either pass directly to the cell output gate or, if a possible veto may occur, into a delay unit.

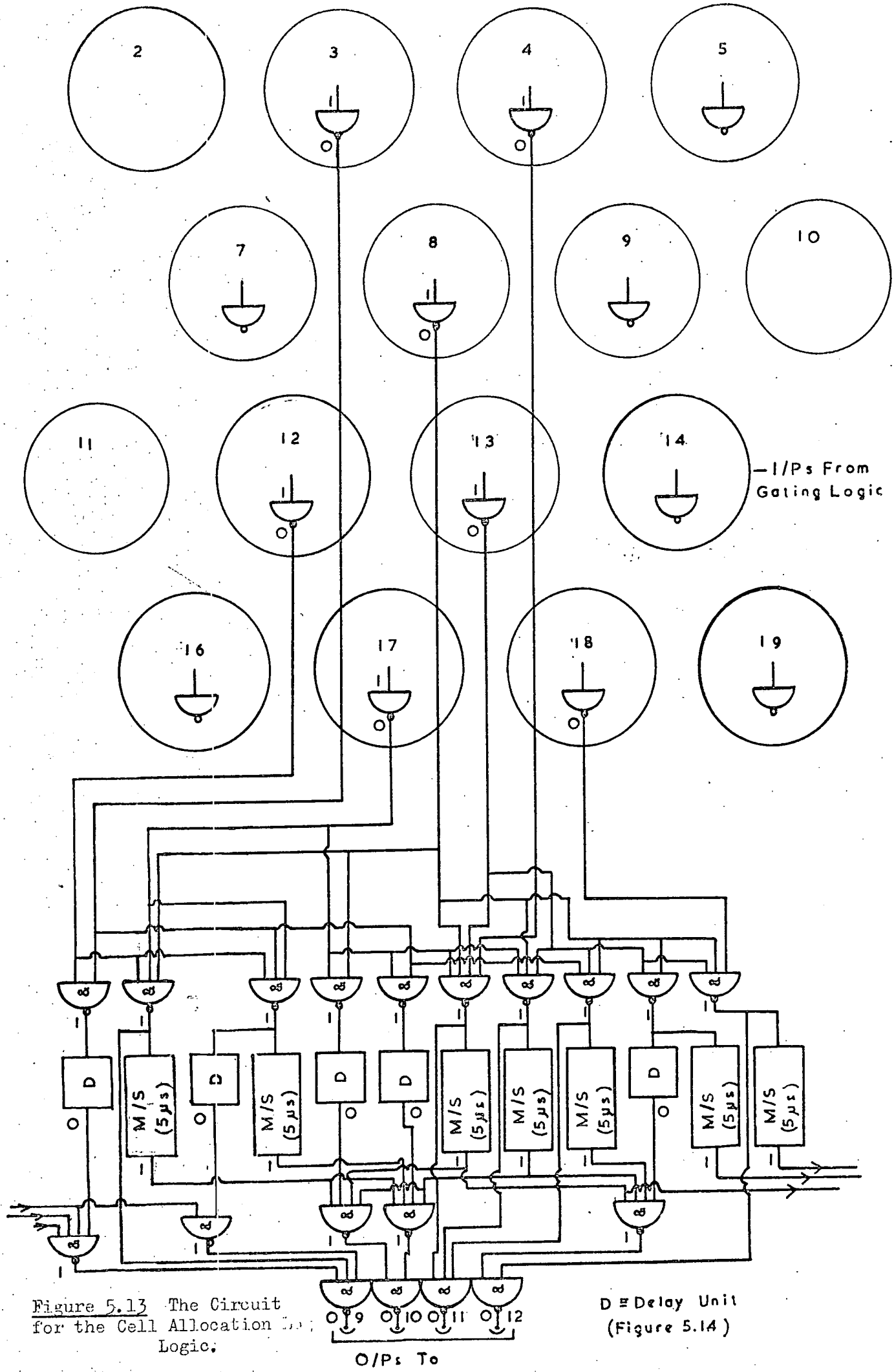

Figure 5.13 The Circuit for the Cell Allocation [illegible] Logic.

The purpose of the delay unit is to delay the pulse by about 0.85 μs during which time a possible veto pulse will have been produced. The circuit for the delay unit is shown in figure 5.14, which also shows the logic levels in the off mode. The delay is obtained by differentiating the output pulse from the first gate in the delay unit by means of the capacitor and input impedance of the gate and resistor. The final gate is triggered by the negative edge of the differentiated pulse. The output pulse is of length 0.15 μs delayed by about 0.85 μs. This delay unit has been incorporated in the logic as a precaution in case of some delay in the veto circuit which would cause a pulse to be sent from the logic from an incorrect cell as well as the correct cell.

The output from the delay unit is connected to an input of a coincidence gate. The other inputs to the gate are the veto inputs. These veto inputs are normally at a logical 1 state. If a veto is required then the corresponding veto input changes to a logical 0 state for 5 μs. Thus when the delayed positive pulse is produced the logical 0 on the veto input prevents the output of the gate from changing. The veto pulse is produced by a monostable, or pulse shaper, whose circuit is described in Appendix A.

The outputs from the coincidence gates for a given cell are connected to the inputs of a buffer gate. There is thus one buffer gate for each cell and the output pulses from these gates pass into the Momentum Selector as described below. The length of the output pulses from the gates depends on whether the flash tube combination for the cell has to be vetoed. If a veto may occur for the combination then the output pulse is of length about 0.15 μs, otherwise it is of length 1 μs.

The circuits are built on printed circuit boards. Each board contains the logic required for 20 cells and there are 80 integrated circuit blocks mounted on a board. As there are a total of 152 cells the logic required is thus contained on 8 boards. The boards are assembled together in pairs as described below.

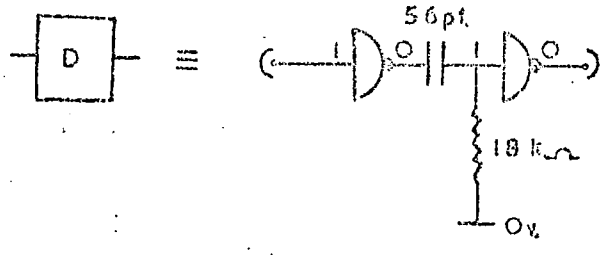

Figure 5.14. The Delay Unit Used in the Cell Allocation Logic.

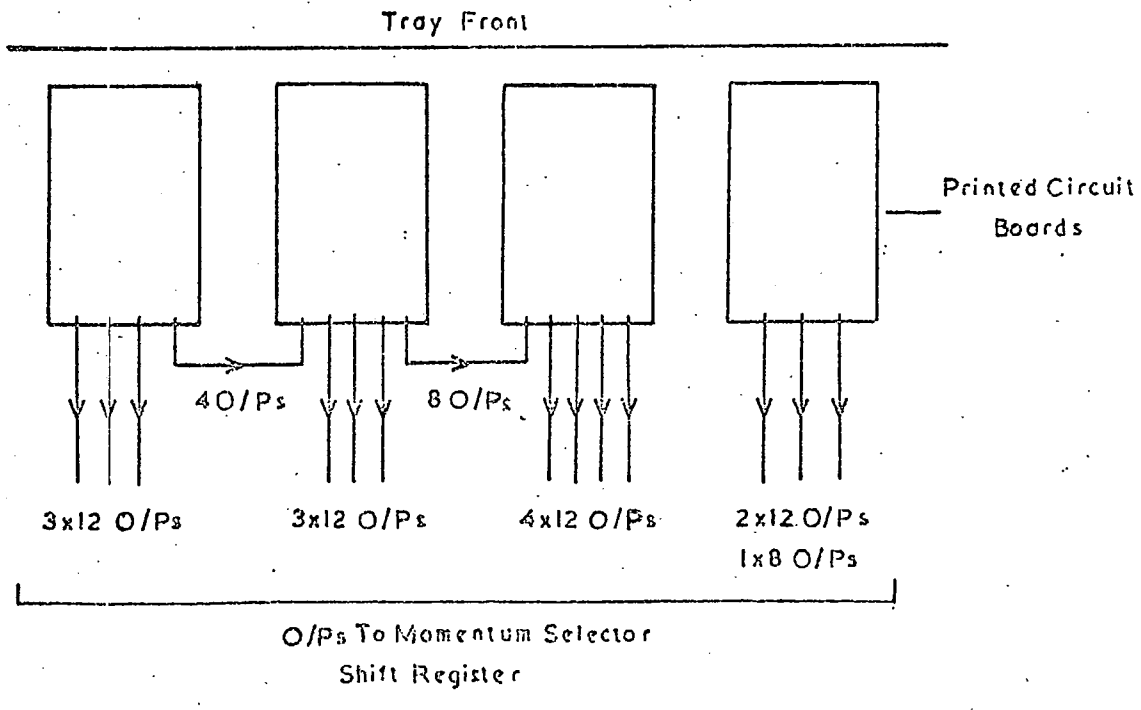

Figure 5.15. The Arrangement of the Cell Allocation Printed Circuit Boards in a Tray.

The blocks on each board were soldered on to individual bases. Interconnection between blocks was made by miniature wire which is on the other side of the board, the wire being soldered to the block base after passing through a small hole drilled for this purpose in the bases. As the wire is on the back of the board, there are no blocks in the way and the wire can pass from block to block in a straight line, thus making a saving on the wire used.

The inputs to each board from the flash tube gating logic are through a pin type edge connector strip which is fixed by adhesive in a Perspex strip of width 3.2 cm as shown in figure 5.10.

The Perspex strip also holds the pair of boards a fixed distance apart. Two $\frac{1}{2}$" diameter Perspex cylinders of the same width as the strip are fixed at the two corners at the opposite end of the boards. The boards are then secured in the framework by screws into the Perspex. The arrangement for two boards joined in this way is shown in figure 5.10. The edge connector also contains the inputs and outputs to adjacent boards for the continuation of the logic between boards, and the power input.

The outputs from the buffer gates for each cell in a tray pass down 12 way individually screened cable to the Momentum Selector, which is situated in a rack near to the spectrograph and is shown in Plate 2. To ensure that all the 12 cables in the multi-core cable are used, thus reducing the amount of cable required, the outputs from the boards are arranged in groups of twelve. As there are forty outputs from each pair of boards, excluding the last pair in a tray, the remainder of the wires, after dividing into groups of twelve, are passed to the adjacent pair of boards through a small length of multi-core cable. Figure 5.15 shows the arrangement for the boards in a tray. The cables are connected to the tray through a 15 way plug on each cable which mates into a 15 way socket fixed on the ends of the pair of boards on the side opposite to the edge connector.

The use of edge connectors and sockets on the boards in this way enables a faulty board to be removed from the tray and repaired. It also allows the

boards to be periodically removed for checking with the test circuit described in §5.8.5.

The boards plug into the corresponding mate for the edge connector on the boards. These edge connectors are contained in a strip of Perspex in a similar way to the edge connector on the boards and are fixed by adhesive in the slit. The Perspex strip is 77 cm long and contains four edge connectors. It is held in front of the tray by a framework of $^{5}/_{16}$" square steel bar which is fixed to the digitisation shield, as shown in figure 5.10, in front of the shield. The outputs from the gating logic on the flash tube memories are connected to the corresponding input on the edge connectors.

The steel bar framework also supports the boards when they are connected to the edge connectors on the tray along the end of the boards opposite to the inputs. This prevents strain and possible damage to the edge connectors.

5.8.5 The Test Circuit for the Cell Allocation Logic

The test circuit for the boards which allocate a cell in each Momentum Selector tray to a particle traversing the spectrograph is shown in figure 5.16. The circuit is designed to test a unit of two circuit boards joined together as described in §5.8.4. For the purpose of this sub-section a board will be taken to imply the two board unit.

The principle of the circuit is to feed known flash tube combinations into the boards under test and to check that the correct cell is indicated. Each input to the board is controlled by a switch situated on the front panel of the chassis containing the electronics. These inputs correspond to the forty flash tube inputs to a board, three inputs from the next board in sequence across the tray, and three inputs from the previous board. The six inputs from other boards are a consequence of the logic circuits continuing across a tube space.

The input pulses to the board under test are pulses of the same length as those which will occur when the board is connected in a tray. These inputs can

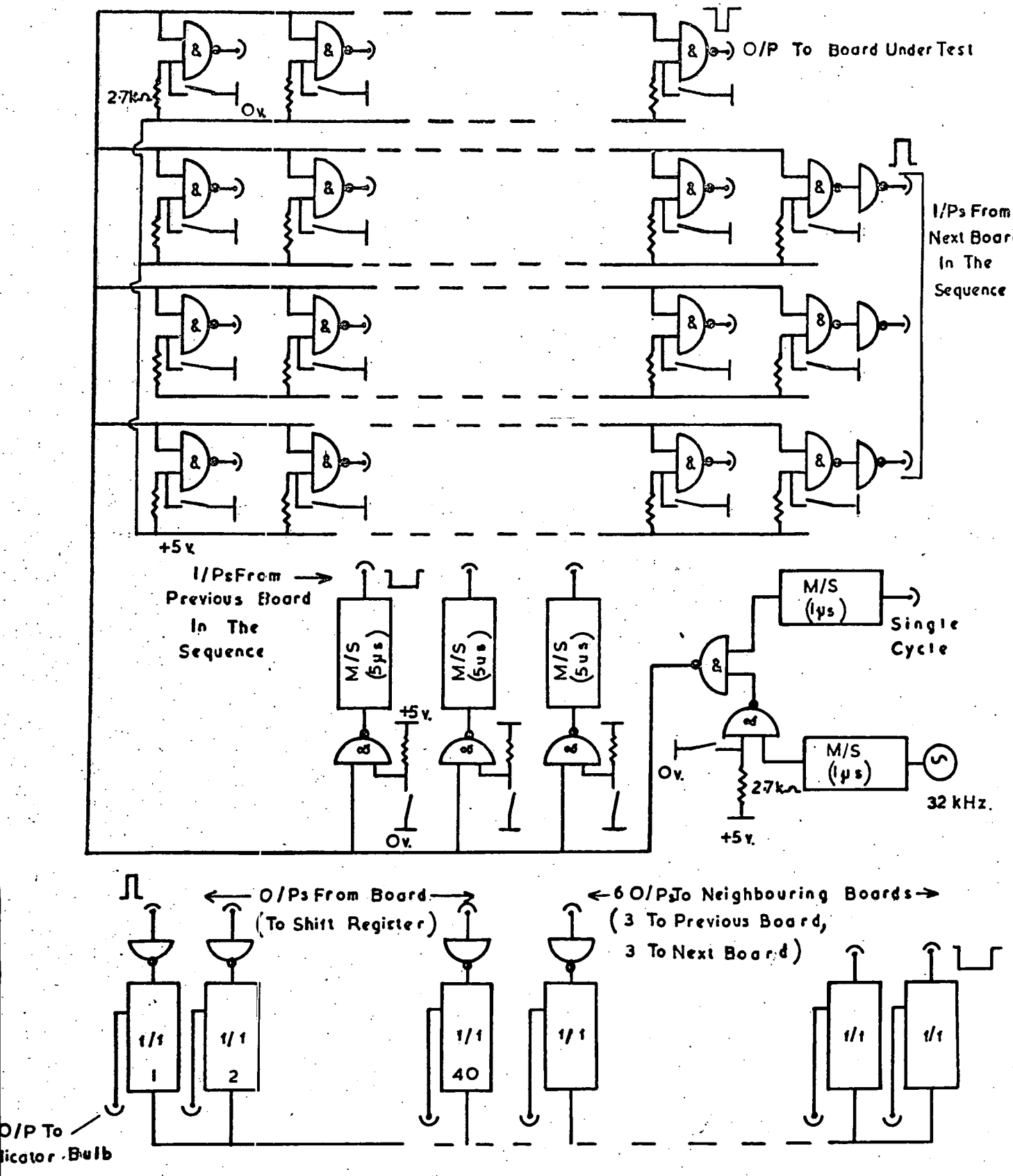

Figure 5.16 The Test Circuit for the Cell Allocation Logic Boards.

be of two forms: a single pulse to an input to the board whose switch is on, whenever a single cycle button is pressed, or a series of pulses of the same length as the single shot pulse but now at a frequency of 32 kHz. These latter pulses are useful for fault finding in the board. The single shot pulse is obtained by triggering a monostable by a push button on the front panel of the chassis. The series of pulse outputs is obtained by a multivibrator running at a frequency of 32 kHz which is connected to a monostable. The monostable output is then gated to the inputs to the board by a switch mounted on the front panel of the chassis. The monostable and multivibrator circuits are described in Appendix A.

The outputs from the board will normally be a single pulse from the cell which the particle traversed. To indicate the outputs which produce a pulse, each output is connected to a flip-flop which changes state on the application of a pulse from the board. The output from each flip-flop is connected to an indicator bulb which thus shows if an output pulse has been obtained. The outputs from a board correspond to the forty outputs from the cells on the board, three outputs to the next board in the sequence, and three outputs to the previous board.

The board is tested by connecting it to the test circuit and feeding in all the possible flash tube combinations which set off a cell and checking to see that the correct cell is indicated. This process is repeated for all the cells on a board.

The boards can then be tested periodically using the test circuit or when any fault is noticed in the outputs from the Momentum Selector Trays to the Momentum Selector.

5.9 The Momentum Selector Electronic Circuits

The circuit for the Momentum Selector shift registers is shown in figure 5.17. Only one shift register is used for each of the three levels so the inputs from the corresponding cells on opposite sides of the spectrograph are fed into the same shift register by the use of logic gates on the input

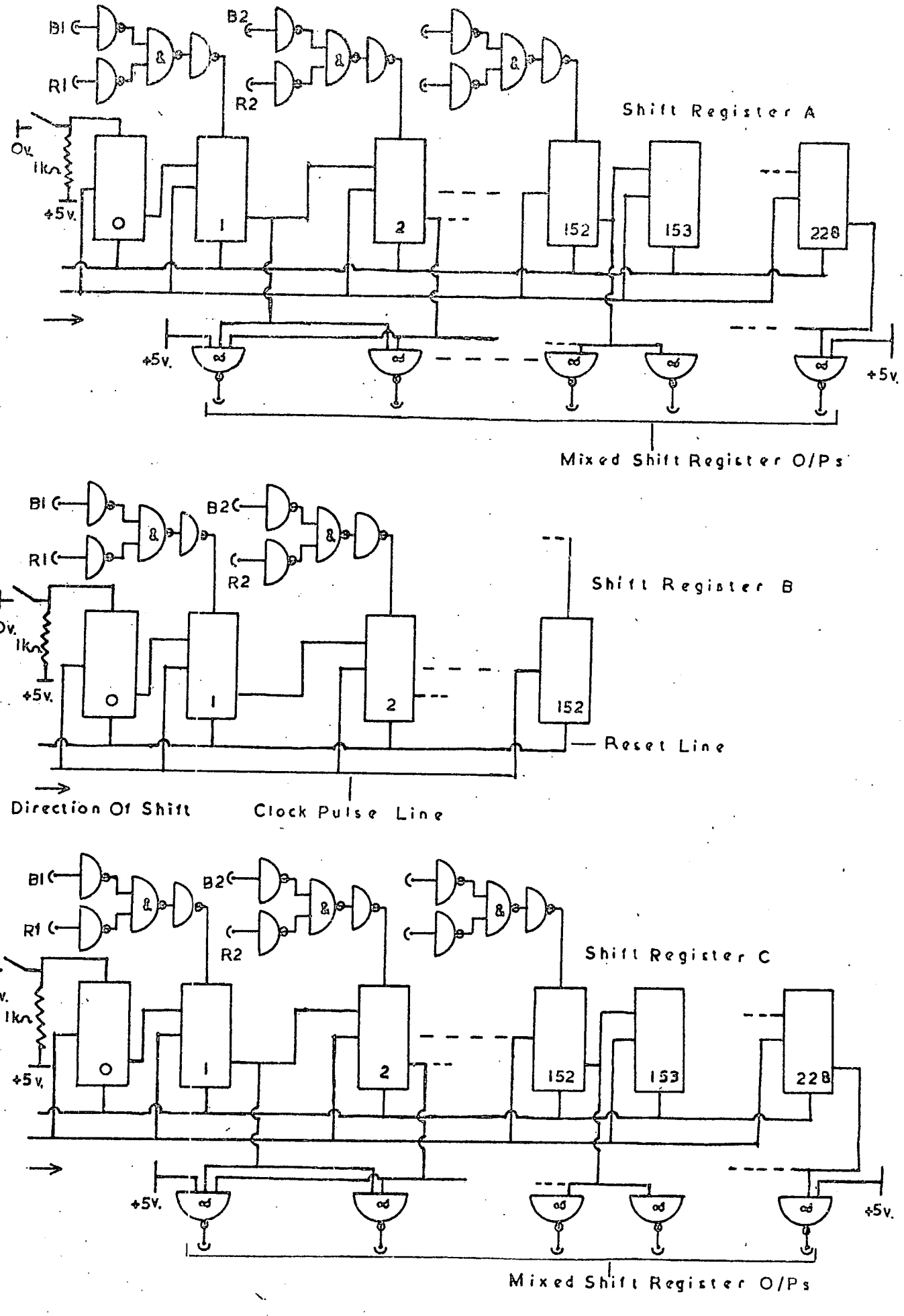

Figure 5.17. The Circuit for the Momentum Selector Shift Registers.

to each shift register bit. The shift registers are made from Mullard integrated circuit blocks type FJJ131. This type of logic circuit is described in Appendix A.

To take account of the cell allocated being out by ± 1 cell, which is mainly due to wrong cell allocation in the logic caused by the bias built into the system as described in §5.6, the outputs of adjacent bits in shift registers A and C are mixed using a three input nand gate. The resultant output is taken as the output for the middle shift register bit of the three.

The information in each shift register bit can be shifted into its neighbour in the direction shown in figure 5.17 on the application of a clock pulse from the shift register control unit described below. The direction of the shift pulse is such that when it is converted to a shift direction in a Momentum Selector Tray the direction is always towards the centre of the magnet. The reason for this assymmetry is to facilitate the analysis of events using the special device R.U.D.I. It should be pointed out that the shift direction will have no effect on the selection of high momentum particles. Figure 5.18 shows the cell numbers for the Momentum Selector Trays in the spectrograph when viewed from the front of the trays. The corresponding cell numbers on both sides are mixed into the same shift register bit as shown in figure 5.17.

A high momentum event is defined in §5.2 as being when a straight line exists between the cells set off by the particle at the three measuring levels. This is achieved in practice by shifting the cells in the direction shown in figure 5.17 and looking at all the possible straight lines which pass through shift register bit numbers 76 and 152 of shift register B. The straight lines are found by the use of three input nand gates, there being 151 possible straight lines at both shift register B bit numbers 76 and 152.

The extra bits in shift registers A and C are necessary to allow for a straight line to pass out of either A or C shift register bit number 152 before the cell in B reaches bit number 152. There are 76 extra shift register bits in both shift registers A and C to allow for this possibility.

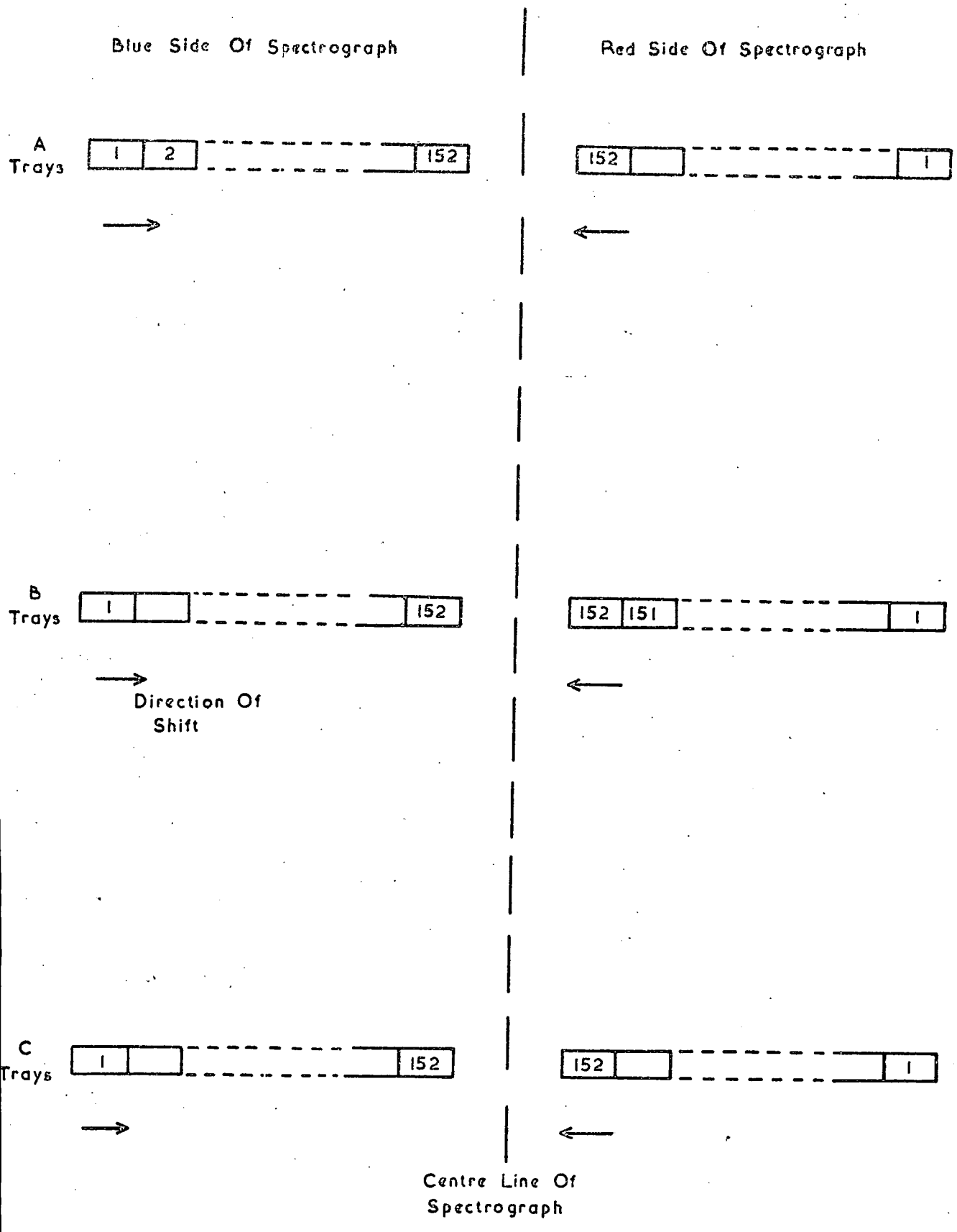

Figure 5.18 The Cell Numbering and Shift Directions in the Momentum Selector Trays.

The outputs from the three input nand gates are mixed so that a flip-flop on the output from the mixer circuit changes state when a straight line is found. The circuit diagram for the mixing circuit is shown in figure 5.19. To prevent the presence of a high momentum event being indicated at a variable time from the mixer circuit, the flip-flop output is gated by a scaler which counts 90 clock pulses. After 90 clock pulses, a pulse is fed to the veto gate and a possible output pulse allowed which triggers a monostable as shown in figure 5.19. The clock pulses are not stopped until a reset pulse is received from the reset unit. Hence output pulses from the unit are vetoed by a flip-flop which is triggered by the output pulse.

The high momentum output pulse is fed to the reset unit to apply a paralysis to the apparatus and to the tray steerage logic to initiate the core store read in of the information in the Measuring Trays in the triggered side and the Azimuth Trays.

The electronic memory resets, the gating logic on the memories, and the Momentum Selector shift register control unit, are all controlled by pulses from the coincidence and reset units which are fed into a control unit. The circuit for the control unit is shown in figure 5.20.

There are two inputs to the control unit from the main coincidence unit to indicate which side has been triggered. A corresponding flip-flop is set which opens the gating pulse outputs to the triggered side. The pulse from the coincidence unit also produces output pulses to the buffer gates on the tray fronts, which control the memory reset, and to the Momentum Selector shift register control unit, which controls the resetting of the shift register bits and the clock pulse to the shift registers. The output pulses to the buffer gates are of sufficient length to ensure that the reset input in the electronic memories are in a logical 0 state when the high voltage pulse is applied. The logical 0 state is removed before the digitisation pulse is obtained from the flash tube. Figure 5.21 shows the sequence of pulses produced after $t = 0$ which is the arrival of a coincidence pulse from the scintillation counters.

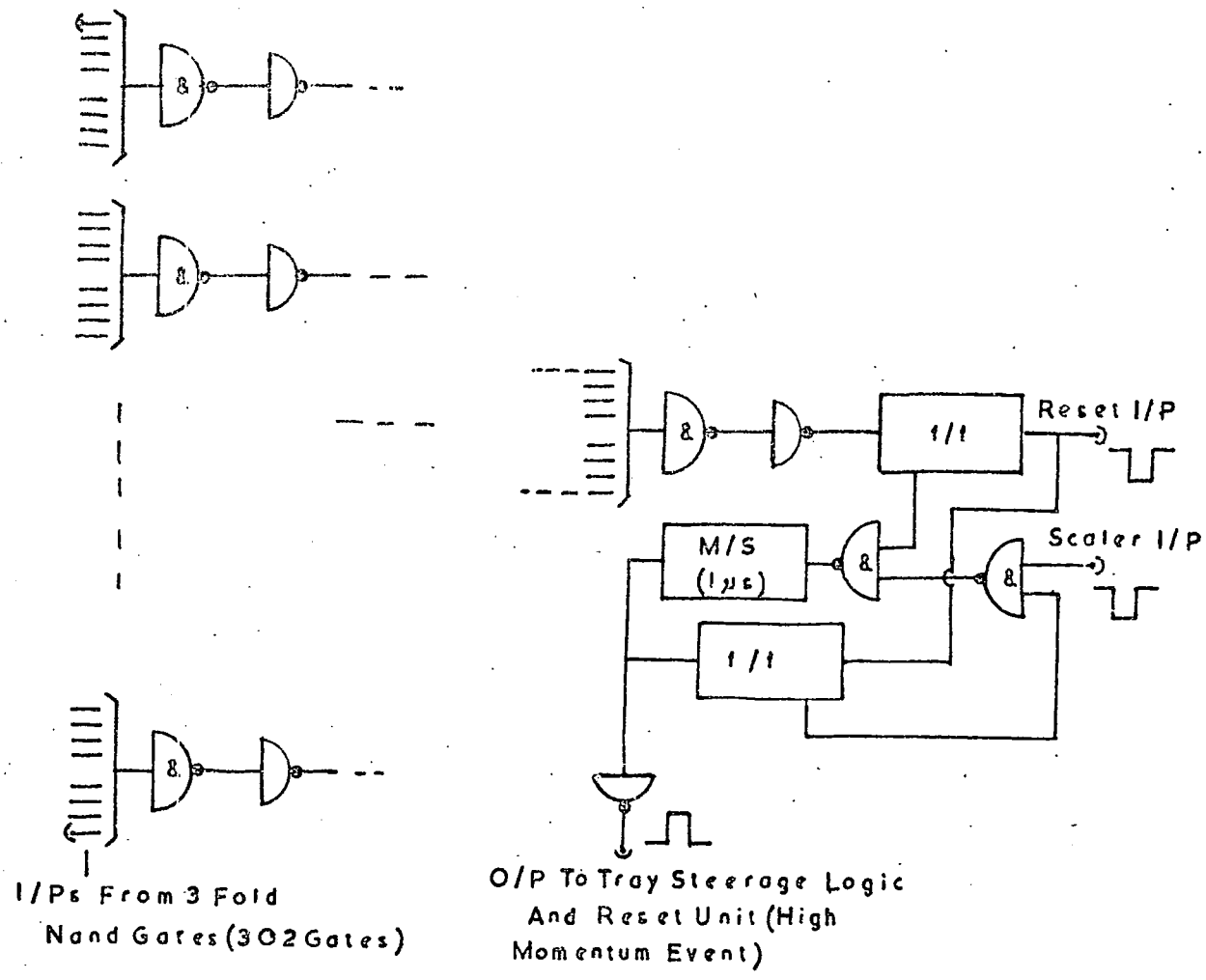

Figure 5.19. The Mixer Circuit of the Momentum Selector.

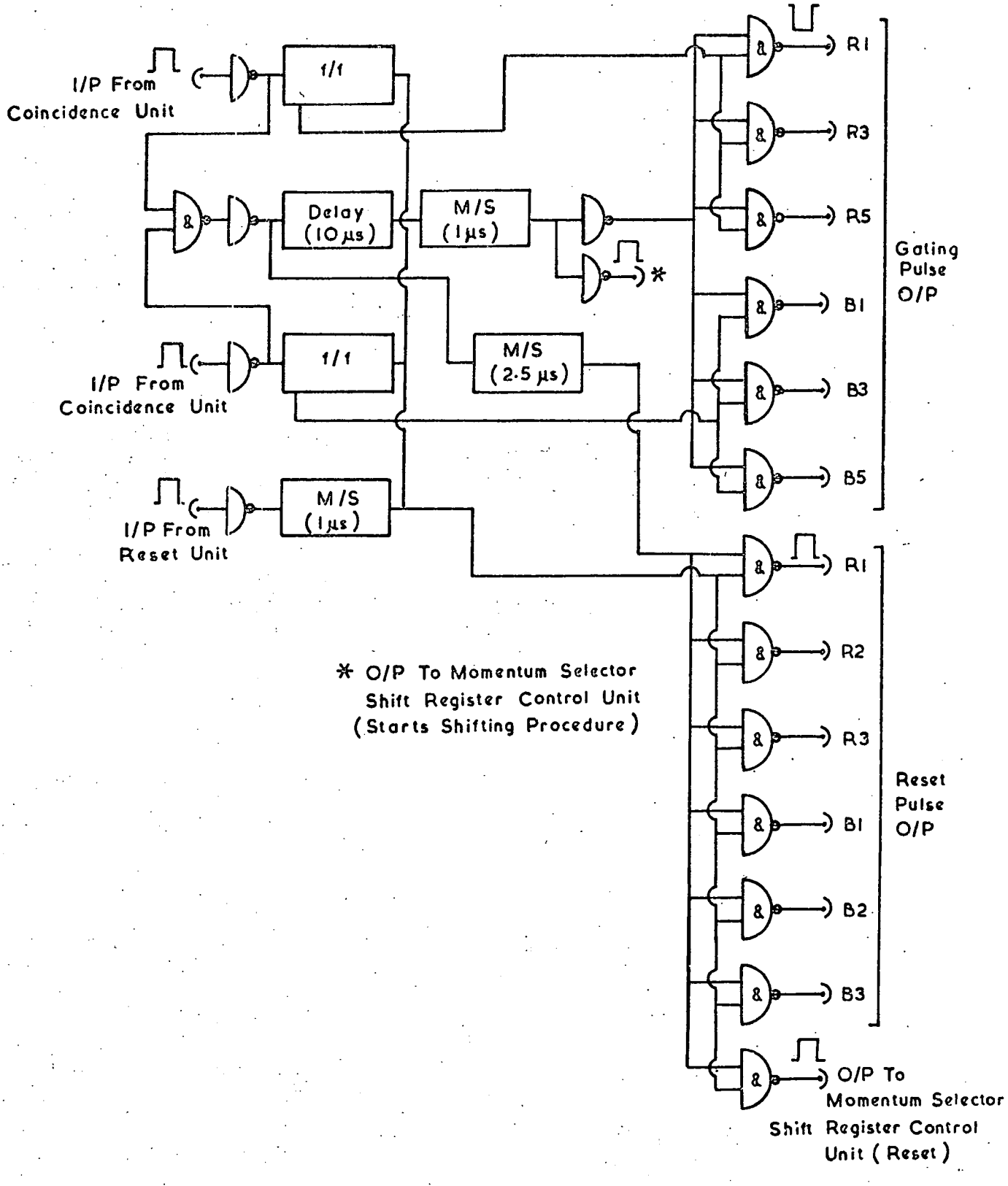

Figure 5.20 The Circuit for the Momentum Selector Control Unit.

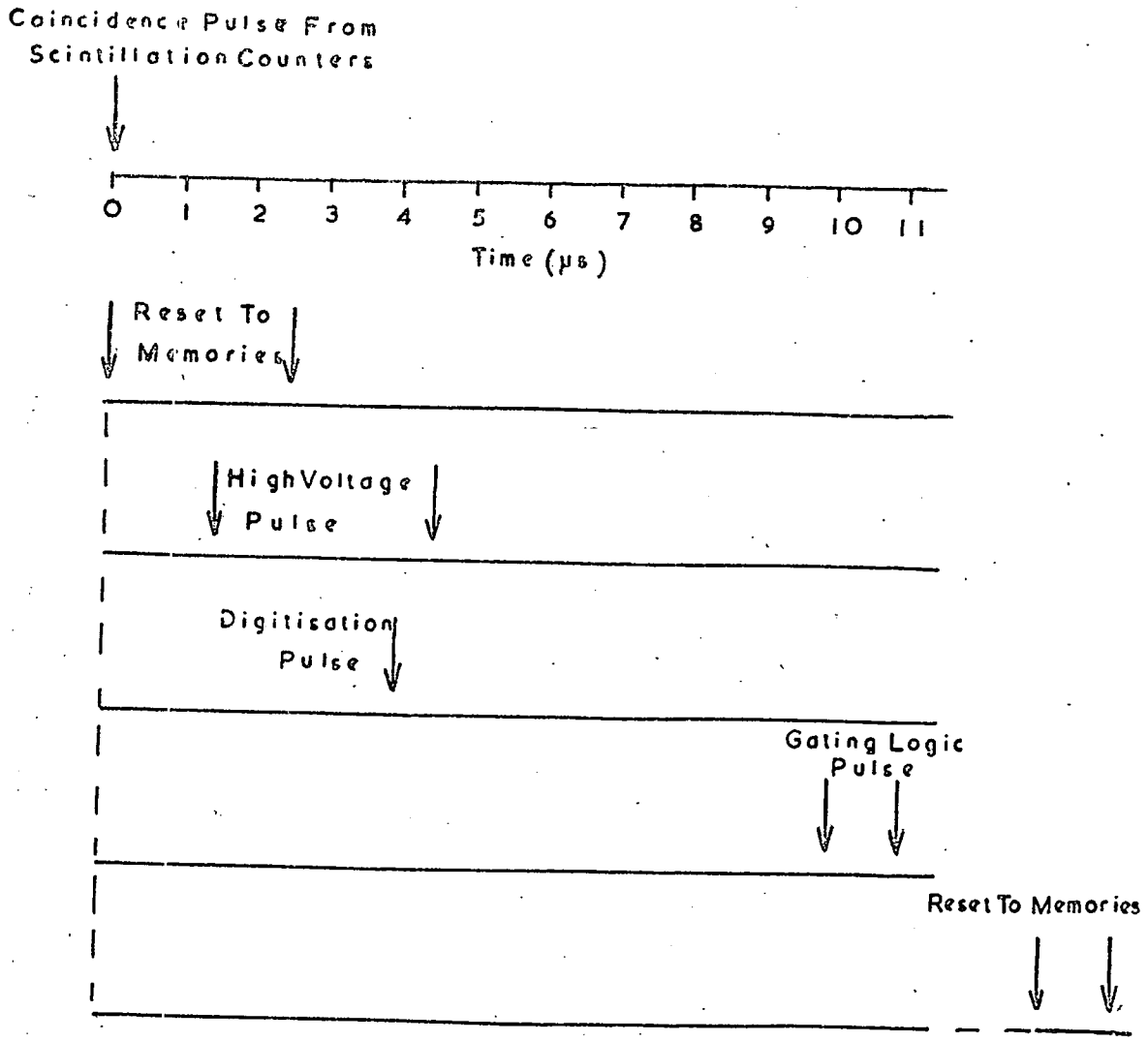

Figure 5.21 The Sequence of Pulses in the Momentum Selector System when a coincidence pulse is obtained from the Scintillation Counters.

The reset pulse on the memories is applied for 2.5 μs. The high voltage pulse on the flash tubes is applied 1.5 μs after t = 0 and the digitisation pulse is produced about 2.5 μs after the start of the high voltage pulse or 4 μs from t = 0. Hence the reset pulse is off before the digitisation pulse. The gating pulse to the memories is produced 10 μs after t = 0 and is of length 1 μs. Finally a further reset pulse is applied to the memories, which is controlled by a pulse from the reset unit as described below. The time of this pulse depends if the particle is a high or low momentum event as explained in §3.4.3.

The output pulse to the Momentum Selector shift register control unit also ensures that the shift register bits are not set by electronic pick up. It should be noted that the reset pulses are used on all Momentum Selector Trays irrespective of which side is triggered. This is again a safety precaution in case of pick up in the memories on the side not triggered.

The inputs from the coincidence unit are mixed as shown in figure 5.20 and the mixed output is delayed by 10 μs, after which a 1 μs pulse is produced, which is fed to the Momentum Selector Trays in the triggered side to allow pulses to be fed into the cell allocation logic from the memories. A pulse is also fed into the Momentum Selector shift register control unit to prepare for pulses from the flash tube trays.

A pulse from the reset unit resets the flip-flop indicating which side had been triggered and the electronic memories. A pulse is then sent to the Momentum Selector shift register control unit to reset the shift registers and stop the clocking of the shift register bits.

The circuit for the Momentum Selector shift register control unit is shown in figure 5.22. In the off state, the clock pulse is vetoed and the output bits of each shift register are in the logical 1 state. After a pulse is fed from the coincidence unit to the Momentum Selector control unit, a pulse is fed from this unit to the reset input. This pulse then triggers a monostable of length 8 μs. The pulse is then fed to the clock control flip-flop and the

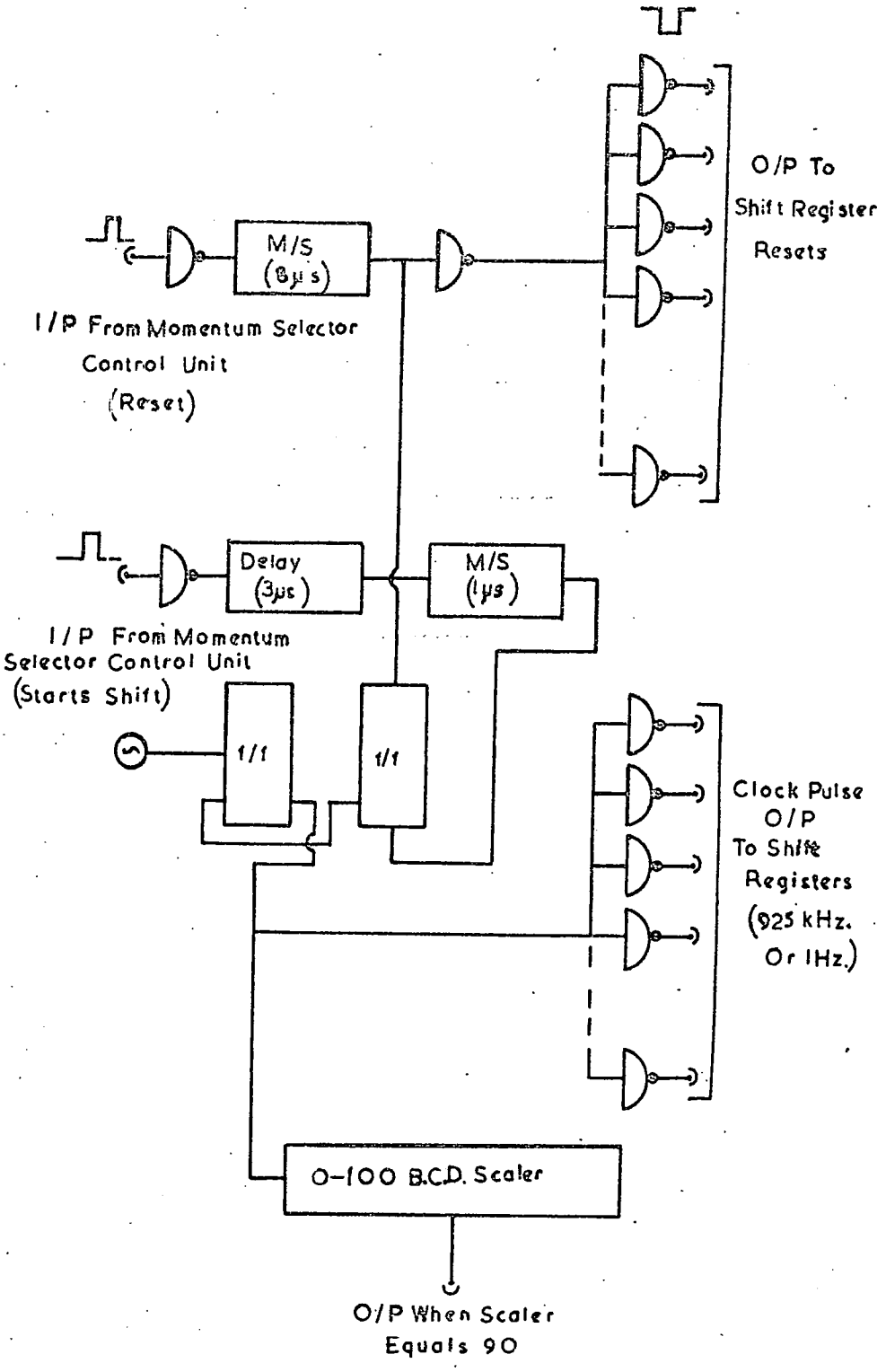

Figure 5.22 The Circuit for the Momentum Selector Shift Register Control Unit.

shift registers to prevent pickup when the high voltage pulse is applied to the flash tubes. The pulse is applied to the shift registers through a series of buffer gates. This fan out is necessary because of the large number of shift register bits, there being a total of 611 shift register bits in the three shift registers. Each buffer gate is then used to drive 12 shift register bits. The clock control flip-flop is normally off at this stage so the application of a pulse is just a precaution.

When the gating pulses are sent to the Momentum Selector Trays, a pulse is also fed to the shift register control unit. After a delay of 3 μs, during which the shift registers are set by pulses from the tray fronts, the flip-flop vetoing the clock pulse is triggered thus enabling clock pulses to be fed to the shift registers. The clock pulses are fed to the shift register bits through a similar system of buffer gates as the reset pulse. The clock pulse is produced by a multivibrator which is described in Appendix A.

Two clock pulse frequencies can be used. The normal clocking frequency is 925 kHz but a shifting frequency of 1 Hz can be used if required. This slow shifting rate has been incorporated in the design as an aid to fault finding.

As mentioned above the clock pulses are counted by a scaler. After the scaler has counted 90 clock pulses an output pulse is produced which gates the output of the flip-flop recording the high momentum event.

The clock pulse is stopped and the shift registers set to their normal off modes by a pulse from the Momentum Selector control unit in a similar way as the initial reset pulse during the application of the high voltage pulse. Again the application of a reset pulse to the shift registers is just a precaution since all the information in the registers will have been shifted to the end of the registers before a reset pulse is obtained.

To keep a visual check on the shift register bits, the bits of each shift register are grouped together consecutively in units of eight and fed into the inputs of an eight input nand gate. Normally the input to the nand gate will

be in a logical 1 state, the output changing to a logical 0 state when the shift register holds relevant information. The outputs to the nand gates are monitored by a bank of indicator bulbs, the bulbs being in the on state when any bit of the shift registers on the inputs to the gates is in the on state.

As a further aid to electronic fault checking, an extra shift register bit has been placed at the beginning of each shift register as shown in figure 5.17. This bit is set in the on state by a push button, it normally being in the off state. The fast or slow clock pulse can then be applied and the movement of information across the shift register can be seen with the use of the indicator bulbs. Any shifting fault can easily be seen.

The Momentum Selector shift register control unit, shift registers, and associated logic for the determination of high momentum events, are contained on plug in type printed circuit boards. The boards plug into edge connectors fixed in a special chassis. The circuits are contained on 55 boards. Interconnection between boards is made by the use of wire soldered between the relevant edge connector pins on the back of the board. The multi-way cable from the logic contained in the tray fronts fit into 15 way sockets fixed on a special designed back to the chassis. Connection to the board is made by wire from the socket to the edge connector. This wire is of sufficient length to enable the back of the chassis to be removed from its correct position to enable any relevant repair or fault finding on the edge connectors to be carried out. The power inputs and other relevant inputs and outputs are also connected to the back plate.

The unit is contained in a rack near to the spectrograph and is shown in Plate 2, the visual indicator display is above the printed circuit boards.

5.10 The Method of Analysis of the Low Momentum Events Using R.U.D.I.

The Restricted Use Digital Instrument (R.U.D.I.) is used in conjunction with the Momentum selector shift registers to determine the deflection, charge, and zenith angle for an event in the spectrograph. The results of the analysis

are stored in a 400 channel pulse height analyser (P.H.A.) in sixteen deflection spectra. Four zenith angle ranges are used and for each range there are four spectra corresponding to the arrival direction and the charge of the particle.

A block diagram of the arrangement is shown in figure 5.23. The scalers AB and BC count the clock pulses applied to the shift registers to shift the information to the end of each register. The scaler AB is started by the first arrival at bit 152 of the shift register of a triggered cell in either shift register A or shift register B and is stopped by the second arrival in the other shift register to the one which started the scaler. The scaler thus records the distance ab in figure 5.23 which shows a typical event through the spectrograph. The scaler BC records in a similar way the distance bc in figure 5.23 by being controlled by the arrival times of the bits in shift registers B and C at the 152nd bit.

The deflection, Δ in figure 5.23 is obtained by either adding or subtracting the scaler values. Which of the two modes is the correct one is determined by the arrival orders of the bits at the 152nd bits of the shift registers. As already mentioned in §5.9 the shift direction for the Blue and Red sides are arranged so that they shift towards the centre of the magnet. This results in the measured deflection for a charged particle to be always in the same direction, irrespective of the side of the spectrograph the particle traversed. The charge of the particle is then obtained from the known field direction.

The zenith angle of the particle when projected in the deflection plane of the magnet will be proportional to the value of scaler AB., the arrival direction of the particle being determined by the arrival sequence at bit 152 of A and B shift registers and the triggered side.

When the Momentum Selector has shifted all the bits to the 152nd bit, which will take 151 clock pulses, the event is stored in the P.H.A. in one of the sixteen possible spectra. The spectrum in which the event is stored is calculated by the logic after taking into account the trigger mode and the

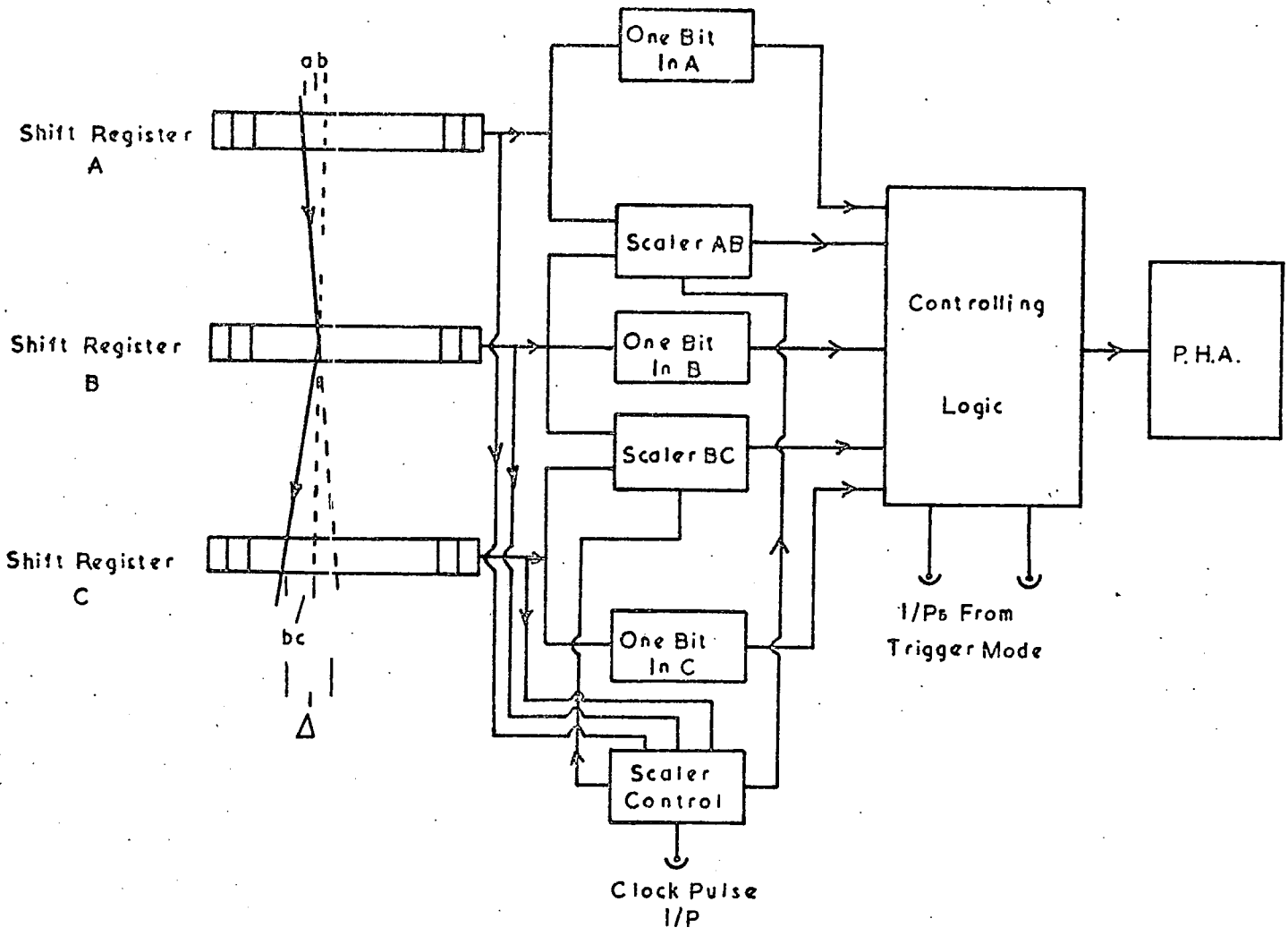

Figure 5.23 Block Diagram of the Digital Device R.U.D.I.

field direction.

Because of the ambiguity which would occur if the Momentum Selector contains more than one cell in any of the three shift registers, a controlling logic circuit is built into the device which checks that there is only one bit in each shift register. If there is more than one bit the event is not stored. Similarly the event is not analysed if there is no bit in any of the shift registers.

As the P.H.A. has 400 channels the sixteen recorded spectra are allocated 25 channels each. This is subdivided into channels corresponding to deflections of 0,1,.....up to 23 cells and each channel can record up to 10^6 events. The final channel is not used, it serves as a gap between spectra and is a useful check on whether R.U.D.I. is working as no information should be recorded in this channel.

CHAPTER 6

The Measuring Trays and Associated Circuits

6.1 Introduction

The Measuring Trays are used to determine the trajectory of a particle which has been flagged by the Momentum Selector as being a high momentum event. Each tray contains 712 neon flash tubes of length 2 metres, mean internal diameter 5.55 mm and filled with neon gas at a pressure of 2.4 atmospheres. The flash tubes were made by International Research and Development Co. Ltd. of Newcastle-on-Tyne, who have had considerable experience in the manufacture of flash tubes of various sizes for a variety of experiments. The tubes are painted black to prevent one flash tube setting off adjacent tubes when it discharges and are digitised using the method discussed in Chapter 4.

This chapter describes the Measuring Trays and associated electronics used in conjunction with the flash tube digitisation technique. Also described briefly are the electronics for the core store and other digital information stored with a high momentum event.

6.2 Construction of the Measuring Trays

The flash tubes are supported by an outer framework made from 1" x $\frac{1}{2}$" bright steel bar of overall size 290cm x 84cm x 12.1cm. This framework is constructed in a similar manner as the Momentum Selector Trays. The trays are similar in external form to those of the Momentum Selector except that each tray contains 8 layers of tubes, there being 89 flash tubes per layer. As there is this similarity between the Momentum Selector Trays and the Measuring Trays only the parts of the tray which differ will be described. The Momentum Selector Tray is described in §5.4.

The electrodes for the trays are made from 18 S.W.G. (1.2 mm) aluminium sheets, which are fixed in position by Tufnol supports in a similar manner to the Momentum Selector Tray. There is similarly an overlap of $\frac{1}{4}$" (6.4 mm) between adjacent electrodes.

The brass supports for the tubes and the digitisation shield were made in a similar manner to the supports and shield for the Momentum Selector Trays. The size of hole used to support the tubes varied from tray to tray because of the slight variation in the diameter of the flash tubes. The flash tubes were arranged in groups depending on their tube diameter, the interval betweeen groups being 0.1 mm. This interval was chosen because it is the standard interval in metric drill sizes. Table 6.1 shows the drill sizes used for the Measuring Trays.

TABLE 6.1

The Hole Diameters Used in the Measuring Tray Supports and Shield

Level	Blue Side	Red Side
1	8.0	8.1
2	8.2	8.1
3	8.1	8.0
4	8.1	8.1
5	8.1	8.0

Before the tray was filled with flash tubes, the tubes were tested for spurious flashing. It was whilst carrying out the tests on spurious flashing that the effects discussed in Appendix B were noticed.

The trays were filled in a similar manner to the Momentum Selector Trays except that a small double-concave shaped spacer made of Tufnol was placed between each tube near to the middle of the tube. This small spacer is used to fix the tubes firmly in position as a tube of this diameter and length is very springy if held only at its ends and any vibration of the tubes when placing the tray in the spectrograph would cause the tubes to move. Thus a hole diameter close to the actual flash tube diameter together with the small spacers hold the tubes in a fixed position in the tray.

These small spacers were made by placing a $\frac{1}{4}$" sheet of Tufnol between the aluminium block and the brass plates before drilling the holes. After drilling

had been completed, a matrix of holes was left in the Tufnol sheet. The sheet was then cut into the required spacers.

When a row of holes had been filled during the construction of a tray, the small Tufnol spacers were placed between each tube and fixed by adhesive to the electrode on which it rested. To facilitate ease in fixing the spacers, they were placed into two rows separated by a few inches. Each row then contained the spacers for adjacent tubes. The flash tubes in a layer were then aligned parallel using a similar technique as was used for the Momentum Selector Trays. After alignment, a small white paint spot was applied at the end of the tube to indicate the correct position of the tube in the tray.

The interconnection of alternate electrodes uses the same method as the Momentum Selector Trays and the high voltage pulse is also applied to the tray in a similar manner.

6.3 The Flash Tube Pattern

The stagger of the flash tubes used in the Measuring Trays is shown in figure 6.1. The distance between adjacent tubes in each layer is 8.6 mm. This distance was chosen so that there would be a wall thickness of approximately 0.5 mm between adjacent holes in the flash tube support plates and the digitisation shield. This value was considered to be the minimum wall thickness as below this value the wall would be too weak. The distance between the centres of adjacent layers was equal to the hole diameter plus the electrode thickness.

Bull et al. (1962) compared the uncertainty in particle position obtained with a random stagger of the flash tube layers with the uncertainty obtained with a designed stagger. They concluded that there is no significant difference between random and designed staggers of flash tube layers. A designed stagger was used for the Measuring Trays. The form of the stagger used was chosen after testing various possible stagger arrangements.

Scale diagrams were drawn of the possible staggers. A measuring level was drawn on the diagrams along the centre line of the tray as shown in figure

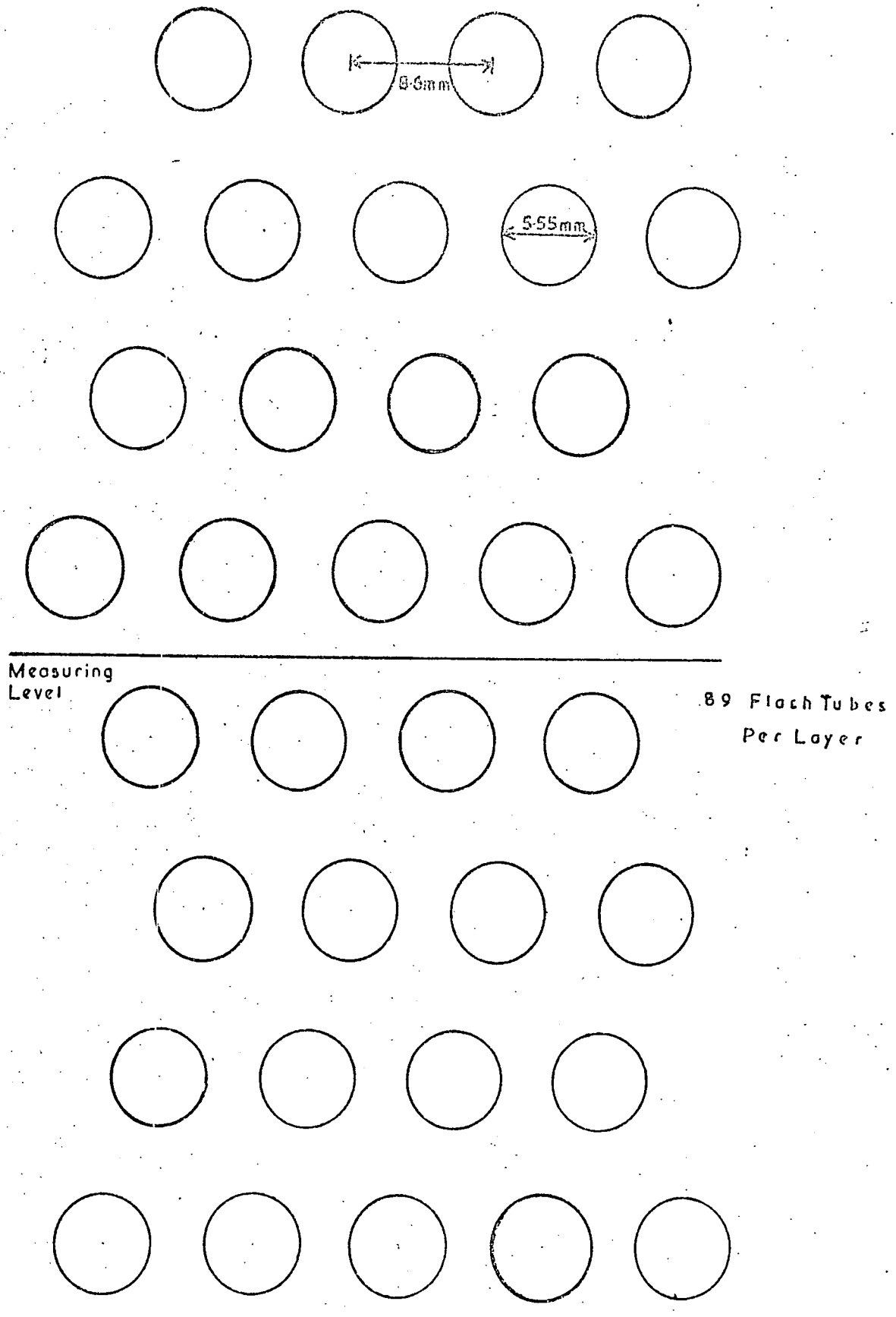

Figure 6.1 The Flash Tube Pattern used in the Measuring Trays.

6.1. For a given angle to the vertical, the number of channel widths in a tube spacing (8.6 mm) was found across the measuring level. The channel width is defined as the distance along the measuring level over which the same pattern of flash tubes is traversed by tracks at the same angle to the vertical. The channel width is then the total uncertainty in position of the particle at the measuring level.

The spectrograph will accept high momentum particles with projected zenith angle up to 7^{o}. A flash tube stagger is thus required which has as near a uniform response as possible over this zenith angle range. This response was measured for the various flash tube patterns by plotting the weighted mean of the channel widths in 2^{o} steps of angle on both sides of the vertical. The channel widths were weighted according to their widths since for a given angle, the probability of a flash tube combination will depend on the channel width for that particular combination. Hence flash tube combinations with a large channel width will occur more often than a smaller channel width.

Figure 6.2 shows the graph of the weighted mean channel widths for the flash tube stagger finally used in the spectrograph. For comparison figure 6.3 (a) shows the corresponding graph for the flash tubes stagger shown in figure 6.3 (b) in which alternate layers of tubes are vertically below one another. This stagger can be seen to have a large uncertainty in position for vertical tracks compared to a closely uniform uncertainty for the flash tube stagger used in the spectrograph. The weighted mean over the angular range was found to be 0.94 mm for the flash tube stagger used in the Measuring Trays and 1.14 mm for the flash tube stagger shown in figure 6.3 (b).

Using a similar method to that described for the Momentum Selector Trays in §5.6, the error in location of a particle in a flash tube tray can be determined for the cell widths over the angular range 0^{o} to 8^{o} on both sides of the vertical. A histogram of the discrepancies is shown in figure 6.4. The distribution is symmetric about the zero value for the discrepancy and has a

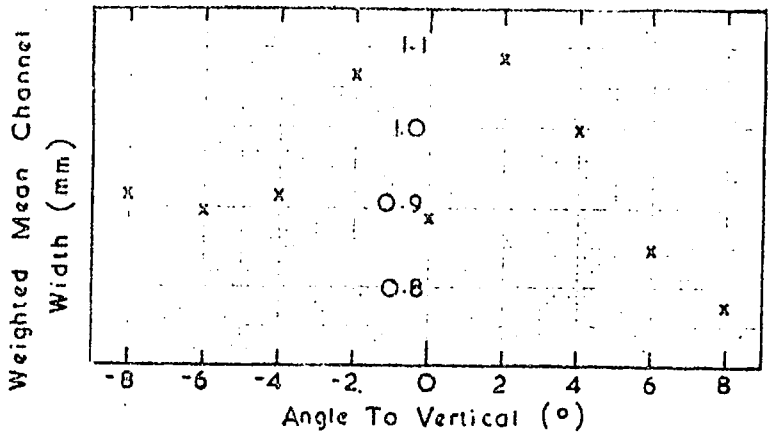

(See Figure 5.7 For Angle Convention)

Figure 6.2 Graph of the Variation of Weighted Mean Channel Width with Angle for the Measuring Tray Pattern.

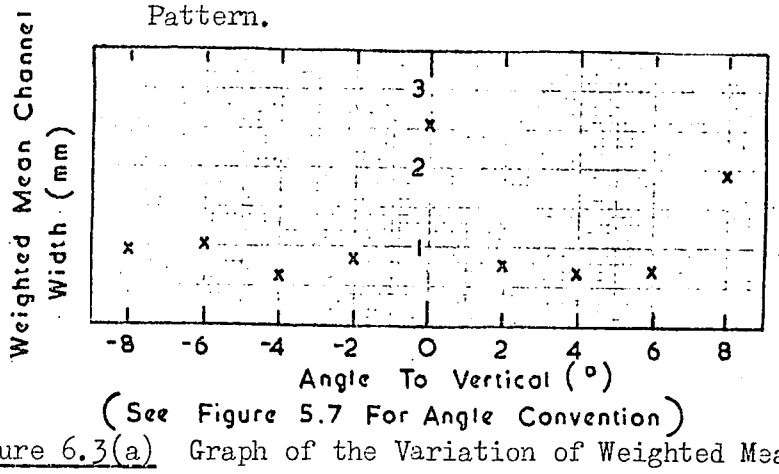

(See Figure 5.7 For Angle Convention)

Figure 6.3(a) Graph of the Variation of Weighted Mean Channel Width With Angle for the Flash Tube Pattern of Figure 6.3(b).

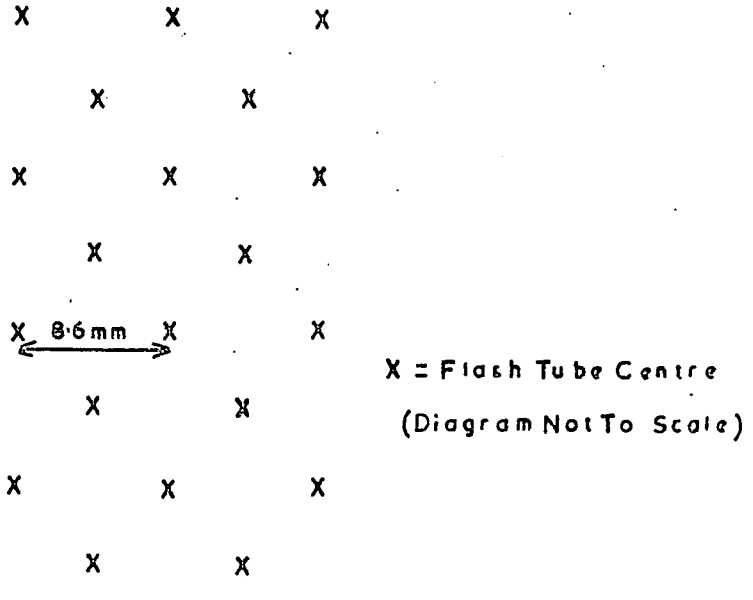

Figure 6.3(b) The Flash Tube Pattern used to obtain the Graph of Figure 6.3(a).

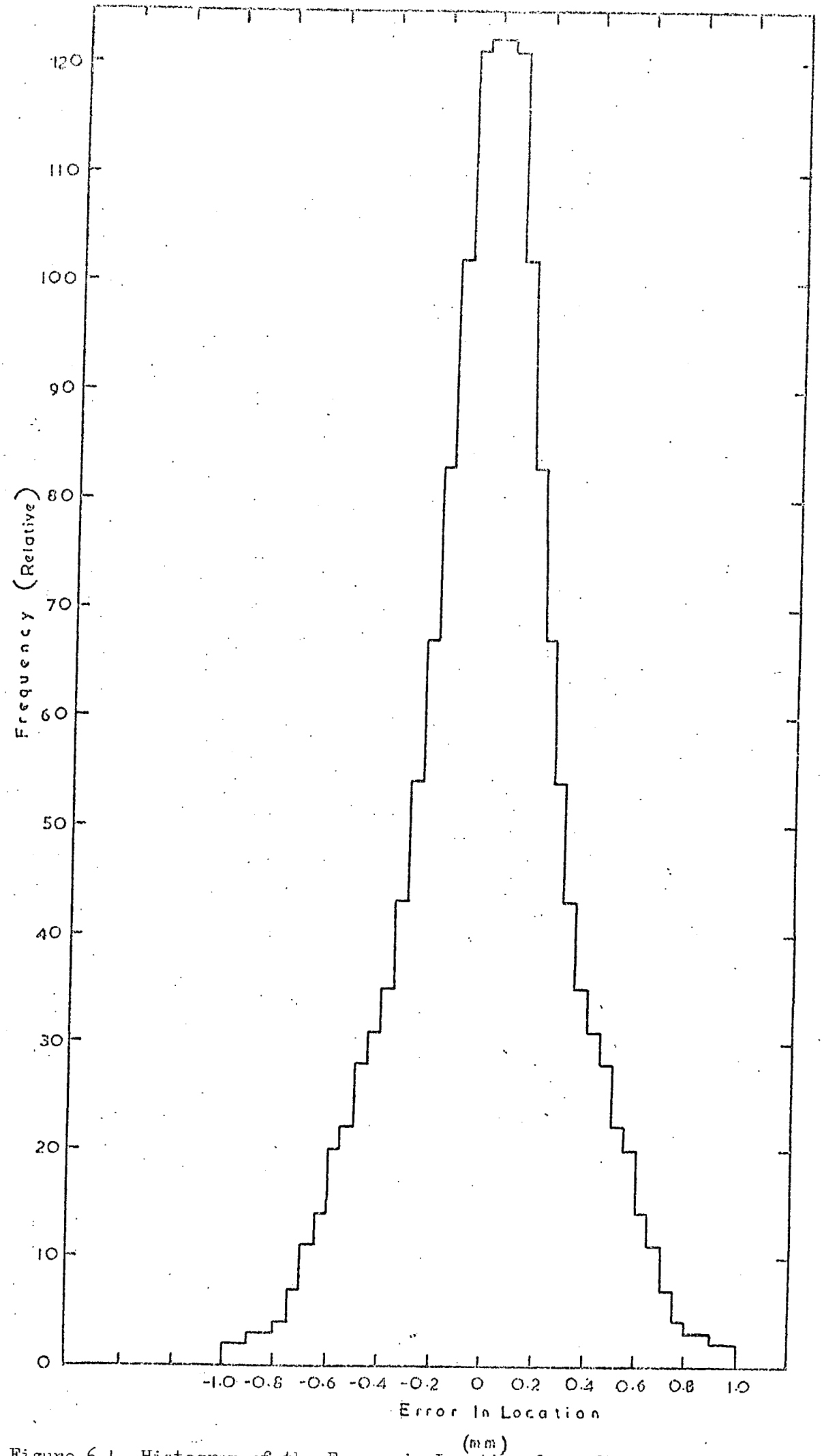

Figure 6.4 Histogram of the Errors in Location for a Measuring Tray Tube Spacing.

mean value, ignoring the signs of the discrepancies, of 0.23 mm and a standard deviation of 0.30 mm. The value of the standard deviation of the distribution is used in §7.4 to estimate the maximum detectable momentum of the spectrograph.

The above analysis assumes that the flash tubes are 100% efficient. Any decrease in efficiency will cause the channel widths to vary and increase the weighted mean channel width and broaden the discrepancy distribution.

The flash tube pattern shown in figure 6.3 is only used in the Measuring Trays in the Blue side of the spectrograph. A mirror image of the pattern is used on the Red side. The 'mirror' is the vertical plane through the centre of the magnet and parallel to the flash tubes.

This arrangement is used as an aid to the computer programme to determine the sign and momentum of the particle traversing the spectrograph. The flash tube pattern is the same on each side of the spectrograph if it is viewed along the magnetic field direction. Then the deflection of particles of the same charge will be in the same direction when viewed along the magnetic field direction in both sides of the magnet.

As will be explained in §6.4, the flash tube information is fed to the computer a column of flash tubes at a time. The flash tube columns are scanned always towards the centre line of the magnet so that the first column in each tray is always on the outside. This ensures that the column stagger for each tray is the same.

6.4 The Readout System of the Flash Tubes

6.4.1 Introduction

This system controls the recording of the information of a flashed tube by an electronic memory and the subsequent readout of the memory output into the core store.

As each Measuring Tray contains 712 flash tubes, an output wire from every flash tube memory in a tray to the core store would cause obvious practical

difficulties. A logic system has thus been devised in which the outputs from each column of flash tubes in a tray can be presented in turn on eight output wires from the tray, which are then fed into the core store logic.

This is achieved by grouping the flash tube memories into vertical columns in the same configuration as the flash tubes in the tray. Each column then comprises 8 memories and the columns are scanned by an electronic scaler until a column is found in which at least one tube has flashed. The memory information of the tubes in this column is then read out into the core store, together with the column number. This process is repeated for all the columns in a tray and for all the trays on the triggered side in turn and finally for the Azimuth Trays. The direction of the scan in the Measuring Trays is always towards the centre of the magnet as mentioned in §6.3.

This method of scanning for the flashed tubes in the columns is used instead of reading out the contents of each flash tube memory because it reduces the storage space required in both the core store and computer disc. Hence more events can be stored on the same disc.

The logic circuits used for the routing procedure are described below. They can be subdivided into two sections: the electronics on the tray fronts, and the tray steerage logic. The tray front electronics contains the electronic memories, gating logic for the flash tube columns, and the mixing circuits for the final outputs from the tray. The tray steerage logic is responsible for the resetting of the electronic memories and the order in which information is passed from the tray logic to the core store logic. But first, the form of the digitisation system for obtaining a output pulse from a flash tube when it flashes is described.

6.4.2 The Digitisation System

The digitising system used on the Measuring Trays is closely similar in form to the system for the Momentum Selector Trays, which was described in §5.8.3, except that there is only one printed circuit board mounted on front of the tray.

The probes used for the Measuring Trays are 1" 8 B.A. brass countersunk screws with a washer on their heads such that the diameter of the probe head is 0.45 cm. Perspex cylinders of length 1.9 cm then hold the probes symmetric in the probe shield in a similar manner to the Momentum Selector Trays.

The printed circuit board on the front of the tray contains the probe resistor and connection is made to the board from the probes using miniature stranded wire. Connection is then made from this board to the electronic memories via a series of sockets held in a steel framework of 5/16" square bar fixed to the digitisation shield. The framework holds 15 sockets, which are used with the circuit boards containing the readout logic from the tray. These boards are described in §6.4.3.

The high voltage pulse applied to the Measuring Trays is obtained by discharging a lumped parameter delay line as explained in §3.5. The value of the resistor used with the delay line is 22 ohm. The variation in layer efficiency as a function of the applied electric field, which is defined as the peak pulse height divided by the distance between electrodes, for this value of resistor, is shown in figure 6.5.

The expected layer efficiency, assuming a 100% internal efficiency for the tubes, is about 64%. The voltage chosen was thus the voltage which gave the nearest layer efficiency to that expected for 100% internal efficient tubes. The voltage chosen has a peak height of 6 kV, producing a peak electric field of 7.5 kV. cm^{-1} and corresponds to a voltage on the delay line of 13 kV.

6.4.3 The Electronics on the Tray Fronts

The electronics for the tray fronts can be subdivided into four main units, which are mounted on seperate printed circuit boards on the tray fronts. These are the circuits for the flash tube memories and the mixing of the memory outputs in a row of tubes; the logic to gate each column in a tray; a circuit to indicate to the tray steerage and core store logic that a column requires to be stored; and the mixer logic for the eight outputs from the tray to the

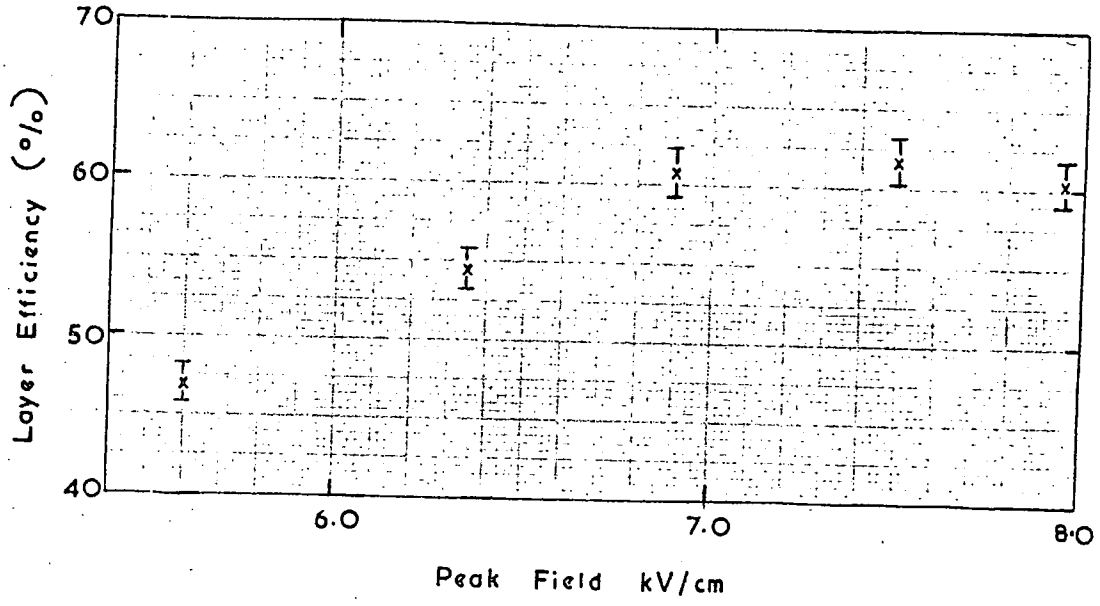

Figure 6.5 The Variation in Layer Efficiency of the Measuring Tray Flash Tubes with Applied Field.

core store. The circuits for these various components are described below. DTL integrated circuit blocks have been used in these circuits as a fast response is not required.

In each Measuring Tray there are 89 columns of flash tubes. These columns are numbered 2 to 90 respectively. Column 1 is a dummy column which contains information on the tray. This information in column 1 is fed into the core store every event so that the computer programme which analyses the event, can group the data on the flashed tubes into the corresponding trays. There are also six dummy columns at the end of the tray, columns 91 to 96 respectively. The eight bits in these columns in every tray will be used by the computer to store information on the processed event.

The integrated circuit blocks for the flash tube memories and the logic for the mixing of memory outputs in a row of tubes are on specially made printed circuit boards. The boards have been designed such that all possible interconnections between the blocks are printed on the board. Single sided board is used so all interconnections between blocks on the same row are printed on the board. Interconnection on the board between integrated circuit blocks on different rows is not possible because of the continuous power lines between the blocks. More, if not all, of the interconnections could have been made using double sided printed circuit boards but then the cost of a board would be greater by an approximate factor of two. The extra expense was felt not to be justified. The blocks and the interconnections between blocks were put on the board in a similar manner to the Momentum Selector boards for the cell allocation logic.

Each board contains the memories and routing logic for eight columns of tubes, 64 tubes in number. As there are 96 real and dummy columns per tray, 12 boards are required. The first board contains the dummy column and 7 real columns. The next 10 boards contain 80 columns and the final twelfth board the remaining two real columns and the six dummy columns. For the dummy columns,

electronic memory blocks are not used but the information to the mixing logic is held permanently in the required state. The output from the dummy columns will contain a coded number for the column so the computer can recognise it as a dummy column.

The logic diagram for a board is shown in figure 6.6(a). There are 74 integrated circuit blocks per board. The electronic memory used is the same as that used for the Momentum Selector flash tubes. Figure 6.6(b) shows the form of the memory. There are two outputs, output 1 and output 2, which are shown in the figure with the logic output states after a negative reset pulse is received. After being set by a pulse from the flash tube probe, the logic states on the two outputs flip over. These two output states are used in the readout logic as explained below.

The gating input to each column opens the output from an eight input nand gate whose inputs are from output 2 of the flash tube memories in the column. If one or more tubes have flashed in a column, a logical 0 state is produced at the corresponding input to the eight fold gate. This results in a logical 1 state on the output from the gate which is fed to a two fold gate, the other input to this gate is from the gating logic. When the gating pulse is produced at this gate, the gate output changes from a logical 1 level to a logical 0 level if one or more tubes in the column have flashed. This change in output is passed to a logic board which produces an output pulse to the tray steerage logic to commence the read in of the particular column into the core store.

If no output pulse is obtained the gating logic continues to scan the columns until it finds a column where one or more tubes have flashed.

The stopping of the gate pulse in its scan results in an input to eight two input nand gates changing from a logical 0 to a logical 1 state. The other input to each gate comes from output 1 of the flash tube memories for the column at which the gating logic stopped. If a tube has flashed the output from the gate is in a logical 1 state, otherwise it is in a logical 0 state.

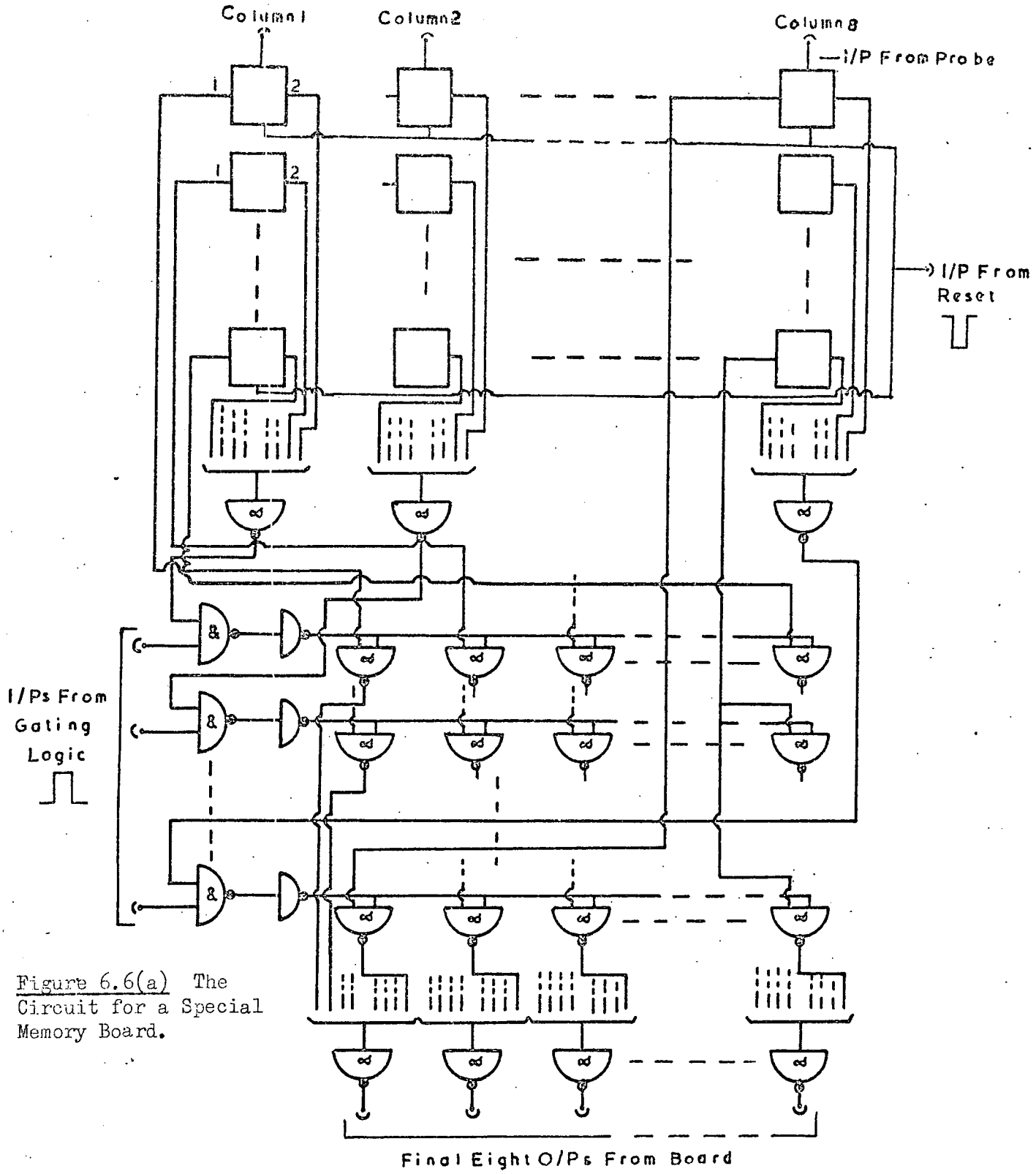

Figure 6.6(a) The Circuit for a Special Memory Board.

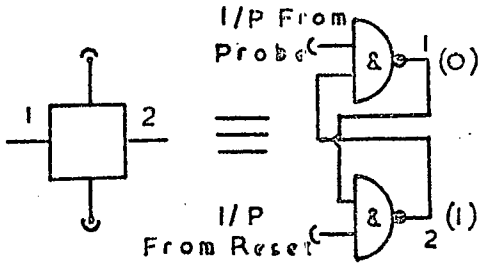

Figure 6.6(b) The Form of the Electronic Memory Used in Figure 6.6(a).

The eight outputs from the two fold gates, corresponding to the eight flash tube memories in each row contained on the board, are fed to the inputs of eight input nand gates. For a given gate, the inputs correspond to the eight flash tubes in the same row so there are eight gates per board. Normally, in the off state, these inputs will be in the logical 1 state, which thus give an output state of logical 0. On scanning the columns, the inputs will remain in the logical 1 state until a column is found where one or more tubes have flashed. Then the inputs to these eight input gates from the tubes in the column which have flashed will change to a logical 0 while the inputs from the rest of the column and the other tubes will remain in the logical 1 state. Thus the outputs from the gates will be at a logical 1 for the tubes in the column which have flashed.

The outputs from each final eight input nand gate on every board in a tray are fed into a mixer circuit which gives the output states of any column in the tray on the eight outputs from the mixer when that particular column is opened. This mixer circuit is described later in this sub-section.

The circuit for the gating logic in the tray is shown in figure 6.7. The function of the circuit is to convert an eight bit B.C.D. number into a decimal output for each column of flash tubes. The B.C.D. number is obtained from a scaler controlled by the tray steerage logic as described in §6.6 and is fed to the board via a twelve way individually screened cable. Each decade of the B.C.D. number is converted to its corresponding decimal number by a B.C.D. to decimal converter which is described in Appendix A.

Normally, the outputs from the circuit will be in the logical 0 state except for the output giving the decimal equivalent for the B.C.D. input number, which will be in the logical 1 state. This then enables the column corresponding to the number to be scanned for possible flashed tubes. The speed of scanning is governed by the frequency of the input pulses to the B.C.D. scaler as explained in §6.6. When a column is found in which one or more

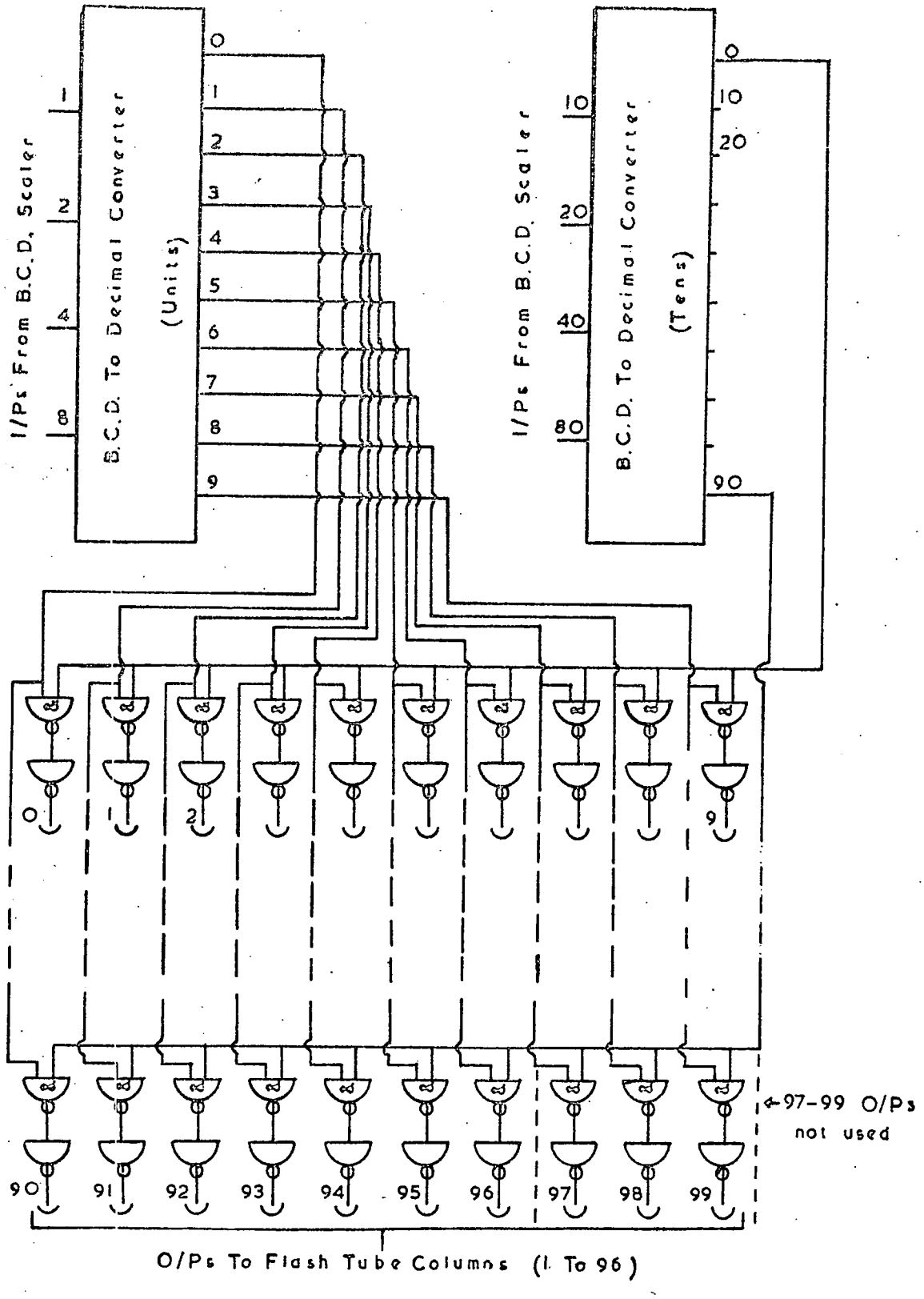

Figure 6.7 The Circuit for the Gating Logic.

tubes have flashed, the tray scaler logic stops the scaler on the column number, thus gating open this particular column.

The circuit is built on specially made printed circuit boards similar to the Momentum Selector boards used for the cell allocation logic, there being 64 blocks on each board.

The circuit which stops the scaler scanning the tray when a column is found in which at least one tube flashed is shown in figure 6.8. There are 96 inputs to the board corresponding to the 96 columns in a tray which are the outputs from the two input gate vetoed by the gating logic as described above. Normally these inputs are in a logical 1 state. When a triggered column is found, the corresponding input to the circuit changes from a logical 1 state to a logical 0 state. This produces an output pulse from the circuit to the tray steerage logic, which stops the scaler scanning the columns. The output states of the column are then fed into the core store and the scaler restarted when the data have been stored.

The output pulse from the circuit is fed from special driving gates designed for use with long cables and uses one of the cables in the twelve core cable used for passing the scaler information to the tray front. This circuit is also built on specially made printed circuit boards, there being 18 blocks on each board.

The mixer circuit used for the final output from the tray is shown in figure 6.9. There are eight outputs from the circuit which give the output states of the flash tubes in each column of the tray when the column is opened by the gating logic. There are twelve inputs controlling each of the eight outputs of the circuit, which correspond to one output from each of the twelve boards containing the flash tube memories.

The outputs from the board are fed via cable driving gates into the core store logic using eight cables of a twelve way individually screened cable. The information on these eight lines is thus read into the core store whenever

27 JAN 1972 LIBRARY

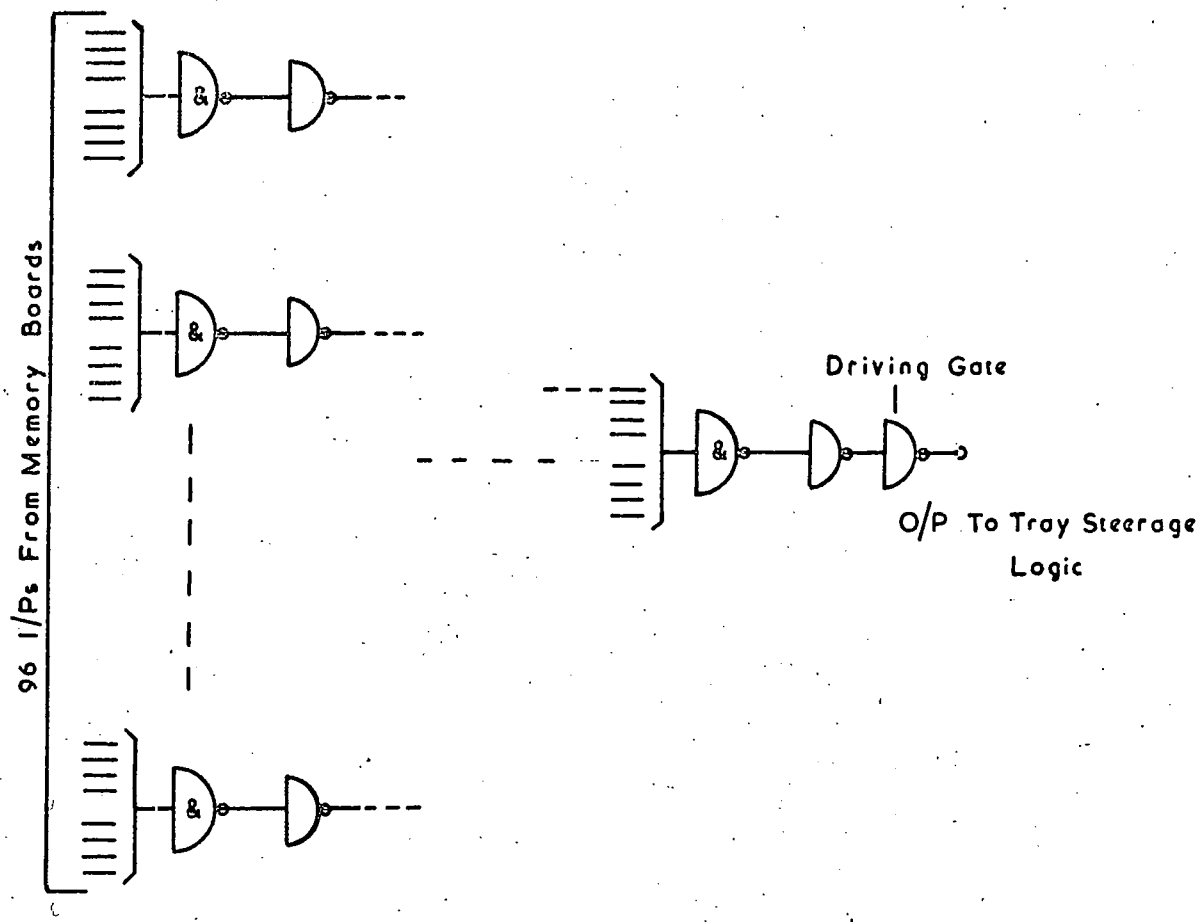

Figure 6.8 The Circuit for the Scan Control Board.

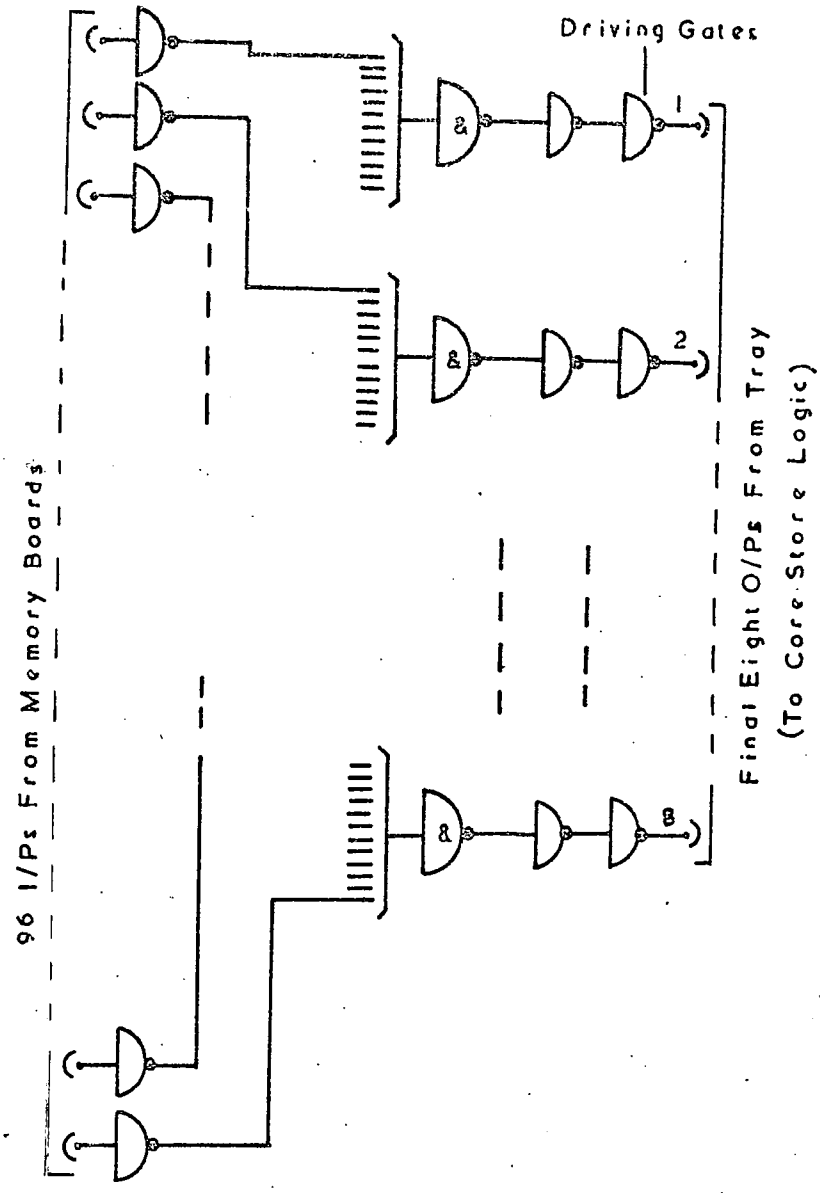

Figure 6.9 The Circuit for the Mixer Board.

a pulse is sent from the tray steerage logic which is itself initiated by a pulse from the tray front. The mixer board is also contained in a special made board with 44 blocks on the board.

Inputs and outputs to the four types of boards on the tray front are made through a plug fixed to the end of the board. The plug then connects into a socket fixed in front of the flash tube tray as described in §6.4.2.

6.5 The Measuring Tray Electronic Checking Systems

6.5.1 Introduction

As the electronics used in the Measuring Trays plays an important role in assuring that the correct data are stored, elaborate checking circuits have been designed for the boards situated at the front of each Measuring Tray. All these boards use multi-way plugs fixed on the ends of the boards which fit into sockets at the front of each tray. The checking circuits have been mounted on portable chasses into which each board can be plugged in turn during the checking period. The special checking circuits are described in the following sub-sections.

6.5.2 The Special Memory Board Tester

The test circuit for the special memory boards is shown in figure 6.10. Each board contains the memories for eight columns of flash tubes, 64 tubes in total. The principle of the check circuits is to feed known combinations into the 64 memories and to check that each memory has the expected information. This is achieved using an 8 bit binary scaler. The binary scaler used in the test circuit is made from Mullard integrated circuit blocks type number FCJ 101 and the form of the circuit is described in Appendix A. The monostable and delay circuits used in the test circuit are also described in Appendix A.

If the binary comparators find a fault, the scanning is stopped and indicator bulbs show the states of the expected output and the output found on the board. The column number where the fault occurred is also indicated. The scanning is also stopped if no output is obtained for the logic which

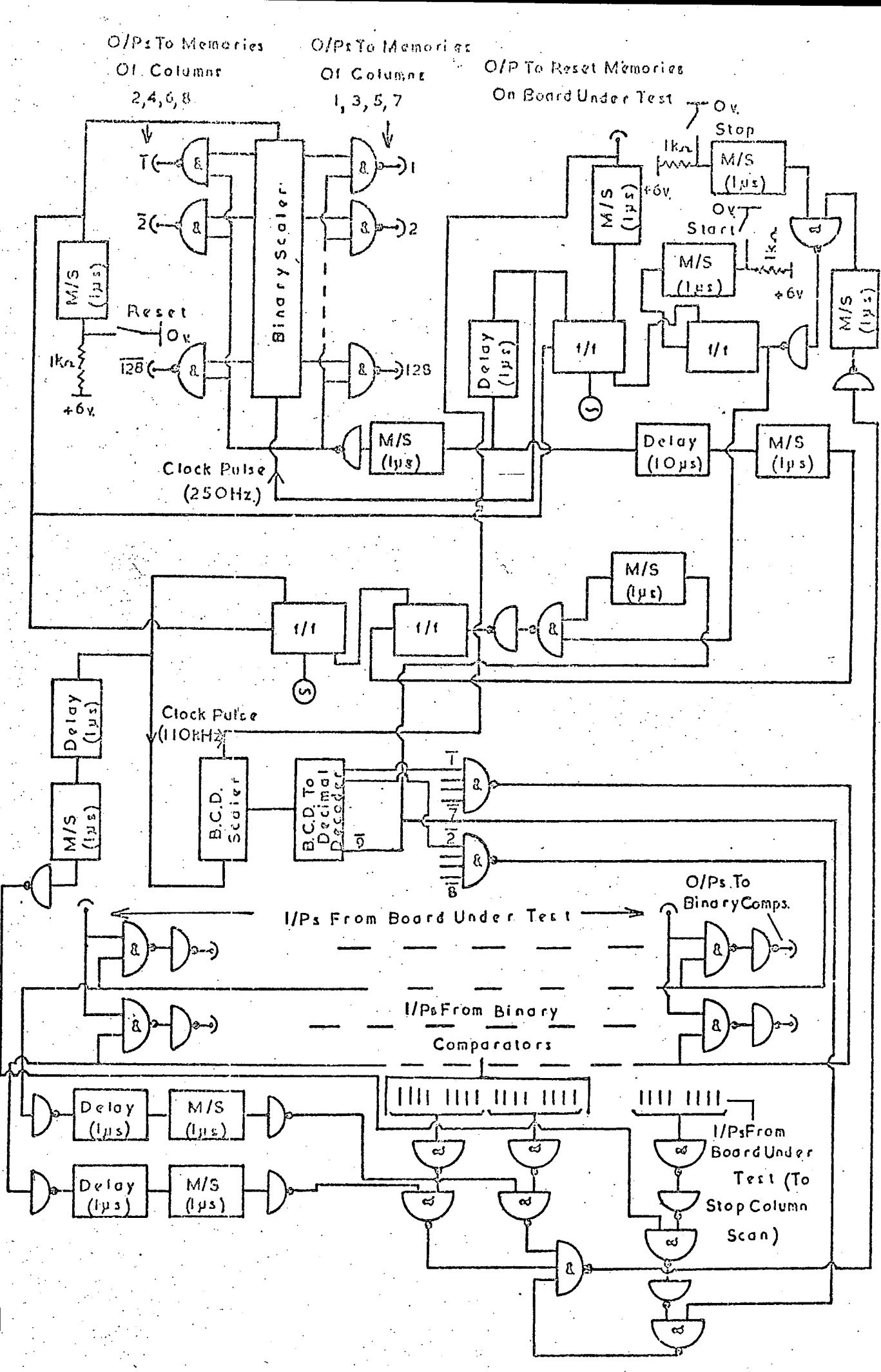

Figure 6.10 The Circuit for the Special Memory Board Tester.

stops the scan when a column with one or more flashed tubes is found. This fault is shown by an indicator bulb.

If no fault is obtained with the binary number fed into the memories, then the memories are reset, the scaler is incremented by 1 and this new number is fed into the memories. The process is repeated for all the possible eight bit scaler numbers (255). If all 255 numbers are fed into the board and no fault is found, then an indicator bulb is switched on to show that there is no fault on the board. The time required for a complete check on a board is about 1 second. Reset, stop, and start buttons are built into the unit to control the testing procedure and to set the flip-flops to the correct state when the power is switched on.

6.5.3 The Gating Logic Tester

The test circuit for the gating logic board is shown in figure 6.11. The logic on the board converts a B.C.D. coded number, which corresponds to a flash tube column number in a tray, into an output which gates the output of the tube configuration in the column.

The test circuit thus feeds into the board a known B.C.D. number which is obtained from a B.C.D. scaler, and compares the output from the board to the value expected using binary comparators.

Pulses are fed into the board under test at the scanning frequency of 100 kHz. The B.C.D. number to the board is also fed to logic in the test circuit to convert the number into the correct column number output. This logic is thus a repeat of the logic on the board under test. The outputs from the board under test are compared with the expected outputs using the binary comparators. The binary comparator outputs are fed into a mixer circuit whose output is gated on the clock pulse from the B.C.D. scaler. The clock pulse is delayed by 1 μs to allow the change in output to be fed into the board. If a fault is found then the scaler is stopped. Indicator bulbs record the scaler output as an aid to fault finding.

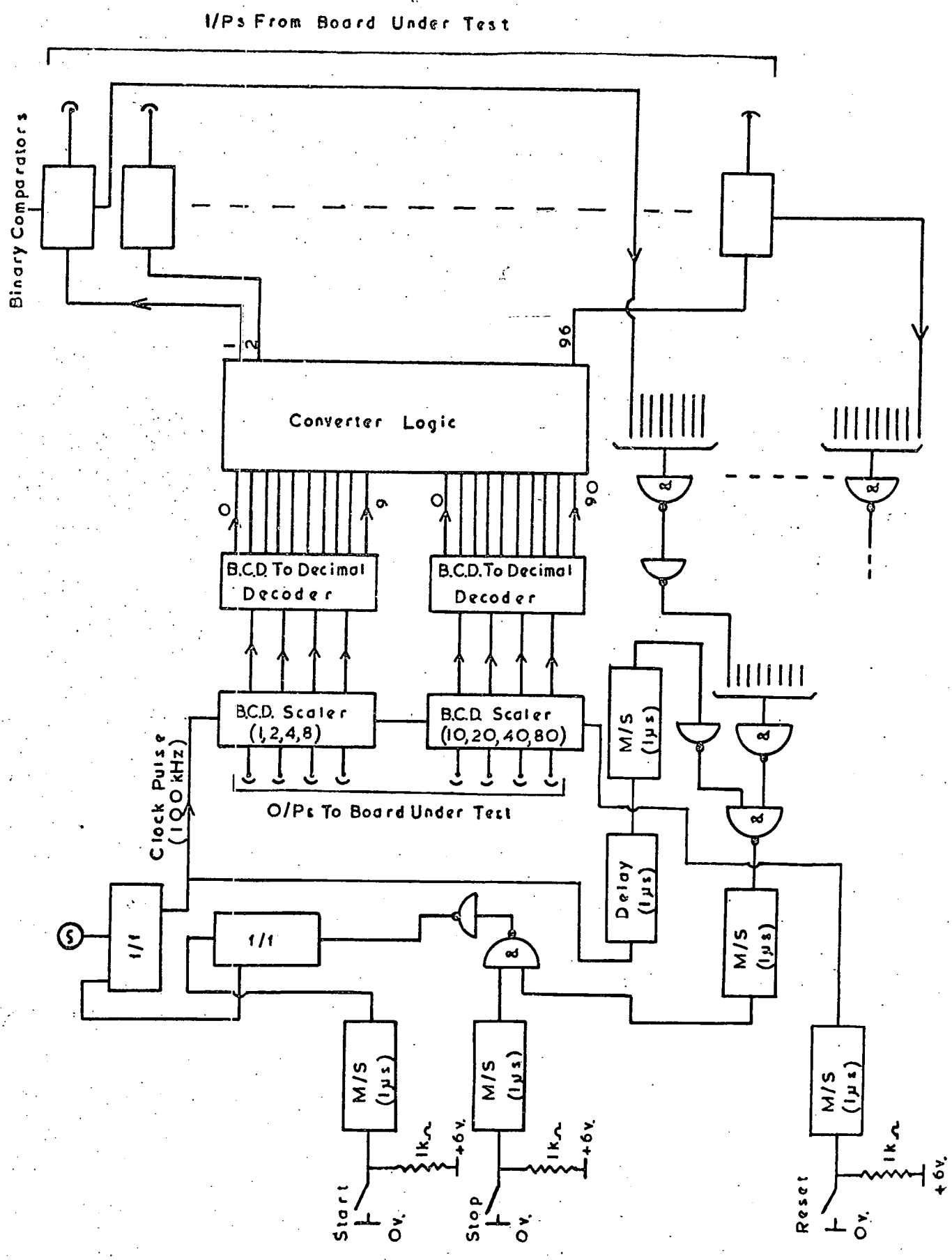

Figure 6.11 The Circuit for the Gating Logic Board Tester.

If no fault is found, the circuit requires a total time of 1 ms for checking. The stop, start and reset controls are built into the front panel of the unit.

6.5.4 The Scan Control Board Tester

The circuit for checking the board used to stop the scan of the columns is shown in figure 6.12. Use is made of a shift register whose bits correspond to the columns. A logical 0 state is set in the shift register bit number 0 and this is fed along the shift register on the application of a clock pulse of frequency equal to the scanning frequency of 100 kHz. The output from the shift register bit is fed to the board under test.

The output from the board under test is normally in the logical 0 state. After inverting, it is connected to an input of a two fold nand gate. The other input is obtained from the clock pulse. The clock pulse is delayed by 1 μs to allow for the input information to be fed to the board under test and an output to be obtained. The delayed clock pulse then triggers a monostable of length 1 μs. If an output is obtained from the board under test, the monostable output is vetoed. If no output is obtained from the board, the monostable pulse stops the clock pulse.

The output from the shift register bits are also fed into the inputs to eight input nand gates arranged in order. The outputs from these gates are used to trigger indicator bulbs. Thus the position of the triggering pulse is known to within eight shift register bits. This helps in the location of any fault on the board. An indicator bulb is triggered when the information reaches the end of the shift register, thus indicating that no fault has been obtained. The total scanning time if no faults are found is about 1 ms. The reset, start, and stop buttons in figure 6.12 are built into the front panel of the unit.

6.5.5 The Mixer Board Tester

The mixer circuit collects the outputs from each of the twelve special memory boards in a tray and presents the contents of each column of flash tubes at the eight outputs from the board when the given column is opened by the scaler.

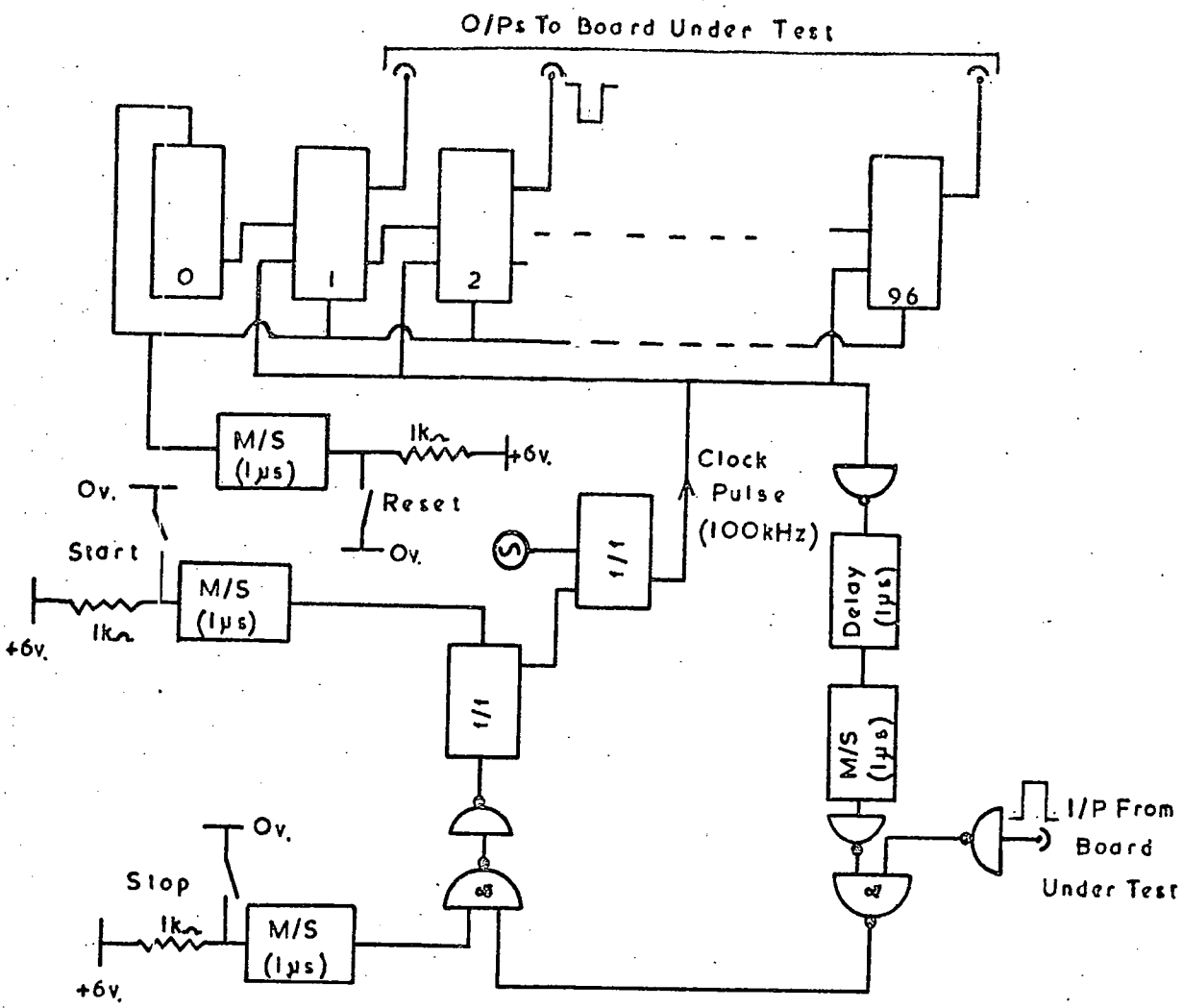

Figure 6.12 The Circuit for the Scan Control Board Tester.

The check circuit for the board is shown in figure 6.13. An eight bit binary scaler is used to feed combinations into the board corresponding to all the possible combinations from one of the special memory boards. The inputs to the board from a given memory board are controlled by a 12 bit shift register.

The board under test is connected to the test circuit and pulses from the binary scaler are fed into the inputs corresponding to the first special memory board. This is achieved by setting the shift register bit 1 to a logical 1 output using the set switch. The scanning frequency of 100 kHz for the columns in a tray is used for the scaler clock pulse.

The eight outputs from the board under test are compared with the expected outputs using binary comparators. The outputs from the binary comparators are fed into an eight fold nand gate whose output is gated on the clock pulse. The clock pulse is delayed by 1 μs to allow for the input pulse to be fed to the board and an output pulse produced. If a fault is found then the clock pulse is stopped.

If no fault is found, then the 8 bit binary scaler counts up to a value of 255 and resets to zero on the next clock pulse. A clock pulse is applied to the shift register when the binary scaler goes to zero. This opens the channel for the inputs from the second board in a tray and closes the channel for the first board. The process is repeated for the inputs from each board in a tray in turn.

Indicator bulbs are used to show the state of the binary scaler and each bit of the shift register. The total time of scanning if there is no fault is about 30 ms. Start, stop, and reset buttons are built into the front of the unit.

6.6 The Tray Steerage Logic

This logic controls the column scaler for each tray, the order in which the information from the Measuring Trays is passed to the core store logic, and the reset for the electronic memories. It can be basically subdivided into

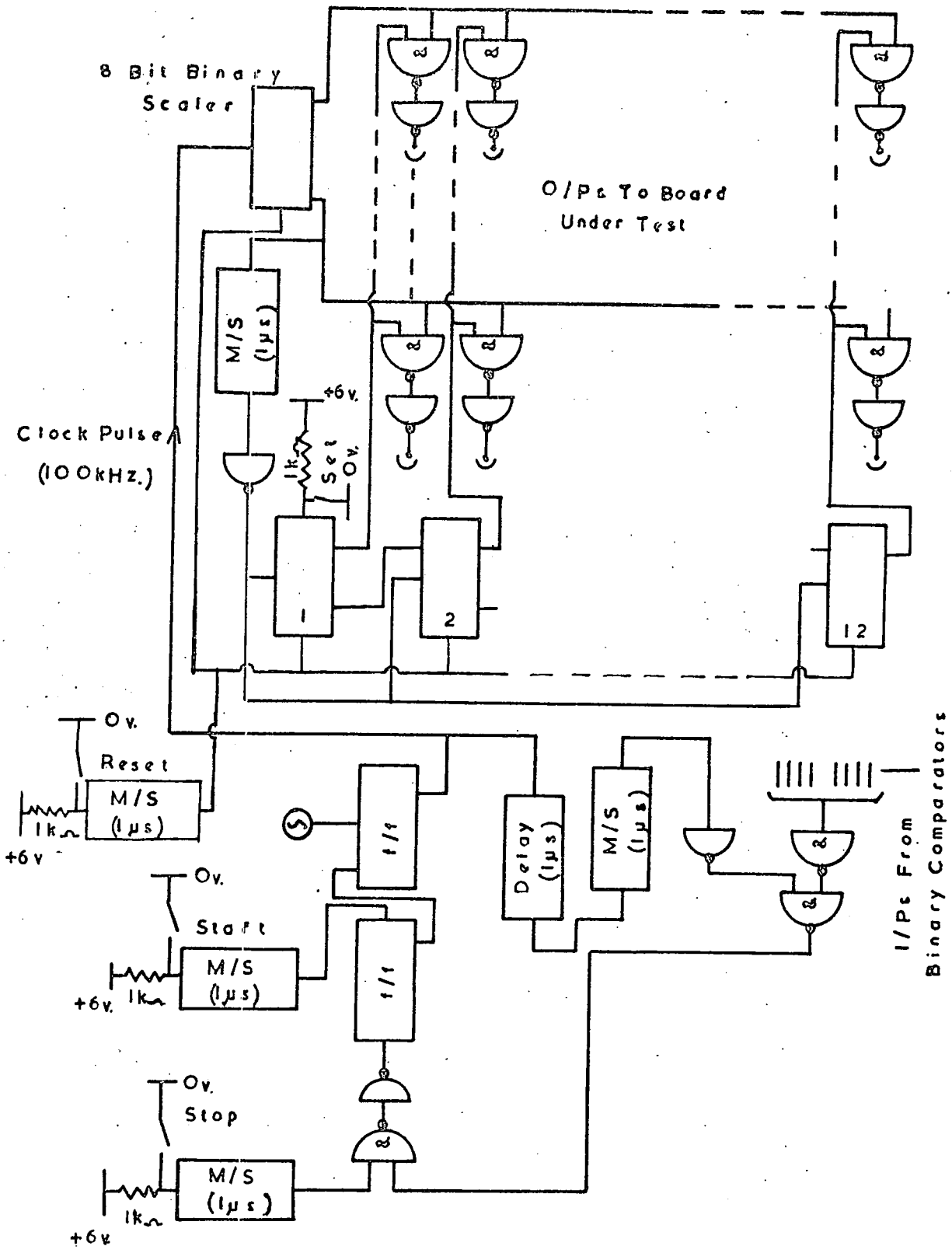

Figure 6.13 The Circuit for the Mixer Board Tester.

two separate parts: the logic for the tray scanning and the logic for the reset of the electronic memories. These two parts are described below.

The circuit diagram for the logic controlling the readout from a tray is shown in figure 6.14. An input from the coincidence unit to the reset logic for the memories described below indicates which side the particle traversed. This produces an output pulse to the corresponding input of the readout logic, which sets a flip-flop to open the scaler output to tray 1 on the triggered side and removes the veto on the input from the Momentum Selector. An input pulse from the Momentum Selector will occur about 110 μs. after the initial trigger input pulse if a high momentum event has been selected by the Momentum Selector. If no pulse is obtained from the Momentum Selector, then a pulse from the reset unit, which occurs 1 ms after the passage of the triggering particle, is given to the reset logic which resets the electronic memories and the flip-flop back to their normal off states.

If a high momentum pulse is obtained from the Momentum Selector, an output pulse is passed to the core store logic. This pulse initiates the core store read in of the digitised information with each high momentum event.

When this information has been stored, a pulse is fed back to the readout logic which starts the scanning of flash tube columns. The speed of scanning is governed by a multivibrator which feeds output pulses to scaler (i) which is a 0 to 99 B.C.D. scaler. The form of a decade of a B.C.D. scaler using integrated circuit flip-flops of Mullard type FCJ 101 is described in Appendix A.

Two scanning frequencies have been incorporated in the multivibrator. Normally, the scanning frequency will be 100 kHz but a frequency of 1 Hz can be introduced if required by closing a switch. This slow scanning speed is useful for fault finding as the output states of the scaler bits are on visual display using small indicator bulbs together with a visual indication of which tray is being scanned.

The outputs from scaler (i) pass initially into the gating logic for the

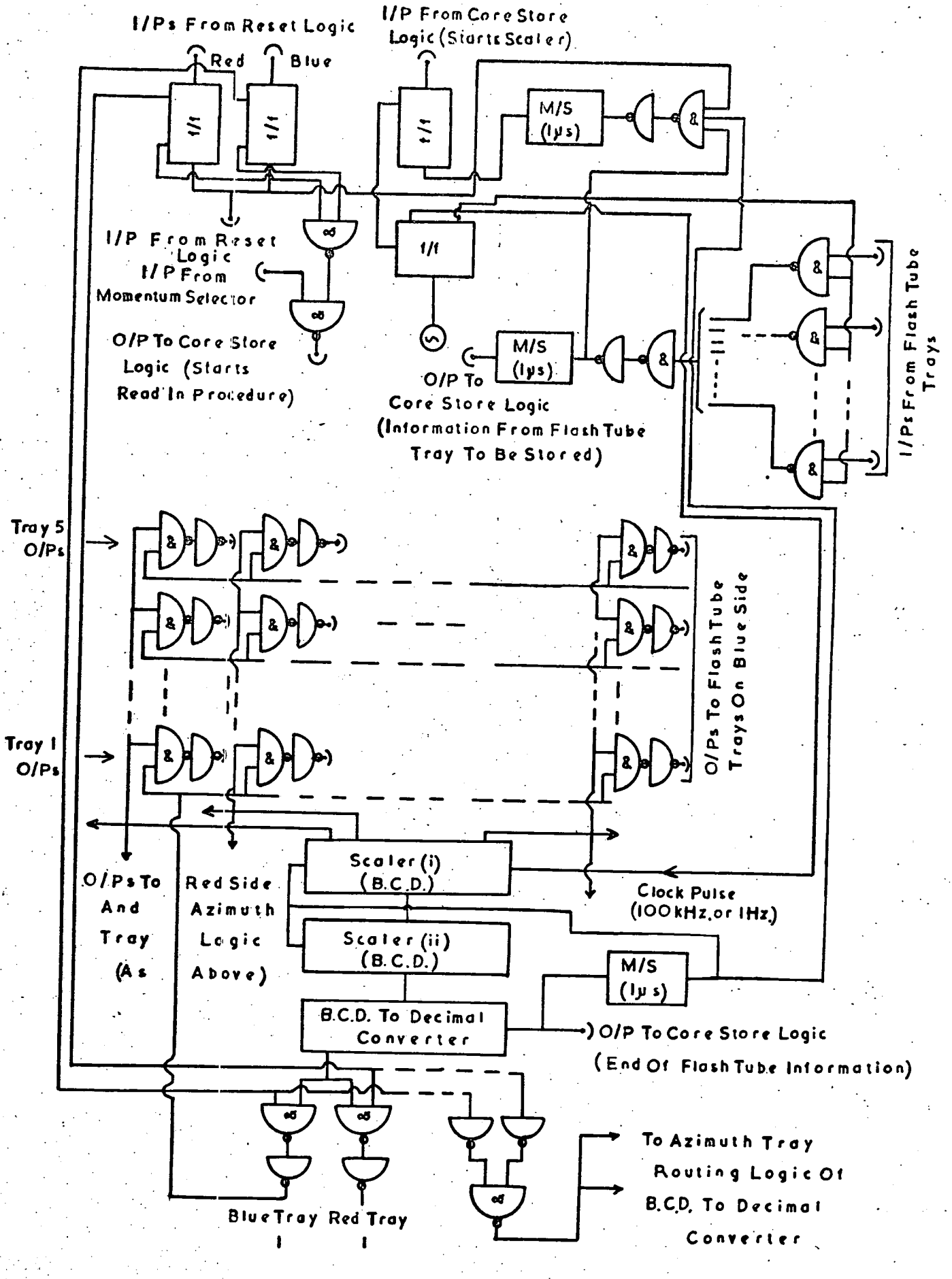

Figure 6.14 The Circuit for the Tray Steerage Readout Logic.

flash tube columns on Measuring Tray 1 on the triggered side. All the scaler outputs to the rest of the trays are vetoed using scaler (ii) as described below. The scaler pulses are fed to each tray using eight cables of a twelve way individually screened cable.

If a column is found in which at least one tube has flashed a pulse is received from the logic on the flash tube tray. This pulse stops scaler (i) and a pulse is sent to the core store logic which indicates to the core store that flash tube information is ready to be stored. The flash tube column number, which is the reading of scaler (i), and tube configuration in the column are then recorded in the core store. When the information on the column has been recorded, a pulse is fed back to the steerage logic to restart scaler (i) and the scanning of a tray continues.

The tray in which the scanning process is being carried out is controlled by scaler (ii) in conjunction with scaler (i). Scaler (i) is a 0 to 99 scaler; it counts 1 to 99, resets to zero on the next pulse, and then continues to count 1 to 99 again on the following pulses. There are 96 columns in a tray so numbers 97 to zero of scaler (i) are not used for scanning the tray. An output pulse is fed to scaler (ii) when scaler (i) counts 98. Scaler (ii) also counts in B.C.D. form and is initially at zero while tray 1 is being scanned. The output from scaler (ii) is fed into a B.C.D. to decimal converter. The converter output is then used to gate the output from scaler (i) into the correct tray. A pulse to scaler (ii) thus changes it to 1 and opens the scanning to tray 2. The reading on scaler (ii) is always one less than the number of the tray being scanned. This process is repeated for each of the Measuring Trays on the triggered side of the spectrogtraph and the Azimuth Trays in turn.

The information from each Azimuth Tray is fed to the core store irrespective of which side of the spectrograph is triggered. Scaler (ii) records numbers 5 and 6 for the two Azimuth Trays. The form of the Azimuth Trays is described in §6.7.

When the final Azimuth Tray has been scanned, scaler (ii) changes from 6 to 7. This produces an output pulse to the core store logic to initiate

the readout of the event into the computer. It also resets the scalers to zero and stops the clock pulse to scaler (i). When the event has been stored by the computer, the paralysis flip-flop is reset in the reset unit and pulses are fed to the reset logic of both the Momentum Selector and tray steerage logic to reset the electronic memories. A pulse is also fed from the reset logic to the readout logic to reset the flip-flop recording the triggered side. The scalers are also reset as a precaution by the reset pulse.

The readout logic is contained on 6 plug in type printed circuit boards, which fit into a specially designed unit. Connection between boards is made by wire joining the edge connectors on the back of the unit. The input and output sockets to the logic are fixed to a panel on the back of the unit. The indicator bulb array is mounted by the side of the plug in boards.

The circuit for the reset logic is shown in figure 6.15. The principle used is similar to the reset for the Momentum Selector. A reset pulse is fed to the Measuring and Azimuth Trays as soon as a coincidence pulse is received from the trigger unit. A veto pulse is then applied to the memories during the rising edge of the high voltage pulse and is taken off before a pulse is obtained from the flash tube. Pulses are fed to all Measuring and Azimuth Trays irrespective of which side is triggered as a precaution. The inputs from the coincidence unit indicate which side has been triggered and a corresponding output pulse is fed to the readout logic. A reset pulse from the reset logic also produces reset pulses to the trays and the readout logic.

The reset pulse is fed to the Measuring Trays via co-axial cable. Output to each memory is via a series of buffer gates placed on the first board in each tray, that is, the board containing column 1. These buffer gates are then connected to the remaining 11 boards on the tray holding the memories and then via a further 4 buffer gates on the boards to the reset inputs of the memories.

The tray steerage logic is contained in a chassis near to the spectrograph and is shown in Plate 2.

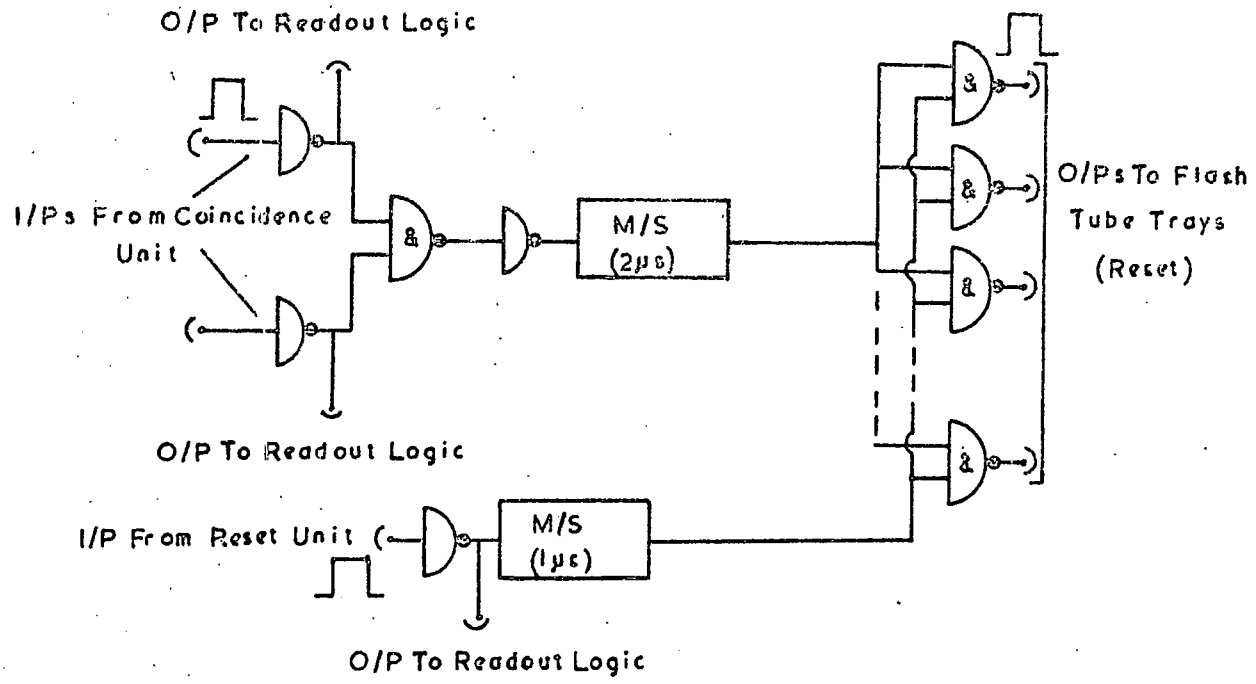

Figure 6.15. The Circuit for the Reset Logic for the Measuring and Azimuth Trays.

6.7 The Azimuth Trays.

Two Azimuth Trays are used with the spectrograph. They are placed on the top of the spectrograph as shown in figures 3.1 and 3.2. The flash tubes used in these trays are of length 2.5 m, mean external diameter 1.75 cm, and filled with neon gas to a pressure of 60 cm of mercury.

The outer framework of the trays is made from the same material as the Momentum Selector and Measuring Trays and is joined together in a similar way. Similarly the flash tube pattern is the same as that used in the Momentum Selector Trays. The brass supports and digitisation shield were drilled as with the previous trays, the only difference being that the dural shield was made out of several sections pinned together because it was not possible to obtain a length of dural of the required size of 244 cm x 10.2 cm. The electronics used with the Azimuth Trays is similar to that already described for the Measuring Trays. The only difference is that the columns are grouped together in twos, thus making a column of eight. There is also a dummy column at the beginning of the tray, indicating the tray number and six dummy columns at the end for holding processed information. In each Azimuth Tray there are 119 columns with four tubes per column. Arranging the columns together in pairs gives 60 columns. The last column will only be one half full of relevant information, the remaining half will be held permanently in the off state. Thus, allowing for the seven dummy columns, there will be 67 columns in each Azimuth Tray.

The overall size of the trays is 305 cm x 244 cm x 12.7 cm and the high voltage electrode has a size of 241 cm x 240 cm. Because of the large size of the electrodes, the electrodes are made from two sheets joined together with the axis of the join parallel to the flash tubes.

6.8 The Core Store

The core store, which is used to store the digitised information of a high momentum event before output to the computer, has a ferrite memory capable of

storing 1024 8 bit words. The data input sequence to the core store is controlled by the core store logic. The output sequence to the computer is controlled by the computer and its ancillary equipment in conjunction with the core store logic.

A block diagram of the system used in the spectrograph is shown in figure 6.16. Information can be stored in an eight bit word by presenting the data on the eight data input lines to the core store. The address of the location is presented on the address input lines. There are 20 address lines corresponding to a 10 bit binary number with its complement. Storage is obtained by applying a series of input pulses to the core store. Similarly, events can be read from a location signified by the address lines by applying a further series of pulses to the core store.

Control of the core store and its associated logic is carried out by a master control circuit. This controls the order in which the event information is stored in the core store and the control pulses for the write and read cycles of the core store. The circuit has input pulses from the Momentum Selector via the tray steerage logic, to signify that the event is a high momentum event; two inputs from the tray steerage logic, one to indicate that a flash tube column is required to be stored and the other to signify the end of the scanning; and an interrupt from the computer during the readout phase to indicate that a core address has been presented and the data output is required from the core store. The logic itself produces output pulses to the tray steerage logic, to restart the scanning; to the computer, to initiate readout of the data; and to the reset unit, to remove the paralysis after the event has been stored in the computer.

The input pulse from the Momentum Selector initiates the readout of the digitial information accompanying each event into the core store. The form of this digitised information is discussed in §6.9. The computer address is gated out from the address to the core store. The data address line is obtained

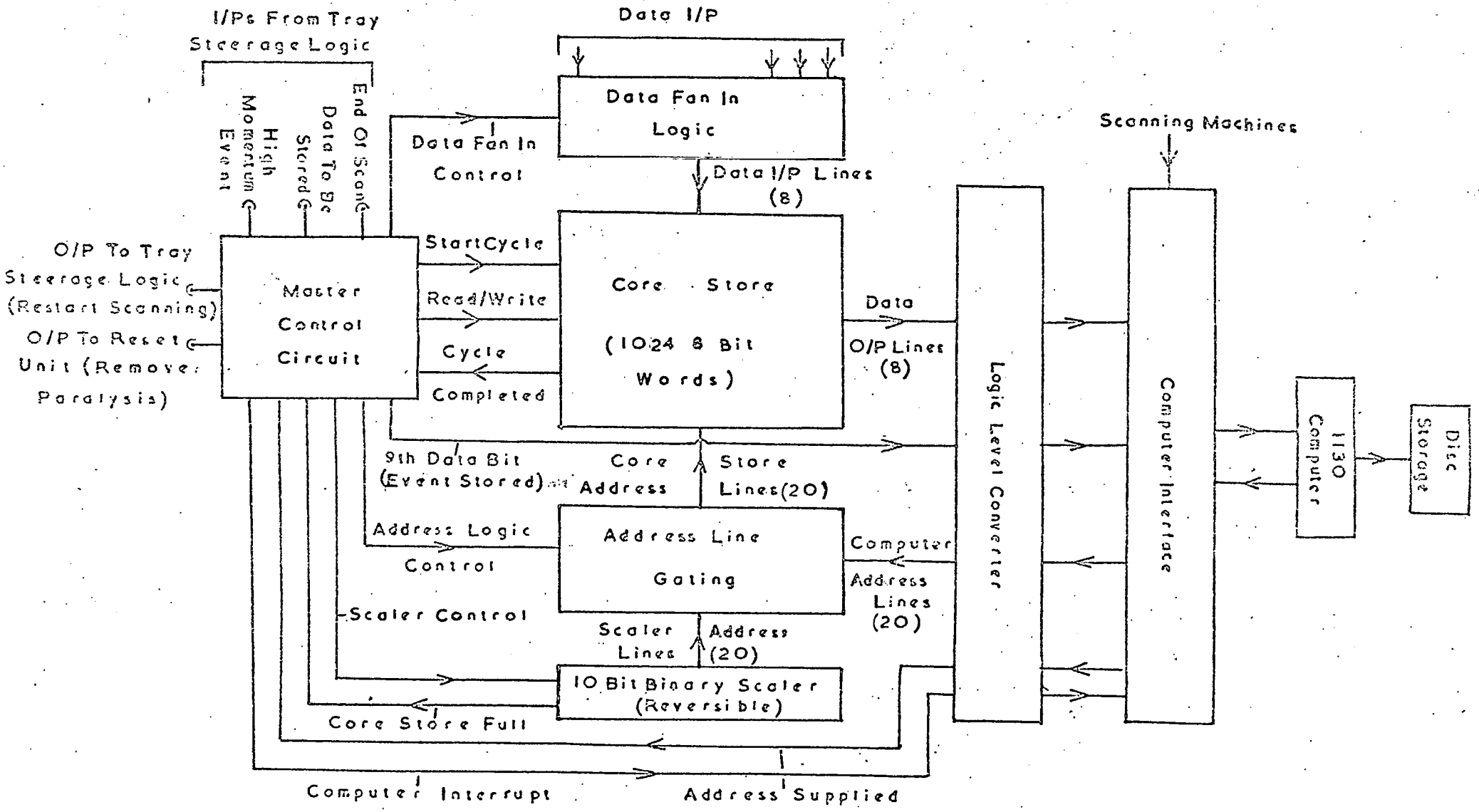

Figure 6.16 Block Diagram of the Core Store Logic.

from a 10 bit reversible binary scaler which starts at zero for the first address and is incremented by 1 after the storage of each word.

To start the recording of the information in the core store, a pulse is fed from the master control circuit to the core store, this pulse is known as the start cycle pulse. This starts a write or read cycle in the core store depending on the logic level on the read/write line from the master control circuit. For a write cycle this level is a logical 0 and a logical 1 for a read cycle. After storage, a cycle completed pulse is fed to the master control circuit and the binary scaler. This increments the scaler by 1 and gates in the next word of the information on the data input lines. The start cycle pulse is then sent to the core store and the process repeated.

The information with each event takes up the first eighteen words in the core store. After their storage, an output pulse is fed to the tray steerage logic to start the scanning of the flash tube trays. When a column is found holding information, a pulse is sent to the master control unit and the scaler number for that column, which is the reading of scaler (i) of the readout logic described in §6.6, is fed into the core store. This is an 8 bit B.C.D. number so it is accommodated by one word. Similarly, the next word stores the flash tube information for the column.

The storage of each relevant flash tube column is continued until the end of scan pulse is received from the tray steerage logic or the core store is full, whichever comes first. Normally, the core store should never be full during an event as it has space for 503 columns of flash tubes with the column number and flash tube configuration. The maximum number of columns in the Measuring and Azimuth trays is 614. This number includes the dummy columns for the tray identifier and storage of processed information. So it can be seen that there would practically have to be nearly one tube in every column which has flashed if the core store is full before the end of the scan. This core store full pulse has been incorporated as a precaution.

When the end of scan pulse or core store full pulse is received, the address lines from the 10 bit binary scaler are vetoed and the computer address lines gated open. The 10 bit binary scaler is put into its reverse mode. A pulse is then sent to the computer by the master control circuit to indicate that information is required to be stored. As mentioned previously, the computer is also used to control measurement of bubble chamber tracks by scanning machines. Hence there will be a delay between the computer interrupt and the readout of information from the core store, depending on whether the computer is in use.

When the computer is ready, a pulse is sent to the master control circuit. This indicates that an address has been supplied to the core store and readout of the data in the address is required. This produces a start cycle pulse to the core store, with the read/write line in a logical 1 state.

After the readout of the data for that address, the 10 bit binary scaler is decreased by 1 and a further address is supplied by the computer accompanied by a pulse to the master control circuit as before. The process is repeated for all the addresses which hold information. The end of information is signified when the 10 bit binary scaler reaches zero. This produces an output pulse from the master control unit to the reset unit to provide pulses for thememory resets and to remove the paralysis. A ninth bit line to the computer is also turned on to indicate to the computer that all the information has been stored.

The data output lines from the core store are fed into special driving gates used for feeding pulses through long cables. The cable used to the computer is a 25 way cable each wire being individually screened.

The computer also has control of up to six measuring machines. A special interface is thus required for control of the input and output lines from the computer. However the logic levels for the interface are +18 volts for a logical 1 and 0 volts for a logical 0. The core store logic has a maximum voltage of +4 volts for a logical 1. Hence the outputs from the core store logic pass through a

logic level converter before input to the interface. Similarly, the outputs from the interface to the core store logic also pass through the logic level converter to reduce the voltage level for a logical 1 to the +4 volts required for the core store.

The data from the core store are presented in 8 bit words. The computer uses 16 bit words. The interface thus joins two 8 bit words together and stores it in the computer as a 16 bit word. Thus one 16 bit word in the computer contains the information on the flash tube column and tube configuration. The words for the events are stored in a part of the computer core allocated for this purpose. When the words stored are equal to 320 16 bit words, this sector is transferred to disc storage, and the sector filled again. The transfer occurs as soon as the sector is full so it could occur during the reading of an event from the core store. This has no effect on the storing as the 320 words are stored sequentially on the disc.

6.9 The Digitised Information Recorded with each High Momentum Event.

6.9.1 Introduction

When a high momentum event is flagged from the Momentum Selector, digitised information on the event is fed into the core store together with the flash tube data as explained in §6.8. This information will be required in any subsequent analysis of the events. The following information is stored with each high momentum event: event number, time of the event, the date, the magnet coil current, the magnetic field direction, the trigger mode, and the atmospheric pressure. The circuits for digitising the required information are described below. The circuits are assembled in special chasses mounted in racks near to the spectrograph. Plate 2 shows the positions of these circuits.

6.9.2 The Event Number

The circuit for the event number is shown in figure 6.17(a). The event number is displayed on a counter consisting of six decade counters suitably joined. The counters are of mechanical form, each decade adds one to its

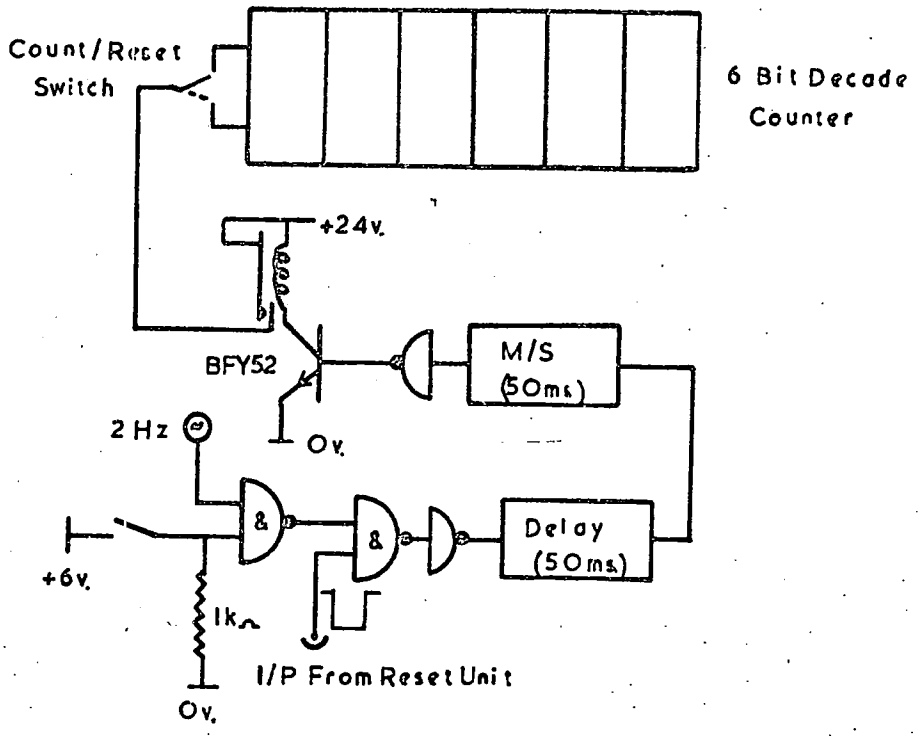

Figure 6.17(a) The Circuit for Digitising The Event Number

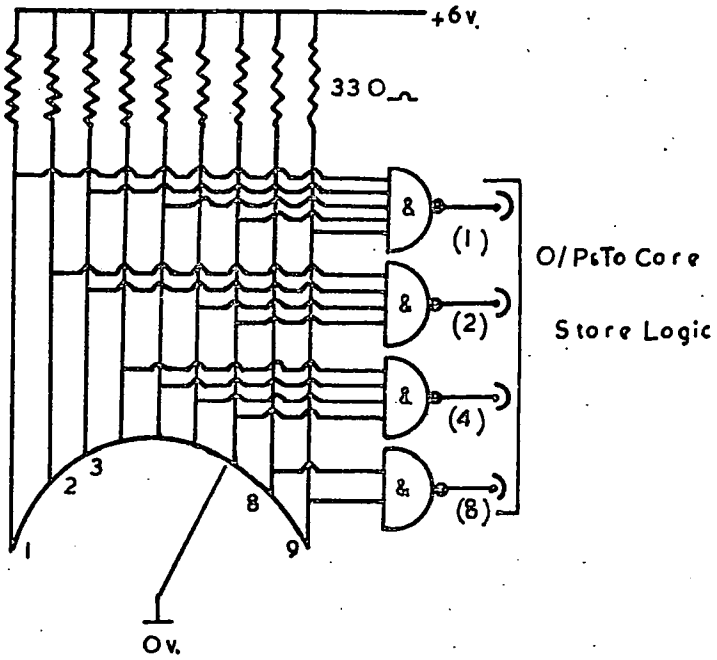

Figure 6.17(b) Circuit for a Decimal to B.C.D. converter.

value when a pulse of 24 volts in height and length 50 ms is applied to a solenoid inside the counter.

The counter is driven by a 24 volt relay which is triggered by a pulse from the reset unit when a high momentum event is flagged. This pulse is delayed by 50 ms for the reason explained below and then triggers a monostable circuit which produces an output pulse of length 50 ms. This monostable pulse is fed after inversion into the base of a BFY 52 npn transistor and this triggers the 24 volt relay, whose coil is the collector resistance of the transistor, and the counter is incremented by one. The counter can be checked by feeding into the circuit pulses from a multivibrator oscillating at 2 pulses per second. The multivibrator only triggers the counters when the push button switch is down. The counter is reset to zero by placing the count/reset switch in the reset mode and applying input pulses from the multivibrator.

The counter displays its value in decimal form. The digitised output is required in binary coded decimal (B.C.D.) form for storage. Use is thus made of the decade contacts on the back of each counter. There are eleven outputs on each decade corresponding to the numbers 0 to 9 and a common line. When an output number is indicated on the counter, the switch between the number and the common line is closed and the other nine outputs are open. Each decade then has a decimal to B.C.D. code converter as shown in figure 6.17(b). When the decade is connected to the code converter, the input to the code converter for the number indicated on the decade counter is at logical 0 level and the rest of the inputs are at logical 1 level produced by the 330 ohm resistors connected to the +6v power line. The code converter then converts this number at the output into B.C.D. form of length 4 bits. The six decades of the counter are thus converted into B.C.D. form of total length 24 bits.

Because of the slow changeover of the number, the previous event number is recorded by the core store, as the number cannot change in the time between a high momentum event being indicated to the core store and the readout of the

event number to the core store. During the 50 ms delay time built into the circuit, the event number is read into the core store.

6.9.3 The Time of the Event.

The circuit for digitising the time of the event is as shown in figure 6.18. The circuit is triggered every second by the electronic sensing head. This device gives an output pulse whenever a metal vane is inserted between two sensing heads. Normally the output is at +6 volts with respect to the common line. When a vane is inserted in the device the output changes to zero volts. The output stays in this state until the metal vane is removed from the device and then the output returns to +6 volts. For the purpose of a clock trigger, four metal vanes are arranged in a windmill shape which is driven by an electric motor at 0.25 revolutions a second such that an output pulse is obtained from the device every second. The pulse from the sensing device is then passed into a monostable circuit to produce an output pulse of length 1 μs which is then used to trigger a series of special B.C.D. scalers which record the time of the event in hours, minutes, and seconds on the 24 hour clock system.

The scalers used in the circuit are not the normal B.C.D. decade type but are composed of two 0 to 60 B.C.D. scalers and a 0 to 24 B.C.D. scaler joined in series. The scalers are arranged as shown in figure 6.18 such that they record the time of the event in seconds, minutes and hours. The bits of the scalers are made from Mullard integrated flip-flops type FCJ 101.

When scaler 1, the scaler recording the seconds, reaches 60 events it is reset to zero and gives an output pulse to scaler 2, which records the minutes, and this adds one on to the reading of scaler 2. When scaler 2 reaches 60 counts, it is also reset to zero and gives an output pulse to the hour scaler, scaler 3. Scaler 3 resets to zero when it reads 24. Indicator bulbs are connected to the outputs of each scaler so the time is indicated on a visual display.

When the power is applied to the circuit, the clock will record a random

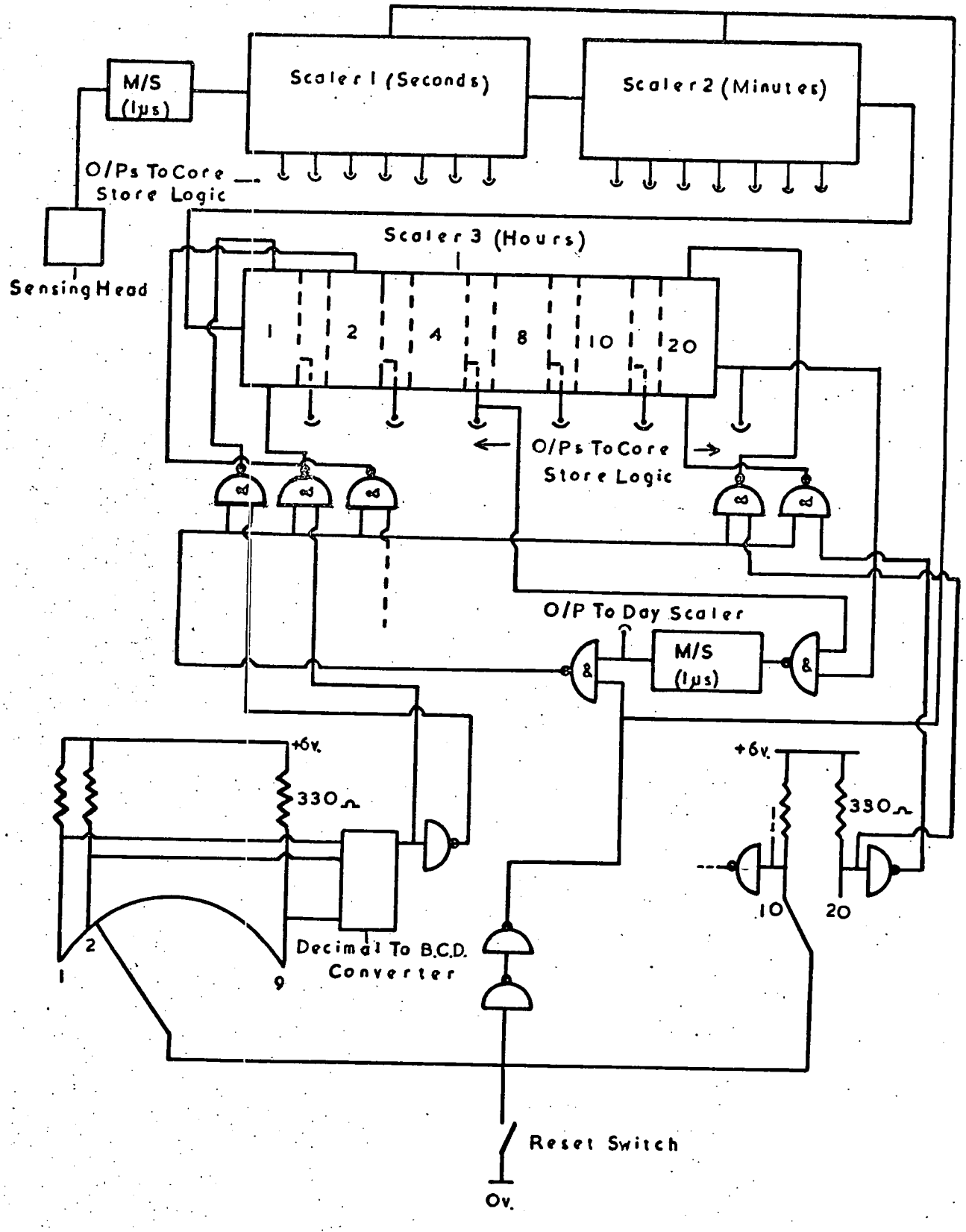

Figure 6.18 The Circuit for Digitising the Time of the Event.

time which depends on the resultant output states of the flip-flops used in the scalers. A reset device has thus been incorporated into the circuit which will reset the clock to any given hour. This hour is set on two decade switches, whose fronts are built into the front panel of the chassis containing the clock circuit. These decade switches also have outputs at the rear of the switch corresponding to the numbers 0 to 9 in the decade and a common output. When a number is shown on the front there is a short circuit between the common and the output for the number on the front. The two decade switches are assembled in the circuit as shown in figure 6.18. The unit decade switch is fed into a decimal to B.C.D. code converter. Only the 10 and 20 outputs of the ten decade switch are used.

Normally, the decade switch outputs are held at a logical 1 level by the 330 ohm resistors connected to the +6 volt power lines which allows the time to be recorded in the normal manner. A push button switch is connected to the common output, the other terminal of the switch being connected to the common of the power lines. The switch is normally open. When the switch is closed, the second and minute scalers are reset to zero and the hour scaler to the time indicated on the hour decade switches. The count starts when the resetting switch is released.

6.9.4 The Date of the Event

The date is produced in days, month, and year. The day output is in B.C.D. code, the month output in binary code, and the year output in B.C.D. code. Only the tens and units of the year are recorded.

The circuit for the day and month recording is shown in figure 6.19. The day is recorded on a B.C.D. scaler which can count from 1 to a maximum value of 31. The day is set initially by means of a single shot device which is triggered by push button switch. When the button is pressed the reading of the day scaler is incremented by one. The day scaler is triggered from the clock circuit (figure 6.18) whever the clock passes through zero time.

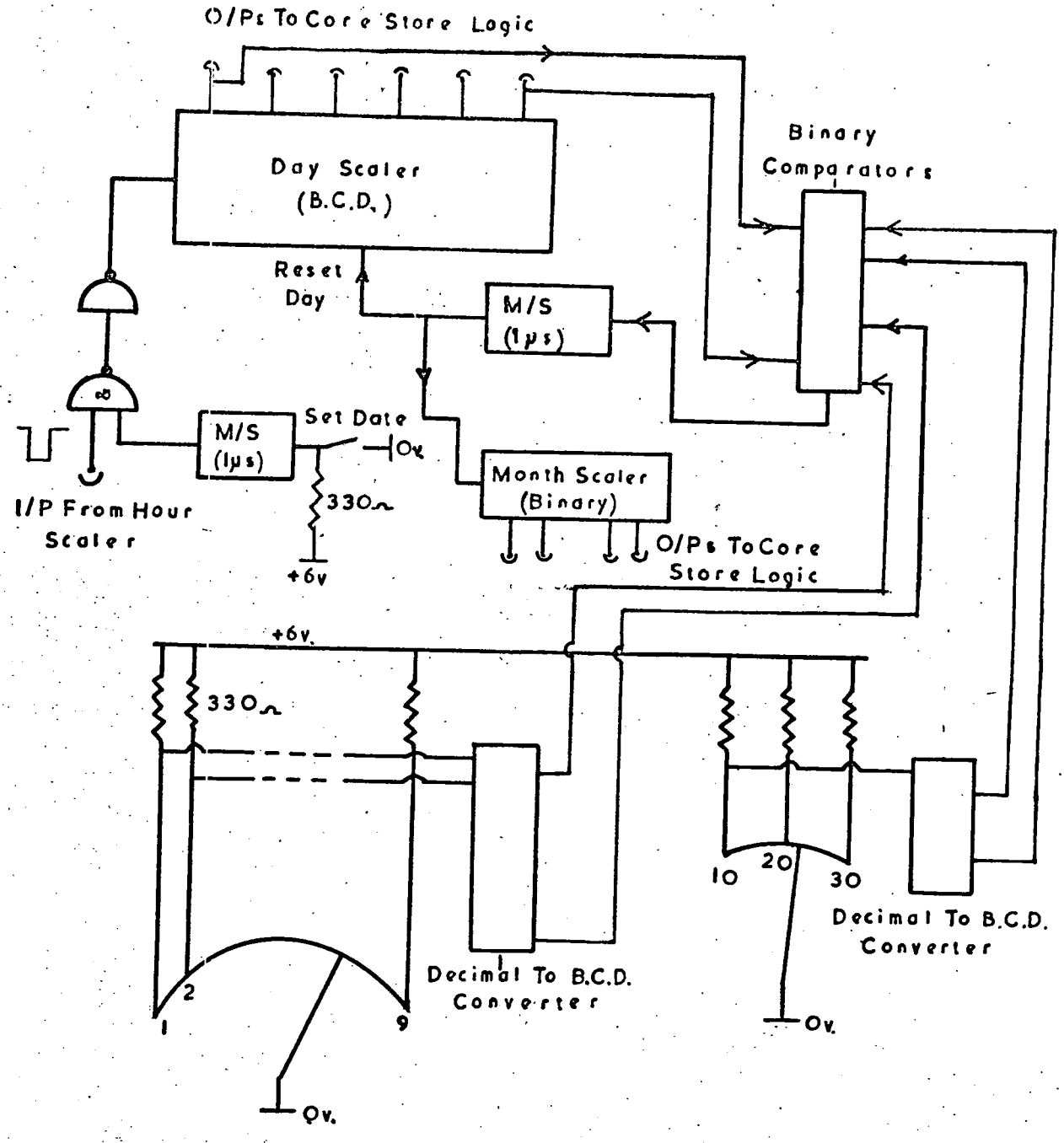

Figure 6.19 The Circuit for Digitising the Date of the Event.

Because of the variation in the number of days in a month, the end of a month is signified by the use of the decade switches as shown in figure 6.19. These switches are the same as those used in setting the time and are built into the front of the unit. The number of days in a given month plus one is indicated on the decade switches. The outputs at the rear of the switches pass through a decimal to B.C.D. code converter as shown in figure 6.19. For the ten decade switch only the 10, 20 and 30 switches are used. The B.C.D. number from the decade switches is then compared with the B.C.D. number on the day scaler using binary comparators. When agreement is found, a pulse is fed to the month scaler and the day scaler resets to 1.

The month scaler is a binary scaler of four bits. A binary code is used rather than B.C.D. code because in binary the month can be represented by four bits compared with five bits in B.C.D. code. The scaler is triggered by an output pulse from the day scaler when the day scaler resets to one. The form of the binary scaler is described in Appendix A.

To obtain the correct day and month after a power interruption or other similar cause, use is made of the single shot device. Pulses are fed into the day scaler which at the end of a month triggers the month scaler. This is achieved quickly by setting the decade switches corresponding to the days in the month to a low value. When the month scaler is at the correct value, the day scaler is set to the required day and the decade switches set to the number of days in a month plus one.

The unit and ten decades of the year are on two decade switches on the front of the chassis. The outputs at the rear of the switches are the inputs to a decimal to B.C.D. code converter, which thus converts the year value into the corresponding B.C.D. number.

6.9.5 The Magnetic Field Direction

The magnet can be operated under normal running mode with the magnetic field zero, or with the magnetic field on in one of two possible field

directions. These two field directions are known as the positive and negative field directions according to a convention. The magnetic field direction is defined to be positive if it is in the direction North to South in the Blue side and negative if it is in the opposite direction in the same side.

The circuit for digitising the field direction is shown in figure 6.20. The field direction is recorded by the use of two microswitches fixed on one of the reversing switches, which control the current direction in the energising coils. In the case when the magnetic field in off, the output for zero field is at a logical 1 level and the outputs for the positive and negative field directions are at a logical 0 level. When the field is on, the output corresponding to the field direction is in the logical 1 state and the two other outputs are in the logical 0 state.

6.9.6 The Magnet Coil Current.

The current flowing through the magnet coils is recorded on an ammeter on the rectifier unit. The value of this reading is the total current from the supply before it is divided into two for the two parallel coils across the output from the rectifier.

At the start of each run the value of this current is noted and recorded on three decade switches of the type used for the time and date resets. The outputs at the back of each decade switch are fed into a decimal to B.C.D. converter. The current is thus represented by 12 bits of a B.C.D. number.

6.9.7 The Trigger Mode.

The circuit for the trigger mode is shown in figure 6.21. The unit records the side through which a three fold coincidence between the scintillators has been detected and also when particles passed through both sides instantaneously. It is controlled by pulses from the coincidence unit and also informs the digital device R.U.D.I. which side has been triggered. The previous side, or sides, to produce a coincidence pulse is recorded on the output until the next event is triggered. The input pulse is of length 1 μs and it first resets all the

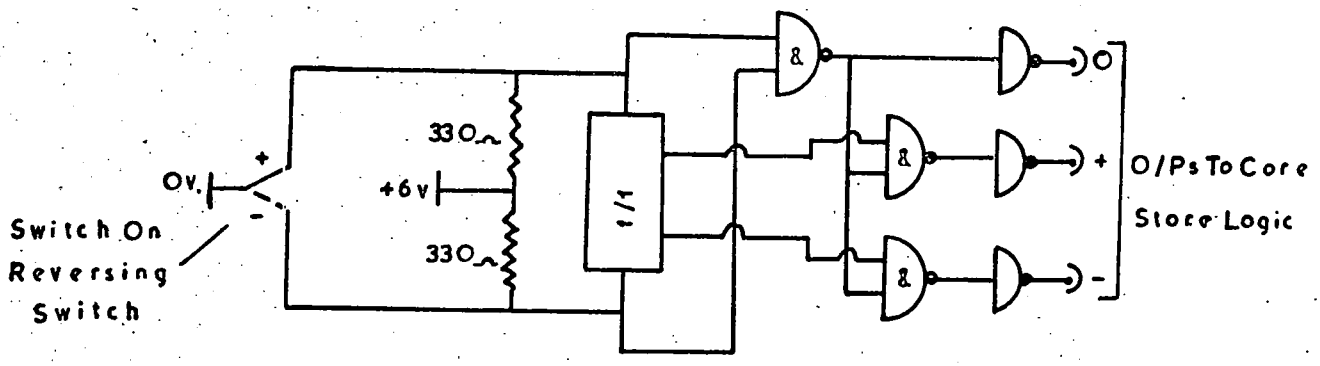

Figure 6.20 The Circuit for Digitising the Magnetic Field Direction.

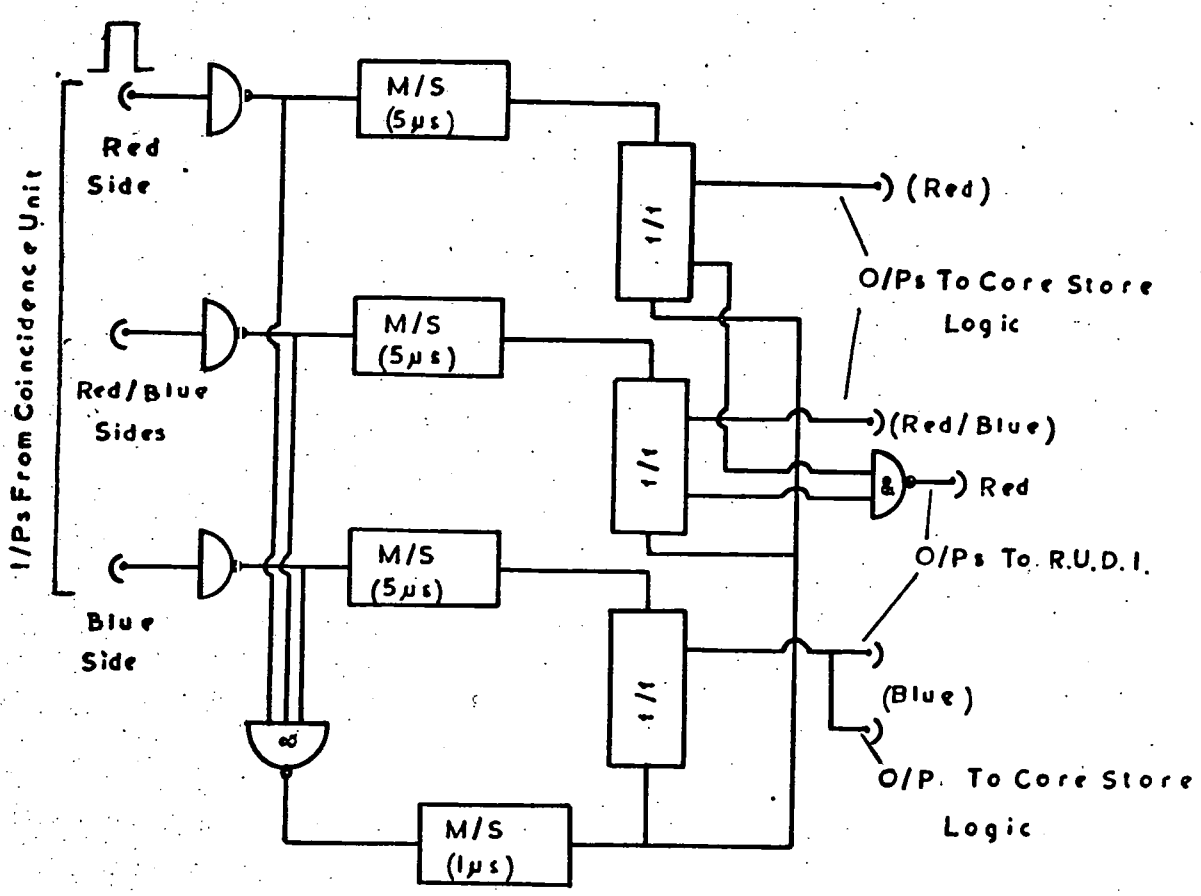

Figure 6.21 The Circuit for Digitising the Trigger Mode.

memories and then sets the required memory by passing through a monostable which lengthens the pulse to 5 μs and thus sets the memory after the 1 μs reset pulse. The outputs from the memories are fed to the core store and are also displayed on indicator bulbs on the front panel.

6.9.8 The Atmospheric Pressure

In order to record the atmospheric pressure, use is made of a pressure transducer connected to a digital voltmeter. The circuit is as shown in figure 6.22. The pressure transducer is of the strain gauge variety in which the atmospheric pressure causes a change in the balance point of a Wheatstone Bridge arrangement of strain gauges. The pressure transducer is driven by a 10v. power supply and gives an output between 0v. and +5v. depending on the pressure. The digital voltmeter is set on the +2v. range and the potentiometer adjusted until the voltmeter reads twice the atmospheric pressure; for example, a pressure of 76 cm of mercury would produce an output on the digital voltmeter of 1.52 volts.

The digital voltmeter provides the output in B.C.D. form automatically. However negative logic is used in which a logical 0 is represented by a voltage between 0v. and -1v. and a logical 1 by a voltage between -5v. and -12v. This has to be converted into positive logic for use with the integrated circuits used in the spectrograph. An integrated circuit device known as a level detector is used. This is a device whose output changes state when the input signal exceeds a certain tripping value set by an external resistance. Each bit of the B.C.D. output from the digital voltmeter is applied to a level detector input as shown in figure 6.22. The external resistor (82Ω) is chosen such that the tripping value is between the two extremes of the logic levels.

The voltage on the input to the digital voltmeter is sampled on the application of a sample pulse to the voltmeter. The output from the voltmeter between these sample pulses is the input voltage at the last sample pulse. The time required to sample the input voltage is about 50 ms so the voltage fed

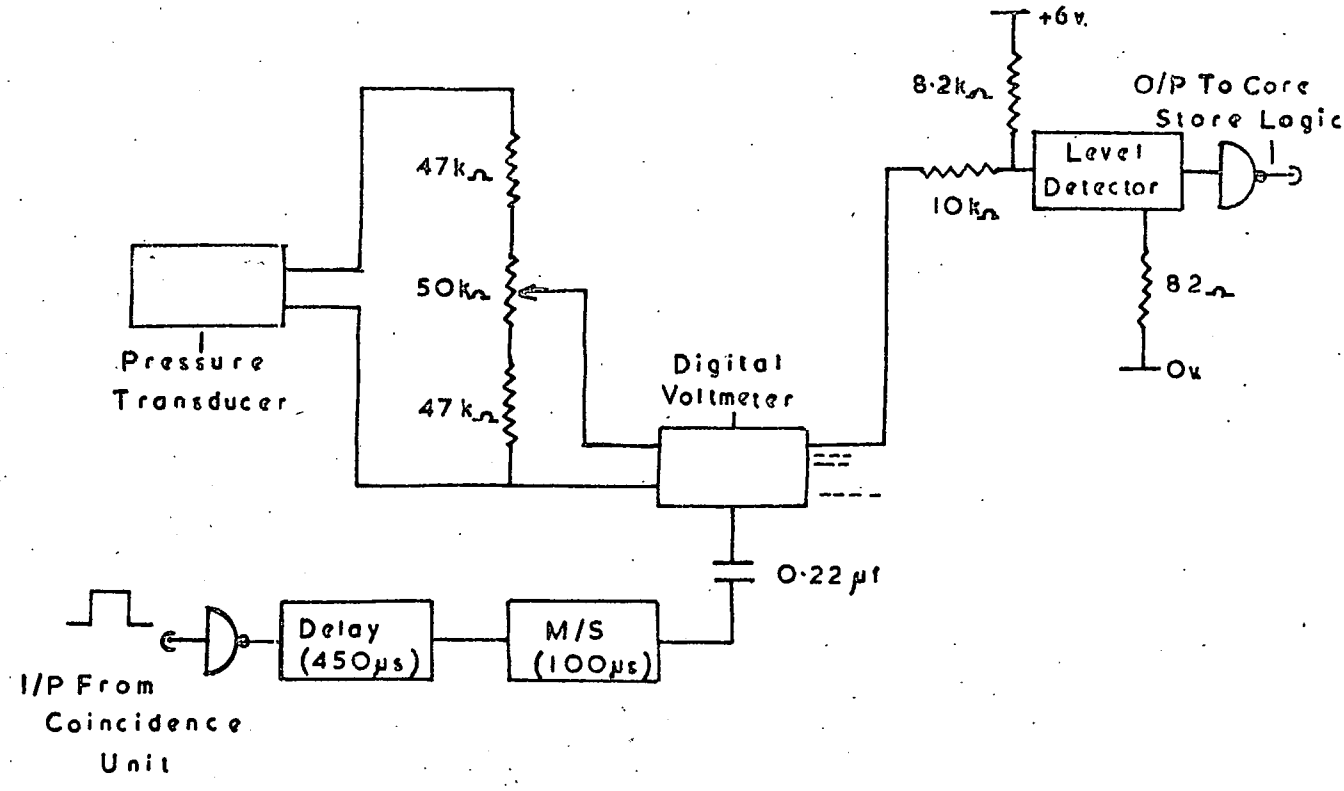

Figure 6.22 The Circuit for Digitising the Atmospheric Pressure.

to the core store is the pressure corresponding to the previous event. This is not detrimental as the previous event will only have been a few seconds before.

The sample pulse for the voltmeter is obtained from the coincidence unit and is delayed by about 450 μs as shown in figure 6.22 to enable the core store to feed in the voltage for the high momentum events before the sample pulse is received.

CHAPTER 7

The Method of Analysis of the Spectrograph Data

7.1 Introduction

This chapter discusses the analysis of the spectrograph data to determine the momenta of particles traversing the spectrograph. The analysis can be divided into two related sections; one section is concerned with the selection of high momentum events by the Momentum Selector together with the variation of the efficiency of detecting a high momentum event with incident momentum, and the other section with the analysis of high momentum events using the data in the Measuring Trays. An estimate of the m.d.m. of the spectrograph is made using the cell width distributions for the Measuring Trays which was discussed in §6.3. Also discussed briefly is the effect of multiple scattering in the magnet blocks on the estimation of the momenta of the incident particles and the variation in the acceptance of the spectrograph with incident particle momentum.

7.2 The Efficiency of the Momentum Selector

Figure 7.1 shows the co-ordinates of a particle which passes through the Momentum Selector Trays at positions a, b, and c from the start of the measuring level in each tray. The measuring levels are assumed to start from the same vertical plane.

The deflection, Δ, of the particle is defined as shown in figure 7.1. From the similar triangles ADB and BEF we have

$$\frac{b - a}{l_1} = \frac{x}{l_2}$$

Hence

$$x = \frac{l_2(b - a)}{l_1} \qquad 7.1$$

Also

$$EC = c - b = \Delta + x$$

Hence

$$\Delta = c - b - x \qquad 7.2$$

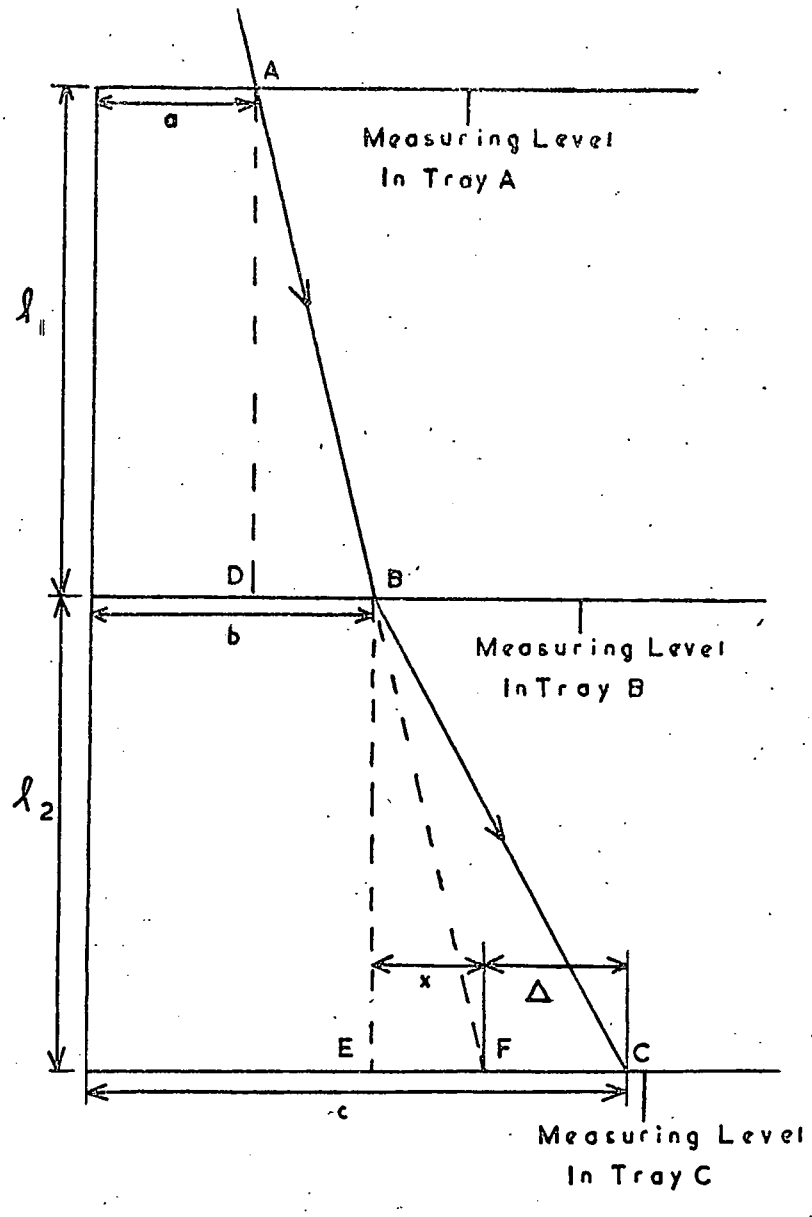

Figure 7.1 The Co-ordinates and Deflection of a Particle Measured in the Momentum Selector Trays.

Substituting for x from equation 7.1 into equation 7.2 we have

$$\Delta = c - b - \frac{l_2}{l_1}(b - a) \qquad 7.3$$

Defining k to be given by the relation

$$\frac{l_2}{l_1} = 1 + k,$$

equation 7.3 becomes

$$\Delta = c - b - (1+k)(b - a)$$

or $$\Delta = a + c - 2b - k(b - a) \qquad 7.4$$

Now for the spectrograph l_1 and l_2 can be measured and have the mean values for both sides of the spectrograph of $l_1 = 3.195$m and $l_2 = 3.141$ m. Hence $\frac{l_2}{l_1} = 0.983$ and $k = -0.017$ so equation 7.4 becomes

$$\Delta = a + c - 2b + 0.017\,(b - a) \qquad 7.5$$

Equation 7.5 has been derived from the trajectory when any value of a, b, and c can be used. In practice, the position of the particle is known only to cells of width 5 mm and the deflection Δ is measured in terms of cell numbers. The Momentum Selector measures Δ', where Δ' is given by the equation

$$\Delta' = a' + c' - 2b' \qquad 7.6$$

In equation 7.6, a', b', and c' are the numbers of the three 5mm wide cells the particle traversed, so no correction is made for the unequal arms of the measuring levels. This correction, however, is small; the maximum effect would be to give the particle an additional deflection, when measured in cell widths, of $\pm$ 2 cells.

The mixing of adjacent cells in the shift registers of the Momentum Selector Trays A and C results in a high momentum event being accepted if Δ' has one of the integer values between -2 and +2. There is thus a wide range of deflection over which the particle traversing the spectrograph will be accepted as a high momentum event. To investigate the efficiency of detecting a high momentum event as a function of the incident momentum, the passage of particles of various momenta and zenith angles was simulated through the spectrograph using

a computer. A magnetic flux density of 16.3 kilogauss was assumed to be present in each magnet block and the effect of the gaps between the blocks was taken into account. The effects of energy loss and multiple scattering on the trajectory were neglected.

By symmetry, particles having the same incident momentum but incoming angles on the opposite side of the vertical will have the same numerical value for the deflection (neglecting the sign) if they have equal and opposite charge and the same value for the incoming angle. Hence the passage of particles having both positive and negative deflection was simulated through the spectrograph for given values of momentum and projected zenith angle.

For a particle of given momentum and projected zenith angle, the positions of the particle in the three Momentum Selector Trays could be found. Then, assuming that the efficiency of correct cell determination is 100%, the particle could be allocated to three 5mm wide cells. The efficiency for the detection of the particle as a high momentum event was found by determining the various cells the particle could traverse in the three trays over a cell width. If, for a given position, the calculated deflection, when measured in cell widths, was in the allowed range, then the event was accepted as a high momentum event. The efficiency is defined as the fraction of the cell width over which the event is accepted as a high momentum event. For a given projected zenith angle, the efficiency was determined for both signs of deflection and the average taken as the overall efficiency for the given projected zenith angle and momentum.

The variation in the efficiency as a function of the incident momentum is shown in figure 7.2 for two values of incident angle. Figure 7.2(a) shows the variation for particles incident in the vertical direction and figure 7.2(b) the variation for particles incident at 3^{o} to the vertical. The sharp peaks in the curves are due to the effect of the cell edges where a small change in position of the particle will move the position into a cell which does not fit the selection criteria.

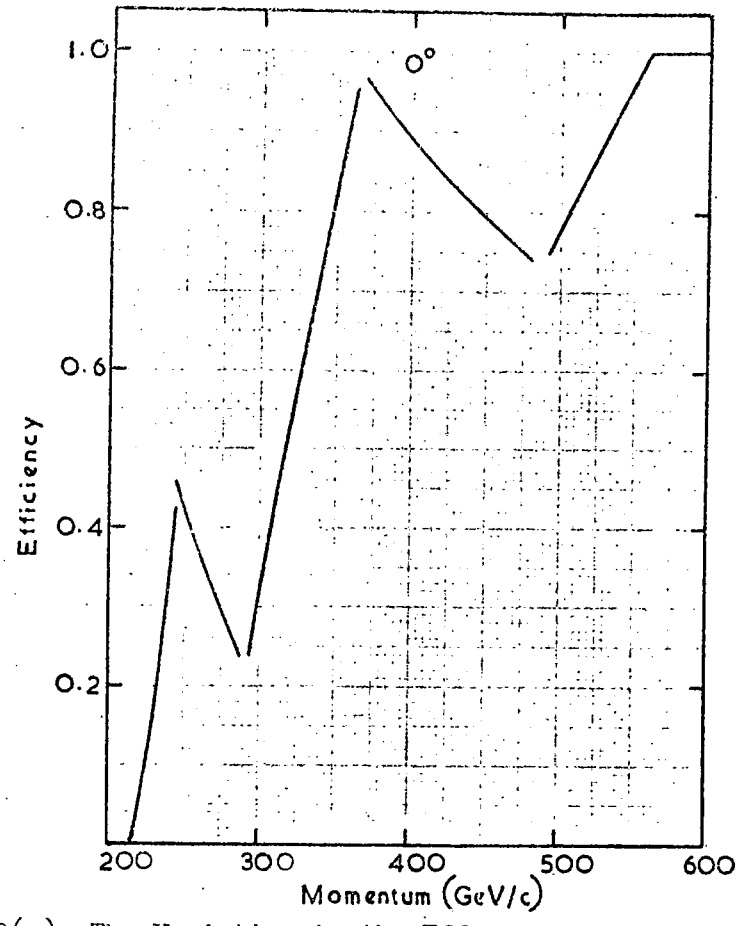

Figure 7.2(a) The Variation in the Efficiency of the Momentum Selector, for Particles Incident at 0°, with Momentum.

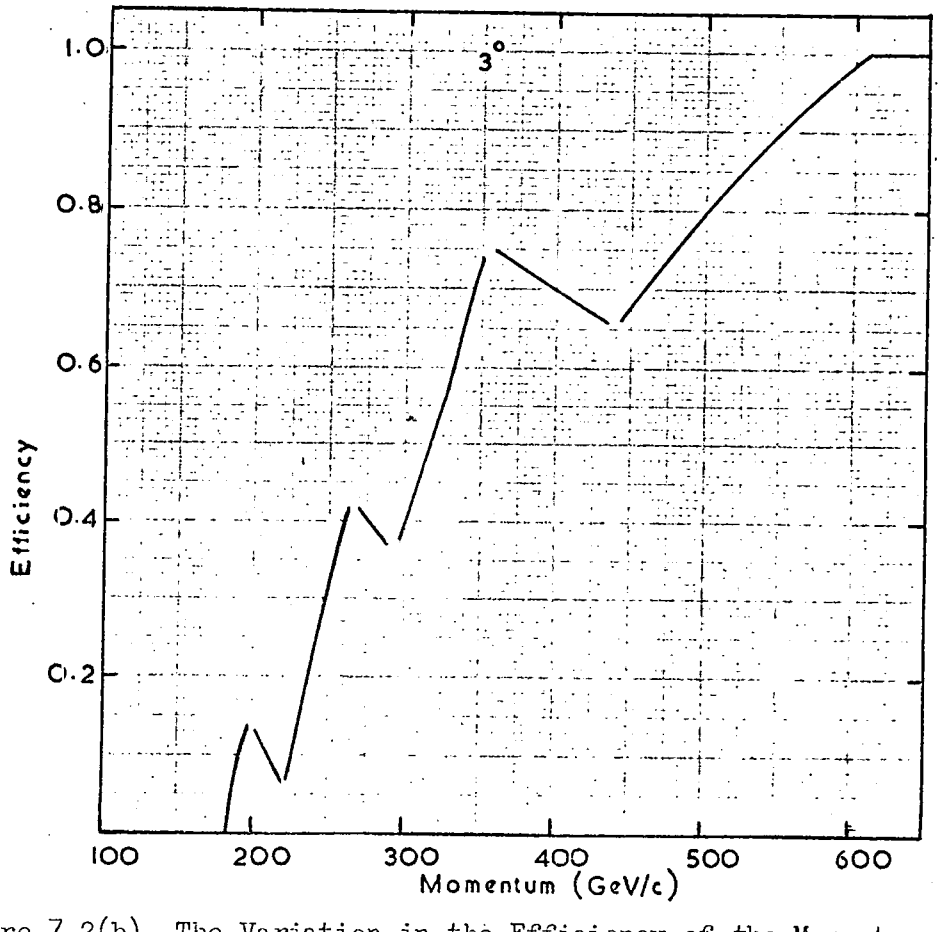

Figure 7.2(b) The Variation in the Efficiency of the Momentum Selector, for Particles Incident at 3°, with Momentum.

The above analysis has been for the ideal case, in which the particle is allocated by the logic to the correct cell. In practice this is not the case, it was shown in §5.6 the correct cell allocation depends on both the position and the angle to the vertical of the particle in a tray. As the mean overall efficiency of correct cell determination is 87%, the above efficiency variation will be a good approximation to that expected experimentally.

7.3 The Equation of Motion of a Charged Particle in the Spectrograph.

The trajectory of a particle through one side of the spectrograph is determined by the five Measuring Trays for the particular side. Figure 7.3 shows the trajectory of a singly charged particle of momentum in the deflection plane of p ev/c passing through one side of the spectrograph in a uniform magnetic flux density of B gauss. Cartesian axes Ox,Oy are drawn as shown in figure 7.3 and axis Oy is chosen so that it is the measuring level of Measuring Tray 3. The measuring level for a Measuring Tray is shown in figure 6.1.

If the energy loss in the magnet is small and the magnet is considered to be a continuous medium of iron then the particle moves in a circular path in the deflection plane of radius ρcm given by equation 2.4.

The equation of the trajectory in figure 7.3 in terms of the cartesian axes is given by

$$(x - P)^2 + (y - Q)^2 = \rho^2 \qquad 7.7$$

where (P,Q) are the co-ordinates of the centre of the circle.

From equation 7.7 we have

$$y = Q \pm \rho\sqrt{1 - \left(\frac{x - P}{\rho}\right)^2} \qquad 7.8$$

For high momentum particles $|x - P| \ll \rho$. This can be seen to be valid by considering the motion in the spectrograph of a particle of momentum 300 GeV/c. Using equation 2.4 with B equal to the value of the magnetic flux density in the magnet (1.63×10^4 gauss) and p equal to 3×10^{11} eV/c, we have $\rho \sim 6.1 \times 10^2$m. For the spectrograph, x varies between - 3.177m and 2.989m and P is of the order

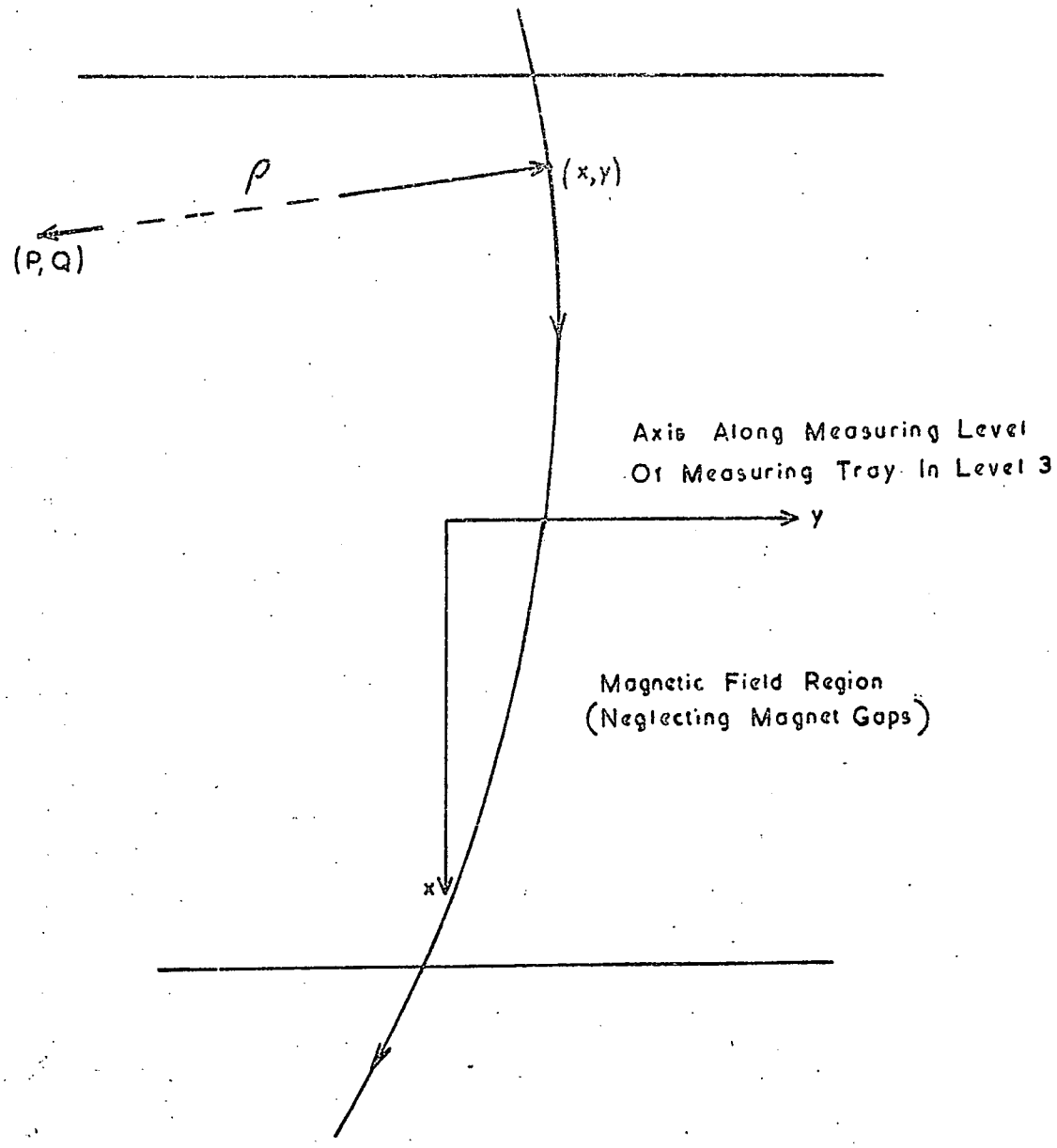

Figure 7.3 The Passage of a Singly Charged Particle Passing Through One Side of the Spectrograph with Cartesian Axes as shown.

of the spectrograph dimensions. Hence the above approximation is valid.

Using this approximation, equation 7.8 can be expanded binominally, which gives

$$y = Q \pm \rho\left(1 - \tfrac{1}{2}\left(\frac{x - P}{\rho}\right)^2 \ldots\ldots\right)$$

$$\text{or} \qquad y = \mp \frac{x^2}{2\rho} \pm \frac{Px}{\rho} \mp \frac{P^2}{2\rho} \pm \rho + Q \qquad 7.9$$

The signs of the coefficients indicate the direction of curvature of the trajectory in the magnetic field and hence the sign of the charge of the particle if the field direction is known.

Equation 7.9 can be written in the general form

$$y = ax^2 + bx + c \qquad 7.10$$

The co-ordinates of the particle trajectory are measured at the five Measuring Trays. The x co-ordinate for a given tray is the same for all events, it is the distance from the origin of co-ordinates to the measuring level of each tray. These x co-ordinates have been measured for the scintillation counters, and the flash tube trays. For the flash tube trays the distances have been measured to the measuring level in the trays and the positions of the mid point of the scintillation counters have been used for their co-ordinates. The x co-ordinates for the components in the spectrograph are shown in figure 7.4. The y co-ordinates for each trajectory are measured by analysing the flash tubes which have flashed along a track in a tray using the 1130 computer.

The coefficients a, b, and c in equation 7.10 are found by the method of least squares as shown in Appendix C. The value of the coefficient a then gives the momentum as comparing equation 7.9 with equation 7.10 we have

$$a = \mp \frac{1}{2\rho} \qquad 7.11$$

Hence substituting for ρ from equation 2.4 into equation 7.11 and re-arranging, we have

$$p = \mp \frac{150B}{a} \text{ eV/c} \qquad 7.12$$

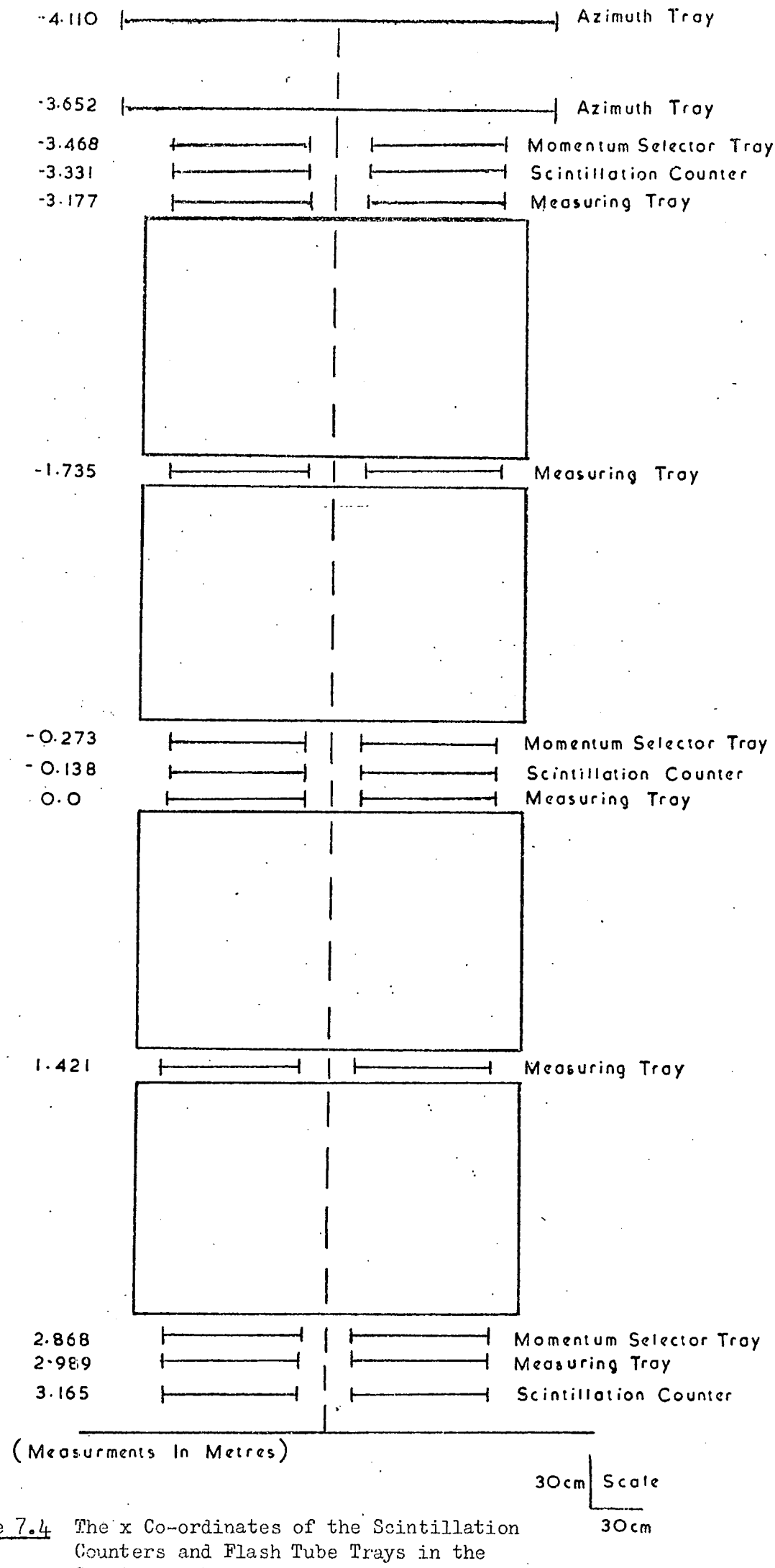

Figure 7.4 The x Co-ordinates of the Scintillation Counters and Flash Tube Trays in the Spectrograph.

if B is measured in gauss and a in $cm.^{-1}$. The sign of a is obtained from the least squares fit of the points and gives the sign of the particle if the field direction is known.

Equation 7.12 can be applied to the spectrograph by using the mean magnetic flux density of 1.63×10^4 gauss for the value of B in equation 7.12. Hence substituting in equation 7.12 and neglecting the sign we have

$$p = \frac{0.245}{a} \text{ GeV/c} \qquad 7.13$$

when a is measured in m^{-1}.

The equations for the motion of the particle in the spectrograph assume that the magnet is a continuum of iron, when in fact this is not the case. To investigate the effect of the gaps in the magnet blocks, particles of various momenta and incident angles were simulated through the spectrograph using a computer. Account was taken of the gaps between the magnet blocks and the co-ordinates of the trajectory in the five Measuring Trays were found. The effect of multiple scattering and energy loss in the magnet blocks were neglected. These co-ordinates were then used to fit a curve of shape given by equation 7.10 using the method of least squares. The momentum given by equation 7.13 could then be compared with the true momentum.

Figure 7.5 (a) shows a graph of calculated momentum against true momentum for an incident angle of 0° and figure 7.5(b) the graph for an incident angle of 5° to the vertical. Figure 7.6 shows the variation in the ratio of the true momentum to the observed momentum over the zenith angular range for an incident momentum of 500 GeV/c. The graphs show that there is only a small variation in the ratio of true momentum to calculated momentum over both the momentum and zenith angle ranges. The ratio is taken to be 0.8 for all ranges and equation 7.13 is reduced by this factor to give

$$p = \frac{0.196}{a} \text{ GeV/c} \qquad 7.14$$

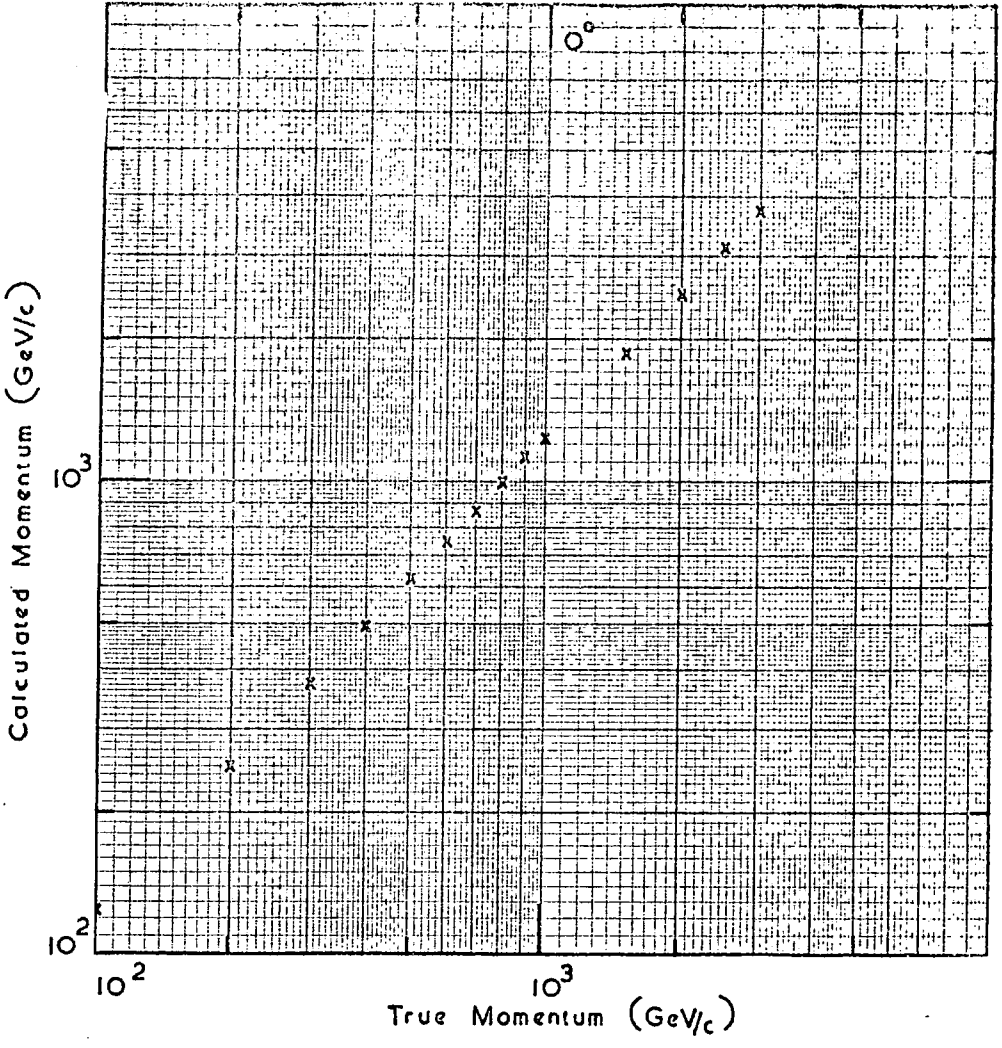

Figure 7.5(a) Graph of Calculated Momentum against True Momentum for an Incident Angle of 0°.

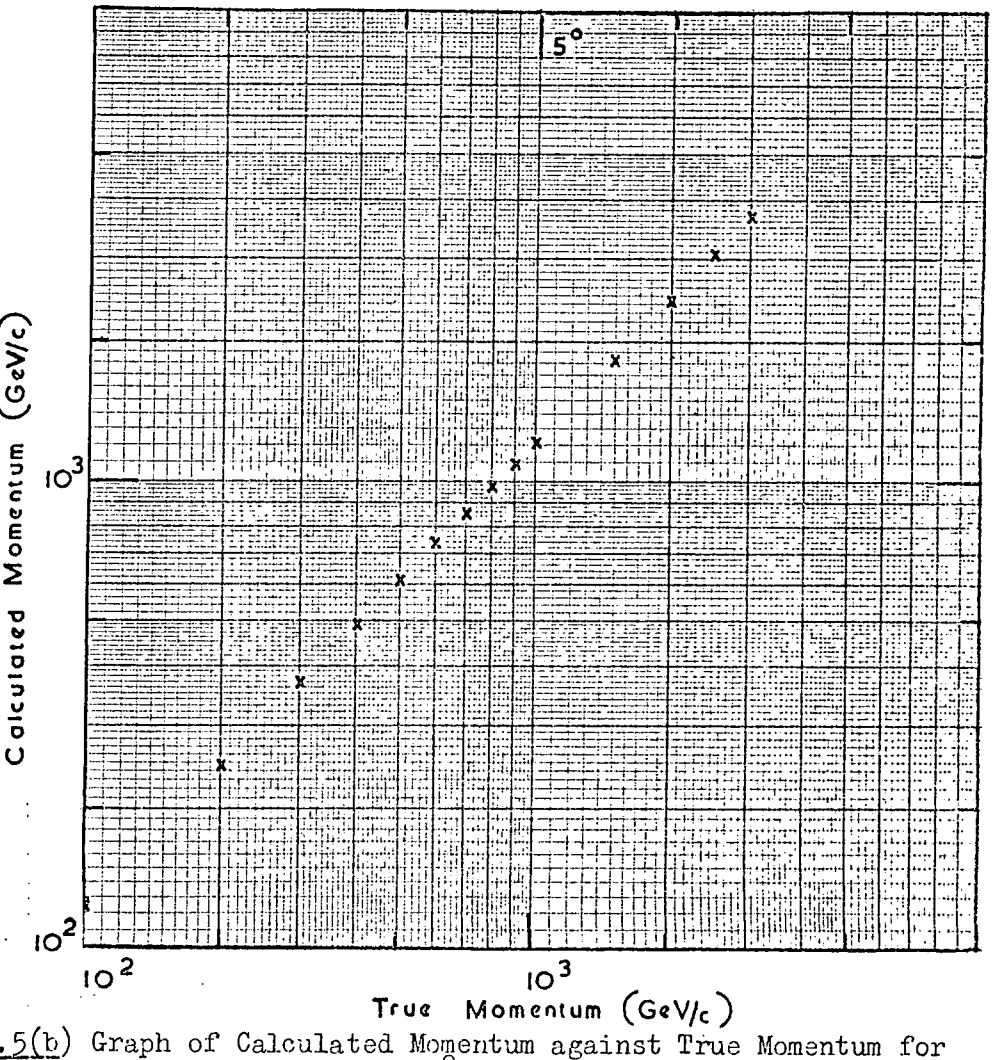

Figure 7.5(b) Graph of Calculated Momentum against True Momentum for an Incident Angle of 5°.

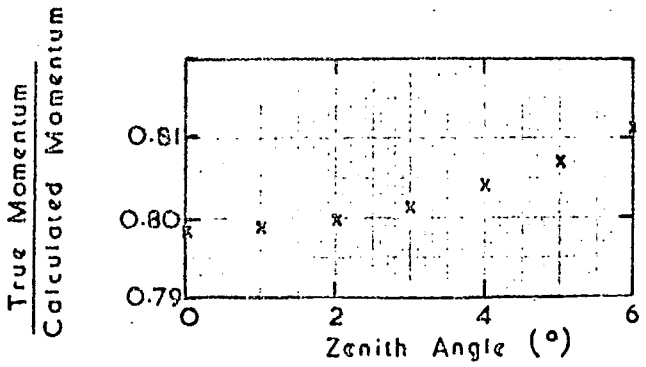

Figure 7.6 The Variation in the Ratio of True Momentum to Calculated Momentum with Zenith Angle.

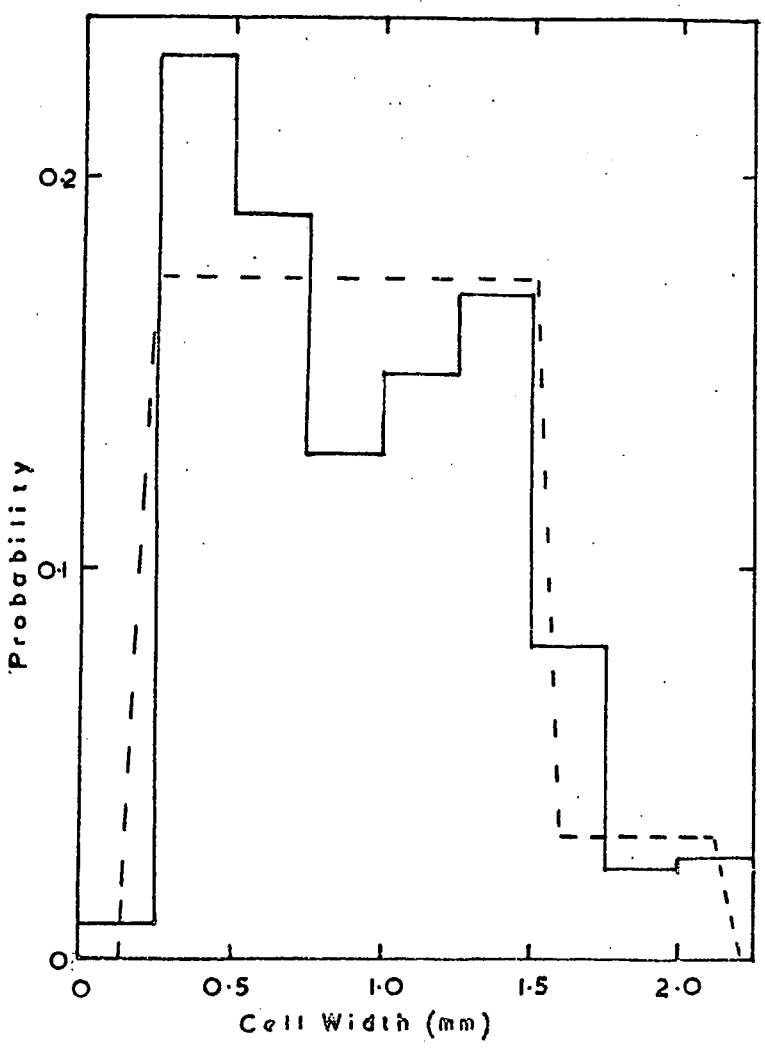

Figure 7.7 Probability Distribution of the Weighted Cell Widths.

Equation 7.14 has been derived for the case when five co-ordinates are known for the track. In general, this may not be so as the flash tube tracks in one or more trays could be distorted due to accompaniment or an interaction in the magnet block above the tray producing a cluster of discharged tubes in the tray.

The coefficients of the quadratic equation for the trajectory of the particle in the spectrograph can be determined if 3,4, or 5 co-ordinates are used. This illustrates an important property of the spectrograph, a measurement can still be made on the momentum of a traversing particle if as few as three co-ordinates are known for the trajectory.

In a similar manner to the method described above, a correction has to be made to the calculated momentum for the 3 or 4 point fits used for the determination of a trajectory.

7.4 The Maximum Detectable Momentum of the Spectrograph

The maximum detectable momentum (m.d.m.) of a spectrograph was defined in §2.1 as being the momentum of that particle, whose deflection is equal to the standard deviation of the error in the deflection. For M.A.R.S., the momentum of a particle is obtained from equation 7.14 if a five point parabola fit is possible on the track of the particle. Hence using the above definition, the m.d.m. of the instrument, p_{mdm}, is given by

$$p_{mdm} = \frac{0.196}{\sigma_a} \quad \text{GeV/c} \qquad 7.15$$

where σ_a is the standard deviation of the coefficient, a, of x^2 in equation 7.10. An expression for σ_a is derived in Appendix D in terms of the x co-ordinates of the measuring levels in the Measuring Trays. The expression is

$$\sigma_a = \sigma_y \sqrt{\frac{n\Sigma x_i^2 - (\Sigma x_i)^2}{\Sigma x_i^4 (n\Sigma x_i^2 - (\Sigma x_i)^2) - (n(\Sigma x_i^3)^2 - 2\Sigma x_i \Sigma x_i^2 \Sigma x_i^3 + (\Sigma x_i^2)^3)}} \qquad 7.16$$

where x_i is the x co-ordinate of the i th Measuring Tray, n is the number of trays used in the curve fitting, and σ_y is the standard deviation of the measurement

in the measuring levels. The summation symbol Σ used in equation 7.16 is equivalent to the symbol $\sum_{i=1}^{n}$

For a five point parabola fit n = 5, so equation 7.16 simplifies, after the summation process, to

$$\sigma_a = \frac{\sigma_y}{8.827} \text{ m.}^{-1} \qquad 7.17$$

if σ_y and x_i are measured in metres.

Hence substituting for σ_a from equation 7.17 into equation 7.16 we have

$$p_{mdm} = \frac{0.196}{\sigma_y} \times 8.827 \text{ GeV/c} \qquad 7.18$$

In § 6.3 a distribution for the discrepancies of a particle from the centre of a cell was obtained and is plotted in figure 6.4. The discrepancy distribution has a standard deviation of 0.3 mm. Hence taking this value as being equal to σ_y we have for the m.d.m.:

$$p_{mdm} = 5770 \text{ GeV/c}$$

As a check on this value of momentum for the m.d.m. of the instrument, a Monte Carlo calculation was carried out on 9990 particles passing through the spectrograph when the position of a particle was taken to be in a cell obtained from the flash tube pattern. The variation in the weighted mean cell width as a function of angle is shown in figure 6.2 for the flash tube pattern used in the Measuring Trays. A probability function for the weighted cell widths is shown in figure 7.7. It is seen that an approximate square distribution is obtained over an appreciable range, which is shown in figure 7.7. It was thus assumed that cell widths between the values 0.19 mm and 1.56 mm, where the probability falls to one half of its plateau value, were possible with equal probability.

A Monte Carlo computer programme was then used to predict a cell width over this range and the position of the particle in the cell. Five of these points were then used as the y co-ordinates of the track of a particle of infinite momentum traversing the spectrograph. The momentum corresponding to the

trajectory was calculated using the least squares parabola fit and equation 7.14. The process was repeated for a total of 9990 events. A histogram of $^{1}/_{p}$, where p is the calculated momentum in GeV/c, for the events is shown in figure 7.8. The distribution has a standard deviation of 1.43×10^{-4} GeV/c^{-1} corresponding to a momentum of 6993 GeV/c.

This value of momentum is in good agreement to that obtained for the m.d.m. of the spectrograph using a r.m.s. positional uncertainty of 0.3 mm in each measuring level. The higher value obtained with the Monte Carlo method could be due to neglecting the effect of the tail in the probability distribution of weigthed cell widths, which would broaden the distribution if included.

7.5 The Effect of Multiple Scattering on the Momentum Determination

The equations used to determine the momentum of a particle traversing the spectrograph have neglected the effect of multiple scattering in the iron of the magnet. The ratio of the r.m.s. angle of scatter to the magnetic angular deflection for the spectrograph is approximately 12%. However, for a single magnet block the ratio is higher by about a factor of 2 on the value for the instrument as a whole and this could be reflected in a higher momentum uncertainty.

To investigate the effect of scattering on the momentum determination, particles of known momentum were simulated through the spectrograph by a computer. The particles entered the spectrograph vertically, no energy loss was assumed, and after traversing each block were subjected to a further angular deflection superimposed on to the magnetic deflection for the block. This additional deflection was selected by a Monte Carlo technique from a Gaussian distribution of the multiple scattering angles, with the mean of the distribution equal to zero and the standard deviation given by equation 2.1 with t of equation 2.1 equal to the thickness of the block. The process was repeated for each block in turn. The effect of further multiple scattering in the flash tube trays and scintillation counter of level 3 were neglected.

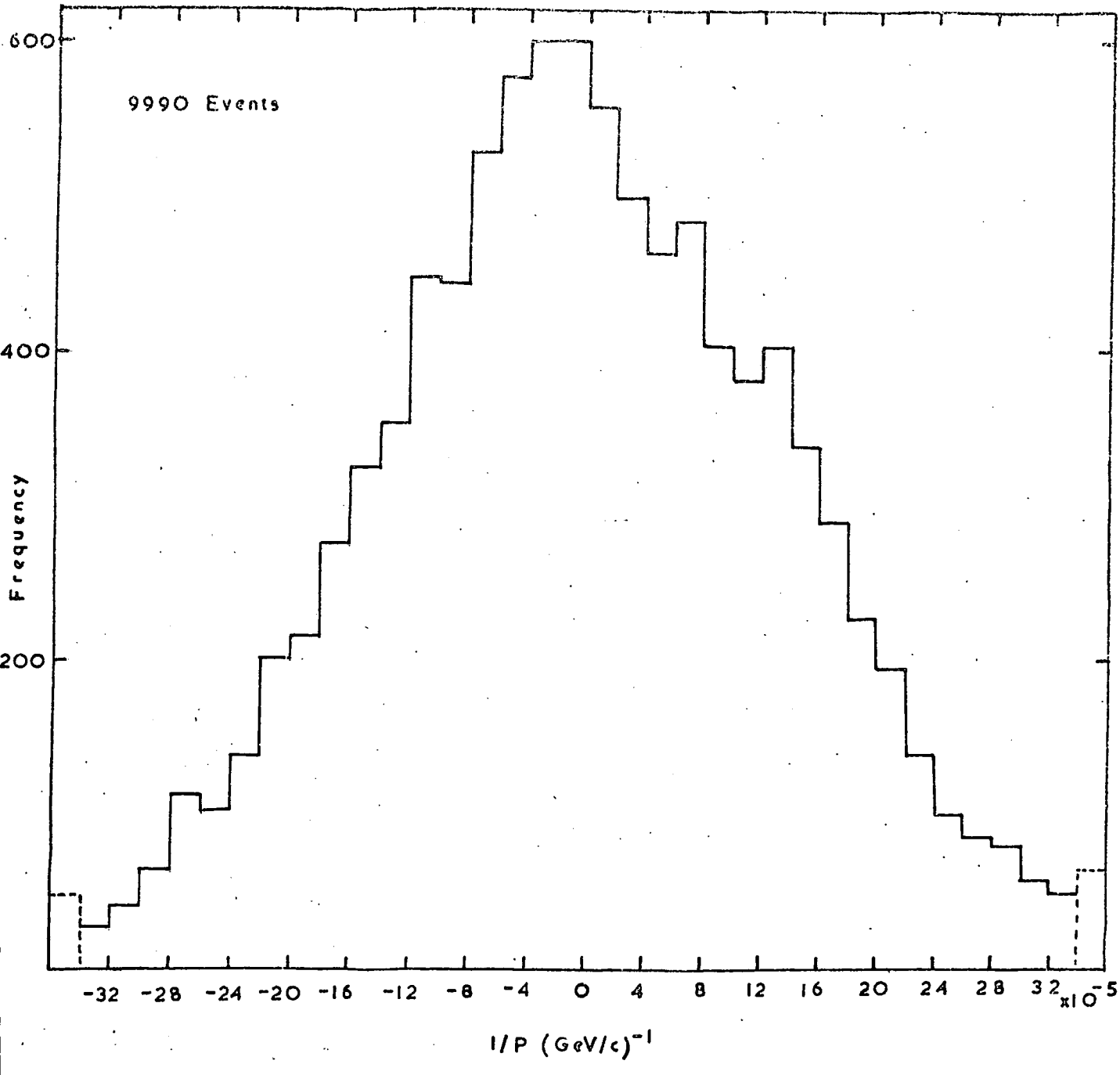

Figure 7.8 Histogram of $\frac{1}{p}$ for 9990 Events.

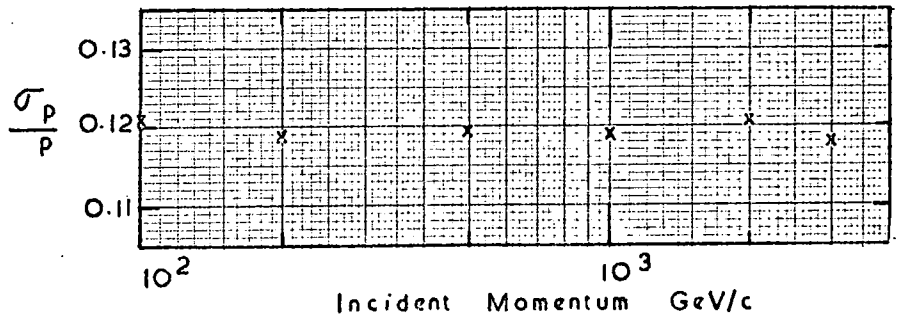

Figure 7.9 Graph of the Variation of $\frac{\sigma_p}{p}$ with Incident Momentum.

From the output positions and angles to the vertical for the particle leaving the blocks, the co-ordinates of the position of the particle in each measuring level could be determined. The co-ordinates were then used to fit a five point parabola fit and the momentum determined using equation 7.14. The procedure was repeated for 1000 events for several values of incident momentum.

For each value of momentum, the standard deviation of the distribution was calculated and in figure 7.9 the ratio of the standard deviation, σ_p, to the incident momentum, p, is plotted as a function of the incident momentum, p. Figure 7.10 shows the distribution obtained for particles of 500 GeV/c incident momentum. This distribution has a mean of 508.2 GeV/c and a standard deviation of 59.9 GeV/c.

The results plotted in figure 7.9 show that the ratio $\frac{\sigma_p}{p}$ is approximately constant over all values of momenta and equal to the expected value, when considering the spectrograph as a whole, of 12%. However, the analysis should only be considered as preliminary as no account has been taken of the effect of lateral scattering, which will be superimposed on the magnetic lateral deflection.

It can be seen from figure 7.10 that the momentum distribution obtained for an incident momentum of 500 GeV/c is not symmetric. This assymmetry in the distributions is obtained in all values of incident momenta comsidered. The reason for this is not clear. It could possibly be caused by the curve fitting technique used in the determination of the momentum from the flash tube co-ordinates but further analysis is required before a satisfactory explanation is obtained.

7.6 The Acceptance of the Spectrograph.

The acceptance of the spectrograph varies with incident momentum, depending for a given value of incident momentum on both the magnetic

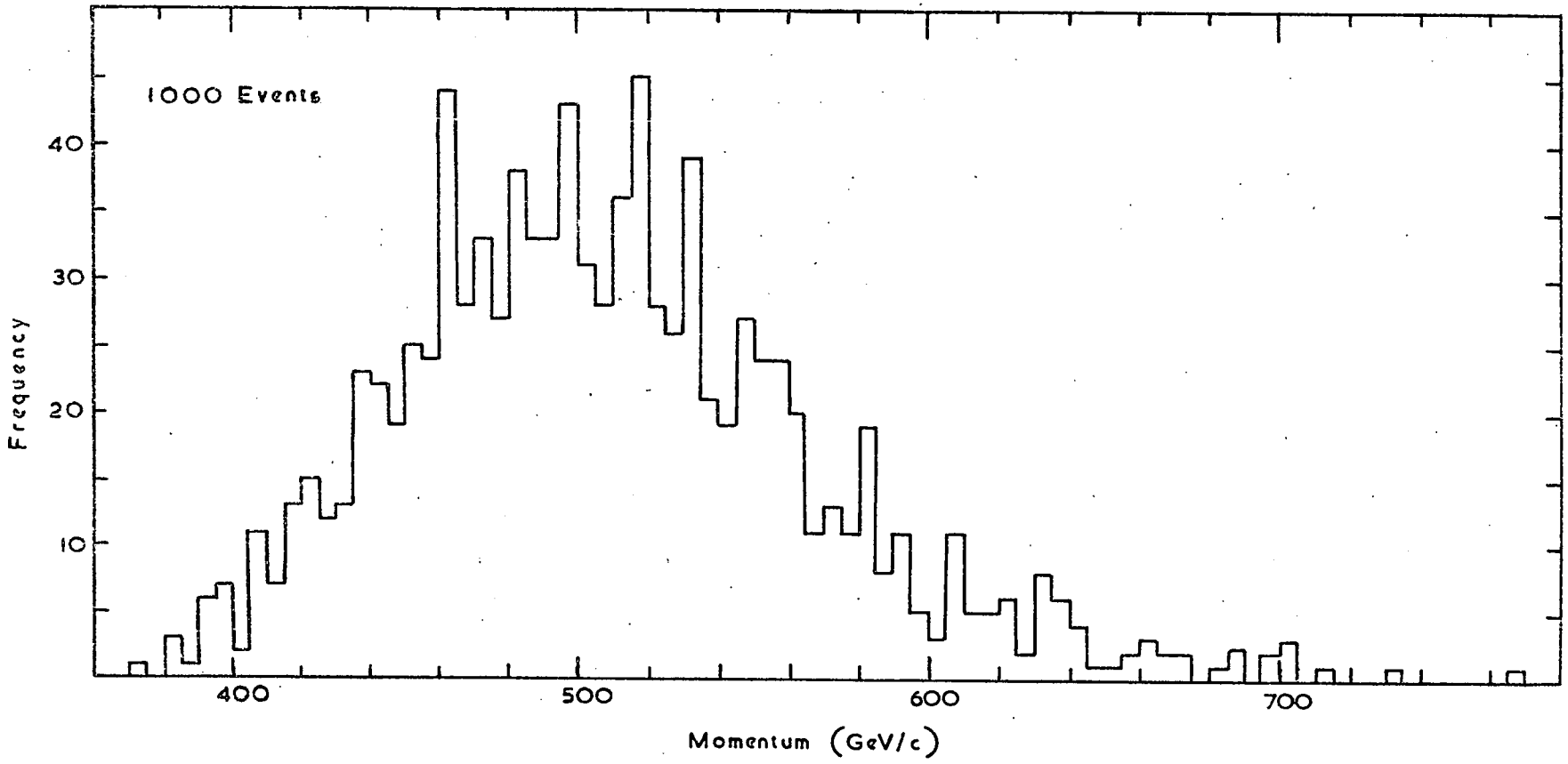

Figure 7.10 Histogram of the Calculated Momentum after Multiple Scattering in the Spectrograph for 1000 Events of 500 GeV/c Incident Momentum.

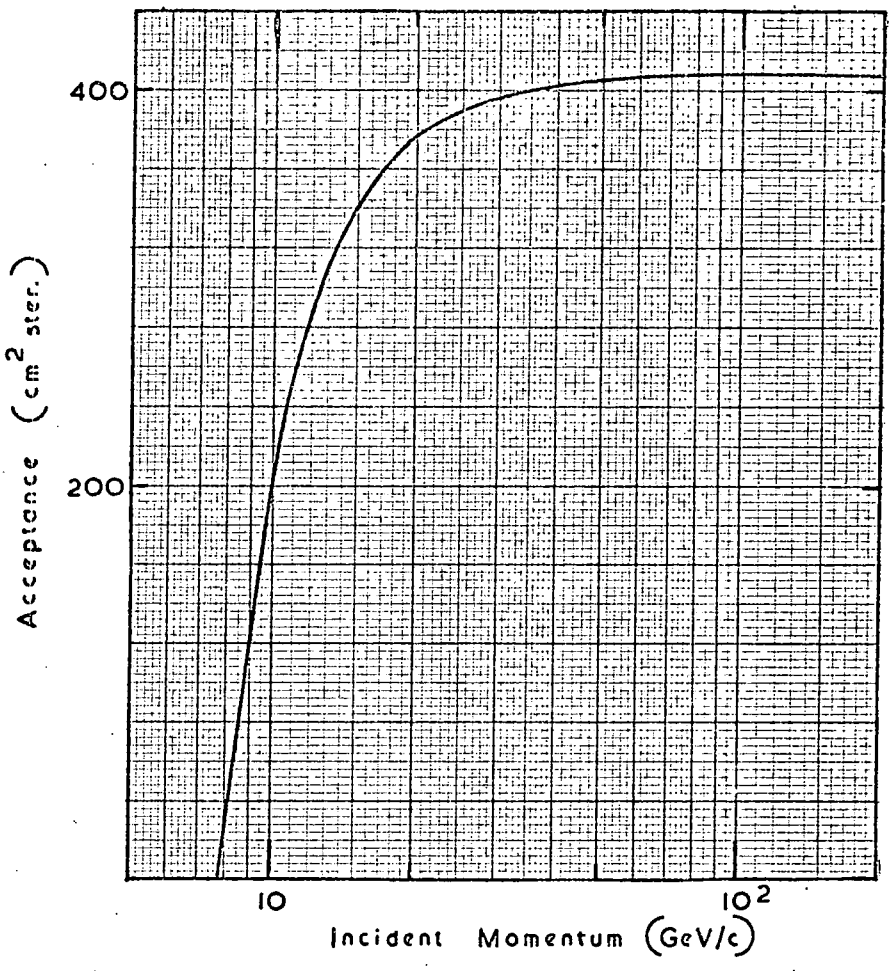

Figure 7.11 The Variation in the Acceptance of one side of the Spectrograph with Incident Momentum.

deflection and the energy loss in traversing the spectrograph. The variation in the acceptance of one side of the spectrograph with incident momentum is shown in figure 7.11. The acceptance was calculated for a given momentum by simulating particles through the spectrograph at various incident angles and calculating the area of the top scintillator through which it was possible for the particle to have passed and be accepted by the instrument. The effect of energy loss and magnetic bending in a field of 16.3 kilogauss was taken into account but the effect of multiple scattering was neglected.

CHAPTER 8

The Present Status of the Experiment

8.1 Introduction

This chapter briefly describes the form of a preliminary experiment using one side of the spectrograph and discusses the present status of the work. Finally, future plans for the spectrograph are discussed.

8.2 The Preliminary Experiment

A preliminary experiment has been performed using one side of the spectrograph (the Red side). The main purpose of this experiment was to test the computer programmes written for the on-line analysis using the 1130 computer. The five Measuring Trays on the Red side were triggered on a three fold coincidence between the scintillation counters. The flash tubes which discharged were recorded in the conventional way on film. For this run, the flash tube digitisation shields were removed from the trays, thus enabling the flash tubes to be photographed. A system of mirrors enabled the five trays to be photographed by the same camera, together with the time of the event and other relevant information.

Figure 8.1 shows the positions of the scintillation counters and Measuring Trays in the Red side for this preliminary run. The positions are slightly different from those which will be used when the Momentum Selector Trays are in position as can be seen from Figure 3.1. With this arrangement, some 7000 events have been photographed and analysed with the magnetic field of the spectrograph at its running value of 16.3 kilogauss.

The films were scanned and the co-ordinates of the discharged flash tubes along a possible track in each tray were punched on to paper tape for input to the 1130 computer. A minimum of three discharged flash tubes along a possible track in each flash tube tray was required before the event was acceptable. The data were stored in the computer in the same format as will eventually be used in the on-line mode, that is, the flash tube column number

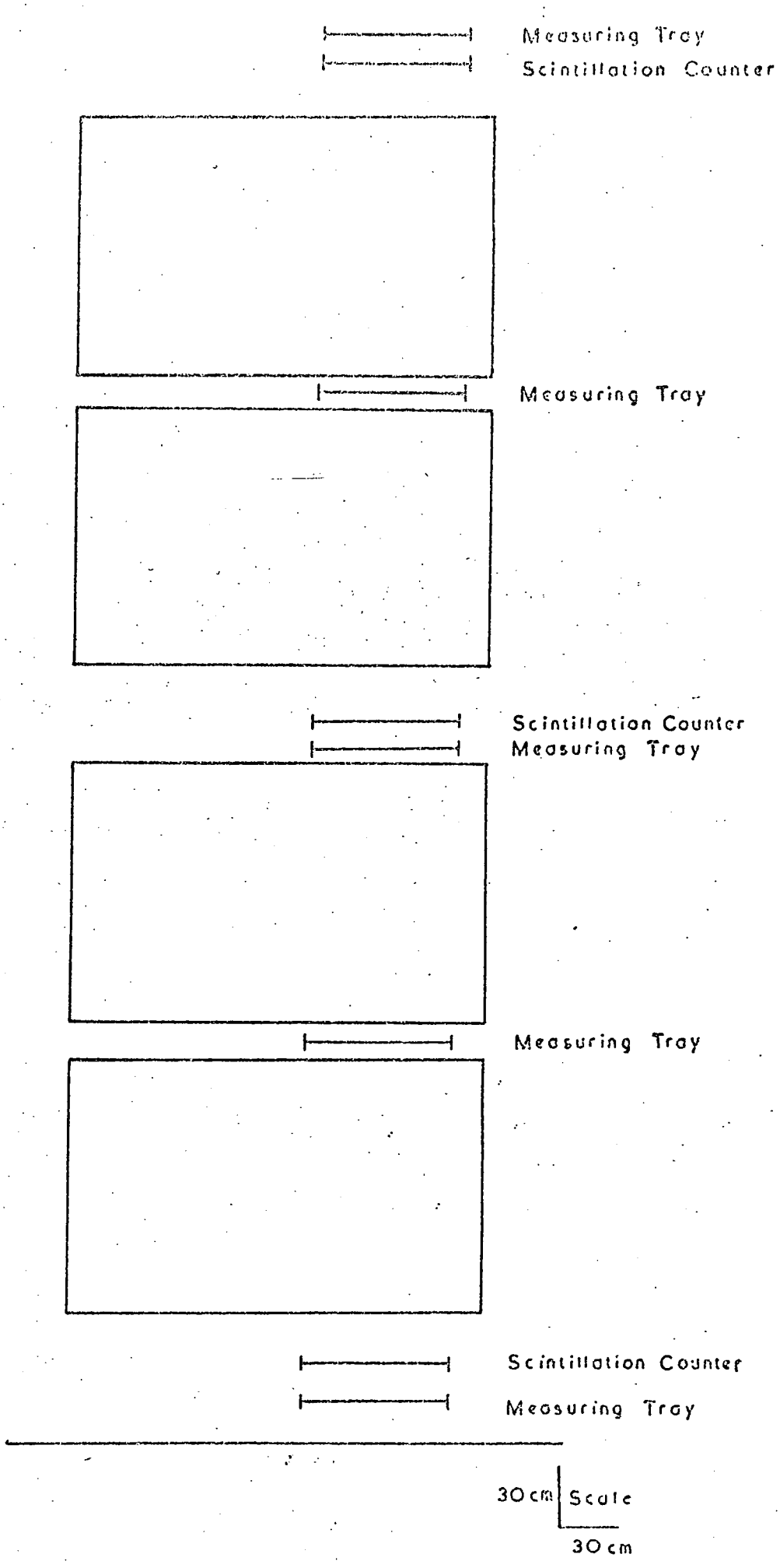

Figure 8.1 The Positions of the Scintillation Counters and Measuring Trays for the Preliminary Experiment.

in an eight bit B.C.D. form and the states of the flash tubes in the column. The events were then analysed by the computer to determine the co-ordinates of the particle in the five Measuring Trays. These co-ordinates were then used to obtain the momentum of the particle using the curve fitting technique described in Chapter 7. A correction was made to the computed momentum for the effect of energy loss in traversing the spectrograph.

An analysis of the events enabled preliminary measurements of the muon spectrum and the variation in the muon charge ratio with muon momentum to be obtained, which are brefly reported here for completeness but with no detailed discussion.

In this preliminary experiment, absolute intensities have not been measured, so the spectrum has been normalised at 22.1 GeV/c to the differential spectrum derived from the integral spectrum of Osborne et al. (1964). The normalised spectrum is shown in figure 8.2, together with the differential spectrum used for the normalisation.

The variation in the charge ratio with muon momentum is shown in figure 8.3. Because of low cell population, the last two cells of the spectrum measurement have been combined for the charge ratio results and plotted at the mean momentum for the new cell.

It should be emphasised that the results plotted in figures 8.2 and 8.3 are preliminary, but reasonable agreement is obtained with previous measurements considering the approximate analysis of the results. The suggestion of a minimum in the charge ratio results at about 80 GeV/c will be investigated further in the future on-line analysis using the digital device R.U.D.I.

8.3 The Present Status of the Work

Work is still being continued on various parts of the spectrograph. This section discusses the latest details and progress of the work.

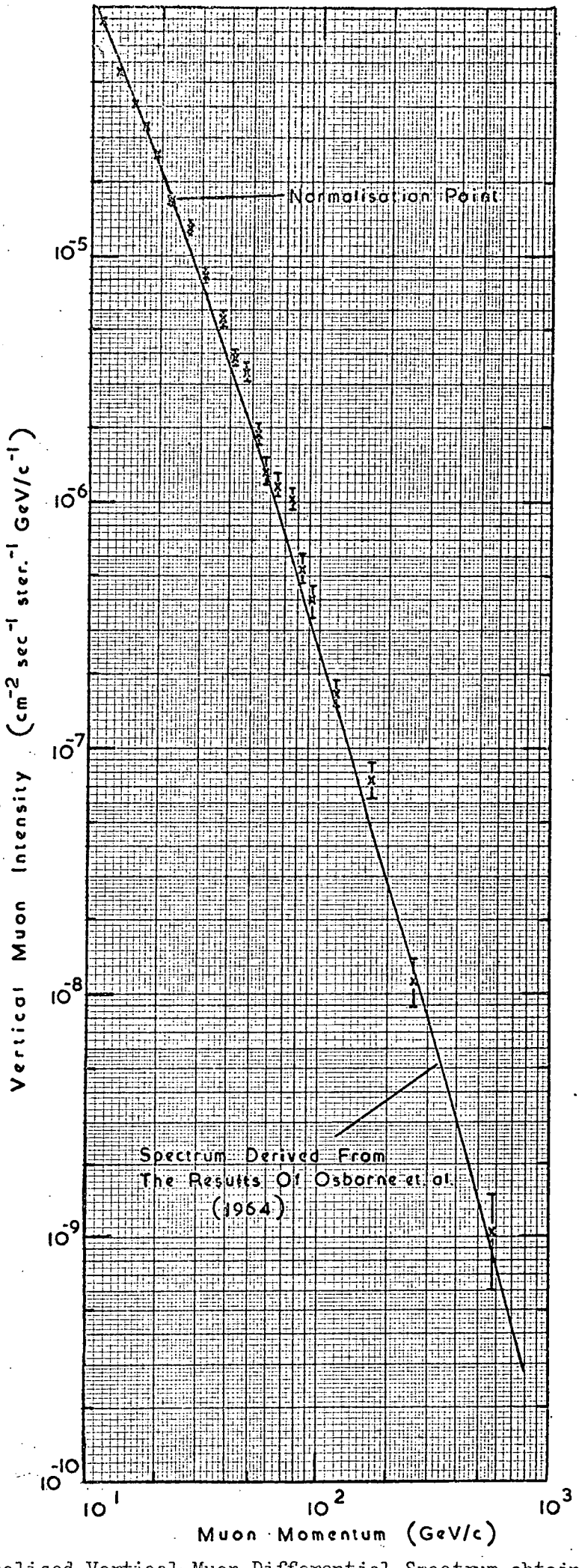

Figure 8.2 The Normalised Vertical Muon Differential Spectrum obtained from the Results of the Preliminary Experiment.

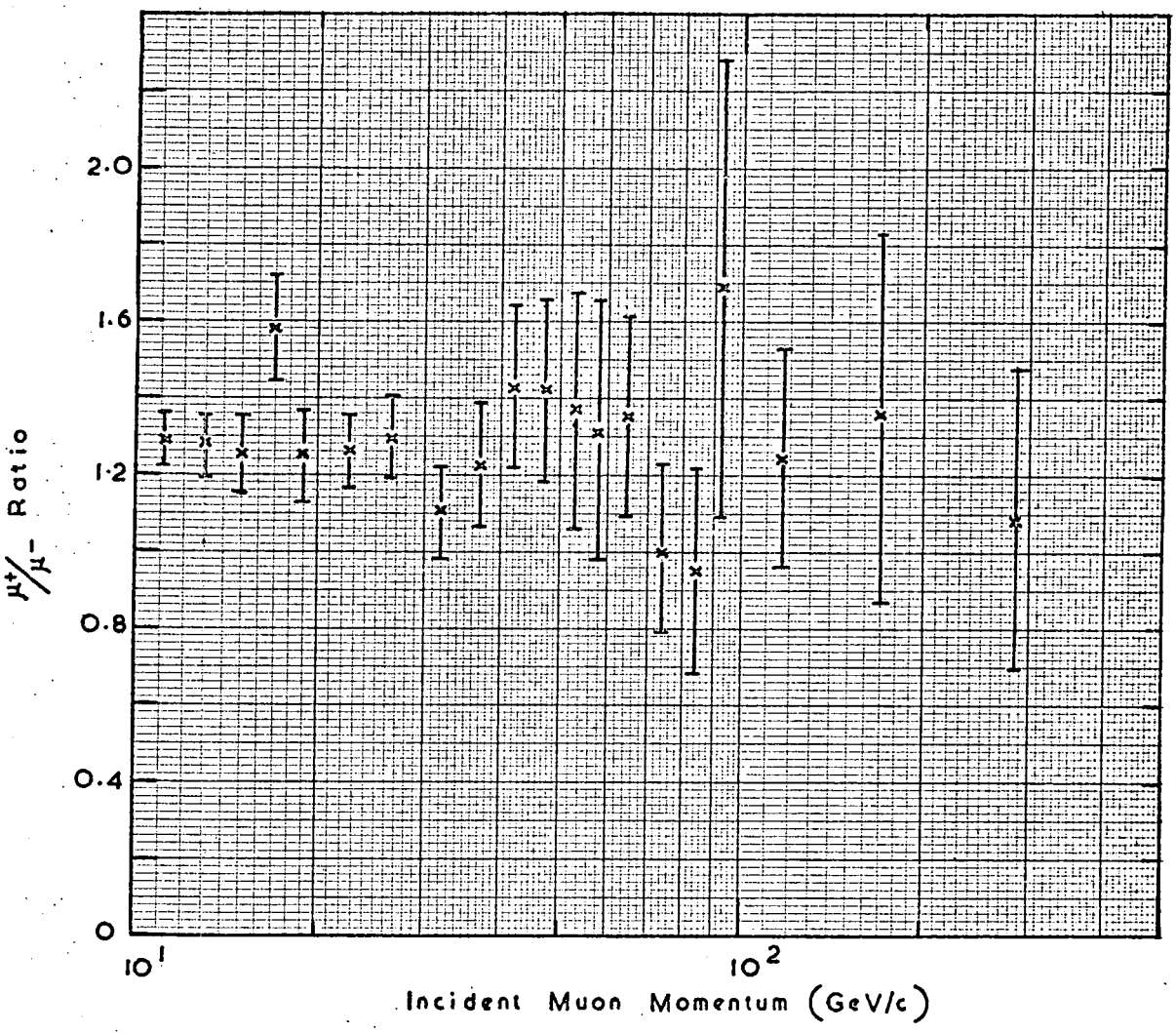

Figure 8.3 The Variation in the Muon Charge Ratio with Momentum from the results of the Preliminary Experiment.

In §8.2, a preliminary experiment using the Red side of the spectrograph has been described. A further photographic run is being performed on the Red side to investigate the interaction properties of the muon by observing the frequency of bursts in the Measuring Trays of levels 1 and 3 produced in the magnet blocks A and C. The three scintillation counters have been modified by the addition of a further two photomultipliers (Mullard Type 56AVP). These photomultipliers are placed on the side of the two Perspex light guides of the scintillation counter.

Eventually, the added pulse heights of these extra photomultipliers will be recorded automatically and stored in digital form in a core store for future analysis. For the present experiment, the extra photomultipliers will be used in conjunction with a three fold coincidence from the scintillation counters of the Red side to apply a high voltage pulse to the five Measuring Trays when a shower of a certain size traverses the scintillation counters in level 1 or level 3, the shower size being set by the discriminator electronics. With the magnetic field in the magnet blocks, an estimation of the momentum of the muon producing the burst can be obtained from the information contained in the Measuring Trays.

The printed circuit boards used in the data recording and readout logic of the flash tubes in the Measuring and Azimuth Trays have been constructed, tested, and any faults found have been rectified. Similarly, the logic circuits of the Momentum Selector system have been tested and found to be working satisfactorily. The computer interrupt and readout facilities from the core store to the computer disc store have been tested and found to be working in the required manner.

Work is now in progress on the Momentum Selector system using the Momentum Selector Trays of the Blue side of the spectrograph. The electronics of the cell allocation logic are now connected to the Momentum Selector and tests are being carried out on the data recording with the spectrograph

under zero field conditions.

8.4 Future Plans

An initial on-line run will be performed using the Momentum Selector Trays of the Blue side of the spectrograph. The Momentum Selector will be connected to R.U.D.I., which will analyse the events and store the computed deflection as a series of spectra in a pulse height analyser as described in §5.10.

During this run, work will begin on connecting the electronic circuits on to the tray fronts of the Measuring Trays of the Blue side. The Azimuth Trays will also be prepared at this stage. After the completion of the muon interaction experiment, the Momentum Selector Trays for the Red side will be placed in position and their electronic circuits, after the initial testing, connected into the Momentum Selector so that the recording on the pulse height analyser of the deflections for particles traversing the spectrograph on both sides will be possible.

This will enable the muon spectrum over the range from about fifty GeV/c to a few hundred GeV/c to be measured from an analysis of the data stored in the pulse height analyser during the completion of the digitisation of the Measuring Trays and eventual on-line analysis by the computer.

APPENDIX A

Some of the Standard Logic Circuits used in the Spectrograph Electronics

A.1 Introduction

Several standard logic circuits made from integrated circuit components are used in the electronics of the spectrograph. Both TTL and DTL systems are used in the spectrograph. The TTL system is incorporated in the circuits of the scintillation counter discriminators, main coincidence unit, and the Momentum Selector. The DTL system is used for the Measuring and Azimuth Tray electronics, the core store logic, and the circuits for digitising the information fed into the core store with every high momentum event.

TTL circuits have a faster switching time than DTL circuits; the switching time for a TTL circuit is typically about 18nS compared with 40 nS for a DTL circuit. Hence the TTL system is used in the spectrograph for all coincidence types of circuits. TTL circuits have also been developed considerably over the past few years compared with DTL circuits. Complex circuits have been produced which now fit into a single integrated circuit block. Previously the circuits would have been built from several blocks. Some of the circuits designed and constructed for the spectrograph using the TTL system could now be built using fewer blocks and thus saving both in the cost of the circuit and in the time required in wiring the circuits.

This Appendix describes some of the standard circuits used in the spectrograph and built in the two logic systems mentioned above.

A.2 TTL System

A.2.1 Introduction

TTL is an abbreviation for Transistor Transistor Logic. Figure A.1 shows a diagram of a two fold input TTL nand gate with the truth table for the logic levels shown in the inset. The logic symbol for the nand gate is also shown in figure A.1. A logical 0 level is obtained for a voltage between 0v. and + 0.8v., and a logical 1 level for a voltage between + 1.4v and + 5v on the inputs. The

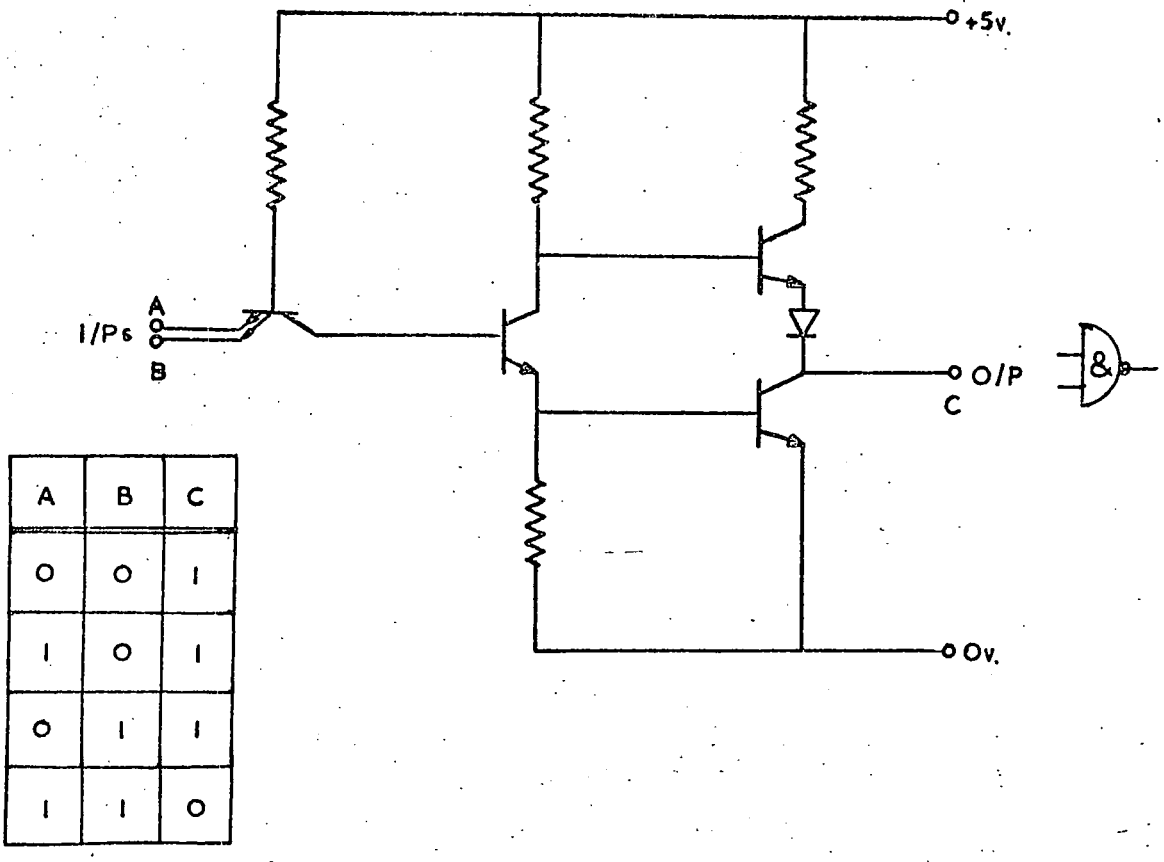

A	B	C
0	0	1
1	0	1
0	1	1
1	1	0

Figure A.1 Schematic Diagram of a Two Fold TTL Nand Gate.

circuit is impregnated on a single chip of silicon. The chip also contains three similar circuits and is encapsulated in an integrated circuit element block. A power supply of + 5v. is required for the block. Gates having various numbers of inputs are available. The various standard circuits using TTL are described below.

A.2.2 The Monostable Circuit and Delay Unit

The monostable circuit is shown in figure A.2(a). A monostable circuit produces an output pulse of length controlled by the capacitor C in figure A.2(a). The output pulse is independent of the length of the input pulse so the circuit is useful as a pulse shaper when triggered from a switch or from an input pulse which has a variable length. Positive and negative output pulses can be obtained from the circuit as shown in figure A.2(a), and figure A.2(b) shows the variation of the output pulse length with value of the capacitor C. The symbol for the circuit is shown in figure A.2(a).

The monostable is triggered by the negative edge of the input pulse. This property makes the circuit a useful device for a delay unit. Two monostables are connected in series via an inverter gate. The input pulse is then delayed by the length of the first monstable and the final output pulse length is controlled by the second monostable. Figure A.3 shows a diagram of the arrangement together with the associated symbol for the delay.

Further development of TTL logic has resulted in the production of an integrated circuit block which has a monostable circuit built inside the block. Pulses of various lengths can be obtained by connecting suitable values of resistor and capacitor to the pins of the block. This block is equivalent in the Mullard range to type number FJK 101.

A.2.3 The Multivibrator Circuit

A multivibrator provides square wave pulses of a certain frequency. The circuit of the multivibrator is shown in figure A.4(a), together with its associated symbol. The frequency of the pulses depends on the value of the capacitors C shown in figure A.4(a). Figure A.4(b) shows a graph of

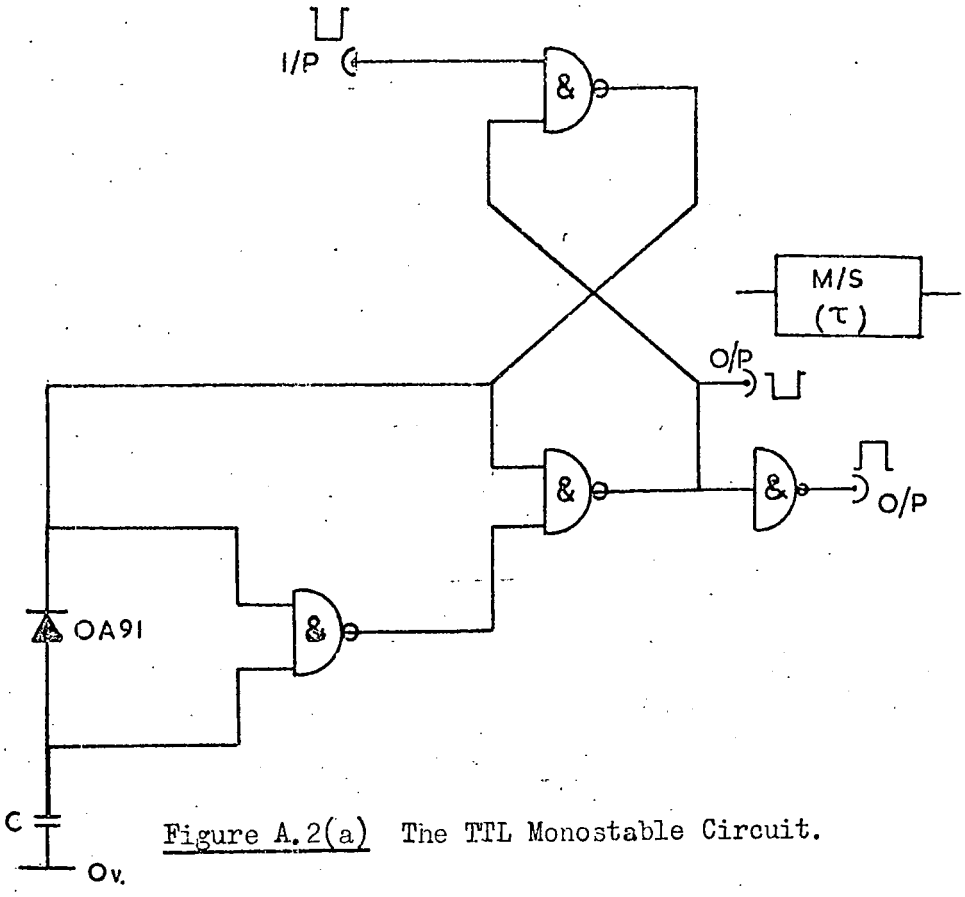

Figure A.2(a) The TTL Monostable Circuit.

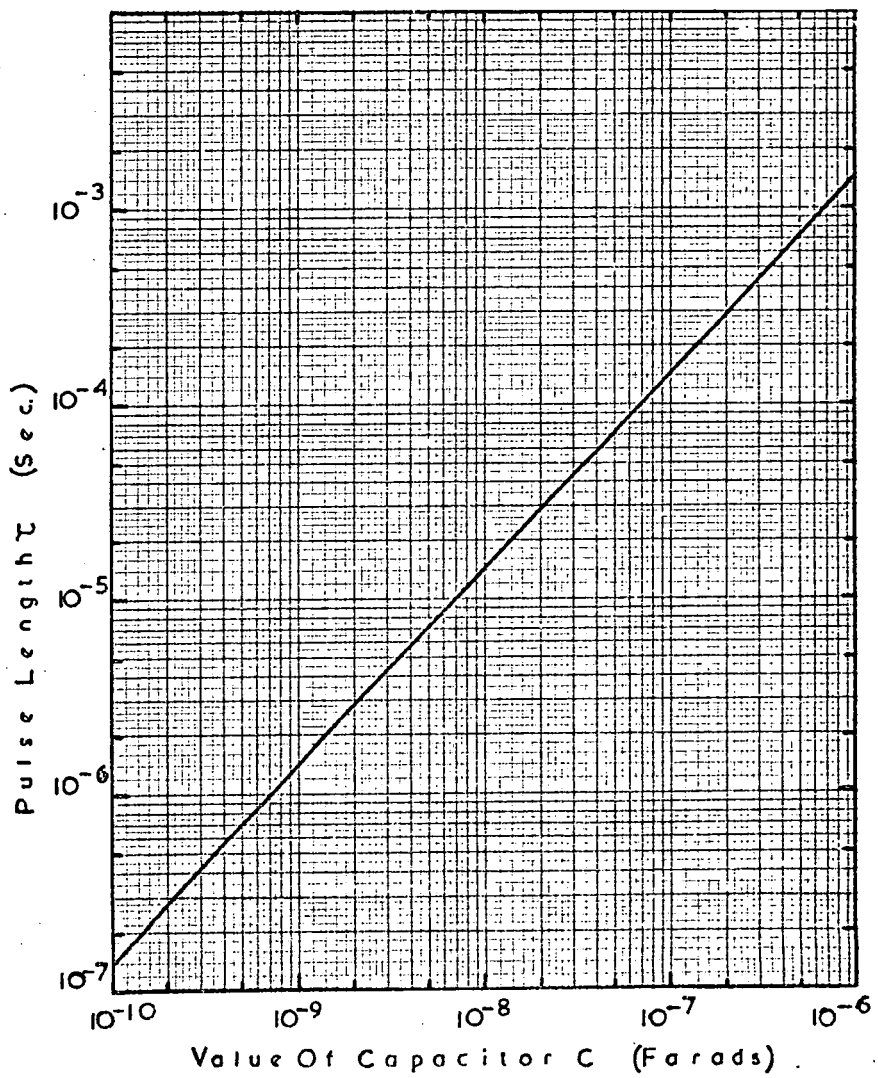

Figure A.2(b) The Variation of Pulse Length, τ, with Capacitor, C.

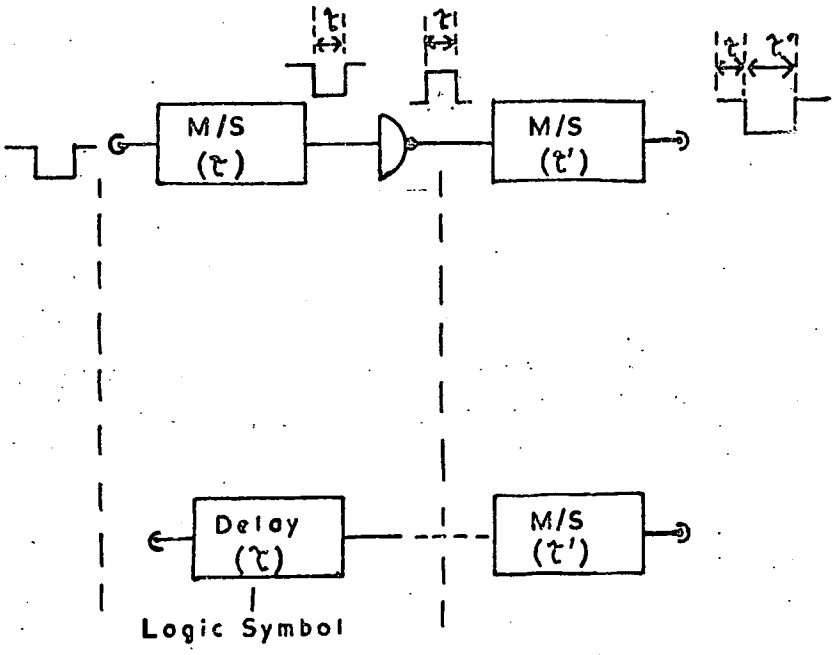

Figure A.3 The Form of the Delay Unit using Two Monostables Connected as Shown.

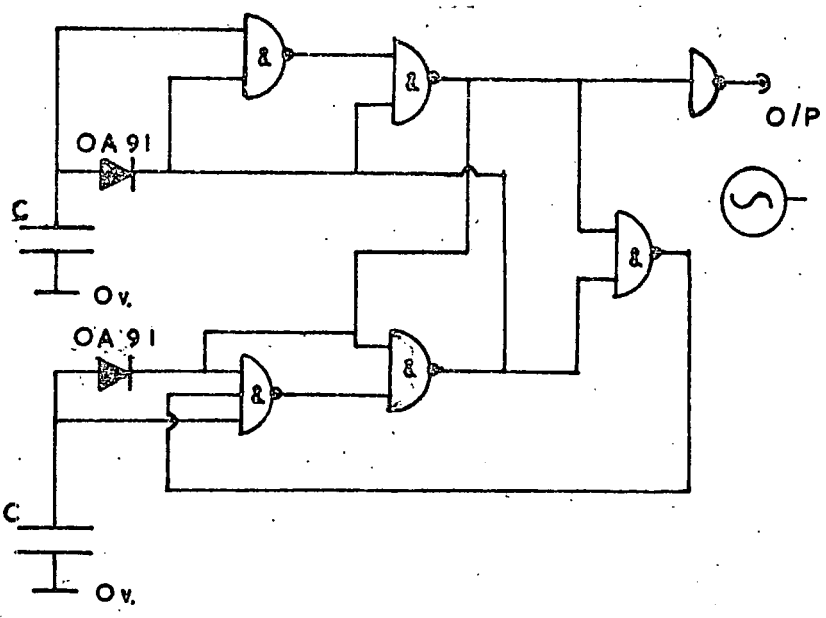

Figure A.4(a) The TTL Multivibrator Circuit.

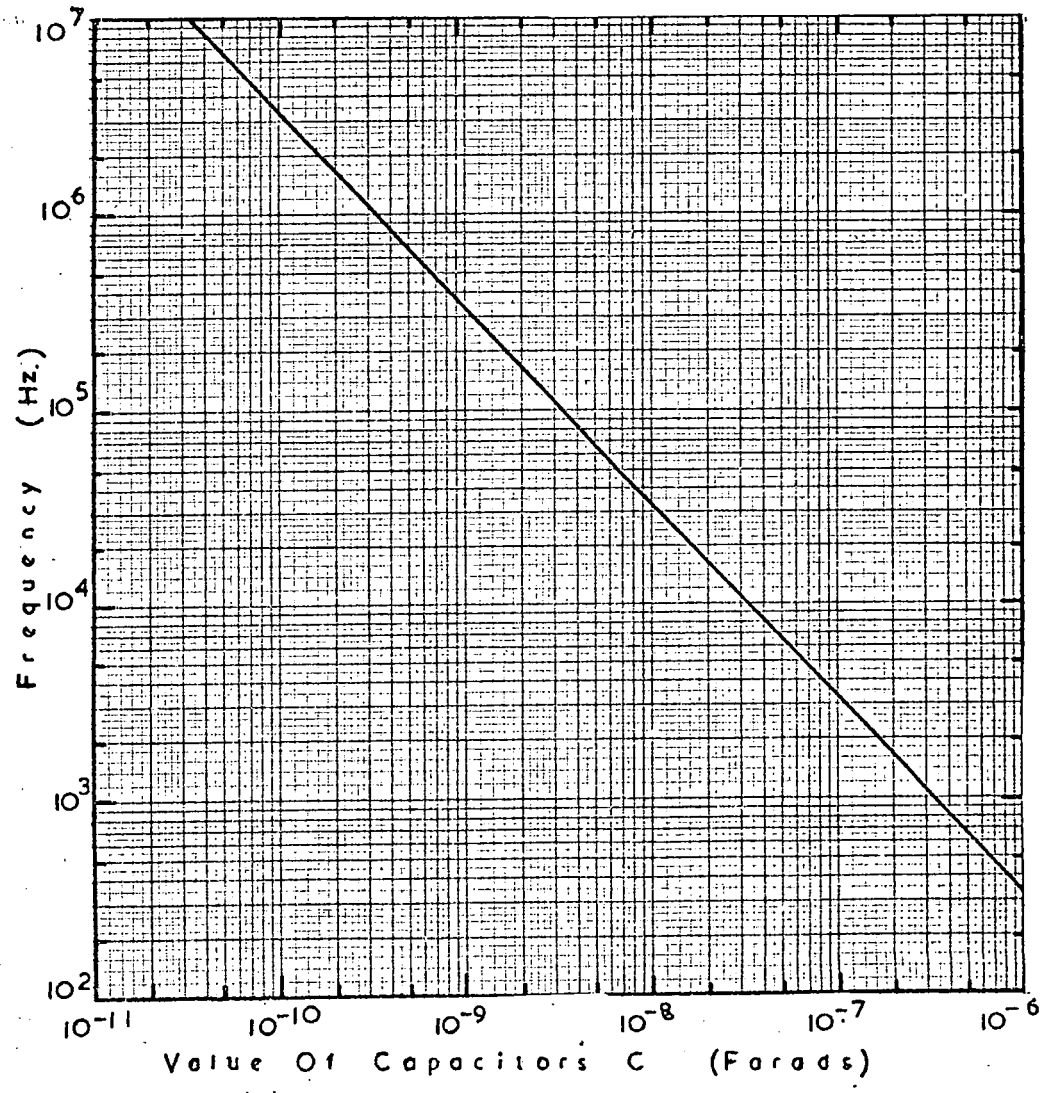

Figure A.4(b) The Variation of Multivibrator Frequency with Capacitors, C.

multivibrator frequency against value of the capacitors. The multivibrator is used as a clock pulse generator for the Momentum Selector shift registers, which were described in § 5.9.

A.2.4 The Basic Shift Register Unit for the Momentum Selector

The shift registers used in the Momentum Selector are made from Mullard integrated circuit blocks type FJJ 131. Each block contains two shift register bits and figure A.5 shows the inputs and outputs of a shift register bit. Each bit has two outputs Q and $\bar{Q}$ (the complement of Q) which can be set to a given initial state by the use of the preset and clear inputs as shown in figure A.5. The logic function of the shift register is such that when both preset and clear inputs are in the logical 1 state, the state on the D input is transferred to the Q output on the positive edge of the clock pulse. Any change in the state of the D input after the positive edge of the clock pulse is not transferred to the Q output.

An example of the improved design of TTL circuits is now the case here. A Mullard-integrated circuit block type FJJ 241 has now been introduced, which incorporates a five bit shift register inside each block and connection between adjacent shift register bits is made internally.

A.3 DTL System

A.3.1 Introduction

DTL is an abbreviation for Diode Transistor Logic. Figure A.6 shows a diagram of a two fold input DTL nand gate together with its associated logic symbol. The circuit is impregnated on a single chip of silicon. The chip also contains three similar circuits and is encapsulated in an integrated circuit element block. A power supply of +6v. is required for the block. A logical 0 level is obtained for a voltage between 0v. and +0.8v. and a logical 1 level for a voltage between +1.5v. and +6v. Gates having various numbers of inputs are available. The various standard circuits using the DTL system are described below.

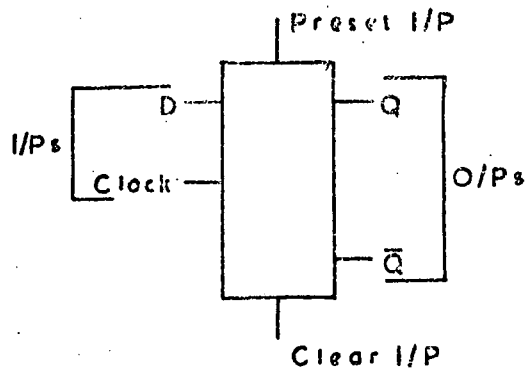

Figure A.5 The Shift Register Bit Used in the Momentum Selector.

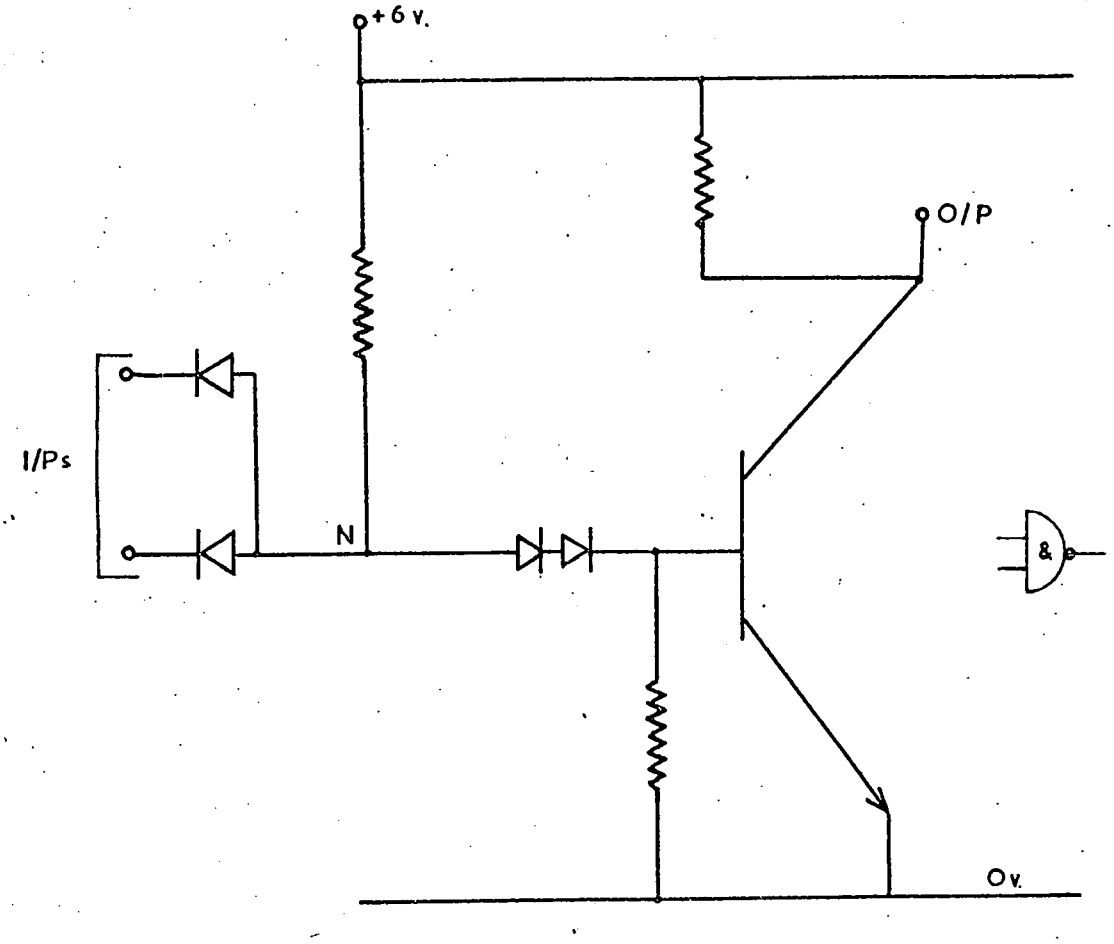

Figure A.6 Schematic Diagram of a Two Fold DTL Nand Gate

A.3.2 The Monostable Circuit and Delay Unit

The monostable circuit using the DTL system is shown in figure A.7(a). As with the TTL monostable, the length of the output pulse depends only on the value of the capacitor C. Figure A.7(b) shows a graph of the variation of pulse length with the value of the capacitance C. The monostable is triggered by the negative edge of the input pulse so a delay unit can be formed in a similar manner to the TTL monostable. The same symbols are used for the DTL monostable and delay unit as for the equivalent TTL circuit.

A.3.3. The Binary Comparator

The form of the binary comparator is shown in figure A.8, with the truth table for the output state for various input states shown in the inset. The binary comparator is used to compare two binary numbers and to indicate if the numbers are the same or differ. It is used in the checking circuits for the printed circuit boards used in the Measuring Trays and in the logic circuit for the date of an event.

As the circuit used only nand gates and inverters, the circuit can be made with both types of logic systems. It has been included with the DTL system because the binary comparators used in the spectrograph are made from DTL circuit blocks.

A.3.4 The J.K flip-flop FCJ 101

This type of flip-flop has many applications in the electronics of the spectrograph. For example, it is used as a simple memory and as the bits of both binary and B.C.D. scalers. The form of the scalers using this flip-flop are described in following sub-sections.

The flip-flop is shown schematically in figure A.9, There are two outputs from the flip-flop, Q_1 and Q_2, which are controlled by the set inputs S_1 and S_2 and the inputs J_1, J_2, and J_3 and K_1, K_2, and K_3 of the flip-flop. A clock input is also incorporated. This sets the outputs to certain states on the negative edge of the clock pulse depending on the states of the set, J, and K inputs at the instant of the negative edge of the clock pulse.

The function of the flip-flop can be seen from the truth tables shown

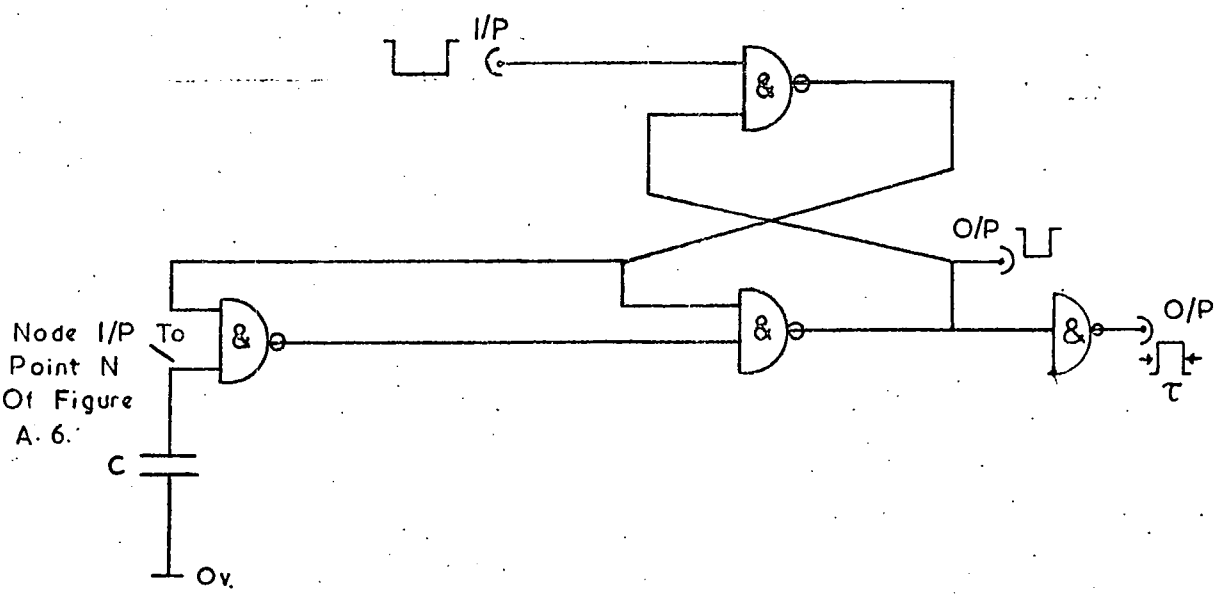

Figure A.7(a) The DTL Monostable Circuit.

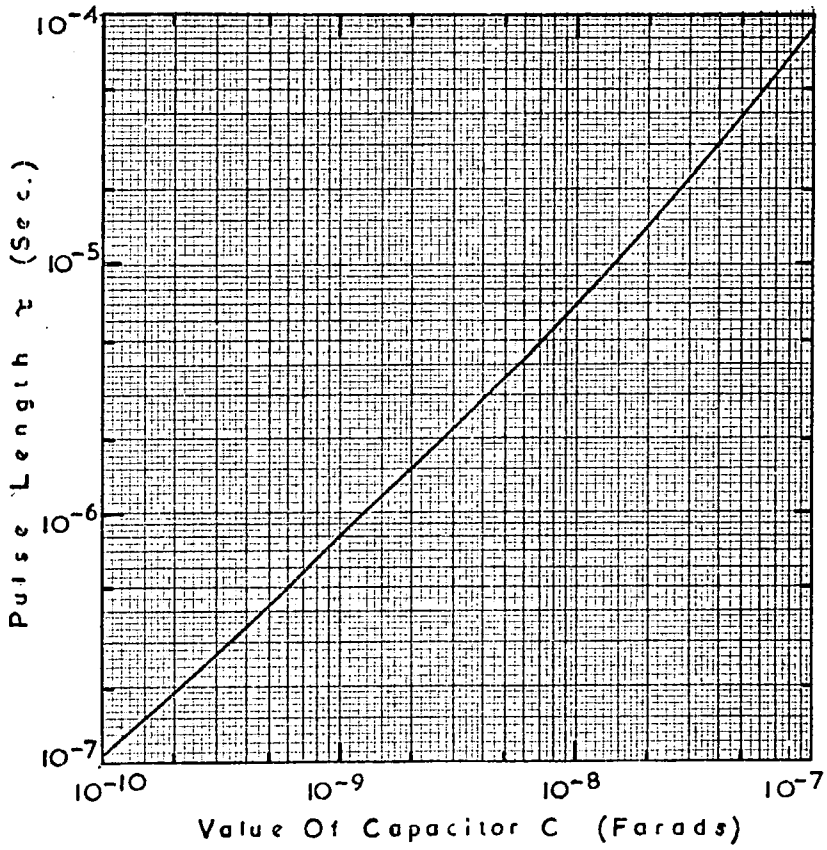

Figure A.7(b) The Variation of Pulse Length with Capacitor C.

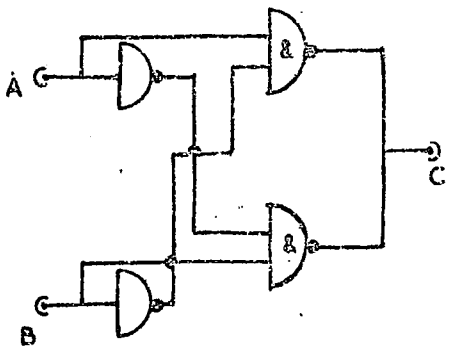

A	B	C
0	0	1
1	0	0
0	1	0
1	1	1

Figure A.8 The Binary Comparator Circuit.

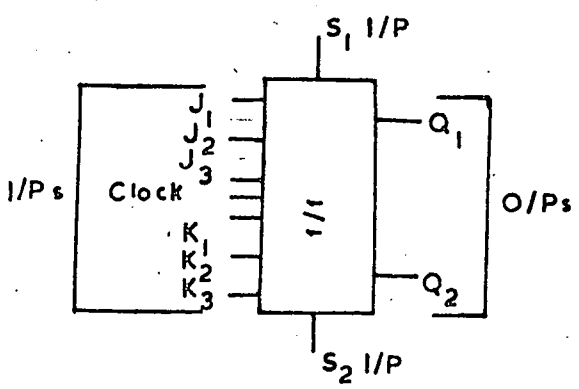

Figure A.9. Schematic Diagram of the DTL Flip-Flop Type FCJ101.

in Table A.1. Table A.1(a) gives the output states of Q_1 and Q_2 for the various states of S_1 and S_2. S_1 and S_2 dominate if at least one is at a logical 0 level. Then Q_1 and Q_2 are independent of the J, K, or clock input states. When S_1 and S_2 are both in the logical 1 state, the outputs Q_1 and Q_2 depend on the J and K input states. Table A.1(b) then gives the output states after the negative edge of the clock pulse for various values of the J and K inputs. When the S_1 and S_2 inputs and all the J and K inputs are in the logical 1 state, the outputs change state on the application of the negative edge of the clock pulse. The flip-flop thus behaves as a divide by two device.

TABLE A.1

The Truth Table for the DTL Flip-Flop Type FCJ 101

(a)				(b)			
S_1	S_2	Q_1	Q_2	J Input	K Input	Q_1	Q_2
0	0	1*	1*	Any Input 0	Any Input 0	No change	
0	1	1	0	Any Input 0	All Inputs 1	1	0
1	0	0	1	All Inputs 1	Any Input 0	0	1
1	1	No change		All Inputs 1	All Inputs 1	Reversed	

* Outputs states indeterminate when S_1 and S_2 go high.

Key Table A1(a): The output states for the logic levels on the Set inputs.

Table A1(b): The output states after the negative edge of the clock pulse for the logic levels on the J and K inputs and the Set inputs at the logical 1 level.

A.3.5 Binary Scaler

Figure A.10 shows a 4 bit binary scaler using FCJ 101 flip-flops. The output states of the bits A, B, C, and D after a given number of clock pulses is shown in Table A.2, which also gives the weights of the four bits. The scaler

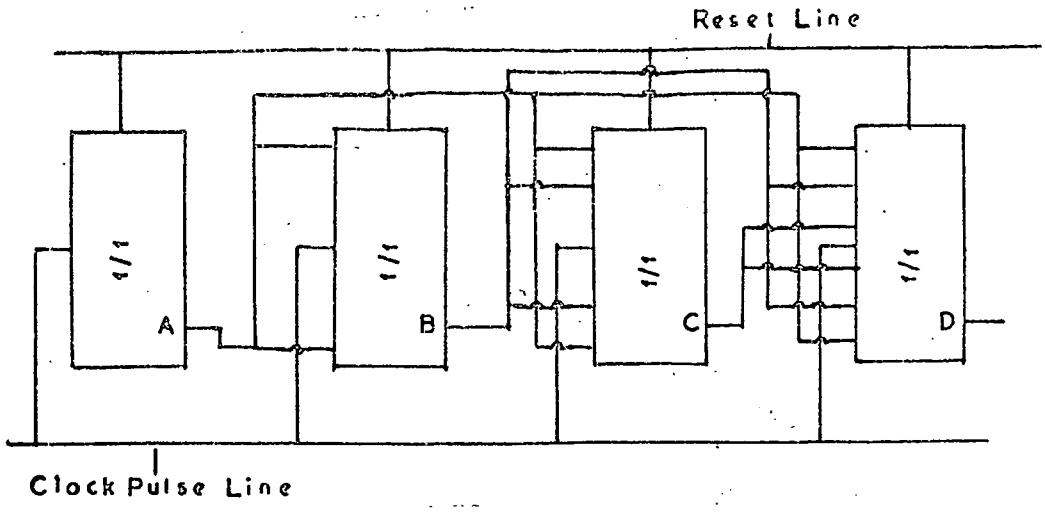

Figure A.10 The Form of a 4 Bit Binary Scaler Using FCJ101 Flip-Flops.

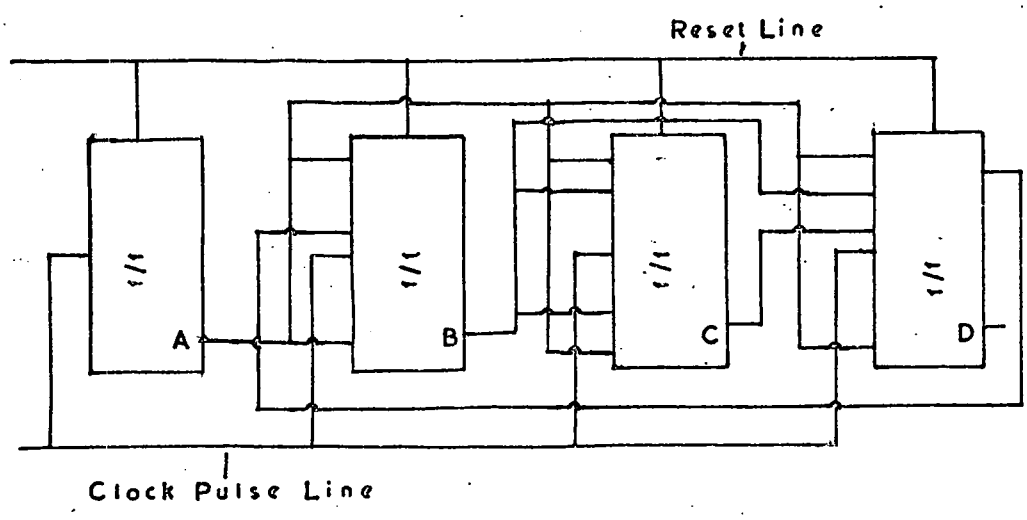

Figure A.11 The Form of a 4 Bit B.C.D. Scaler Using FCJ101 Flip-Flops.

counts on the negative edge of the clock pulse. It can count up to 15 pulses and resets to zero on the sixteenth pulse. Further bits can be connected to the scaler by using the output bit D as the clock pulse for the next stage. The scaler is reset by a negative pulse on the reset line. Binary scalers are used in several of the checking circuits for the electronic circuit boards on the Measuring Trays. The month of the event is also recorded by a binary scaler.

TABLE A.2

The Output States of the Bits of a 4 Bit Binary Scaler

Number of Clock pulses	Bit A(1)	Bit B(2)	Bit C(4)	Bit D(8)
0	0	0	0	0
1	1	0	0	0
2	0	1	0	0
14	0	1	1	1
15	1	1	1	1
16(=0)	0	0	0	0

A.3.6 B.C.D. Scaler

B.C.D. is the abbreviation for Binary Coded Decimal. A B.C.D. scaler consists of four bits A,B,C, and D, weighted as shown in Table A.3. The scaler resets to zero on the tenth clock pulse. This should be compared with a binary scaler of the same number of bits. The binary scaler would reset to zero on the sixteenth clock pulse.

TABLE A.3

The Output States of the Bits of a 4 Bit B.C.D. Scaler

Number of Clock pulses	Bit A(1)	Bit B(3)	Bit C(4)	Bit D(8)
0	0	0	0	0
1	1	0	0	0
2	0	1	0	0
8	0	0	0	1
9	1	0	0	1
10(=0)	0	0	0	0

A 4 bit B.C.D. scaler using FCJ 101 flip-flops is shown in figure A.11. The scaler counts on the negative edge of the clock pulse and is reset by the application of a negative pulse to the reset line. The scaler only counts one decade but further decades can be added if the D output bit of the scaler is used as the clock pulse for the next decade. The weight for the outputs on the next decade will be higher by a factor of 10 on the corresponding outputs of the previous decade.

B.C.D. Scalers are used extensively in the electronics for the tray steerage logic, which is described in § 6.6., and in several of the checking circuits for the electronics in the Measuring Trays, which are described in § 6.5.

A.3.7 B.C.D. to Decimal Converter

The form of the B.C.D. to decimal converter is shown in figure A.12. It converts a 4 bit B.C.D. number into its corresponding decimal output using a series of nand gates. With the system shown in figure A.12, the bits for a given number will be at a logical 1 level if the bit is on and the rest of the bits will be in the logical 0 level. The output for the corresponding decimal number will be at a logical 1 level and the remaining 9 outputs will be at a

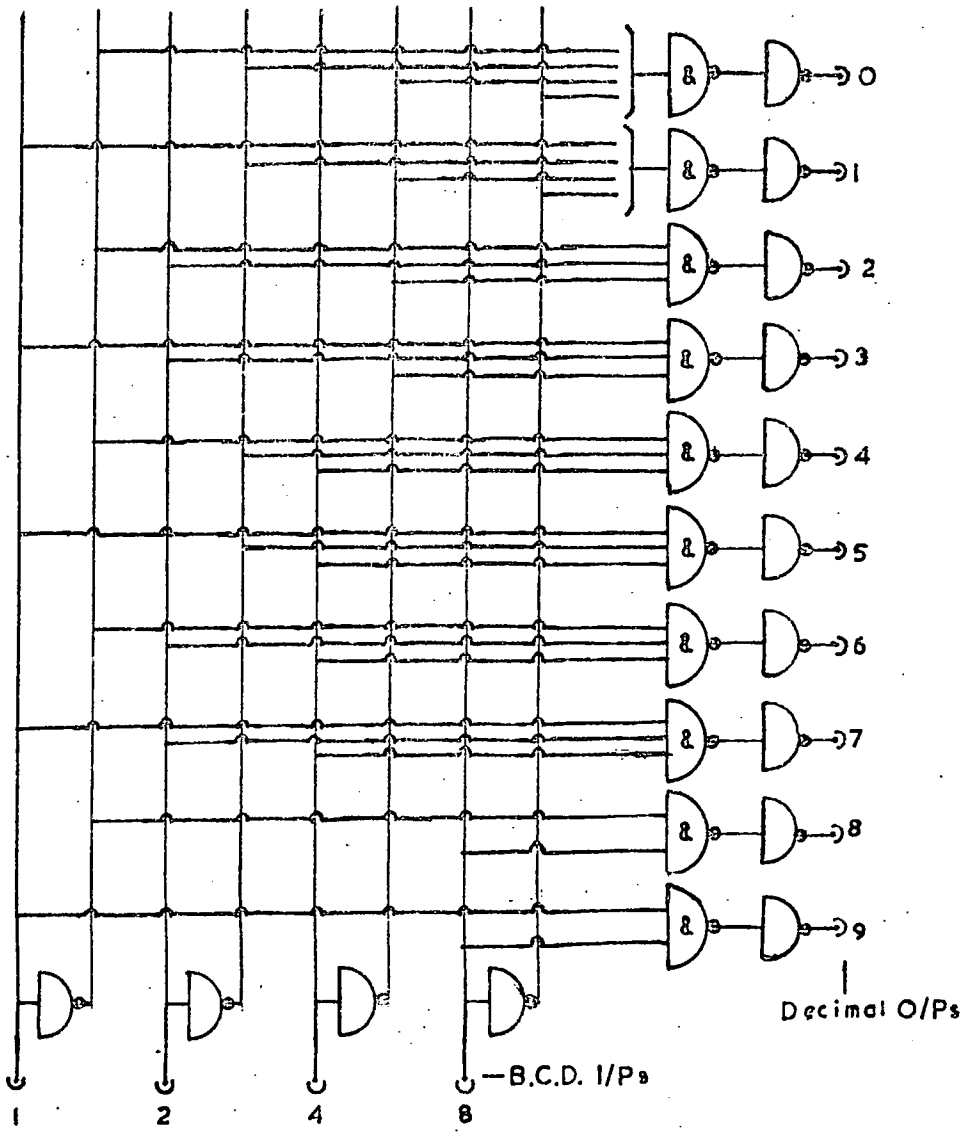

Figure A.12 The Form of the B.C.D. to Decimal Converter.

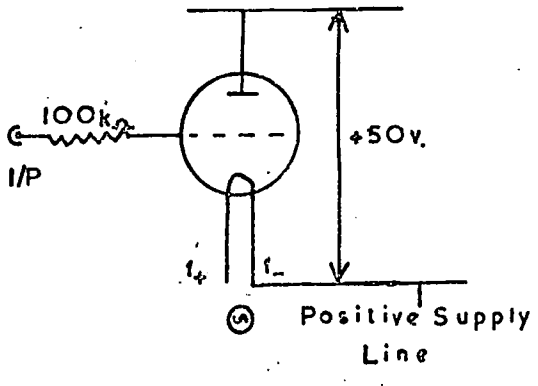

Figure A.13 Schematic Diagram of the Indicator Bulb Type DM160.

logical 0 level.

A B.C.D. number having more than one decade can be converted into a decimal output by using converters for each decade and gating the outputs of each decade. This circuit is used in the gating logic circuit for the Measuring Trays as explained in § 6.4.3 and in several of the checking circuits for the electronics in the Measuring Trays.

A.4 The Indicator Bulb

The indicator bulb has been used in the electronics to indicate the states of such circuits as controlling flip-flops, scalers, and shift registers. The indicator used is a Mullard subminiature voltage indicator type DM 160. A schematic diagram of the indicator is shown in figure A.13. The filament of the device uses a 1v. a/c power supply. The f_- input of the filament is connected to the positive power line of the integrated circuit blocks. A+50v. D.C. voltage is applied between the f_- and anode terminals. The 100kΩ resistor is used to prevent high current flow through the grid circuit.

The valve, when connected to the output from the logic gate, is on when the gate output is in a logical 1 state and off when the gate output is in the logical 0 state. When the valve is on, it displays a characteristic green colour. The DM 160 valves are mounted on printed circuit boards behind the front panel of the chassis containing the logic and are viewed through slits cut in the front panel.

APPENDIX B

The Spurious Rate of the High Pressure Flash Tubes

B.1 Introduction

When arrays of flash tubes are constructed, it is desirable to have a low spurious rate of flashing. A spurious flash tube is defined to be a flash tube which flashes whenever a high voltage pulse is applied across the tube. If an array has a high spurious rate, the tracks of particles will be difficult to distinguish from the background of spurious tubes.

The spectrograph has a large rate in its unparalysed mode ($\sim$0.3 $sec.^{-1}$ for each side with the magnetic flux density at a value of 16.3 kilogauss), so it is important to ensure that the flash tubes do not have a high spurious rate when pulsed at rates comparable to the maximum trigger rate. A spurious background will also effect the analysis of the events by the computer as the computer may try to fit a track through spurious tubes when these tubes would be rejected by the conventional scanning of a photographic film of the events.

Consequently, the flash tubes were tested before being used in any of the flash tube trays. A layer of tubes was placed between parallel electrodes and a high voltage pulse applied to the electrodes at a rate of 1.2 $sec.^{-1}$. The pulse was of similar height and length to the pulse expected to be used in the spectrograph. A pulsing rate of 1.2 $sec.^{-1}$ was used as this was about four times the maximum trigger rate and thus any tubes rejected would include all the spurious tubes obtained at small pulsing rates.

The 2m tubes of the Momentum Selector Trays were found to have a low rejection rate of less than 1% after 500 random pulses. However the 2m tubes for the Measuring Trays were found to have a spurious rate of $\sim$10% after 500 pulses. This was a far higher spurious rate than had been expected.

B.2 The variation of the spurious rate with pulsing rate and pulse length.

The above results have been achieved with a single layer of tubes so the applied high voltage pulse was of different shape to the pulse obtained when applied to a tray. This is the effect of the high capacitance of the tray (0.028μf) distorting the pulse. Hence a tray of flash tubes containing eight

layers of tubes was constructed and used for the investigations described below. The delay line used was the same as the delay line described in §3.5 for the Measuring Trays, which gave a pulse of peak field 7.5 $kVcm^{-1}$ and total length 1.5μs when applied to the flash tube tray. Unless stated otherwise this pulse was used in the investigations.

In order to see how the number of spurious flash tubes varied with the pulsing rate, the tray was pulsed randomly for various pulsing rates and the spurious rate plotted against the number of applied pulses. The results are shown in figure B.1 for pulsing rates of 0.1, 0.2, 0.33, and 0.5 $sec.^{-1}$; the spruious rate is expressed in figure B.1 as a percentage of the total number of tubes.

The tray was first pulsed at the slow rate of 0.1 $sec.^{-1}$, the rate increasing up to 0.5 $sec.^{-1}$. The interval between pulsing at the various rates depended on the rates, being ~2 hours for the low rate to ~15 hours for the faster rates in order to give any effect of a memory in the spurious tubes time to recover.

After the pulsing rate of 0.5 $sec.^{-1}$, the pulsing was stopped for ~15 hours and a pulsing rate of 0.1 $sec.^{-1}$ used again. The results of this run were within the errors for the initial run showing that the flash tubes had completely recovered from any memory imposed by the fast pulsing rate within this time. A further check on the complete recovery of the tubes was shown by pulsing the tray at 5.0 pulses $sec.^{-1}$ for ~1.86×10^5 pulses. After this number of pulses, about 80% of the tubes were flashing spuriously. A pulsing rate of 0.1 $sec.^{-1}$ was then used immediately after this fast rate. There was a quick reduction in spurious rate and the previous value for the spurious number for this rate was obtained.

The effect of the pulse length on the spurious rate was investigated by measuring the spurious rate for the same pulsing rate but with different pulse lengths. The results are shown in figure B.2 where the percentage of spurious

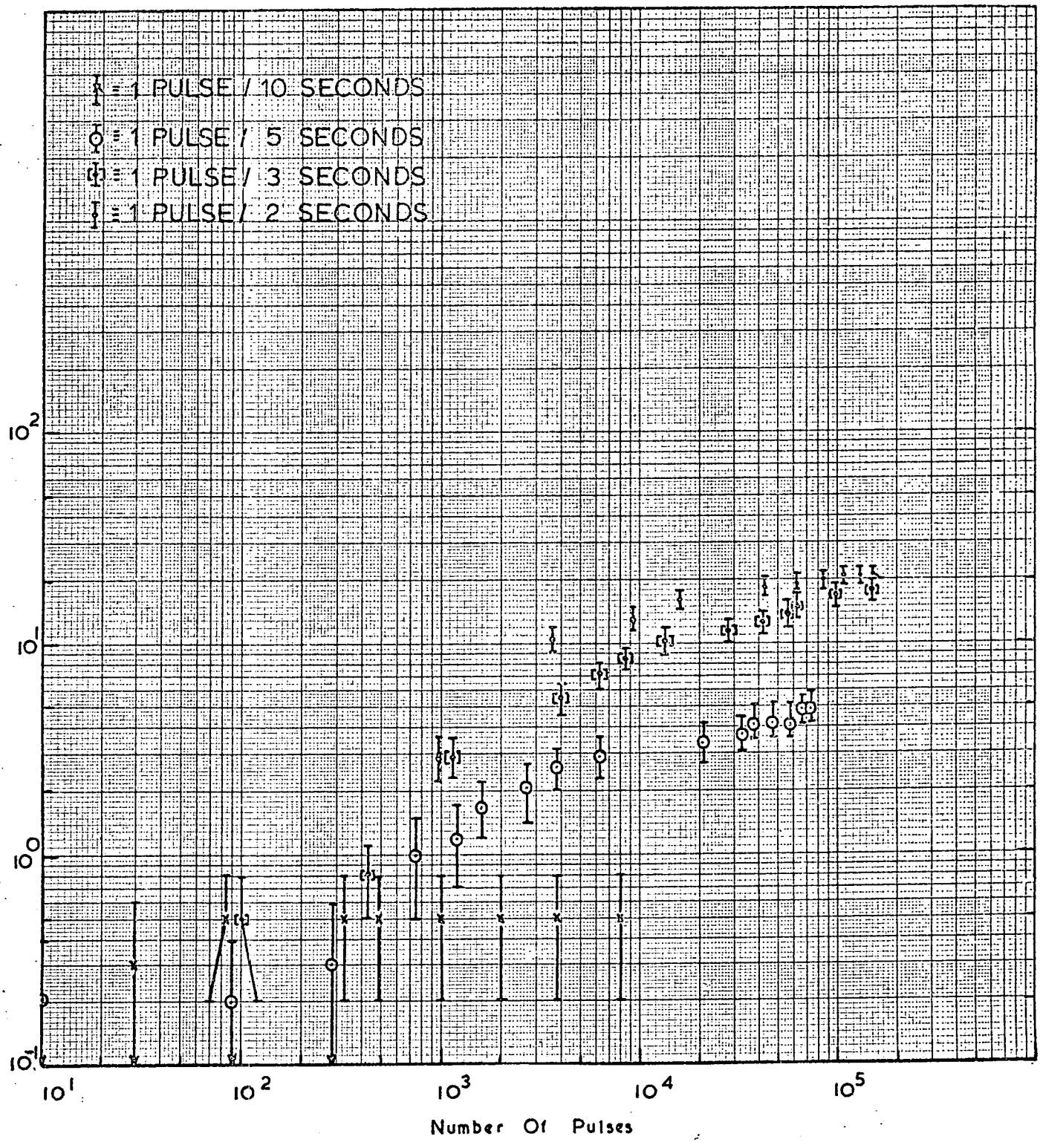

Figure B.1 Graphs of the Spurious Rate against Number of Pulses for Various Pulsing Rates.

flash tubes is plotted against the number of pulses for a pulsing rate of 0.5 $sec.^{-1}$ and two pulse widths. The pulses in the two cases had a peak field of 7.5 $kV.cm^{-1}$ and the overall pulse lengths were 1.5μs and 3.0μs, the pulse length is defined as the time from the start of the pulse to the point where the voltage is again zero.

The above results show that the spurious rate is dependent to a large extent on both the pulse length and the time between pulses. In normal conditions, the form of the pulse applied to an array of flash tubes is chosen after measuring the variation in efficiency of the tubes with the applied peak field. The pulse which produces the highest efficiency is normally the pulse which is used. Hence the results described above suggest that the spurious rate for a pulse giving the best efficiency will depend on the time interval between the successive pulses of the array.

B.3 The Spurious Rate for Tubes of Smaller Length and Various Electrode Sizes

The above results were obtained using flash tubes of length 2m with the electrodes covering 1.8m of the tubes. To see whether the high spurious rate is present for tubes of smaller length, an array was constructed using flash tubes of the same diameter as the 2m tubes but of length 38cm and pressure 2.3 atmospheres. The high spurious rate was not found with these tubes; at a pulsing rate of 5 $sec.^{-1}$ and the electrodes covering 28cm of the flash tube length, the spurious rate was ~ 0.3%.

As the effect is not present using tubes of smaller length, the 2m tubes were again pulsed at a rate of 0.5 $sec.^{-1}$ but now smaller electrodes were used such that they only covered part of the flash tubes. The high voltage pulse applied to the tubes was obtained from the same delay line as was used in §B.2 but now of course, as the capacitance of the electrode - flash tube system had decreased, there was less distortion on the applied pulse. The results are shown in figure B.3 for the electrodes of the lengths shown. The electrodes of length 102cm were used at both the front and back of the tray and the results

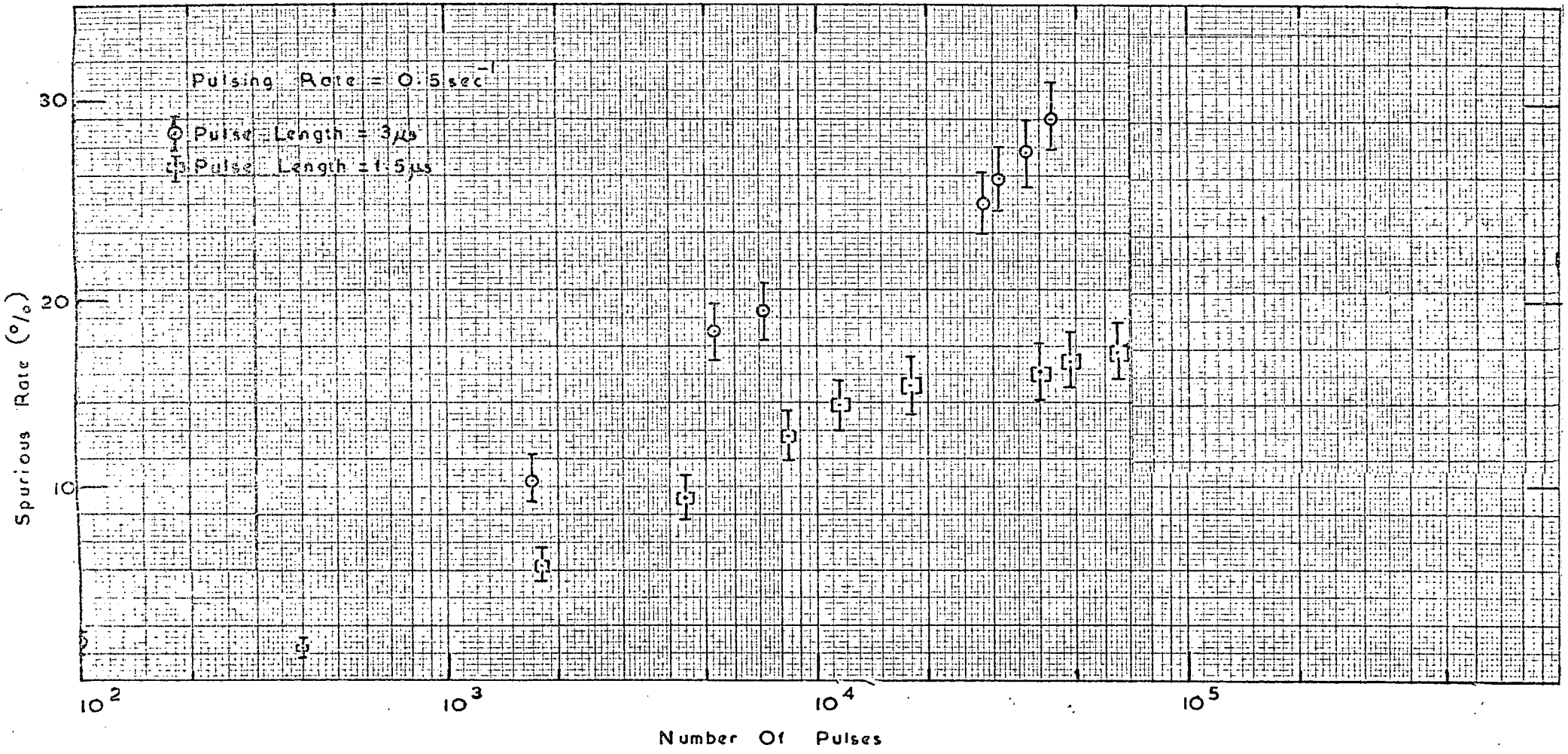

Figure B.2 Graphs of the Spurious Rate Against Number of Pulses for Different Pulse Lengths.

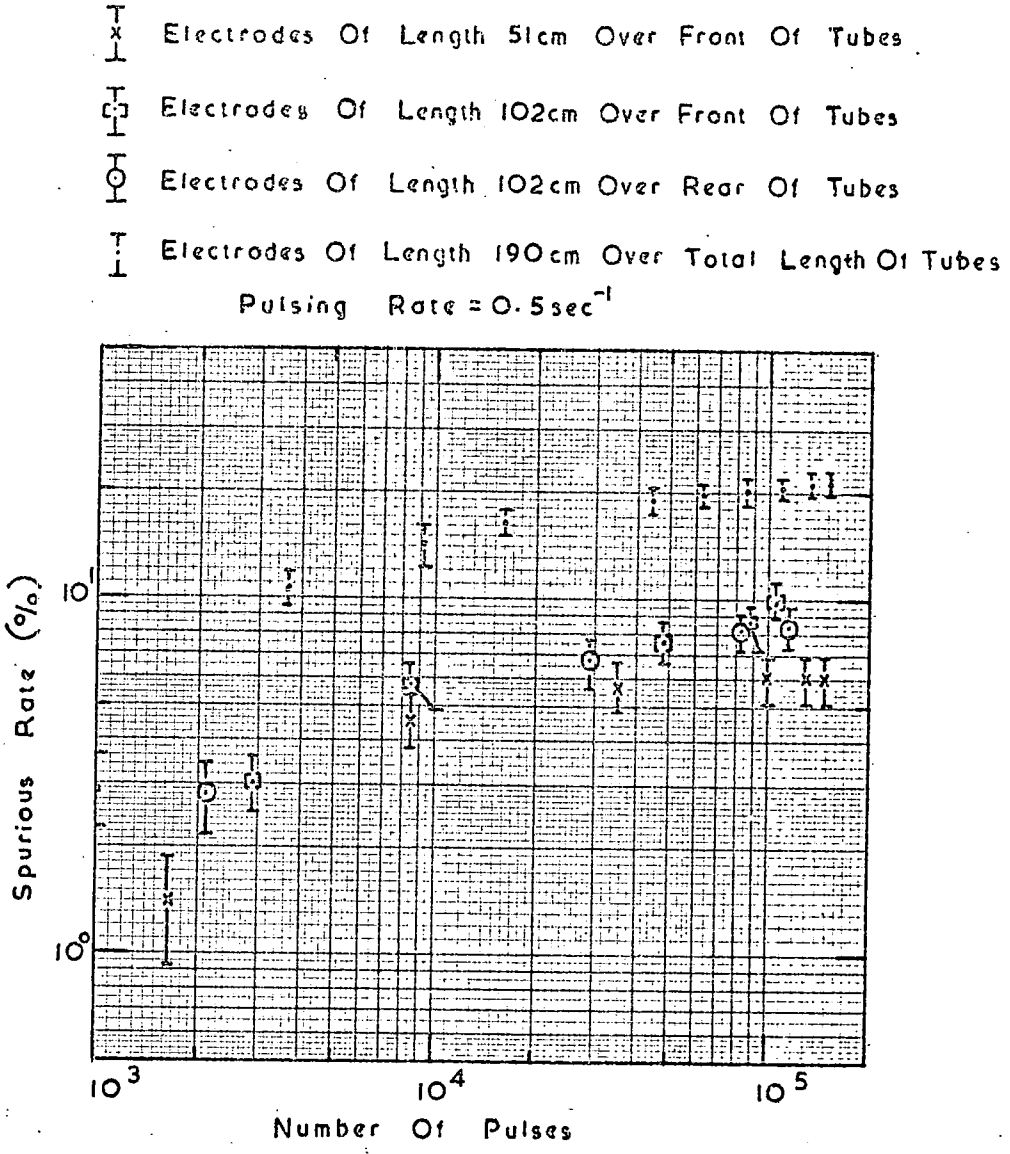

Figure B.3 Graphs of the Spurious Rate against Number of Pulses for Various Electrode Sizes.

for these two positions are plotted in figure B.3. For comparison, the results obtained at the same pulsing rate with the electrodes which covered the total length of the tubes and plotted in figure B.1 have been re-plotted in figure B.3.

The results plotted in figure B.3 show that there is a reduction in the spurious rate depending on the electrode sizes. One interesting point to note is that the values for the spurious rate, when the electrodes of approximately half the flash tube length are used at the front and back of the tubes, are nearly the same. Also the sum of the spurious rates for the two positions of the electrodes is nearly equal to the value obtained for a single electrode across the tube length. This effect suggests that the spurious rate obtained with electrodes along the complete length of the tubes could be caused by some local effect in the tube which causes it to flash when a high voltage pulse is applied across the irregularity.

However the tubes which flashed spuriously when the electrodes were placed at the back of the tray were marked and 38% of these were found to be still spurious when the electrodes were moved to the front of the tray. Although this in itself is not sufficient to completely refute the idea of some irregularity in the tubes - there could be several positions of an irregularity in a tube - it does cast some doubt and further work is required on the spurious rate using various pulsing rates and electrode sizes.

B.4 The Spurious Rate for a Different Applied High Voltage Pulse.

The results obtained above were for a high voltage pulse produced by a lumped parameter delay line. To see whether there was any effect on the spurious rate for a different shape of applied pulse, a pulse obtained by discharging a capacitor through a resistor was applied across the flash tubes. The pulse was used with the electrodes of length 102 cm when they covered the rear half of the tubes. The peak field across the flash tubes was equal to the peak field using the delay line pulse ($7.5 kV.cm^{-1}$) but the pulse was now

exponential in shape, the total length depending on the values of the capacitor and resistor.

The results are shown in figure B.4 for a pulsing rate of 0.5 sec^{-1}, and two values for the total length of the applied high voltage pulse of 14μs and 30μs. These results are for electrodes used only on one half of the tray so that the spurious rates plotted in figure B.4 will be approximately a factor of two higher when considered for the whole tray. The spurious rate is thus considerable for an exponential shaped pulse and is again dominant on the pulse length.

B.5 Discussion

The results described in the above sections show that the spurious rate of the high pressure flash tubes depends on both the rate of pulsing of the flash tubes and on the length of the flash tube. Reducing the length of the 2m flash tubes covered by the electrodes reduced the spurious rate. This suggests that the spurious effects are dependent on the flash tube length, since the rate would be uneffected if it was some property of the gas producing the effect.

One possible cause could be contamination in the tube producing some form of irregularity. This could be dust or other foreign body present in the tube before being filled with neon. A point discharge could then be produced by the dust which consequently causes the tube to flash. As the pulsing rate increases, the increase in spurious rate could be produced by an after-flashing effect on the initial discharge caused by the contamination in the flash tube.

The effect of impurities in a batch of flash tubes on their spurious rate was investigated by Coates (1967). A small quantity of iron filings was added to a batch of flash tubes of internal diameter 1.55 cm and containing commercial neon gas at a pressure of 60 cm of mercury. The spurious rate

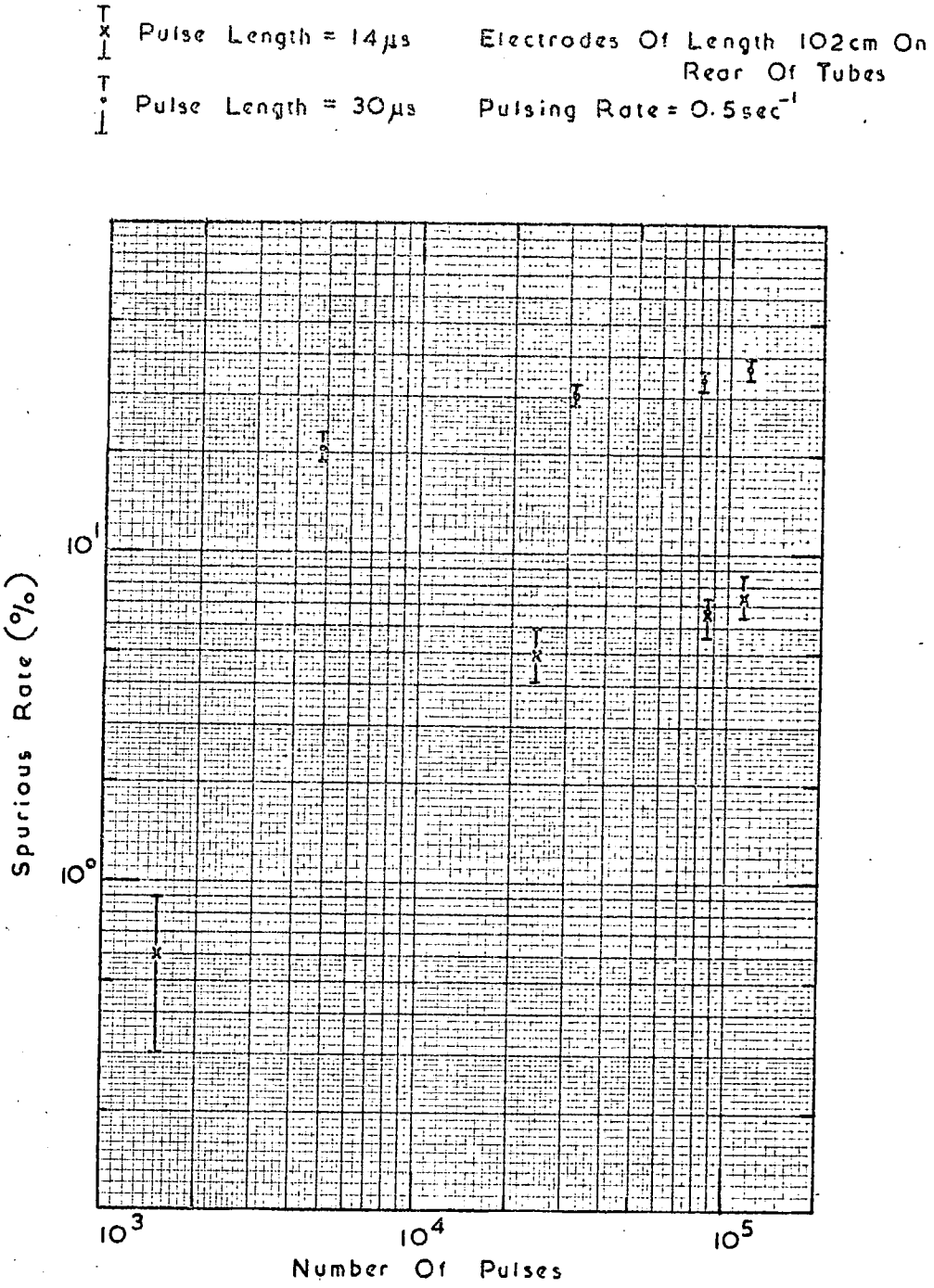

Figure B.4 Graphs of the Spurious Rate against Number of Pulses for Different Exponential Pulse Lengths.

of these tubes was compared with a normal batch of tubes of the same diameter and pressure. He found that the probability of a spurious flash in the contaminated batch was 0.5 tube^{-1} pulse^{-1} compared to 0.012 tube^{-1} pulse^{-1} for the normal batch. These figures were obtained for a pulse of peak field 6kV cm^{-1} and length 4μs with the flash tubes pulsed randomly at a rate of 1 pulse every 7 seconds. It can be seen from these results that the spurious number of tubes is increased by the addition of an impurity in the tubes.

It could be argued that the initial flash of a spurious tube is caused by a charged particle traversing the flash tube during its sensitive time and any subsequent flash then being caused by an after-flashing effect. However, this is thought not to be the case as, on average, the same flash tubes were found to be spurious when the tubes were pulsed at different times under the same conditions, which indicates that it is some property of the flash tube causing the effect.

B.6 Possible Further Investigations

It is obvious that further investigations into this problem need to be performed. One possible extension is to compare the spurious rates of flash tubes made in different batches to see if there is any systematic difference in their spurious properties. The 2m flash tubes were made in batches of 40 on the same filling rig but they were not stored after manufacture in separate batches, so no check could be made on the differences in the various batches. Also the spurious rates of flash tubes made in the normal manner and a batch made with the inside of the tube chemically cleaned before evacuating and filling could be compared. Chemical cleaned tubes have one main disadvantage in that the cost could prove to be excessive, the extra cost depending on the method of cleaning.

The results so far have been obtained with flash tubes pulsed randomly.

When a flash tube array is pulsed after the passage of a charged particle, the spurious rate will almost certainly increase due to an after-flashing effect in the flash tubes which discharged along the track of a particle. Thus an investigation of both the spurious rate after 'genuine' triggers of an array and the after-flashing effect for various average pulsing rates and electrode sizes needs to be carried out on the high pressure flash tubes.

APPENDIX C

The Curve Fitting Technique using the Method of Least Squares

The equation of motion for a charged particle in the magnet has been shown to obey the relation given by equation 7.10:

$$y = ax^2 + bx + c$$

with the Cartesian axes as shown in figure 7.3.

The coefficients a, b, and c are determined from the co-ordinates of the track obtained from the information contained in the five Measuring Trays.

In general, consider the case where n co-ordinates are known for the track where n, for a quadratic equation, has a minimum value of 3.

Let $$Q = \sum_{i=1}^{n} \left(y_i - ax_i^2 - bx_i - c \right)^2 \qquad C.1$$

The best fit is obtained when Q is a minimum. This is obtained when

$$\frac{\partial Q}{\partial a} = \frac{\partial Q}{\partial b} = \frac{\partial Q}{\partial c} = 0, \text{ that is}$$

$$\Sigma \left(y_i - ax_i^2 - bx_i - c \right) x_i^2 = 0 \qquad C.2$$

$$\Sigma \left(y_i - ax_i^2 - bx_i - c \right) x_i = 0 \qquad C.3$$

$$\Sigma \left(y_i - ax_i^2 - bx_i - c \right) = 0 \qquad C.4$$

where the summation symbol Σ used above is equivalent to the symbol $\sum_{i=1}^{n}$

Simplifying the above, we have

$$a \Sigma x_i^4 + b \Sigma x_i^3 + c \Sigma x_i^2 - \Sigma x_i^2 y_i = 0 \qquad C.5$$

$$a \Sigma x_i^3 + b \Sigma x_i^2 + c \Sigma x_i - \Sigma x_i y_i = 0 \qquad C.6$$

$$a \Sigma x_i^2 + b \Sigma x_i + \Sigma c - \Sigma y_i = 0 \qquad C.7$$

From these 3 linear equations the coefficients a, b, and c can be determined as shown below

$$a = \frac{\begin{vmatrix} \Sigma x_i^3 & \Sigma x_i^2 & -\Sigma x_i^2 y_i \\ \Sigma x_i^2 & \Sigma x_i & -\Sigma x_i y_i \\ \Sigma x_i & n & -\Sigma y_i \end{vmatrix}}{\begin{vmatrix} \Sigma x_i^4 & \Sigma x_i^3 & \Sigma x_i^2 \\ \Sigma x_i^3 & \Sigma x_i^2 & \Sigma x_i \\ \Sigma x_i^2 & \Sigma x_i & n \end{vmatrix}} \qquad C.8$$

$$b = -\frac{\begin{vmatrix} \Sigma x_i^4 & \Sigma x_i^2 & -\Sigma x_i^2 y_i \\ \Sigma x_i^3 & \Sigma x_i & -\Sigma x_i y_i \\ \Sigma x_i^2 & n & -\Sigma y_i \end{vmatrix}}{\begin{vmatrix} \Sigma x_i^4 & \Sigma x_i^3 & \Sigma x_i^2 \\ \Sigma x_i^3 & \Sigma x_i^2 & \Sigma x_i \\ \Sigma x_i^2 & \Sigma x_i & n \end{vmatrix}} \qquad C.9$$

$$c = \frac{\begin{vmatrix} \Sigma x_i^4 & \Sigma x_i^3 & -\Sigma x_i^2 y_i \\ \Sigma x_i^3 & \Sigma x_i^2 & -\Sigma x_i y_i \\ \Sigma x_i^2 & \Sigma x_i & -\Sigma y_i \end{vmatrix}}{\begin{vmatrix} \Sigma x_i^4 & \Sigma x_i^3 & \Sigma x_i^2 \\ \Sigma x_i^3 & \Sigma x_i^2 & \Sigma x_i \\ \Sigma x_i^2 & \Sigma x_i & n \end{vmatrix}} \qquad C.10$$

where $\Sigma c = nc$

The value of n used in the equations to determine the coefficients depends on the number of track co-ordinates obtainable from the flash tubes, although n can only have the values 3, 4, or 5. The summation of the x co-ordinates raised to the given power is then taken only over the flash tube trays for which a y co-ordinate of the trajectory is known.

APPENDIX D

Derivation of the Formula used to Determine the m.d.m. of M.A.R.S.

The m.d.m. of the instrument using a five point fit on the trajectory has been defined by equation 7.15 as

$$p_{mdm} = \frac{0.196}{\sigma_a} \text{ GeV/c} \qquad \text{D.1}$$

where σ_a is the standard deviation of the coefficient, a, of x^2 in the five point parabola fit. The value of σ_a is derived below.

From Appendix C we have the general expression for a of

$$a = \frac{\begin{vmatrix} \Sigma x_i^3 & \Sigma x_i^2 & -\Sigma x_i^2 y_i \\ \Sigma x_i^2 & \Sigma x_i & -\Sigma x_i y_i \\ \Sigma x_i & n & -\Sigma y_i \end{vmatrix}}{\begin{vmatrix} \Sigma x_i^4 & \Sigma x_i^3 & \Sigma x_i^2 \\ \Sigma x_i^3 & \Sigma x_i^2 & \Sigma x_i \\ \Sigma x_i^2 & \Sigma x_i & n \end{vmatrix}}$$

$$= \frac{\Sigma x_i^3 \left(-\Sigma x_i \Sigma y_i + n \Sigma x_i y_i\right) - \Sigma x_i^2 \left(-\Sigma x_i^2 \Sigma y_i + \Sigma x_i \Sigma x_i y_i\right) - \Sigma x_i^2 y_i \left(n \Sigma x_i^2 - (\Sigma x_i)^2\right)}{\Sigma x_i^4 \left(n \Sigma x_i^2 - (\Sigma x_i)^2\right) - \Sigma x_i^3 \left(n \Sigma x_i^3 - \Sigma x_i \Sigma x_i^2\right) + \Sigma x_i^2 \left(\Sigma x_i \Sigma x_i^3 - (\Sigma x_i^2)^2\right)}$$

Defining k to be equal to the denominator and re-arranging the numerator we have

$$a = \frac{\left((\Sigma x_i^2)^2 - \Sigma x_i^3 \Sigma x_i\right) \Sigma y_i + \left(n \Sigma x_i^3 - \Sigma x_i \Sigma x_i^2\right) \Sigma x_i y_i - \left(n \Sigma x_i^2 - (\Sigma x_i)^2\right) \Sigma x_i^2 y_i}{k} \qquad \text{D.2}$$

The standard deviation of a, σ_a, is given by the relation

$$\sigma_a = \sqrt{\Sigma_i \left(\frac{\partial a}{\partial y_i}\right)^2 \sigma_{y_i}^2} \qquad \text{D.3}$$

From equation D.2 we have

$$\frac{\partial a}{\partial y_i} = \frac{(\Sigma x_i^2)^2 - \Sigma x_i^3 \Sigma x_i + (n\Sigma x_i^3 - \Sigma x_i \Sigma x_i^2)\, x_i - \left(n\Sigma x_i^2 - (\Sigma x_i)^2 \right) x_i^2}{k} \qquad D.4$$

as k is a function of x_i only.

Now σ_{y_i} is the standard deviation in the measurement at the measuring levels which is the same for all layers as the same measuring system is used. Hence defining σ_y as this standard deviation we have:

$$\sigma_a = \frac{\sigma_y}{k} \sqrt{\Sigma \left((\Sigma x_i^2)^2 - \Sigma x_i^3 \Sigma x_i + (n\Sigma x_i^3 - \Sigma x_i \Sigma x_i^2) x_i - (n\Sigma x_i^2 - (\Sigma x_i)^2) x_i^2 \right)^2} \qquad D.5$$

Simplifying the above, we obtain

$$\sigma_a = \frac{\sigma_y}{k} \sqrt{k \left(n\Sigma x_i^2 - (\Sigma x_i)^2 \right)} \qquad D.6$$

which reduces to

$$\sigma_a = \sigma_y \sqrt{\frac{n\Sigma x_i^2 - (\Sigma x_i)^2}{\Sigma x_i^4 (n\Sigma x_i^2 - (\Sigma x_i)^2) - (n(\Sigma x_i^3)^2 - 2\Sigma x_i \Sigma x_i^2 \Sigma x_i^3 + (\Sigma x_i^2)^3)}} \qquad D.7$$

Substituting in equation D.1 for σ_a we have

$$p_{mdm} = \frac{0.196}{\sigma_y} \sqrt{\Sigma x_i^4 - \frac{n(\Sigma x_i^3)^2 - 2\,\Sigma x_i \Sigma x_i^2\, \Sigma x_i^3 + (\Sigma x_i^2)^3)}{n\Sigma x_i^2 - (\Sigma x_i)^2}} \qquad D.8$$

The m.d.m. is then obtained by summing over the x co-ordinates of the flash tube trays for n = 5.

ACKNOWLEDGEMENTS

The author is grateful to Professor G.D. Rochester, F.R.S. for providing facilities and for his interest in all aspects of the work.

He is indebted to his supervisor, Dr. M.G. Thompson, for the helpful guidance given throughout the period of the work. Professor A.W. Wolfendale is thanked for many useful comments and suggestions.

The discussions with past and present members of the Cosmic Ray Group, in particular Dr. M.J.L. Turner, Mr. S.C. Wells, and Mr. M.R. Whalley, are acknowledged with gratitude.

With a project of the size described in this thesis, the number of Technical Staff involved has been numerous. Particular thanks, however, must go to Mr. W. Leslie and members of the Physics Main Workshop for their construction of the magnet; to Mr. Dennis Jobling and members of the Physics Student Workshop for the manufacture of the flash tube trays and numerous other equipment; and to Mr. E.W. Lincoln and members of the Physics Electronics Workshop for building the majority of the electronics.

Past and present members of the Technical Staff, who have been connected with the M.A.R.S. group, in particular Mr. P. Armstrong, Mr. B. Carr, Mr. M.P. Scott, and Mr. J. Webster, are thanked for their help. Mr. K. Tindale, the technician assigned to the project since its inception, is thanked for the conscientious way he has performed his duties.

A special acknowledgement must be reserved for Mr. R. McDermot, who has painstakingly made the supports and shields for the flash tube trays.

Mrs. P.A. Russell is gratefully thanked for her conscientious preparation of the diagrams.

For her painstaking efforts in typing this thesis, Mrs. A. Harris is sincerely thanked.

Finally, the Science Research Council is thanked for providing a Research Studentship.

REFERENCES

Achar, V.C., Menon, M.G.K., Marasimham, V.S., Ramana Murthy, P.V., Streekantan, B.V., Hinotani, K., Miyake, S., Creed, D.R., Osborne, J.L., Pattison, J.B.M., and Wolfendale, A.W., 1965, Phys. Lett., 18, 196.

Alchudjian, S.V., Asatiani, T.L., Badalian, H.V., Gazarian, K.A., Mekilov, G.I., Krishchian, M.V., Prokhorov, A.N., Prokhorov, V.N.,1968, Canad. J. Phys., 48, S1169.

Allkofer, O.C., Carstensen, K., Dau, W.D., Heinrich, W., Kraft, E., and Weinert, M., 1970, Acta Phys. Hung., 29, Supp.4, 13.

Asbury, J.G., Cooper, W.A., Voyvodic, L., Walker, R.J., and Wangler, T.P., 1970, Nuovo Cim., 66, 169.

Ashton, F., Kisdnasamy, S., and Wolfendale, A.W., 1958, Nuovo Cim., 8, 615.

Ashton, F., and Wolfendale, A.W., 1963, Proc., Phys., Soc., 81, 593.

Ashton, F., Coates, R.B., Holyoak, B., Simpson, D.A., and Thompson, M.G., 1965, Nuc. Inst. and Meth., 37, 181.

Ashton, F., and Coates, R.B., 1966, Proc. IX Int. Conf. Cosmic Rays, London; Inst. of Phys. and Phys. Soc., 2, 959.

Ashton, F., Kamiya, Y., MacKeown, P.K., Osborne, J.L., Pattison, J.B.M., Ramana Murthy, P.V., and Wolfendale, A.W., 1966, Proc. Phys. Soc., 87, 79.

Ashton, F., Coates, R.B., King, J., Tsuji, K., and Wolfendale, A.W. J. Phys. A. (in the press).

Aurela, A.M., MacKeown, P.K., and Wolfendale, A.W., 1966, Proc. Phys. Soc., 89, 401.

Aurela, A.M., and Wolfendale, A.W., 1967, Ann. Acad. Sci. Fenn., A6, 226.

Ayre, C.A., and Thompson, M.G., 1969, Nucl. Inst. and Meth., 69, 106.

Ayre, C.A., Breare, J.M., Holroyd, F.W., Thompson, M.G., Wells, S.C. and Wolfendale, A.W., 1970, Acta Phys. Hung., 29, Supp. 4, 547.

Ayre, C.A., and Thompson, M.G., 1970, Acta Phys. Hung., 29, Supp. 4, 541.

Ayre, C.A., Hamdan, M.A., Hume, C.J., Thompson, M.G., Wells, S.C., Whalley, M.R., and Wolfendale, A.W., 1971, J. Phys. A., 4, L75.

Baber, S.R., Nash, W.F., and Rastin, B.C., 1968a, Nucl. Phys., B4, 539.

Baber, S.R., Nash, W.F., and Rastin, B.C., 1968b, Nucl. Phys., B4, 549.

Bacon, D.F., and Nash, W.F., 1965, Nucl. Inst. and Meth., 37, 43.

Barnaby, C.F., and Barton, J.C., 1960, Proc. Phys. Soc., 76, 745.

de Beer, J.F., Holyoak,B., Wdowczyk, J., and Wolfendale, A.W., 1966, Proc. Phys. Soc., 89, 567.

Bennett, H.W., and Nash, W.F., 1960, Supp. Nuovo Cim., 15, 193.

Bergeson, H.E.,Keuffel, J.W., Larson, M.O., Martin, E.R., and Mason, G.W., 1967, Phys. Rev. Lett., 19, 1487.

Bergeson, H.E., Bolingbroke, G.L., Carlson, G., Groom, D.E., Keuffel, J.W., Morrison, J.L., and Osborne, J.L., 1971, Phys. Rev. Lett., 27, 160.

Brooke, G., Gardener, M., Lloyd, J.L., Kisdnasamy, S., and Wolfendale, A.W., 1962, Proc. Phys. Soc., 80, 674.

Bull, R.M., Coates, D.W., Nash, W.F., and Rastin, B.C., 1962, Supp. Nuovo Cim., 23, 39.

Bull, R.M., Nash, W.F.,and Rastin, B.C., 1965, Nuovo Cim., 40, 348.

Caro, D.E., Parry, J.K., and Rathgeber, H., 1951, Aust. J. Sci. Res. A, 4, 16.

Chin, S., Hanayama, Y., Hara, T., Higashi, S., Kitamura, T., Miono, S., Nakagawa, M., Ozaki, S., Takahashi, T., Tsuji, K., Watase, Y., Kobayakawa, K., and Shibata, H., 1970, Acta Phys. Hung., 29, Supp. 4, 65.

Coates, D.W., and Nash, W.F., 1962, Aust. J. Phys., 15, 420.

Coates, R.B., 1967, Ph.D Thesis, University of Durham.

Coccoini, G., 1966, Proc. IX Int. Conf. Cosmic Rays, London; Inst. of Phys. and Phys. Soc., 2, 616.

Conversi, M., and Gozzini, A., 1955, Nuovo Cim., 2, 189.

Cousins, J., Harrison, D.J., Hoque, M.T., and Rastin, B.C., 1970, Acta Phys. Hung., 29, Supp. 4, 585.

Coxell, H., and Wolfendale, A.W., 1960, Proc. Phys. Soc., 75, 378.

Coxell, H., Meyer, M.A., Scull, P.S., and Wolfendale, A.W., 1961, Supp. Nuovo Cim., 21, 7.

Earnshaw, J.C., Orford, K.J., Rochester, G.D., Somogyi, A.J., Turver, K.E., and Walton, A.B., 1967, Proc. Phys. Soc., 90, 91.

Flatté, S.M., Decoster, R.J., Stevenson, M.L., Toner, W.T., and Zipf, T.F., 1971, Phys. Lett., 35B, 345.

Flint, R.W. and Nash, W.F., 1970, Acta Phys. Hung., 29, Supp. 4, 99.

Fugii, Z., Iida, S., Kamiya, Y., Kawaguchi, S., and Takenaka, A., 1969, Lett. Nuovo Cim., 1, 845.

Gardener, M., Kisdnasamy, S., Rössle, E., and Wolfendale, A.W., 1957, Proc. Phys. Soc. B, 70, 687.

Greisen, K., 1966, Proc. IX Int. Conf. Cosmic Rays, London; Inst. of Phys. and Phys. Soc., 2, 609.

Harrison, D.J., and Rastin, B.C., 1970, Nuc. Inst. and Meth., 77, 181.

Hayman, P.J., and Wolfendale, A.W., 1962, Proc. Phys. Soc., 80, 710.

Holmes, J.E.R., Owen, B.G., and Rodgers, A.L., 1961, Proc. Phys. Soc., 78, 496.

Hyams, B.D., Mylroi, M.G., Owen, B.G., and Wilson, J.G., 1950, Proc. Phys. Soc. A, 63, 1053.

Judge, R.J.R., and Nash, W.F., 1965a, Nuovo Cim., 35, 999.

Judge, R.J.R., and Nash, W.F., 1965b, Nuovo Cim., 35, 1025.

Kamiya, Y., Sagisaka, S., Ueno, H., Kato, S., and Sekido, Y., 1962, J. Phys. Soc. Japan, 17, Supp. A - III, Part III, 315.

Kasha, H., Hawkins, C.J.B., and Stefanski, R.J., 1968, Canad. J. Phys., 46, S306.

Keuffel, J.W., Osborne, J.L., Bolingbroke, G.L., Mason, G.W., Larson, M.O., Lowe, G.H., Parker, J.H., Stenerson, R.O., and Bergeson, H.E., 1970, Acta Phys. Hung., 29, Supp. 4, 183.

Krishnaswamy, M.R., Menon, M.G.K., Narasimham, V.S., Kawakami, S., Miyake, S., and Mizohata, A., 1970, Acta Phys. Hung., 29, Supp. 4, 221.

MacKeown, P.K., Said, S.S., Wdowczyk, J., and Wolfendale, A.W., 1966, Proc. IX Int. Conf. Cosmic Rays, London,; Inst. of Phys. and Phys. Soc., 2, 964.

Miyake, S., Narasimham, V.S., and Ramana Murthy, P.V., 1964, Nuovo Cim., 32, 1524.

Moroney, J.R., and Parry, J.K., 1954, Aust. J. Phys., 7, 423.

Nandi, B.C., and Sinha, M.S., 1970, Acta Phys. Hung., 29, Supp. 4, 529.

Osborne, J.L., Wolfendale, A.W., and Palmer, N.S., 1964, Proc. Phys. Soc., 84, 911.

Pak, W., Osaki, S., Roe, B.P. and Greisen, K., 1961, Phys. Rev., 121, 905.

Palmer, N.S., and Nash, W.F., 1969, Nucl. Phys., B9, 315.

Pine, J., Davisson, R.J. and Greisen, K., 1959, Nuovo Cim., 14, 1181.

Reines, F., 1967, Proc. Roy. Soc. A, 301, 125.

Rossi, B., and Greisen, K., 1941, Rev. Mod. Phys. 13, 240.

27 JAN 1972